LA-UR-01-4083

GSI-191: PARAMETRIC EVALUATIONS FOR PRESSURIZED WATER REACTOR RECIRCULATION SUMP PERFORMANCE

TECHNICAL LETTER REPORT

AUGUST 2001, REVISION 1

PREPARED BY
D. V. RAO, B. LETELLIER, C. SHAFFER, S. ASHBAUGH, AND L. BARTLEIN

LOS ALAMOS NATIONAL LABORATORY
DECISION APPLICATIONS DIVISION
PROBABILISTIC RISK ANALYSIS GROUP (D-11)

M. L. MARSHALL, NRC TECHNICAL MONITOR

PREPARED FOR
US NUCLEAR REGULATORY COMMISSION
OFFICE OF NUCLEAR REGULATORY RESEARCH
DIVISION OF ENGINEERING TECHNOLOGY

EXECUTIVE SUMMARY

The purpose of the Generic-Safety-Issue (GSI) 191 study is to determine if the transport and accumulation of debris in a containment following a loss-of-coolant accident (LOCA) will impede the operation of the emergency core cooling system (ECCS) in operating pressurized water reactors (PWRs). In the event of a LOCA within the containment of a PWR, thermal insulation and other materials (e.g., coatings and concrete) in the vicinity of the break will be damaged and dislodged. A fraction of this material will be transported to the recirculation (or emergency) sump and accumulate on the screen. The debris that accumulates on the sump screen forms a bed that acts as a filter. Excessive head loss across the debris bed may exceed the net positive suction head (NPSH) margin of the ECCS or containment spray (CS) pumps. For sump screens that are only partially submerged by water on the containment floor, excessive head loss across the debris bed may prevent water from entering the sump. Thus, excessive head loss can prevent or impede the flow of water into the core or containment. Also, excessive head loss across the debris bed may lead to ECCS- or CS-pump damage. Excessive head loss will be referred to as "sump failure."

As part of the GSI-191 study, the parametric evaluation documented in this report was performed to demonstrate whether sump failure is a plausible concern for operating PWRs. The results of the parametric evaluation form a credible technical basis for making a determination of whether sump blockage is a generic concern for PWRs. However, the parametric evaluations have a number of limitations that make them ill-suited for making a determination of whether a specific plant is vulnerable to sump failure.

Approach

PWR sump and containment design features vary widely between plants. The focus of this parametric evaluation was to examine the range of conditions present in operating PWRs and to incorporate variations such as insulation type in proportion to their occurrence in the population so that the plausibility of sump blockage could be assessed generically for the PWR population as a whole. This objective necessitated an adequate representation of individual plant features, so parametric cases were developed to represent specific plants. Although the best information available to Los Alamos National Laboratory (LANL) was applied for each parametric case, it is recognized that these cases do not provide a complete perspective of the sump-blockage potential at the corresponding plants. However, the cases do provide a reasonable description of operating PWRs, and they focus parametric evaluations on a realistic range of conditions. The development of the parametric cases was a key feature of this study.

Two primary sources of information were used to construct the parametric cases.

(a) Licensee responses to a recent industry survey on sump and containment design related to GSI-191
(b) Licensee responses to Nuclear Regulatory Commission (NRC) Generic Letter (GL) 97-04.

As appropriate, this information was augmented by plant-specific information from

(a) the Unresolved Safety Issue (USI) A-43 study (Serkiz, 1985),
(b) Updated Final Safety Analysis Reports (UFSARs), and
(c) Individual Plant Examinations (IPEs).

Another key feature of this study involves the use of "reasonable" parameter ranges. These ranges were defined through the judicious application of completed and ongoing test results from the GSI-191 study and test results from the NRC-sponsored Boiling Water Reactor (BWR) Strainer Blockage Study. Also, results from tests and analyses that were sponsored by the Boiling Water Reactor Owner's Group

(BWROG) during the recent modification of BWR ECCS strainers[1] were used to establish "reasonable" parameter ranges. Parameter values that reduced the potential for sump blockage were considered to be "favorable," whereas parameter values that increased the potential for sump blockage were viewed as "unfavorable." An example of this approach is the designation of design ECCS flow as "unfavorable" because it would increase the head loss caused by a debris bed and designation of 1/2 of the maximum flow (i.e., one train of the ECCS operating) as a "favorable" assumption because it would decrease the head loss caused by a debris bed. Both flow rates are realistic and reasonable.

Final determination of the sump failure likelihood for each parametric case was expressed with a qualitative grade of **unlikely**, **possible**, **likely**, and **very likely**. Under this approach, a parametric case with debris-bed head losses that exceed the sump failure criterion when evaluated under favorable conditions indicates that blockage is **very likely** to occur for the assumed plant configuration. A case that meets the sump failure criterion even under unfavorable assumptions indicates that blockage is **unlikely** to be a concern. Intermediate cases that fail over part of the parameter range and succeed over the remainder of the range are more difficult to judge. These require consideration of features of the parametric case like the orientation of the screen, the location of the sump, and the predominance of insulation types in the containment. Qualitative grades of **likely** and **possible** were assigned to this intermediate spectrum of cases using engineering judgment based on associated calculations and related test data.

Results

Table ES-1. Summary of Sump Failure Potential for 69 Parametric Cases.

Sump Failure Potential	SLOCA	MLOCA	LLOCA
Very Likely	25	31	53
Likely	7	6	7
Possible	4	6	1
Unlikely	33	26	8
Total	69	69	69

Table ES-1 summarizes the results of the parametric evaluation. The 69 parametric cases developed for this evaluation provide a reasonable representation of operating PWRs, so the results form a credible technical basis for making a determination of whether sump blockage is a generic concern for PWRs. However, the parametric evaluations have a number of limitations that make them ill-suited for making a determination of whether a specific plant is vulnerable to sump failure.

Some of these limitations include the following.

(a) The locations of thermal insulation and other debris sources for the various plants that the parametric cases are based on were not modeled.
(b) Changes in $NPSH_{Margin}$ for the various plants that the parametric cases are based on were not modeled.
(c) The variability in responding to SLOCAs for the various plants on which the parametric cases are based was not modeled.

[1] ECCS strainers in BWRs perform the same function that recirculation sump screens do in PWRs.

(d) Only the thermal insulations and other debris sources that are widely used were included in the evaluation.

Useful Insights

(a) Accumulation of very large quantities of damaged reflective metallic insulation (RMI) would be necessary to cause sump failure by the assumed head-loss criteria. The potential for sump failure caused by transport of RMI debris was found to be unlikely for all parametric cases except 3 out of the 69.

(b) Transport and accumulation of small quantities of fibrous and particulate debris are sufficient to cause sump failure by the assumed head-loss criteria. Approximately 1/2 ft^3 of fibrous insulation combined with only 10 lb of particulates would be sufficient to raise sump blockage concerns for 30 out of 69 parametric cases. This finding is a direct reflection of the fact that a significant number of parametric cases included sump-screen areas less than 100 ft^2 and $NPSH_{Margins}$ less than 4 ft-water.

(c) In numerous parametric cases, the estimated quantities of debris reaching the sump far exceeded the minimum amount of debris necessary to cause sump failure. The actual number of parametric cases where failure was predicted varied depending on the break size. In general, a large LOCA (LLOCA) tended to generate and transport substantially larger quantities than the failure-threshold debris loadings. Although estimates for the quantity of debris transported following a small LOCA (SLOCA) depended strongly on assumptions related to CS actuation, a small subset of parametric cases was capable of transporting quantities of debris sufficient for failure even without sprays. In these parametric cases, recirculation sumps are located inside the missile shield and have special features such as horizontal screens at or below the containment floor level.

(d) For many parametric cases, head-loss estimates (evaluated using both favorable and unfavorable assumptions) exceeded the $NPSH_{Margin}$ for the ECCS and/or CS pump(s). Typically, head-loss estimates following a LLOCA were much larger than the $NPSH_{Margin}$.

(e) Greater uncertainties and variability in SLOCA accident sequences introduce greater uncertainties in the conclusions of this study for SLOCA. Large debris volumes and more standard plant responses to medium LOCAs (MLOCAs) and LLOCAs increase the confidence placed in the conclusions for these accidents.

TABLE OF CONTENTS

LIST OF TABLES

LIST OF FIGURES

LIST OF ACRONYMS AND ABBREVIATIONS

AHU	Air Handling Unit
AJIT	Air-Jet Impact Testing
B&W	Babcock and Wilcox
BWR	Boiling Water Reactor
BWROG	Boiling Water Reactor Owners' Group
CCW	Component Cooling Water
CE	Combustion Engineering
CFD	Computational Fluid Dynamics
CP	Corrosion Products
CS	Core Spray
DBA	Design Basis Accident
DEGB	Double-Ended Guillotine Break
ECCS	Emergency Core Cooling System
EOP	Emergency Operating Procedure
EQ	Equipment Qualification
ESF	Engineered Safeguard Feature
FSAR	Final Safety Analysis Report
FTDL	Failure-Threshold Debris Loading
FY	Fiscal Year
GL	Generic Letter
GSI	Generic Safety Issue
HDR	Heissdampfreaktor
HEPA	High-Efficiency Particulate Air
HPSI	High-Pressure Safety Injection
IPE	Individual Plant Examination
L/D	Range-of-Damage Zone Divided by Pipe Diameter
LANL	Los Alamos National Laboratory
LDFG	Low-Density Fiberglass
LLOCA	Large LOCA
LOCA	Loss-of-Coolant Accident
LPSI	Low-Pressure Safety Injection
MLOCA	Medium LOCA
NEI	Nuclear Energy Institute
NPSH	Net Positive Suction Head
NRC	Nuclear Regulatory Commission
NRR	Nuclear Regulatory Research
PORV	Power-Operated Relief Valve
PRA	Probabilistic Risk Assessment
PWR	Pressurized Water Reactor
RCP	Reactor Coolant Pump
RCS	Reactor Coolant System
RHR	Residual Heat Removal
RMI	Reflective Metallic Insulation
RWST	Refueling Water Storage Tank
SAT	Spray Additive Tank
SER	Safety Evaluation Report
SI	Safety Injection

SLOCA	Small LOCA
SRS	Savannah River Site
UFSAR	Updated Final Safety Analysis Report
URG	Utility Resolution Guidance
USI	Unresolved Safety Issue
ZOI	Zone of Influence

ACKNOWLEDGEMENT

The U. S. Nuclear Regulatory Commission (NRC) office of Nuclear Regulatory Research (NRR) sponsored the work reported here. Mr. Michael Marshall, RES/DET, is the Technical Monitor for this task. He provided critical technical direction, actively participated in the design of the experiments reported here, and provided an in-depth review of this report. Mr. Kenneth Karwoski and Mr. John Boardman of the NRC also provided valuable input throughout this effort. The authors would like to thank Mr. Robert Elliott, NRC/NRR, for taking time to review earlier versions of this report and for providing valuable comments.

The authors would particularly like to acknowledge the contributions of Dr. A. Maji of the University of New Mexico and his student assistants. These individuals conducted many of the experimental investigations described in this report.

The Nuclear Energy Institute coordinated a comprehensive industry survey and collected much of the descriptive data used in this study. The authors would like to acknowledge the contributions of Mr. T. Andreycheck of the Westinghouse Owner's Group, Mr. Barry Lubin of the Combustion Engineering Owners Group, and Mr. Gilbert Zigler of ITS Corporation for their input and cooperation during this study.

Finally, the authors would like to thank Mr. D. Stack, Dr. H. Sullivan, and Dr. J. Ireland of Los Alamos National Laboratory for their counsel and guidance during the preparation of this document.

1.0 INTRODUCTION

1.1 Description of Safety Concern

In the event of a loss-of-coolant accident (LOCA) within the containment of a pressurized water reactor (PWR), piping thermal insulation and other materials in the vicinity of the break will be dislodged by break-jet impingement. A fraction of this fragmented and dislodged insulation and other materials such as paint chips, paint particulates, and concrete dust will be transported to the containment floor by the steam/water flows induced by the break and by the containment sprays. Some of this debris will eventually be transported to and accumulated on the recirculation sump suction screens. Debris accumulation on the sump screen may challenge the sump's capability to provide adequate, long-term cooling water to the emergency core cooling system (ECCS) and to the containment spray (CS) pumps. The Generic Safety Issue (GSI) 191 study titled "Assessment of Debris Accumulation on PWR Sump Performance" addresses the issue of debris generation, transport, and accumulation on the PWR sump screen, and its subsequent impact on ECCS performance. Los Alamos National Laboratory (LANL) has been supporting the U.S. Nuclear Regulatory Commission (NRC) in the resolution of GSI-191.

In the GSI-191 study, the sump is defined as the space enclosed by the trash rack (see Fig. 1-1), and the space enclosed by the sump screen is referred to as the sump pit or sump region. Figure 1-1 is a generic representation of a pressurized water reactor (PWR) sump layout. Actual sump designs vary significantly from this figure, but all share similar geometric features. The purpose of the trash rack and sump screen is to prevent debris that may damage or clog components downstream of the sump from entering the ECCS and reactor coolant system (RCS). The area outside of the sump is referred to as the containment floor or pool.

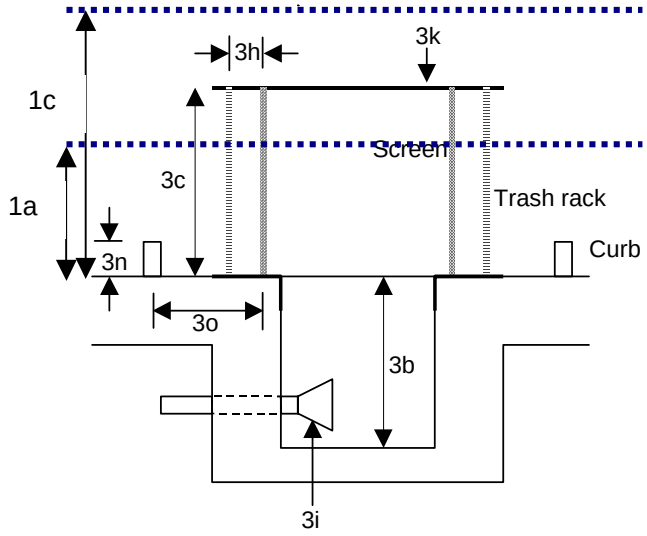

Symbol	
3b	Sump depth
3c	Height above floor
3h	Distance between trash rack and screen
3i	Vortex suppressor
3k	Solid plate
3n	Debris curb height
3o	Distance between debris curb and screen
1a	Height of water pool on containment floor at time of switchover
1c	Max. Height of water pool on containment floor

Fig. 1-1. Illustration of Sump Parameters Queried in the GSI-191 Industry Survey.

An examination of plant drawings, preliminary analyses, and ongoing tests suggests that a prominent mechanism for recirculation sump failure involves pressure drop across the sump screen induced by debris accumulation. However, sump-screen failure through other mechanisms is also possible for some configurations. Three failure mechanisms were considered as part of the GSI-191 study.

(1) Loss of net positive suction head (NPSH) margin caused by excess pressure drop across the screen resulting from debris buildup. This concern applies to all plant units having sump screens that are completely submerged in the containment pool in combination with other plant features that permit generation and accumulation of debris on the sump screen.

(2) Loss of the static head necessary to drive recirculation flow through a screen because of excess pressure drop across the screen resulting from debris buildup. This concern applies to all plant units having sump screens that are not completely submerged in combination with other plant features that permit generation and accumulation of debris on the sump screen.

(3) Blockage of water-flow paths may (a) cause buildup (and retention) of water in some regions of the containment and result in lower water levels near the sump and thus lower $NPSH_{Margin}$ than estimated by the licensees or (b) altogether prevent adequate water flow through these openings.

Realistically, only the licensees are capable of judging their plant's vulnerability to the third safety concern because (a) vulnerability to this mechanism is highly plant-specific and (b) the plant-specific data necessary to make such a judgment are not widely available. Although plant vulnerability to debris accumulation on the sump screen (i.e., the first two safety concerns) is also plant-specific, the NRC and industry groups have compiled much of the information that is necessary to effectively judge the vulnerability of ECCS systems during recirculation following specific accidents [e.g., large LOCA (LLOCA), medium LOCA (MLOCA), and small LOCA (SLOCA)] and to draw insights regarding the potential severity of the problem for classes of reactors with similar design features (e.g., sub-atmospheric containments, ice condenser containments, etc.). The focus of the present study is to perform "representative" parametric analyses to address the following safety questions for each plant to the extent possible.

If a LOCA of a given break size were to occur, would the amount and type of debris generated from containment insulation and other sources of debris cause significant buildup on the ECCS recirculation sump? If so, would such blockage be of sufficient magnitude to challenge the ECCS function either by reducing the $NPSH_{available}$ below the $NPSH_{required}$ or by reducing flow through the sump screen below the ECCS pump flow demand?

Other concerns related to debris generated during postulated accidents are beyond the scope of the GSI-191 study and the parametric analyses presented in this report. Examples of such concerns include (a) the potential for debris to pass through the sump screen, enter the RCS, and damage or block ECCS or RCS components and (b) structural failure of sump screens as a result of loads from debris or direct jet impingement.

1.2 Scope and Objectives of the Parametric Calculations

The present study has two objectives.

1. Perform parametric analyses that can be used effectively to judge the potential for sump-screen blockage following postulated LLOCA, MLOCA, and SLOCA events in representative PWRs. This includes performing appropriate technical calculations that provide estimates for debris generation, debris transport, debris accumulation, and the resulting head loss across the sump screen. This effort also includes providing defensible bases for all of the assumptions made in the

analyses and explanations of how some of the prominent calculational uncertainties were factored into the decision process.

2. Interface with the ongoing probabilistic risk assessment (PRA) study [LANL, 2001f] and provide a conditional probability range for loss of recirculation caused by LOCA-generated debris that can be used to estimate the risk-significance of this issue for the overall PWR population.

Clearly, this safety concern is plant-specific in nature, and a firm determination of the vulnerability of any individual plant could require a plant-specific evaluation. Such an evaluation may have to incorporate plant features such as

- physical layouts of primary and auxiliary piping in the containment;
- possible locations of the postulated breaks and the likely ECCS response to these breaks;
- locations, types, and quantities of insulation used on each piping system and equipment component;
- physical layouts of intervening structures that may inhibit debris transport;
- a physical description of the sump geometry and its location in containment; and
- the time until switchover to recirculation and the required flow rates through the sump.

Detailed plant-specific analyses are complex and unique, and performing them for each of the 69 operating PWRs is beyond the present scope of work.[2] The objective of this parametric study is to examine the range of possible conditions present in the industry and to incorporate variations such as insulation type in proportion to its occurrence in the population so that the plausibility of sump blockage can be assessed. This objective necessitates approximations of individual plant features, so throughout the parametric analysis, individual cases are developed to represent specific plants in the industry. Although the best information available to LANL was used for each unit, it is recognized that these cases do not describe conditions at any single plant in great detail. Therefore, the individual entries for each unit will be referred to as "cases" or as "parametric cases" rather than as "plant analyses" so that it is understood that the individual cases do not provide a complete perspective of sump-blockage risk at the corresponding plants.

Even with the necessary approximations, valuable insights regarding the relative potential for plant susceptibility to sump-screen blockage can be drawn by performing representative parametric evaluations. This can be demonstrated by considering the following examples.

1. Consider two plants that have sump screens with flow areas of only 11.64 ft^2 and use fibrous insulation on essentially all of their piping.[3] A LOCA in these plants would almost certainly result in thick beds of fibrous insulation on the screen. With or without the addition of some particulate materials (e.g., concrete dust and paint chips), a substantial head loss would result that could easily overcome the plant's NPSH margin (estimated to be about 2.6 ft-water based on plant responses to NRC GL 97-04 [US NRC, 1997]). Several representative parametric evaluations can be performed in this case to demonstrate that sump-screen blockage and loss of $NPSH_{Margin}$ are **very likely** for these plants .

2. There is a set of plants whose primary piping is insulated with large quantities of both calcium silicate (cal-sil) and fibrous insulation (e.g., fiberglass or mineral wool). The combination of cal-sil and fibrous insulation is known to induce very large head losses across a sump screen (even at very small debris loadings), and hence, this class of plants would be susceptible to sump-

[2]Plant-specific analyses are underway as part of the continuing GSI-191 study for two volunteer plants and six USI A-43 reference plants (for which detailed drawings are available).
[3]Source of information: Plant submittal to Industry Survey.

screen blockage. Representative parametric evaluations also can be performed in this case to judge the potential for blockage.

3. Finally, consider a plant that has a screen area of 330 ft^2. Its insulation consists of 90% reflective metallic insulation (RMI) and 10% fibrous insulation, and it has a relatively large $NPSH_{Margin}$ of 5.25 ft. RMI debris is known to cause substantially less strainer blockage than other types of insulation debris. Also, recent testing has shown that RMI is less likely to transport to the sump in significant quantities. Given these facts, parametric evaluations can be used again to show that this plant is **unlikely** to have a strainer head-loss problem. Despite the conclusions of a parametric evaluation, only a thorough analysis can confirm that this plant is not susceptible to sump-screen blockage.

The terms "very likely" and "unlikely" are described in Sec. 3 along with the rationale used to assign these grades to each parametric case.

1.3 Description of Relevant Plant Features and Other Parameters

Some general conclusions regarding important plant features that influence accident outcome are listed below.

Sump Design and Configurations

- The ECCS and/or CS pumps in nearly one-third of the plants have an $NPSH_{Margin}$ less than 2 ft-water, and another one-third have an $NPSH_{Margin}$ between 2 ft-water and 4 ft-water. In general, PWR sumps have low $NPSH_{Margins}$ compared with the head-loss effects of debris accumulation on the sump screen.

- PWR sump designs vary significantly, ranging from horizontal screens located below the floor elevation to vertical screens located on pedestals. The sump-screen surface areas vary significantly from unit to unit, ranging from 11 ft^2 to 700 ft^2 (the median value is approximately 125 ft^2). Some plants employ curb-like features to prevent heavier debris from accumulating on the sump screen, and some do not have any noticeable curbs. All these plant-specific features should be captured adequately in the parametric cases.

- In 19 PWR units, the sump screen would not be completely submerged at the time that ECCS recirculation starts. As described in Sec. 1.4, the mode of failure is strongly influenced by sump submergence.

- Sump-screen clearance size varies considerably. A majority of the plants used a sump-screen opening size of 0.125 in., reportedly to ensure that the maximum size of the debris that can pass through the sump screen is less than the smallest clearance in the RCS and the CS system. However, 26 PWR units indicated that sump-screen clearance is higher than 0.125 in., reaching up to 0.6 in. Two units reported not having fine screens, other than the standard industrial grating used to filter out very large debris.

Sources and Locations of Debris

- US PWRs employ a variety of types of insulation and modes of encapsulation, ranging from non-encapsulated fiberglass to fully encapsulated stainless-steel RMI. A significant majority of PWRs have fiberglass and cal-sil insulations in the containment, either on primary piping or on supporting

systems.[4] The types of fibrous insulation varied significantly, but much of it is in the form of generic low-density fiberglass (LDFG) and mineral wool. It appears that many of the newer plants (or plants replacing steam generators) have been replacing RMI insulation on the primary systems with "high-performance" fiberglass. In general, the smaller pipes and steam generators are more likely to be insulated with fiberglass and cal-sil than the reactor pressure vessel or the hot leg or cold leg. Other sources of fibrous materials in the containment for some plants include up to 12,985 ft^2 of filter media on the air-handling units (AHUs) and up to 1500 ft^3 of fibrous insulation (e.g., Kaowool) used as fire barrier materials. Given that (a) very small quantities of fibrous insulation would be necessary to induce large pressure drops across the sump screens (less than 10 ft^3) and (b) most plants have comparatively very large inventories of fibrous insulation, it is not clear that any plant can be screened out from this safety evaluation without the benefit of detailed evaluations.

- Other sources of debris in the PWR containments include cement dust and dirt (either present in the containment *a priori* or generated by a LOCA), particulate insulations used on the fire barriers (e.g., Marinite), failed containment coatings (a median PWR has approximately 650,000 ft^2 of coated surfaces in the containment), and precipitants (zinc and aluminum precipitation by-products).[5] Estimates for this type of debris ranges from 100 lb to several 1000 lb; either of these bounds would result in very large head losses when combined with fibrous material .

Containment Features Affecting Debris Transport

- CS set points typically are defined based on LLOCA and equipment qualification (EQ) considerations. Consequently, sprays may not (automatically) actuate during SLOCAs[6] because peak containment pressures are expected to be lower than for an LLOCA. CS actuation following an SLOCA event plays an important role in the transport of debris to the sump, and at the same time, it affects the timing of sump failure. Set points for CS actuation vary considerably and span a wide range: 2.8 psig to 30 psig. Consistently lower values are observed in sub-atmospheric and ice condenser containment designs, as would be expected. Nevertheless, values at or below 10 psig[7] are observed for several plants, including large dry containments.

1.4 Criteria for Evaluating Sump Failure

The sump failure criterion applicable to each plant is determined primarily by sump submergence. Figure 1-2 illustrates the two basic sump configurations of fully and partially submerged screens. Although only vertical sump configurations are shown here, the same designations are applicable for inclined screen designs. The key distinction between the fully and partially submerged configurations is that partially submerged screens allow equal pressure above both the pit and the pool, which are potentially separated by a debris bed. Fully submerged screens have a complete seal of water between the pump inlet and the containment atmosphere along all water paths passing through the sump screen. The effect of this difference in evaluation of the sump failure criterion is described below.

[4]About 40 PWR units have in excess of 10% of the plant insulation in the form of fiberglass and another 5-10% in the form of cal-sil. A typical plant has approximately 7500 ft^3 of insulation on the primary pipes and supporting systems pipes that are in close proximity to the primary pipes.

[5]PWR DBAs evaluate the potential for precipitation of aluminum and zinc when they are subjected to high-pH, hot, borated water because these chemical reactions generate H_2.

[6]Fan cooler response to LOCAs also plays a vital role in determining spray actuation following SLOCA. These concerns are not applicable to LLOCA or MLOCA, where automatic actuation of sprays is expected in every plant.

[7]The 10-psig set point is important because MELCOR simulations showed that if both fan coolers in a large dry containment are not operating at full capacity, containment pressure could exceed 10 psig for breaks $\geq$ 2 in [LANL, 2001b].

1.4.1 Fully Submerged Sump Screens

Figure 1-2(a) is a schematic of a sump screen that is fully submerged at the time of switchover to ECCS. Sump failure is likely to occur for sumps in this configuration because of cavitation within the pump housing when head loss caused by debris accumulation exceeds the $NPSH_{Margin}$. For this set of plants (in which sump screens are fully submerged at the time of switchover), the onset of cavitation is determined by comparing the plant $NPSH_{Margin}$, as reported by plants responding to NRC Generic Letter (GL) 97-04 [US NRC, 1997] with the screen head loss calculated in the parametric study. Therefore, for this case, the sump failure criterion (ΔH_f) is assumed to be reached when $\Delta H_{screen} \geq NPSH_{Margin.}$

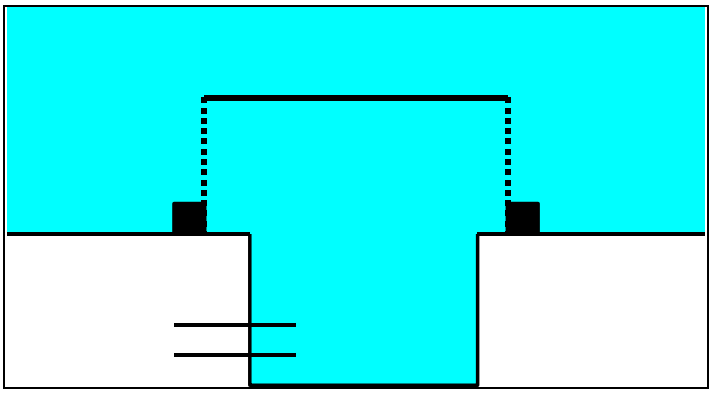

(a) Fully submerged screen configuration showing solid water from pump inlet to containment atmosphere.

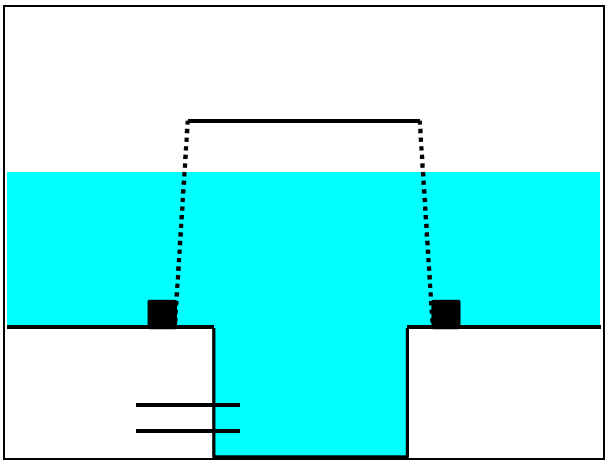

(b) Partially submerged screen configuration showing containment atmosphere over both the external pool and the internal sump pit with water on lower portion of screen.

Fig. 1-2. Sump-Screen Schematics.

1.4.2 Partially Submerged Sump Screens

Figure 1-2(b) is a schematic of a sump that is partially submerged at the time of switchover. Failure can occur for sumps in this configuration in one of two ways: by pump cavitation as explained above or when head loss caused by debris buildup prevents sufficient water from entering the sump. This flow imbalance occurs when water infiltration through a debris bed on the screen can no longer satisfy the volumetric demands of the pump. Because the pit and the pool are at equal atmospheric overpressure, the only force available to move water through a debris bed is the static pressure head in the pool. Numeric simulations confirm that an effective head loss across a debris bed approximately equal to ½ of the pool height is sufficient to prevent adequate water flow. For all partially submerged sump screens, the sump failure criterion (ΔH_f) is assumed to be reached when

$$\Delta H_{screen} \geq \text{NPSH}_{\text{Margin}} \text{ or } \Delta H_{screen} \geq \text{½ of pool height.}$$

After switchover to ECCS recirculation, some plants can change their sump configuration from partially submerged to fully submerged. This can occur for a number of reasons, including accumulation of CS water, continued melting of ice-condenser reservoirs, and continued addition of refueling water storage tank (RWST) inventory to the containment pool. As the pool depth changes during recirculation, the "wetted area" (or submerged area) of the sump screens can also change. The wetted area of the screen determines the average approach velocity of water that may carry debris. Because information about time-dependent pool depths is difficult to obtain and because the most significant debris transport will occur early in the scenario when the pool is shallow, only the pool depth at the time of switchover to the ECCS was used in the parametric evaluations.

1.5 Industry Survey and Other Sources of Information

Based on the findings of the boiling water reactor (BWR) ECCS strainer blockage study, e.g., BWR Utility Resolution Guidance (URG) [BWROG, 1998], review of updated safety analysis reports (UFSARs), and several plant visits, the NRC and LANL identified a set of plant design features (e.g., sump design) and sources of debris (e.g., insulation materials and containment coatings) that were judged to strongly influence debris generation, transport, and accumulation in PWRs. One of the tasks under GSI-191 is to compile a database of insulation, containment, and recirculation sump design and operation information for each of the operating US PWRs.

The NRC (and LANL) formulated a set of questions that captured some of the information needs and forwarded them to the industry groups formally organized by Nuclear Energy Institute (NEI). The licensee response to these survey questions was voluntary and consisted of written responses and engineering drawings (as deemed necessary by the individual licensees). This information is contained in the NEI database *Results of Industry Survey on PWR Design and Operations* [NEI, 1997]. LANL performed a thorough review of the industry responses to draw inferences regarding the plant designs and features that affect the generation, transport, and accumulation of debris on the sump screen. From this data base, LANL also compiled the most up-to-date information on insulations, other sources of debris, and containment and sump configurations at each of the operating PWRs. This database is the primary source of information for the parametric evaluations described here [LANL, 2001a]. This information was supplemented, as necessary, using two sources of additional information.

1. PWR licensee responses to Generic Letter 97-04, "Assurance of Sufficient Net Positive Suction Head for Emergency Core Cooling and Containment Heat Removal Pumps" [US NRC, 1997]. These provide the $\text{NPSH}_{\text{Margin}}$ and licensing-basis ECCS flow rate for each plant following a postulated LLOCA.

2. PWR UFSARs, individual plant examination (IPE) submittals, and emergency operating procedures (EOPs) for selected plants. These provided information regarding plant accident progression and the basis for recirculation sump flow rates following a SLOCA.

1.6 Integration of Parametric Calculations with Ongoing GSI-191 Research

The parametric analysis documented in this report took advantage of the following aspects of the ongoing GSI-191 research program.

Preliminary results from ongoing debris generation testing [LANL, 2001e] were used to define the zone of influence (ZOI)[8] for fiberglass and cal-sil insulations in this parametric study. The preliminary findings suggest that two-phase jets with a stagnation pressure of approximately 1400 psia (290°C and 20-s blowdown duration)[9] can inflict significant damage at distances much farther away than those measured either in USI A-43 studies or the BWR air-jet impact test (AJIT) program. Further testing is under way to collect similar test data for other insulations (other than fiberglass and cal-sil) and to examine the effect of larger nozzle sizes and longer blowdown duration on insulation damage.

Results from the ongoing transport testing program [LANL, 2001c; LANL, 2001d] played a key role in determining the containment transport fractions and thus the quantity of insulation expected to reach the sump. Given the preliminary nature of the results coupled with the fact that computational fluid dynamics (CFD) simulations of the parametric plant containment floors is lacking, the experimental results were used to deduce "favorable" and "unfavorable" estimates rather than best estimates. A set of transport tests using a three-dimensional tank facility were conducted to specifically obtain transport data that can be used to define "favorable" and "unfavorable" bounds.

The results from head-loss modeling activities were used to estimate the head-loss effects of debris accumulation on the sump. The primary basis for head-loss models is a BWR study [Zigler, 1995] that provided a semi-theoretical model for head-loss estimation. This correlation is known to under-predict head loss for cal-sil beds for which head-loss data were not measured in the NRC test apparatus (these experiments are currently in progress). Once again, the head-loss model was used to deduce "favorable" and "unfavorable" estimates for cal-sil contribution.

A set of tests was specifically designed and carried out in support of this parametric study [LANL, 2001d]. These tests examined the ability of small fiberglass insulation shreds and loosely attached fibers to build a contiguous and uniform debris bed on the simulated sump screens with openings of 1/4 in. and 1/8 in., respectively. These tests confirmed that at a "nominal" or "theoretical" thickness of approximately 1/10-in. fiberglass beds can be built on a vertical sump screen and that the beds can start to filter out cal-sil passing through them. In addition, these tests confirmed that cal-sil insulation can form debris beds by itself even without presence of fiberglass.

It also should be noted that this parametric study took full advantage of (a) containment and RCS analytical models developed as part of GSI-191 (see Sec. 2 and [LANL, 2001b]) and (b) a debris generation CAD model, also built to support the GSI-191 study (see Sec. 3).

Finally, the study results were provided to both LANL and NRC PRA analysts for use in their determination of the risk significance of GSI-191 to US PWRs. The PRA studies benefited significantly from the thermal-hydraulics simulations described in the following sections.

---

[8] The ZOI is defined as the zone within which the break jet would have sufficient energy to generate debris of transportable size and form.

[9] These conditions are significantly less severe than those expected in a PWR (2250 psia and 300°C).

2.0 DESCRIPTION OF POSTULATED ACCIDENTS

2.1 Overview

This section presents the results of thermal-hydraulic simulations performed to achieve the following objectives.

1. Identify important RCS and containment thermal-hydraulic parameters that influence the generation and/or transport of debris in PWR containments.

2. Perform plant simulations using NRC-approved computer codes to the determine the value of each parameter as function of time and, where applicable, as a function of the assumed system's response. Of particular interest are plant simulations of small and medium LOCAs for which information regarding accident progression is not readily available.

3. Use the calculated plant response information to construct accident progression sequences that form the basis for strainer blockage evaluations and probabilistic risk evaluations.

Originally, evaluations were made for seven accident scenarios: (1) LLOCA (cold- and hot-leg breaks), (2) MLOCA (6-in. cold leg), (3) SLOCA (2-in. cold leg), (4) small-small LOCA (1/4-in. cold leg), (5) pressurizer surge line break, (6) loss of offsite power with simultaneous failure of feedwater, and (7) false lifting and stuck-open power-operated relief valve (PORV).

Figure 2-1 shows the major steps involved in the calculational effort. These include the following.

- RELAP5/MOD3.2 [Lockheed, 1995] was used for simulating the RCS response to each of the postulated accident sequences. The RELAP5 simulations incorporated realistic initial and boundary conditions and a full representation of a Westinghouse four-loop RCS design. Selected simulations were also performed for Combustion Engineering (CE) plants. No RELAP simulations were performed for Babcock and Wilcox (B&W) plants. Information regarding B&W plants was obtained primarily from their IPEs.

- MELCOR Version 1.8.2 [Summers, 1994] was used for simulating the response of the ice condenser containment, large dry containment, and sub-atmospheric containment to a release of steam/water into the containment as a result of each accident sequence (as predicted by RELAP5).

The parameters tracked for each code simulation are shown in Fig. 2-1. These parameters were limited to those that could influence debris generation and transport following a LOCA. A brief description of each of the important parameters and their potential effect is provided in Table 2-1.

Brief discussions of the simulation results are provided in Secs. 2.2 through 2.4 for an LLOCA, an MLOCA, and an SLOCA, respectively. An examination of the data summarized in these sections reveals that accident progression differs markedly with event type and containment type. The important differences are as follows.

Table 2-1. Important Parameters Tracked and Their Relevance to the Study.

RCS PRESSURE AND TEMPERATURE: The flow through an RCS breach would be choked as long as the RCS temperature (and hence pressure) remain elevated. The critical (choked) flow rate through the breach would depend strongly on upstream pressure and temperature, which define the thermodynamic state of the fluid. The state of the fluid largely determines the expansion characteristics of a two-phase flashing jet as evident from Ref. 5.
BREACH FLOW CONDITIONS (FLOW RATE, VELOCITY, AND QUALITY): The destructive potential of a break jet depends strongly on break flow conditions. The velocities of both phases (liquid and vapor) are important here. The values calculated are the velocities at the choke plane. The moisture content of the fluid exiting the breach influences the damage potential of the jet. The quantity calculated here is the ratio of vapor mass flow rate to total mass flow rate at the choke plane.
ECCS SAFETY INJECTION FLOW: The rates of ECCS safety injection determine when the inventory of the RWST would be depleted, requiring switchover to ECCS recirculation through the emergency sump. The timing of switchover is important with regard to debris settling opportunities. Flow patterns in the water pool formed on the floor of containment would be influenced by injection rates. Injection rates determine accident progression as related to the rate at which the RCS is cooled down.
ECCS RECIRCULATION FLOW: The rate at which flow is recirculated through the emergency sump will determine the flow patterns, velocities, and turbulence levels in the containment pool. The potential for debris transport is governed by these traits.
CONTAINMENT SPRAY FLOW: Containment sprays have the potential to wash settled debris from containment structures and suspended debris from the containment atmosphere down to the containment pool. Whether the sprays are operating or not largely determines the time at which the RWST inventory is expended and the magnitude of the recirculation flow through the emergency sump. The flow patterns and turbulence levels in the containment pool may be affected by where and how the sprays drain. The potential for containment sprays to influence debris transport is thought to be considerable. As such, it is important to note the large variability in spray activation logic that exists from plant to plant, e.g., containment high-high pressure set points. Additionally, actions taken by the operators to shut containment sprays down would influence debris transport.
CONTAINMENT SPRAY TEMPERATURE: In some plants, recirculated spray water passes through heat exchangers. The heat removal would influence containment pressure and temperature trends. This phenomenon is of particular interest in ice-condenser containments. Therefore, special emphasis was put on modeling residual heat removal (RHR) heat exchangers and determining spray temperatures as close to reality as possible.
POOL DEPTH AND TEMPERATURE: The available NPSH at the recirculation pumps depends on the depth of the containment pool and its temperature. The velocities, flow patterns, and turbulence levels (and hence debris transport potential) in the pool depend on pool depth.
POOL PH: Basic or acidic tendencies in recirculating water may change the corrosion, dissolution, or precipitation characteristics of metal or degraded metal-based paints in containment. A specific concern is the possible precipitation of ZnOH formed from chemical interaction between zinc (in the zinc-based paints) and water at high temperature. The dissolution/precipitation of ZnOH in water is influenced by the degree of boration.
CONTAINMENT ATMOSPHERIC VELOCITY: The atmospheric velocities generated in the containment in response to an RCS breach determine to what degree generated debris initially disperses within the containment. These are the velocities developed as containment is subjected to the shock and pressurizing effects of the flashing break jet.
PAINT TEMPERATURE: Sustained elevated temperatures may degrade containment paints. An elaborate paint representation model was included in the MELCOR input model.

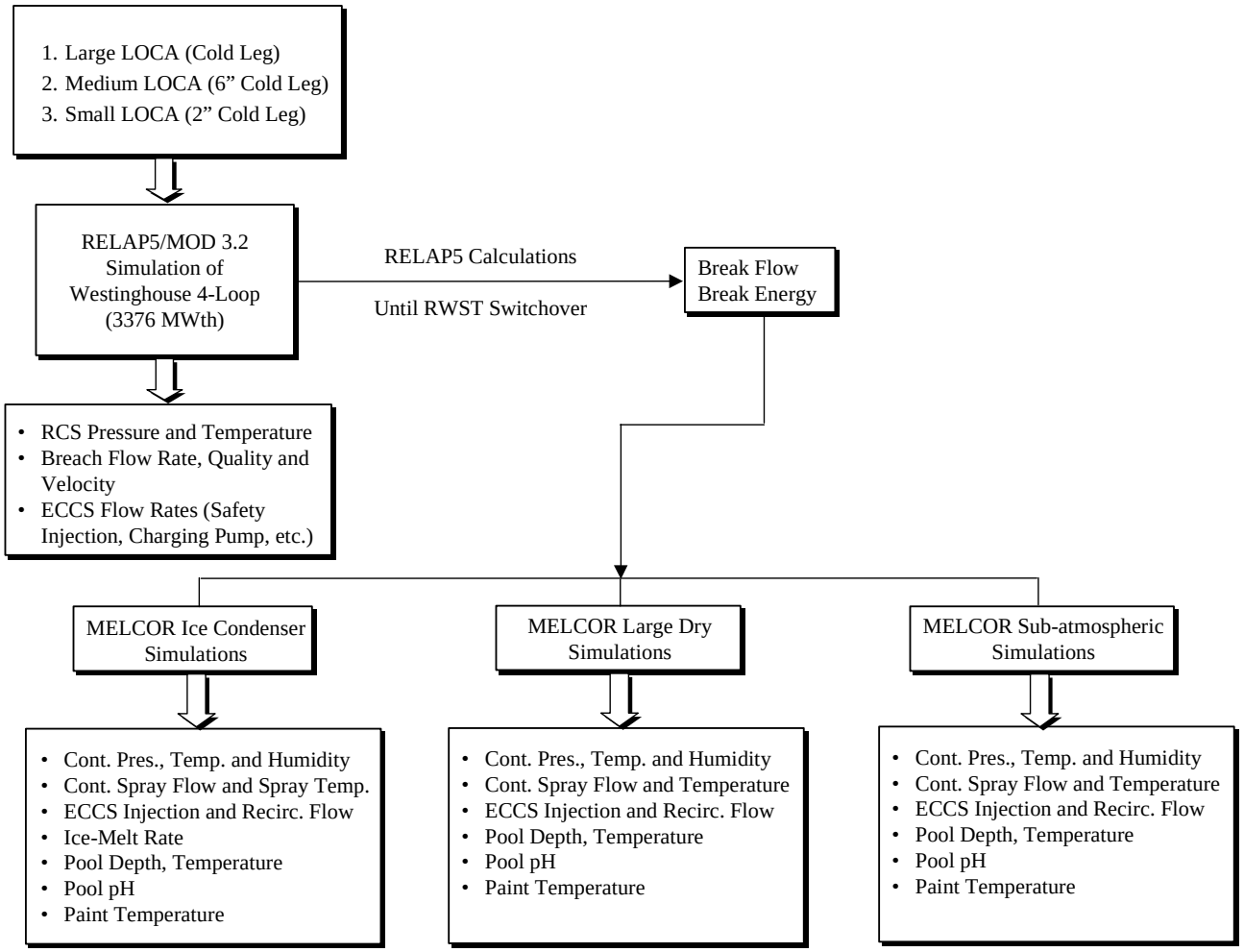

Fig. 2-1. Flow Chart of Analysis Process.

1. *Time at which blowdown commences and the duration over which blowdown occurs varies considerably with accident type*. In one extreme, the RCS blowdown following an LLOCA commences immediately and terminates within 30 s. The stagnation pressure at the break plane over that time period varies between 2000 and 300 psia. On the other extreme, blowdown following the SLOCA occurs over the first hour of the transient; even after 1 h, it is possible that the pressure vessel remains at pressures as high as 500 psi. Debris generation estimates must account for these differences, especially for those insulations for which generation is driven by erosion. It is possible that a small-break ZOI may be characterized by a larger L/D compared with large or medium breaks.[10]

2. *The magnitude of the ECCS recirculation flow through the emergency sump varies between events.* In the case of an SLOCA, the maximum ECCS flow through the sump during recirculation corresponds to the make-up flow for the high-presure spray injection (HPSI) and charging pump discharge into the RCS (at about 500 psi) and subsequently leaking into the containment through the breach. On the other hand, following a LLOCA or a MLOCA, the maximum ECCS flow approaches the design flow (which is approximately 11,000 gpm for the cases simulated). The implication is that the potential for debris transport would be higher following an LLOCA than for the SLOCA analyzed. The plant-specific estimates for ECCS recirculation flow for each case can be obtained as follows.

    - A generic value of 10,000 gpm (large break) could be used for most plants, or alternately, the plant response to NRC Generic Letter (GL) 97-04 [US NRC, 1997] may be used.

    - A generic value of 2500 gpm (small break) could be used for most plants. A survey of plant data suggests that actual ECCS flow following a SLOCA could vary between 1800 gpm and 4800 gpm, with a median value of 2500 gpm [LANL, 2001a].

3. *CS actuation is accident- and plant-specific.* In an accident where containment fan coolers sufficiently managed containment pressure and temperature to below the engineered safeguard feature (ESF) actuation set point, sprays would not actuate. If the sprays were not used or were used only sparingly, the length of time that ECCS injection could draw from the RWST would be largely increased. This also would minimize the potential for debris washdown by the cascading spray water. Note that for SLOCA events, sprays were not required for large dry containments whose actuation set points are higher than 10 psi, thereby limiting the maximum flow expected through the sump. Sprays were required for the ice condenser containment, resulting in sump flow rates nearly four times that required for the large dry plants. Sprays are also required for many large dry plants (including but not limited to sub-atmospheric containment) whose actuation set points are equal to or lower than 10 psi[11]. This is because of the following.

    - In several plants, the chilled water supply to the fan coolers is isolated following the LOCA, which reduces the efficiency of the fan coolers for removing containment heat. [The ultimate heat sink is the component cooling water (CCW), which may not be sufficiently sized to handle such heat loads.]

[10]The ZOI is defined as the zone within which the break jet would have sufficient energy to generate debris of transportable size and form. L/D (read 'ell over dee') is a unitless measure of the size of the ZOI, where L is the maximum linear distance from the location of the break to the outer boundary of the ZOI and D is the diameter of the broken pipe.

[11]A SLOCA simulation was performed assuming fan coolers were not operational. Maximum containment pressure for this calculation was estimated to be approximately 18 psi, as opposed to 5 psi (See Table 2-7) for the case where fan coolers are assumed to operate [LANL, 2001b].

- Degradations in fan coolers may also be possible if LOCA debris reaches or deposits on the fan cooler heat exchangers.

- Fan coolers are not safety-class equipment in most PWRs. It is not clear that fan coolers can be relied on for pressure control for a variety of reasons ranging from the fact that their functionality is not tested for these conditions to the fact that the heat removal source for fan coolers may be isolated as a result of a hi-hi or hi containment pressure set point (differs from containment to containment).

The plant estimates for CS recirculation flow for each plant can be obtained as follows.

- A generic value of 6000 gpm can be used for most PWRs or alternatively one can use appropriate flow rates applicable to each plant. Individual plant flow is generally not significantly different, and thus will not influence the accident outcome.

2.2 Large Loss-of-Coolant Accident

The LLOCA simulated was a cold-leg, pump-discharge, double-ended guillotine break (DEGB). The RCS pressure and average temperature before the break were 2250 psia and 570°F. The cold-leg inside diameter was 27.5 in., corresponding to a cross-section area of 4.12 ft^2. The break was assumed to be instantaneous with a discharge coefficient of unity. A cold-leg break was chosen as the LLOCA event because design-basis accidents typically are cold-leg breaks. With respect to debris generation and transport, any differences between a cold-leg and hot-leg break likely would be small. This is not the case for core response, but with respect to emergency sump blockage, differences between large hot-leg and large cold-leg breaks are probably negligible. This assumption is supported by the results (not presented here) of a supplementary RELAP5 large-hot-leg-break calculation that compares closely with the results of the large-cold-leg-break calculation with respect to break flow characteristics.

The calculated results for the LLOCA events in large dry and ice condenser containments are provided in Tables 2-2 and 2-3, respectively.[12] These simulations were used to develop a generic description of LLOCA accident progression in a PWR, both in terms of the system's response and its implications on debris generation and transport. Table 2-4 provides a general chronology of events for a PWR LLOCA sequence. Figure 2-2 summarizes key findings to supplement the tabulated results, with further explanation as follows.

2.2.1 RCS Blowdown

In this report, the RCS blowdown refers to the event (or process) by which elevated energy in the RCS inventory is vented to containment as the RCS vents through the breach. Blowdown and the subsequent flashing[13] in containment causes rapid decay in the RCS pressure and rapid buildup of containment pressure. Either of these initiates reactor scram,[14] and with delay built-in, it is expected that reactor scram would occur within the first 2 s. It is during RCS blowdown that flow from the break occurs and the highest (and most destructive) energy is released. Therefore, debris generation by jet impingement would be greatest during this time. Also, debris could be displaced from the vicinity of the break as the flashing two-phase break jet expands into the containment. Large atmospheric velocities

[12]Large dry containment LLOCA results are representative of those expected for sub-atmospheric containments as well, with the exception that inside recirculation pump flow for the sub-atmospheric containment would have to be added.

[13]Flashing refers to the phenomenon by which the mainly liquid inventory of the RCS turns into a steam and liquid mixture as it is expelled into the containment atmosphere, which is at a significantly lower pressure.

[14]The accident progression in sequences in which scram does not occur is significantly different and will not be discussed in this document.

may develop in the containment (approaching 200 ft/s in the ice condenser containment and 300 ft/s in the large dry containment) as breach effluent quickly expands to all regions of the containment. In the vicinity of the breach, containment structures would be drenched by water flowing from the breach. Increase in containment pressure also causes immediate automatic actuation of containment sprays (for all plant types), condensing steam and washing structures throughout containment. Spray water drains over and down containment walls and equipment, carrying both insulation and particulate (e.g., dirt and dust) debris to a growing water pool on the containment floor. In most containments, NaOH liquid stored in the spray additive tank (SAT) will be added to the borated water to facilitate absorption of iodine that may be released to the containment. Therefore, a secondary CS effect is a potential increase in pool pH, which in turn, could play a role in particulate debris precipitation caused by the interaction of hot, borated, high-pH water with zinc and aluminum surfaces. The rates of these reactions are used in many FSARs to estimate the hydrogen source term and evaluate the potential for hydrogen accumulation in the containment.

Accurate characterizations of conditions that exist during the blowdown phase are important for estimating debris generation and, to some degree, debris transport. For LLOCA events, RCS blowdown occurs over a period of approximately 30 s, during which vessel pressure goes from 2250 psia to near atmospheric pressure. During this time, the reactor pressure vessel thermodynamic conditions undergo a rapid change. Initially, the break flow is subcooled at the break plane and flashes as it expands into the containment. Within 2 s, the vessel pressure drops below 2000 psi and the flow in the pipes and the vessel becomes saturated. Thereafter, the break flow quality is equal to or higher than 10%. On the other hand, the void fraction increases to approximately 1.0, clearly indicating that the water content would be dispersed in the vapor continuum in the form of small droplets. The corresponding flow velocity at the break plane reaches a maximum of about 930 ft/s. This clearly indicates that jets would reach supersonic conditions during their expansion upon exiting the break. Based on these simulations, the energetic blowdown terminates within 25-30 s as the vessel pressure decreases to near 150 psig. Although steam at high velocities continues to exit, the stagnation pressure is not sufficient to induce very high pressures at distances far from the break. Thus, it is reasonable to assume that debris generation following a LLOCA occurs within the first minute. (Note: Debris generation by non-jet-related phenomena may occur over a prolonged period of time as a result of high temperature and corrosion.) The RCS blowdown continues until the vessel pressure falls below the shut-off head for the accumulator tank,[15] the HPSI, and the LPSI. This causes increasingly large quantities of cooler, borated RWST water to quench the core and terminate blowdown.

2.2.2 ECCS Injection Phase

The injection phase refers to the period during which the RCS relies on safety injection, drawing on the RWST for decay heat removal. In the case of LLOCA, the injection phase immediately succeeds the initial RCS blowdown. During this phase, core reflood is accomplished and quasi-steady conditions are arrived at in the reactor, where decay heat is removed continually by injection flow. In ice condenser containments, the ice condenser compartment doors open and the recirculation fans move the containment atmosphere through the ice condensers. Opportunities would exist for debris to settle in the pool during this relatively quiescent time before ECCS recirculation. Containment pressure would largely decrease from its maximum value (reached in the blowdown phase). The injection phase is considered to be over when the RWST inventory is expended and switchover to sump recirculation is initiated.

Accurate characterization of conditions that exist during injection phase may be important for estimating the quantity of debris transported from the upper containment to the pool and for estimating the quantity of debris that may remain in suspension. Following the initial break, safety injection (SI) begins immediately because of the combined operation of the accumulators, the charging pump, the

[15]The accumulators are also known as safety injection tanks in some designs.

HPSI pumps, and the low-pressure safety injection (LPSI) (RHR) pumps. The SI flow approaches the design value (which is 11,500 gpm in the plant simulated) in about a minute and continues at that rate until switchover. Current simulations did not take credit for potential reduction in the injection flow (e.g., system-failure scenarios). Containment sprays continue to operate; spray water and water exiting the break will cause washdown of debris from the upper portions of the containment to the pool on the containment floor.

In conclusion, it has been determined that large quantities of water would be introduced into the containment within a few minutes following a LLOCA. As a result, the water pool depth on the containment floor increases steadily. In the case of a large dry containment, the peak pool height is reached at the end of the injection phase; in an ice-condenser containment, the peak value is reached several hours into the accident after all the ice has melted.

2.2.3 Recirculation Phase

After the RWST inventory is expended, the ECCS pumps would be realigned to take suction from the emergency sump in the containment floor. This would begin the ECCS recirculation phase, in which water would be pulled from the containment pool, passed through heat exchangers, and delivered to the RCS, where it would pick up decay heat from the reactor core, flow out the breach, and return to the containment pool. Pool depth would reach a steady state during the recirculation phase, and containment pressure and temperature would be gradually decreasing. It would be during this accident phase that the potential would exist for debris resulting from an RCS breach (or residing in containment beforehand) to continue to be transported to the containment emergency sump. Because of the suction from the sump, this pool debris may accumulate on the sump screens, restrict flow, and either reduce available NPSH or starve the ECCS recirculation pumps.

The primary observation regarding the RCS and containment conditions during the recirculation phase is that the sump flow rate reaches the design capacity of all the pumps (which in the plants analyzed is 17,500 gpm for the large dry and sub-atmospheric containments and 18,000 gpm for the ice condenser containment).

2.3 Medium Loss-of-Coolant Accident

The MLOCA simulated was a 6-in.-diam (0.1963-ft^2) circular hole in a cold leg downstream of the reactor coolant pump (RCP). The hole became full-sized instantaneously. It was situated on the side of the cold leg and centered halfway up. A discharge coefficient of unity was used, which made these simulations very conservative. The cold-leg location of the hole was chosen arbitrarily and is not expected to be a determining factor in the simulation results.

The calculated results for the MLOCA events in large dry and ice condenser containments are provided in Tables 2-5 and 2-6, respectively. Figure 2-3 presents the time scales associated with the occurrence of some of the events. The following sections highlight the differences between the MLOCA event and the LLOCA event described above.

2.3.1 RCS Blowdown

In the case of an MLOCA, RCS blowdown occurs over a prolonged period (3 min) compared with the that in an LLOCA. Blowdown starts at 0 s when the vessel is at 2250 psia and terminates as the RCS pressure and liquid subcooling decrease. Peak break flow for the MLOCA is at least a factor of 15 less than that observed for the LLOCA. In addition, the resulting vapor velocity in the containment peaks around 30 ft/s, as opposed to 200-300 ft/s for the LLOCA. These observations suggest less severe debris generation and transport caused by the LOCA jet itself. Another significant observation is that after

MLOCAs, the exit flow at the break plane remains subcooled throughout the blowdown (at least until the vessel pressure falls to a point where blowdown would have little effect on debris generation). This may affect the ZOI over which debris would be generated.

2.3.2 ECCS Injection Phase

The fundamental differences between an MLOCA and an LLOCA are as follows.

- ECCS injection begins before termination of the RCS blowdown. Initiation of injection occurs after 20-60 s, whereas the blowdown phase is not terminated until approximately 180 s.
- The LPSI does not inject significant quantities of water into the core in the short term. The LPSI (or RHR) pumps start injecting into the core at about 15 min.
- In the plants analyzed, spray actuation occurs shortly after ECCS injection begins (approximately 3 min, right around the termination of the RCS blowdown).

2.3.3 Recirculation phase

The recirculation phase accident characteristics for the MLOCA are similar to those described in Sec. 2.2.3 for the LLOCA. The sump recirculation flow rate for each plant analyzed was approximately half of that for the LLOCA simulation. No further observations are made for the MLOCA.

2.4 Small Loss-of-Coolant Accident

The SLOCA studied was a 2-in.-diam (0.0218-ft^2) circular hole in a cold leg downstream of the RCP.[16] The hole became full-sized instantaneously. It was situated on the side of the cold leg and centered halfway up. A conservative discharge coefficient of unity was defined. The cold-leg location of the hole was chosen arbitrarily and is not expected to be a determining factor in the simulation results. The 2-in. specification of this hole was made with the expectation that RCS pressure would stabilize above the accumulator pressure such that the accumulators would not inject.

The calculated results for the SLOCA events in large dry, ice condenser, and sub-atmospheric containments are provided in Tables 2-7 through 2-9, respectively. Figure 2-4 the presents time scales associated with the occurrence of some of the events.

2.4.1 RCS Blowdown

RCS blowdown in the case of an SLOCA occurs over a prolonged period (60 min). Blowdown starts at 0 s when the vessel is at 2000 psia and terminates mainly as the RCS pressure and liquid subcooling decrease. Peak break flow velocities for the SLOCAs are a factor of 30 less than those for the LLOCA and a factor of 2 less than those for the MLOCA. Containment atmosphere velocities are a factor of 30-60 less than those for the LLOCA and a factor of 2 less than those for the MLOCA. Another significant observation is that following SLOCAs, the exit flow at the break plane remains subcooled throughout the blowdown (at least until the vessel pressure falls to a point where blowdown would have little effect on debris generation). This may affect the ZOI over which debris would be generated.

[16]The study also simulated a 1.75-in. break. The results were found to be very similar to the 2-in. break.

2.4.2 ECCS Injection Phase

The fundamental differences between a SLOCA and a LLOCA are as follows.

- The LPSI does not inject into the core at all; the HPSI and charging pumps are sufficient to make up for lost inventory.
- Actuation of containment sprays is highly plant specific and may not be needed at all. In the large dry containment plant analyzed (which has a CS actuation set point of 9.5 psig), spray operation is not required[17]. Spray actuation is seen after 30 min in the ice condenser simulation and after 15 min in the sub-atmospheric plant. Even then, the operator may terminate sprays during the SLOCA event to prolong RWST availability and rely on fan coolers (or the ice condenser) for decay heat removal from the containment. Note that washdown of debris from the upper containment to the floor pool may be limited to more localized areas (near the break) for plants in which containment sprays are not required.

2.4.3 Recirculation Phase

The recirculation phase accident characteristics for the SLOCA are similar to those described in Sec. 2.2.3 for the LLOCA. The primary difference is that the required flow rates for the SLOCA are significantly less than those for the LLOCA (as low as 2500 gpm for plants in which containment sprays do not actuate).

[17] Again, the results presented herein are for an accident scenario in which fan coolers operate. Other calculations suggest a peak containment pressure during a SLOCA in a large-dry containment could reach values nearing 18 psig if fan coolers fail to operate [LANL, 2001b].

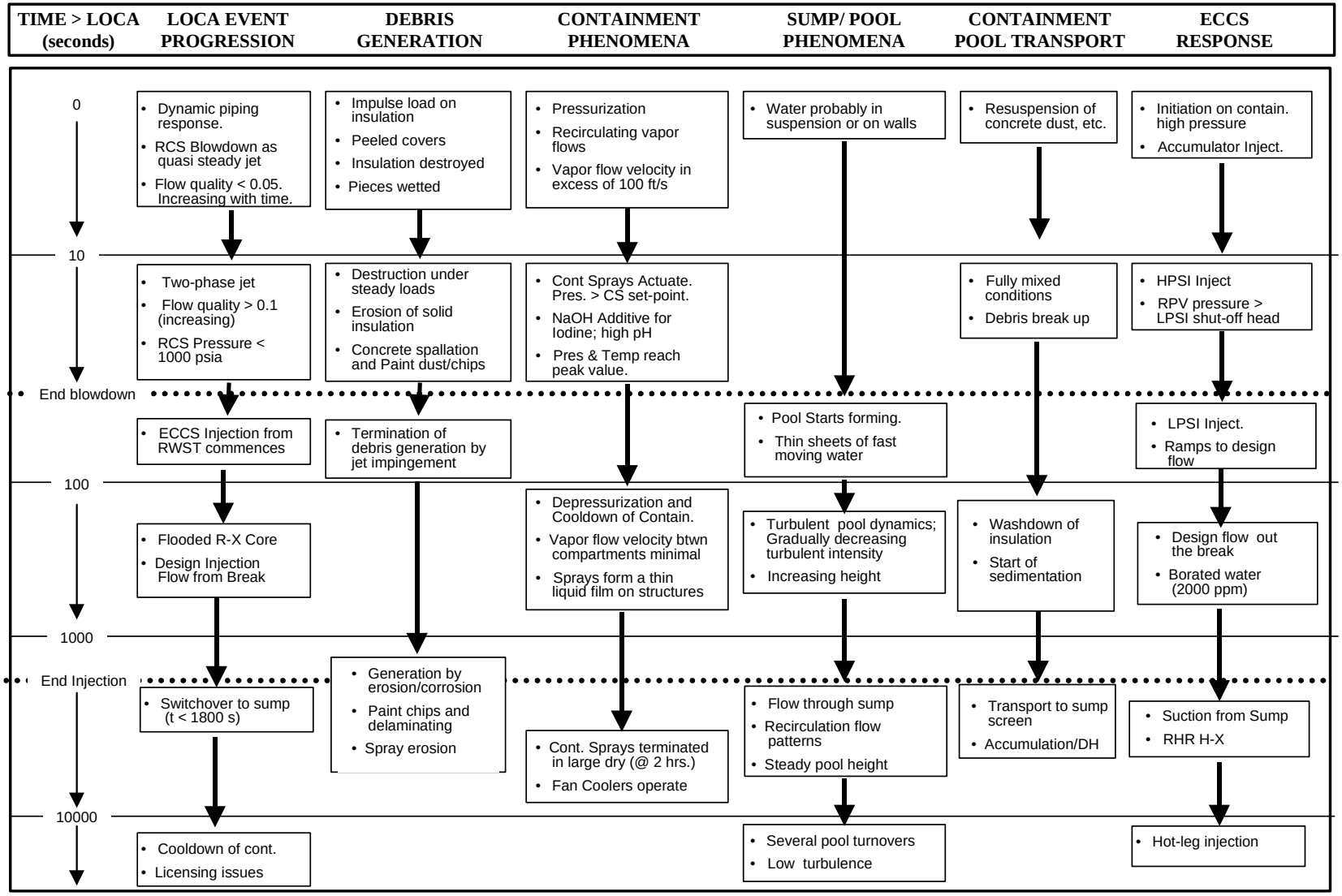

Fig. 2-2. PWR LLOCA Accident Progression in a Large Dry Containment.

Table 2-2. Debris Generation and Transport Parameters: LLOCA—Large Dry Containment.

Parameter	Blowdown Phase			Injection Phase			Recirculation Phase		
	0+	20 s	45 s	45 s	15 min	27 min	27 min	2 h	24 h
RCS pressure at break (psia)	2250	393	55						
RCS temperature at break (°F)	531	291	250	250	173	144	144		
Break flow (lb/s)	7.97e4	1.28e4	4.89e3						
Break flow velocity (ft/s)	296	930	100						
Break flow quality	0	0.25	0.3	0.3	0				
Safety injection (gpm)				11500	11500	11500			
Recirculation flow (gpm)							17500	11800	11800
Spray flow (gpm)				0	5700	5700	5700	0	
Spray temperature (°F)					105	190	190		
Containment pressure (psig)	0	36	33	33	11.5	7	7	1.5	0
Containment temperature (°F)	110	305	250	250	190	163	163	115	95
Pool depth (ft)					2	3.5	3.5	3.5	3.5
Pool temperature (°F)					212	187	187	125	100
Pool pH									
Containment atmosphere velocity (ft/s)	282		7						
Containment relative humidity (%)	50	100	100	100	100	90	90	100	100
Paint temperature (°F)	100			215	240	220	220	145	112

Peak break flow: 7.97e4 lb/s at 0+ s
Quality at peak break flow: 0
Peak containment pressure: 36 psig at 20 s

Peak break flow velocity: 930 ft/s at 21 s
Quality at peak break flow velocity: 0.25
Peak containment atmosphere velocity: 282 ft/s at 0+ s

Table 2-3. Debris Generation and Transport Parameters: LLOCA—Ice Condenser Containment.

Parameter	Blowdown Phase			Injection Phase			Recirculation Phase		
	0+	20 s	45 s	45 s	10 min	17 min	17 min	2 h	24 h
RCS pressure at break (psia)	2250	393	55						
RCS temperature at break (°F)	531	291	250	250	200	160	160		
Break flow (lb/s)	7.97e4	1.28e4	4.89e3						
Break flow velocity (ft/s)	296	930	100						
Break flow quality	0	0.25	0.3	0.3	0				
Safety injection (gpm)				11500	11500	11500			
Recirculation flow (gpm)							18000	18000	18000
Spray flow (gpm)				6400	6400	6400	6400	6400	6400
Spray temperature (°F)				105	105	97	97	95	89
Containment pressure (psig)	0+	14	10.1	10.1	4.5	4.5	4.5	3	2
Containment temperature (°F)	100	168	160	160	103	105	105	98	100
Pool depth (ft)				4	8.5	10.75	10.75	10.8	10.1
Pool temperature (°F)				180	157	159	159	148	126
Pool pH									
Containment atmosphere velocity (ft/s)	184	18	1						
Containment relative humidity (%)	0	50	100	100	80	96	96	97	98
Paint temperature (°F)	100	106	112	112	113	112	112	90	90

Peak break flow: 7.97e4 lb/s at 0+ s
Quality at peak break flow: 0
Peak containment pressure: 14.4 psig at 15 s

Peak break flow velocity: 930 ft/s at 21 s
Quality at peak break flow velocity: 0.25
Peak containment atmosphere velocity: 184 ft/s at 0+ s

Table 2-4. PWR LLOCA Sequences

Time after LOCA (s)	Accum. (SI Tanks)	HPSI	LPSI	CS	Comments
0-1	Reactor scram. Initially high containment pressure. Followed by low pressure in the pressurizer. Debris generation commences caused by the initial pressure wave, followed by jet impingement. The blowdown flow rate is large. But mostly saturated water. Quality $\leq$0.05. Saturated jet-models are appropriate. SNL/ANSI Models suggest wider jets, but pressures decay rapidly with distance				
2		Initiation signal	Initiation signal	Initiation signal	Initiation signal from low pressurizer pressure or high containment pressure/temp
5	Accumulator injection begins	Pumps start to inject into vessel (bypass flow out)	Pumps start (RCS P > pump dead head)	Pump start and sprays on	In cold-leg break, ECCS bypass is caused by counter-current injection in the downcomer. Hot-leg does not have this problem.
10	The blowdown flow rate decreases steadily from ≈20,000 lb/s to 5000 lb/s. Cold-leg pressure falls considerably to about 1000 psia. At the same time, effluent quality increases from 0.1 to 0.5 (especially that from steam generator side of the break). Flow is vapor continuum with water droplets suspended in it. Saturated water or steam jet-models are appropriate. At these conditions, SNL/ANSI models show that jet expansion induces high pressures far from the break location.				
25		End of bypass; HPSI injection			
25-30	Break velocity reaches a maximum > 1000 ft/s. Quality in excess of 0.6. Steam flow at less than 500 lb/s. Highly energetic blowdown is probably complete. However, blowdown continues as residual steam continues to be vented.				
35	Accumulators empty		Vessel LPSI ramps to design flow.		
40	Blowdown is terminated, and therefore, debris generation is complete. Blowdown pressure at the nozzle less than 150 psi. Debris would be distributed throughout the containment. Pool is somewhat turbulent. Height < 1 ft.				
55-200	Reflood and quenching of the fuel rods (T_{max} ~ 1036 °F). In cold-leg break, quenching occurs between 125 and 150 s. In the case of hot-leg break, quenching occurs between 45 and 60 s (T_{max} ~ 950 °F).				
200-1200	Debris added to lower containment pool by spray washdown drainage and break washdown. The containment floor keeps filling. No directionality to the flow. Heavy debris may settle down.				
1200	RWST low level indication received by the operator. Operator prepares to turn on ECCS in sump recirculation mode. Actual switchover when the RWST low-low level signal is received.				
1500		Switch suction to sump	Switch suction to sump	Terminate or to sump	Many plants have containment fan coolers for long-term cooling.
1500-18000	Debris may be brought to the sump screen. Buildup of debris on the sump screen may cause excessive head loss. Containment sprays may be terminated in large dry containments at the 2-h mark.				
>36000		Switch to hot-leg recirculation.	Switch to hot-leg recirculation		

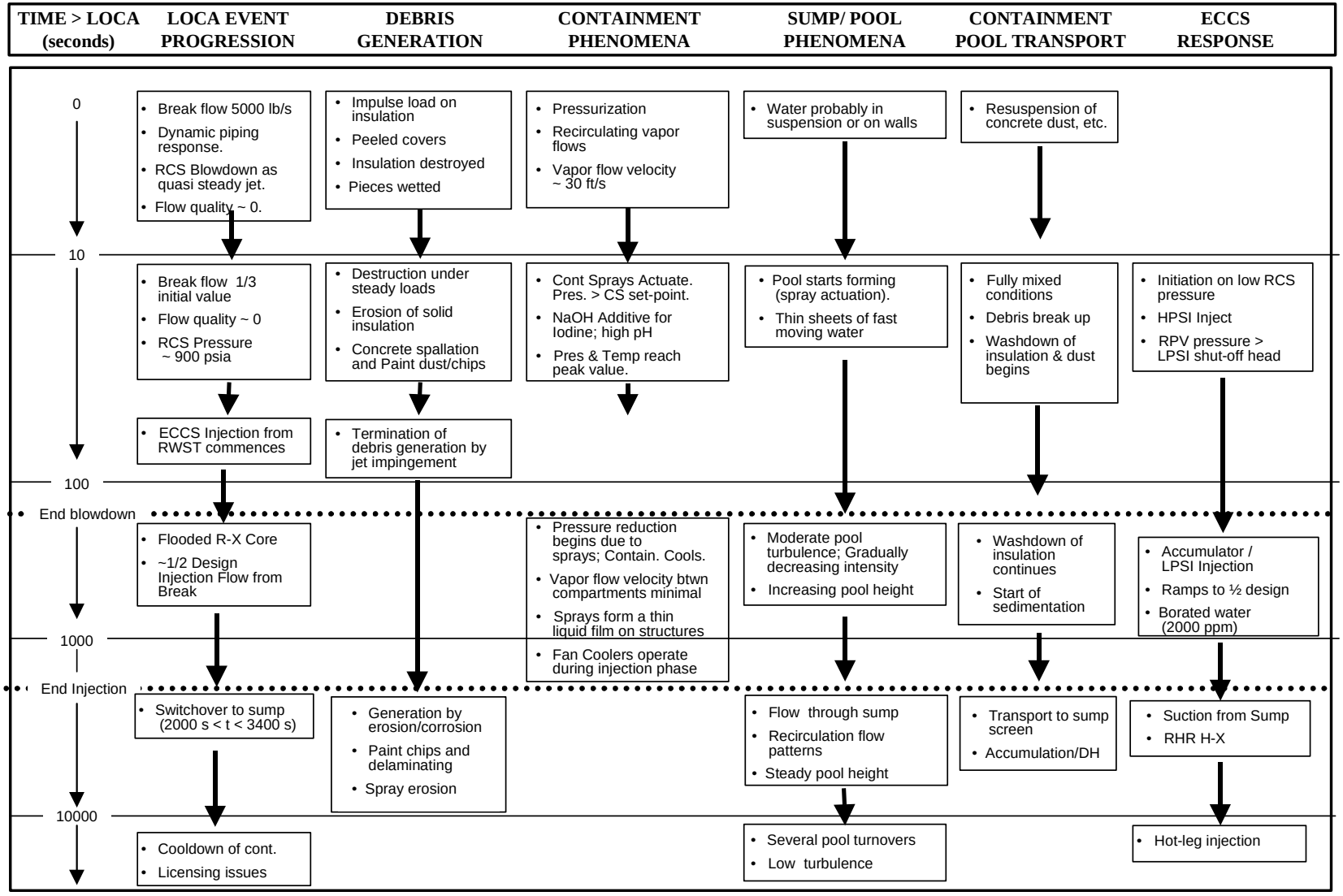

Fig. 2-3. PWR MLOCA Accident Progression in a Large Dry Containment.

Table 2-5. Debris Generation and Transport Parameters: MLOCA—Large Dry Containment.

Parameter	Blowdown Phase			Injection Phase			Recirculation Phase		
	0+	30 s	180 s	20 s	15 min	57 min	57 min	2 h	24 h
RCS pressure at break (psia)	2250	900	508						
RCS temperature at break (°F)	537	521	392		330	274	274		
Break flow (lb/s)	4940	1670	1000						
Break flow velocity (ft/s)	510	190	108						
Break flow quality	0	0	0		0.03	0.03	0.03	0	
Safety injection (gpm)				885	2500	2500			
Recirculation flow (gpm)							8250	2550	2550
Spray flow (gpm)		0	5700		5700	5700	5700	0	
Spray temperature (°F)			105		105	150	150	150	
Containment pressure (psig)	0	6	9.5		5	3	3	4.2	1.5
Containment temperature (°F)	110	170	182		160	140	140	148	120
Pool depth (ft)					0.9	3.3	3.3	3.3	3.3
Pool temperature (°F)					170	145	145	147	125
Pool pH									
Containment atmosphere velocity (ft/s)	35	10	5						
Containment relative humidity (%)	50	100	100		98	98	98	98	100
Paint temperature (°F)	110		160		175	160	160	155	121

Peak break flow: 4940 lb/s at 0+ s
Quality at peak break flow: 0
Peak containment pressure: 10.2 psig at 2 min

Peak break flow velocity: 510 ft/s at 0+ s
Quality at peak break flow velocity: 0
Peak containment atmosphere velocity: 35 ft/s at 0+ s

Table 2-6. Debris Generation and Transport Parameters: MLOCA—Ice Condenser Containment.

Parameter	Blowdown Phase			Injection Phase			Recirculation Phase		
	0+	30 s	180 s	20 s	15 min	34 min	34 min	2 h	24 h
RCS pressure at break (psia)	2250	900	508						
RCS temperature at break (°F)	537	521	392		330	300	300		
Break flow (lb/s)	4940	1670	1000						
Break flow velocity (ft/s)	510	190	108						
Break flow quality	0	0	0		0.03	0.03	0.03	0	
Safety injection (gpm)				885	2500	2500			
Recirculation flow (gpm)							9000	9000	9000
Spray flow (gpm)		0	6400		6400	6400	6400	6400	6400
Spray temperature (°F)			105		105	105	92.5	86.5	84
Containment pressure (psig)	0+	9.8	7.8		4	4	4	1.8	1.4
Containment temperature (°F)	100	145	151		110	110	110	87	90
Pool depth (ft)					4	7.9	7.9	8	9.6
Pool temperature (°F)					150	146	146	117	104
Pool pH									
Containment atmosphere velocity (ft/s)	30	2.5	1.25						
Containment relative humidity (%)	0	10	40		80	97	97	97	98
Paint temperature (°F)	100	101	125		130	125	125	95	90

Peak break flow: 4940 lb/s at 0+ s
Quality at peak break flow: 0
Peak containment pressure: 11 psig at 55 s

Peak break flow velocity: 510 ft/s at 0+ s
Quality at peak break flow velocity: 0
Peak containment atmosphere velocity: 30 ft/s at 0+ s

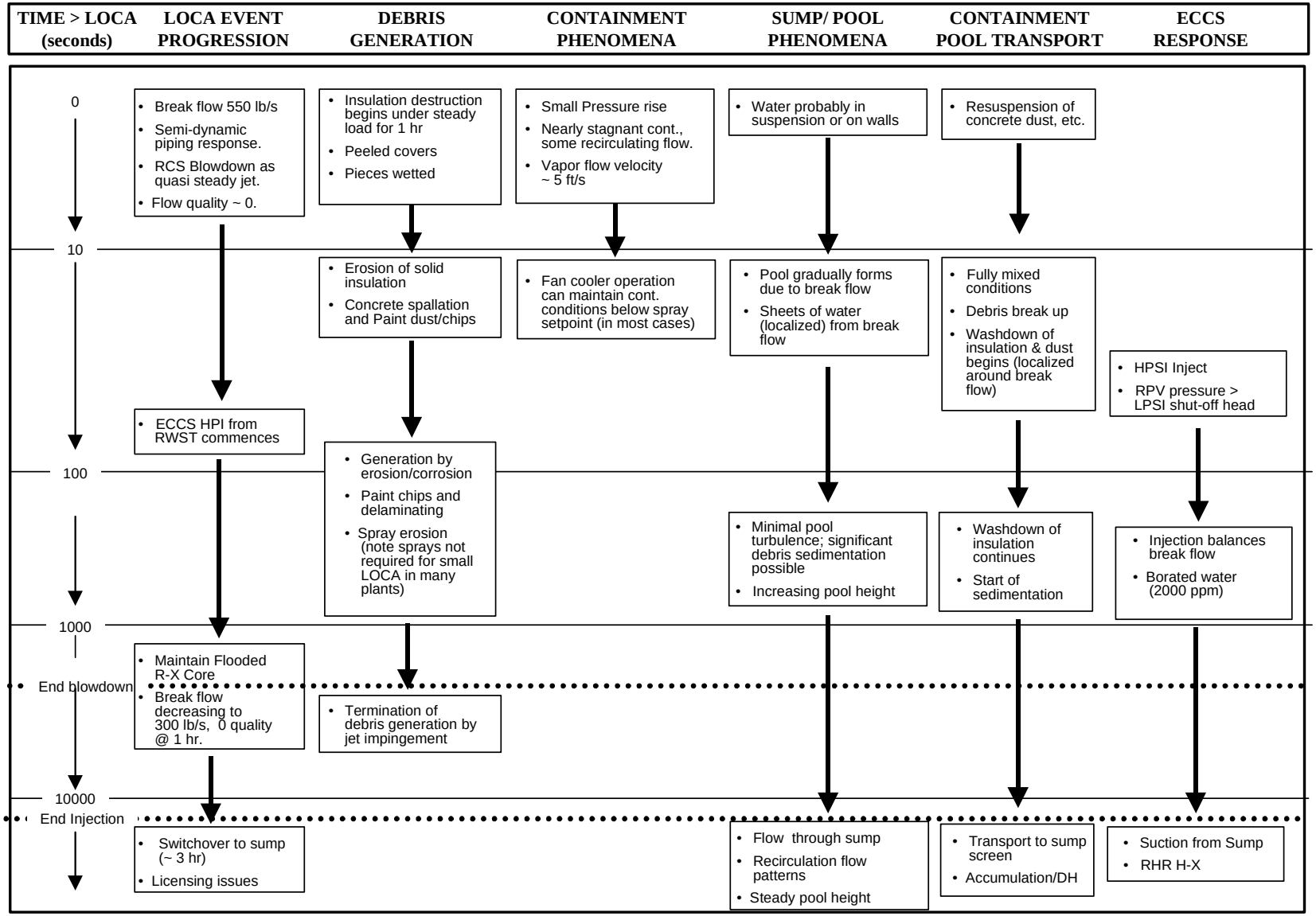

Fig. 2-4. PWR SLOCA Accident Progression in a Large Dry Containment.

Table 2-7. Debris Generation and Transport Parameters: SLOCA—Large Dry Containment.

Parameter	Blowdown Phase			Injection Phase			Recirculation Phase		
	0+	30 min	1 h	60 s	2 h	3 h	3 h	12 h	24 h
RCS pressure at break (psia)	2250	605	512						
RCS temperature at break (°F)	538	354	371		270	236	236		
Break flow (lb/s)	550	343	300						
Break flow velocity (ft/s)	320	320	320						
Break flow quality	0	0	0						
Safety injection (gpm)				1500	2500	2500			
Recirculation flow (gpm)							2500	2500	2500
Spray flow (gpm)	Sprays not required								
Spray temperature (°F)									
Containment pressure (psig)	0	5	5		4	3	3	1	0.75
Containment temperature (°F)	110	160	160		150	140	140	115	110
Pool depth (ft)			0.8		1.5	2.25	2.25	3	3
Pool temperature (°F)			157		157	150	150	125	118
Pool pH									
Containment atmosphere velocity (ft/s)	9	4	4						
Containment relative humidity (%)	50	100	100		100	100	100	100	100
Paint temperature (°F)	100	160	160		157	153	153	127	117

Peak break flow: 550 lb/s at 0+ s
Quality at peak break flow: 0
Peak containment pressure: 6 psig at 38 min

Peak break flow velocity: 320 ft/s at 0+
Quality at peak break flow velocity: 0
Peak containment atmosphere velocity: 9 ft/s at 20 s

Table 2-8. Debris Generation and Transport Parameters: SLOCA—Ice Condenser Containment.

Parameter	Blowdown Phase			Injection Phase			Recirculation Phase		
	0+	30 min	1 h	60 s	15 min	35 min	35 min	5 h	24 h
RCS pressure at break (psia)	2250	605	512						
RCS temperature at break (°F)	538	354	371		391	362	362		
Break flow (lb/s)	550	343	300						
Break flow velocity (ft/s)	320	320	320						
Break flow quality	0	0	0						
Safety injection (gpm)				1500	2500	2500			
Recirculation flow (gpm)							9000	9000	9000
Spray flow (gpm)		6400	6400	0	6400	6400	6400	6400	6400
Spray temperature (°F)		105	91		105	105	91	87.5	86
Containment pressure (psig)	0+	4.1	3.6	3.4	4.4	4.2	4.2	2.25	1.8
Containment temperature (°F)	100	111	96.5	94	112	110	110	92	95
Pool depth (ft)		5.5	6.75		2.5	6.5	6.5	9	8.9
Pool temperature (°F)		137	132		137	137	137	120	114
Pool pH									
Containment atmosphere velocity (ft/s)	2.9	0.7	0.7						
Containment relative humidity (%)	0	97	97	6	100	97	97	97	97
Paint temperature (°F)	100	110	104	100	106	110	110	92	96

Peak break flow: 550 lb/s at 0+ s
Quality at peak break flow: 0
Peak containment pressure: 4.4 psig at 15 min

Peak break flow velocity: 320 ft/s at 0+
Quality at peak break flow velocity: 0
Peak containment atmosphere velocity: 2.9 ft/s at 23 s

Table 2-9. Debris Generation and Transport Parameters: SLOCA—Sub-Atmospheric Containment.

Parameter	Blowdown Phase			Injection Phase			Recirculation Phase		
	0+	30 min	1 h	60 s	1 h	3 h	3 h	12 h	24 h
RCS pressure at break (psia)	2250	605	512						
RCS temperature at break (°F)	538	354	371		270	236	236		
Break flow (lb/s)	550	343	300						
Break flow velocity (ft/s)	320	320	320						
Break flow quality	0	0	0						
Safety injection (gpm)				1500	2500	2500			
Recirculation flow (gpm)							2500	2500	2500
Spray flow (gpm)					9000	9000	9000	9000	9000
Spray temperature (°F)					105	150	150	125	120
Containment pressure (psig)	0	5	5		4	3	3	1	0.75
Containment temperature (°F)	110	160	160		150	140	140	115	110
Pool depth (ft)			0.8		1.5	2.25	2.25	3	3
Pool temperature (°F)			157		157	150	150	125	118
Pool pH									
Containment atmosphere velocity (ft/s)	9	4	4						
Containment relative humidity (%)	50	100	100		100	100	100	100	100
Paint temperature (°F)	100	160	160		157	153	153	127	117

Peak break flow: 550 lb/s at 0+ s
Quality at peak break flow: 0
Peak containment pressure: 6 psig at 38 min

Peak break flow velocity: 320 ft/s at 0+
Quality at peak break flow velocity: 0
Peak containment atmosphere velocity: 9 ft/s at 20 s

2.5 Other Plant Design Features That Influence Accident Progression

Other plant design features (beyond those previously discussed) may influence the debris-related accident progression. For example, in many plants, heat exchangers are installed directly in the core cooling recirculation flow paths to ensure that the water is cooled before it is returned to the core. However, in some plants, the core cooling recirculation systems do not have dedicated heat exchangers and instead make indirect use of heat exchangers from other systems (i.e., CS) to ensure that heat is removed from the reactor coolant. Examples of plants where core cooling makes indirect use of heat exchangers from CS includes the plants with sub-atmospheric containments and CE plants. For these types of plants, successful core cooling during recirculation will require (1) direct sump flow from the core cooling system and (2) sump recirculation cooling from the CS system.

For plants with sub-atmospheric containments, switchover for the set of "inside" recirculation spray pumps is performed quickly (approximately 2 min), whereas the switchover for ECCS pumps and CS pumps is considerably longer (on the order of 30 min or more depending on LOCA type). The relatively quick switchover of the inside recirculation spray pumps is accomplished to minimize containment pressure and temperature. The inside recirculation spray system is equipped with a heat exchanger, and it appears that its actuation is credited in estimating the $NPSH_{Margin}$ for the ECCS and CS system during the recirculation phase.

Recovery from a stuck-open PORV may be possible at many plants through operator actions to close the associated block valve. The need for sump recirculation could be avoided by this action.

The containment structures are sufficiently robust that failure of CS is not expected to cause containment failure from overpressure (~ 3 times design pressure).

3.0 TECHNICAL APPROACH

Subsection 3.1 provides a comprehensive overview of the technical approach used in these evaluations. The remainder of this section discusses specific assumptions important to the treatment of insulation debris generation, debris transport, and debris accumulation and head loss. The step-by-step process used in the parametric evaluations is described in Secs. 4 and 5.

3.1 Overview

The objective of this parametric study is to assess the vulnerability of the PWR population to potential blockage of the recirculation sump screen following a LOCA. Regardless of the break size, as discussed in Sec. 2, the LOCA accident sequence in any PWR involves (1) debris generation, (2) containment transport during depressurization, (3) debris washdown and degradation caused by containment sprays if they are actuated manually or automatically, (4) pool transport to the sump, and (5) debris-bed formation and head loss. Although a great deal has been learned about the individual processes through testing and simulations performed as part of the ongoing GSI-191 program, an integrated analysis of blockage potential requires plant-specific spatial information that is not part of the parametric assessment.[18] Therefore, the methodology developed here to assess vulnerability for each parametric case focuses first on the range of debris loadings needed for the plant to fail to meet the recirculation flow requirements and second on the range of debris volumes and compositions that can be generated. Assessment of the cumulative transport fraction required to fail the sump is considered last. This approach does not follow the chronological accident sequence, but, as shown in Fig. 3-1, it does introduce the highest quality information and the most refined models before more subjective arguments must be invoked.

Figure 3-2 provides a simplified description of the technical approach and the scope of evaluations performed. This approach consists of three major steps.

1. *Construct a representative parametric case for each PWR*. To the extent possible, these cases were constructed using actual plant information collected from sources described in Sec. 1.5. Table 3-1 provides a list of parameters used to construct each parametric case. Typically, information with high fidelity is available for the following parameters: (a) ECCS and CS flow rates following LLOCAs and MLOCAs, (b) $NPSH_{Margin}$ for each pumping system, (c) time to ECCS switchover following LLOCAs and MLOCAs, (d) expected water levels on the containment floor at the time of ECCS switchover, (e) containment-averaged fraction of insulation in each insulation type, and (f) recirculation-sump geometry and containment-layout information.[19] For these parameters, parametric variations addressed issues such as the comparison between a single operational ECCS train and design-basis performance. For some other parameters, information with high fidelity is not available. Primary examples of these parameters are the location of each insulation type in the containment[20] and the flow through the recirculation sump following an SLOCA. For these parameters, a variety of supporting analyses were performed to define a

[18] Even when detailed information is available for a single plant, variability in these parameters and uncertainty in the physical models creates a range of possible outcomes that must be interpreted by comparing the completeness of the available information and the confidence one has in the predictive capability of the methodology with the safety philosophy upon which decisions are based. These difficulties are further compounded for the industry-wide evaluations by the wide range of plant configurations that exist among operating PWRs.

[19] Most plant licensees provided such information in the form of engineering drawings, and the information was validated in many cases by comparing it with UFSAR descriptions.

[20] This information is available for two volunteer plants for which CAD drawings are available and, to some extent, information is available for 6 USI A-43 reference plants.

reasonable range over which they may vary. The "favorable" end of this range establishes values that tend to minimize the potential for sump-screen blockage. Conversely, the "unfavorable" end of this range provides values that enhance the potential for sump-screen blockage. Table 3-2 documents the favorable and unfavorable bounds for each parameter and describes the analytical tools used to define this range. The following sections provide further discussions of how some of the uncertainties in choosing these favorable and unfavorable parameter estimates are factored into the vulnerability assessment for each parametric case.

2. *Perform parametric case evaluations*. For each parametric case, calculations were used to estimate (a) the quantity of debris that would be necessary to cause sump-screen blockage of sufficient magnitude to render the ECCS and/or CS inoperable, (b) the quantity of each type of debris that might be generated for postulated breaks of different sizes, (c) the transport fractions applicable to each type of insulation and each break size, (d) the quantity of insulation that could be transported to the sump, and finally, (e) the head loss caused by debris accumulation. These case evaluations were used to calculate four parameters that formed the basis for decisions regarding the potential for sump failure. These parameters (or metrics) are described in Table 3-3.

3. *Judge the potential for blockage for each parametric case*. The potential for blockage is estimated for each case for each LOCA size using two general criteria.

    - To determine parametric cases that are **unlikely** to have a blockage problem, the analyses apply "unfavorable" estimates of parameters used in the evaluations. If the parametric case is proven to perform well even under these assumed unfavorable operating conditions, it is very likely that it would perform well following a real LOCA.
    - Conversely, when "favorable" assumptions are used in the analyses, parametric cases that fail are **very likely** to be susceptible to sump-screen blockage following a LOCA.

The favorable and unfavorable assumptions are itemized and discussed more fully in Table 3-2. Based on the criteria described above, some parametric cases were identified as **very likely** to experience blockage following a LOCA and some were identified as **unlikely** to experience a problem. Numerous parametric cases that lie between these extremes are further graded into two categories: **likely** to have a problem and **possible** to have a problem. Assignment to these categories is made when performance comparisons made under the favorable and unfavorable bounds do not indicate a clear decision. Additional features of the case such as the presence of curbs, the sump geometry, and the predominance of fiber or cal-sil insulation types must be considered to make the final judgment of vulnerability in these cases.

Table 3-1. List of Parameters Used to Construct Parametric Cases.

Parameter	Source of Information
Sump-Screen Area (wetted)	**LANL Analysis of GSI-191 Database**. Answers to Question 3e of GSI-191 survey provided the total screen area. LANL used plant drawings (provided for each plant) to estimate what fraction of this screen area would be submerged at the time of switchover.
$NPSH_{Margin}$	**NRC GL 97-04 database**. This value was not available for four plant units. A surrogate range was used for those plants.
Recirculation Flow Rates SLOCA (2-in.) Flow MLOCA/LLOCA Flow	**NRC GL 97-04 database**. Review of NUREG/CR-5640 for HPSI and charging pumps
Spray Activation Pressure	**LANL Survey of UFSARs for several plants.**
Containment Free Area (unobstructed flow paths near sump)	**GSI-191 Database**
Fan Cooler	**LANL Survey of UFSARs for several plants.**
Pool Levels At Switchover Maximum Height	**GSI-191 Database** **Question 1(a)** **Question 1(c)**
Sump Submergence	**LANL Analysis of GSI-191 Database.** LANL used plant drawings to determine if the sump would be submerged or not at the time of ECCS switchover.
Sump Location	**GSI-191 Database**
Sump-Screen Orientation	**GSI-191 Database**
Sump-Screen Approach Velocity	**LANL analyses** that used data from GSI-191 Database and NRC GL 97-04 database.
Sump-Screen Clearance	**GSI-191 Database**
Insulation Types	**GSI-191 Database**
Relative Fractions of Insulation Fibrous (Fiberglass and Kaowool) Cal-sil Reflective Metallic Insulation (RMI)	**GSI-191 Database**. Information for this field is not complete. Several plants provided no estimates. A surrogate range was developed by LANL based on qualitative descriptions provided by the licensees (such as RMI on RPV and steam generator and rest is fibrous insulation).

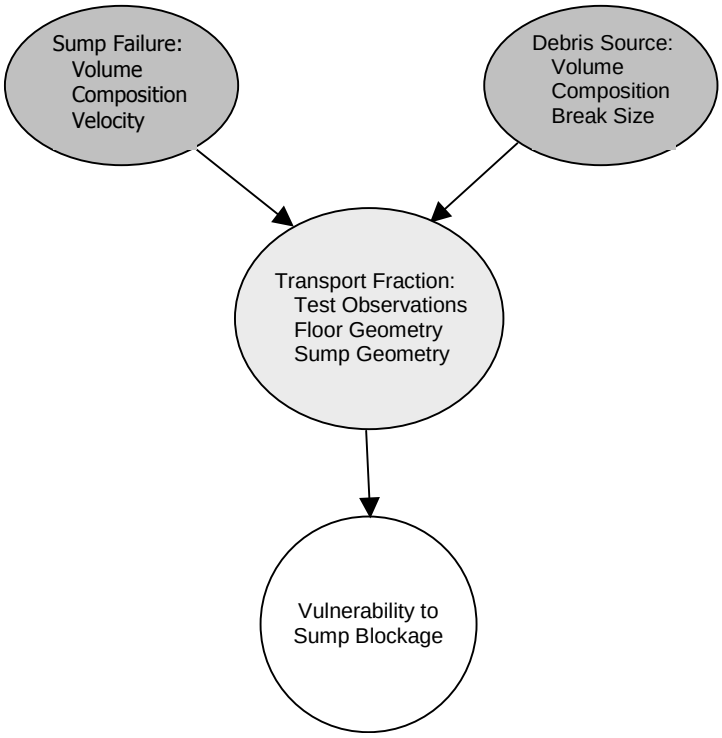

Fig. 3-1. Schematic of Parametric Methodology that Focuses First on Sump Failure, Second on Debris Generation, and Finally on Necessary Debris Transport.

Table 3-2. Summary of Analyses and "Favorable" and "Unfavorable" Modeling Assumptions Used in the Parametric Evaluations.

Parameter	Analyses Conducted	Modeling Assumptions[21]	
		Favorable Analysis	Unfavorable Analysis
Accident Scenario	• RELAP simulations of RCS • MELCOR simulations for dry, ice condenser, and sub-atmospheric containments	• Spray actuation on set point • Degraded fan-cooler • One operating train (LLOCA)	• Spray actuation on set point • No fan cooler • Design pump flows
ZOI Model	• CAD simulations for two GSI-191 volunteer plants • Detailed calculations for four USI A-43 plants • Simplified model for 63 plants	(No differences between "Favorable" and "Unfavorable") • BWROG URG data for ZOI (corrected for PWRs) • Homogenized mixture of insulations for SLOCA • Spherical ZOI	
Destruction Model	• No analyses. Approximate estimates based on URG data and other test data	• Incomplete destruction within ZOI. 1/3 into small fragments; 1/3 into larger fragments; remaining into torn blankets	• Use results from preliminary debris generation testing for cal-sil and fiberglass (50% into powder/small fragments)
Debris Transport	• GSI-191 test data applied similar to NUREG/CR-6369 • Detailed estimates for volunteer plants • Approximate estimates for non-volunteer plants	• 5% of ZOI debris volume deposits on sump when no sprays on for SLOCA • 10% of ZOI debris volume deposits on sump when sprays on for SLOCA or for LLOCA and MLOCA **Same for particulates**	10% and 25% were used for no-spray and spray sequences Also examined potential for transport of large pieces • By blowdown for exposed sumps • By floating up to the sump and sinking on the sump for horizontal sumps
Particulate (Paint Chips, Dirt, Dust, etc.)	• Oxidation calculations and models for zinc and aluminum • Approximate calculations for dust, dirt, and corrosion products (CPs) • SRS paint study	Relatively small quantities. Transport of about 10-20 lb • BWROG estimates • No paint contribution • No oxidation of zinc and aluminum contribution	Relatively large quantities • Dust/dirt estimates for PWR • SRS paint contribution • STUK and ANS model oxidation of zinc and aluminum contribution
Sump Flow	• RELAP results • Survey of HPSI and charging pump flow for each plant • GL 97-04 responses	• HPSI/charging + one train spray (if on) for SLOCA. • 1 residual train ECCS and spray for LLOCA/MLOCA	All ECCS and containment sprays (EOPs and GL 97-04)
Head Loss Model	• NUREG/CR-6224 model • Bump-up factors for miscellaneous debris • Cal-sil head-loss model (still underestimates head loss) • Validated for use	• Neglect RMI contribution • Treat cal-sil as just another particulate debris • Treat all fiber insulation as LDFG (per ft^3 LDFG results in lower head loss than Min-wool, Kaowool or some other fibrous insulation)	• RMI contribution • Treat cal-sil as just another particulate debris • Fiber represented by mineral wool or Tempmat when they are present

[21] Although the philosophy of "favorable" and "unfavorable" analyses was rigorously followed in assessment of debris transport and accumulation, it is less uniformly applied for other parts of the evaluations. In some cases (e.g., ZOI model), point estimates were used instead of a range of possibilities.

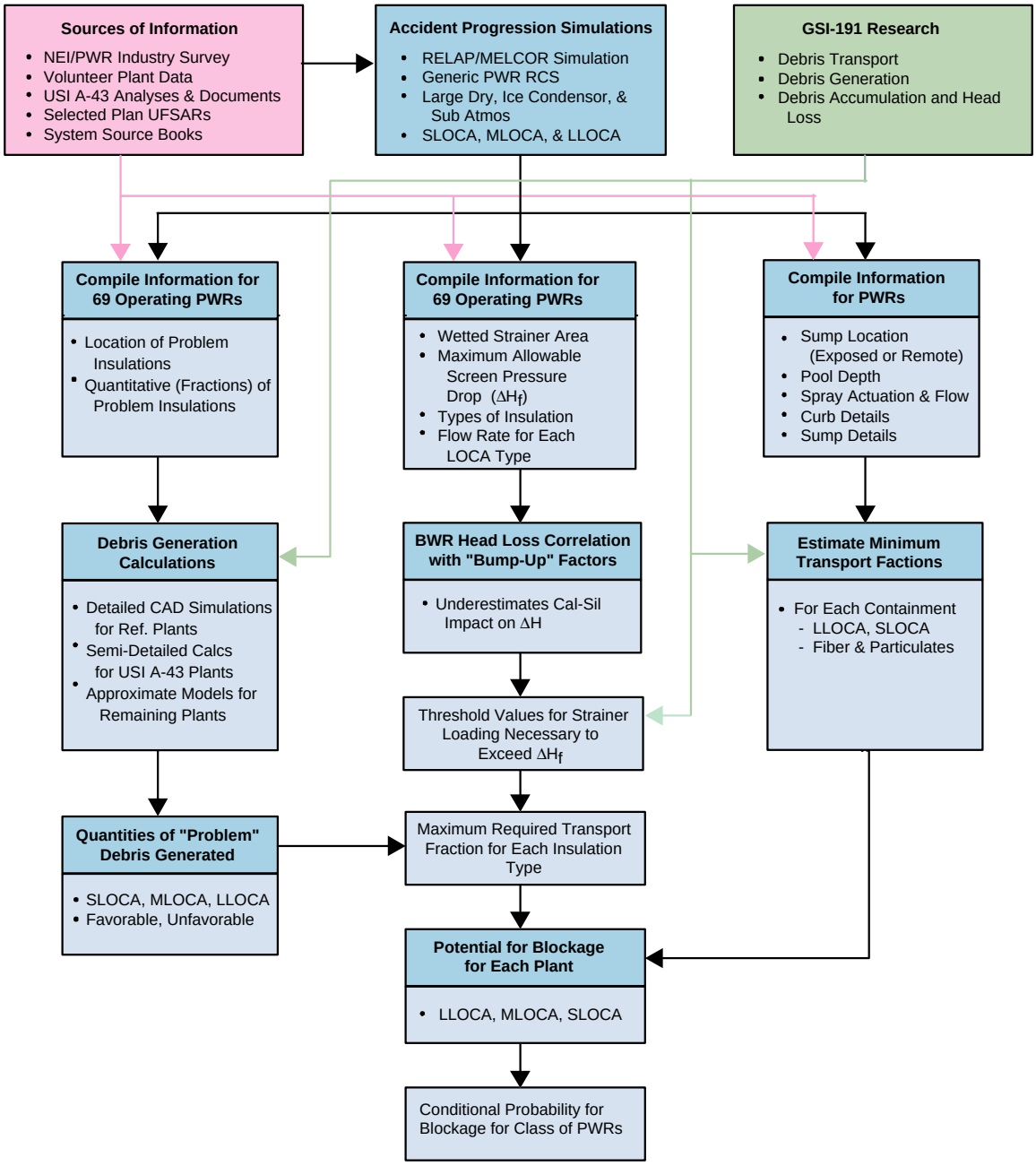

Fig. 3-2. Technical Methodology Used to Identify Plants Vulnerable to GSI-191 Related Safety Concerns.

Table 3-3. Description of Metrics Used in the Decision Process.

Failure-Threshold Debris Loading (FTDL). This metric represents the minimum sump screen debris loading necessary to induce head loss across the sump in excess of the failure criterion (e.g., $\Delta H_{screen} > NPSH_{Margin}$). Typically, data and models with high fidelity are available to estimate FTDL values, and thus, estimates of FTDL played a key role in determining the likely outcome of each parametric case. Figs. B-1 through B-69 present these values for each parametric case and each accident sequence. Section 3.4 describes how this metric was calculated.

Minimum Cumulative Transport Fraction. Defined as the ratio of FTDL to quantity of debris generated, this metric provides insights into the cumulative transport fraction required to reach the sump failure criterion. It is very instructive to calculate this ratio for each postulated accident condition because it forces one to consider the plausibility of the required transport processes before assigning a vulnerability to the parametric case. For example, a case that requires 2 ft^3 of fiber on the screen to induce failure that may generate as much as 200 ft^3 of fiber at the source requires a cumulative transport fraction of only 1%. Testing and simulation performed to date may either be viewed as (a) supporting a transport fraction of 10% under similar conditions or (b) failing to preclude this level of transport as a possibility. In either case, the plausibility of transport is much greater for this case than if the source can only generate 2.5 ft^3 of fiber. The later scenario would require an 80% transport fraction for failure, and current testing does not support a cumulative transport process of this efficiency except under very special circumstances. Important plant features (e.g., the presence of curbs, the sump geometry, and the predominance of fiber or cal-sil insulation types) were also considered on a case-by-case basis in addition to the failure-threshold transport fraction to make a final vulnerability assignment.

Range of Expected Debris. Testing and simulations performed as part of the ongoing GSI-191 program were used to obtain "favorable" and "unfavorable" estimates for debris loading on the sump screen. CFD-based simulations were performed for selected containment layouts, and engineering judgments were relied on to extend test data and analysis findings to each parametric case. Judgments regarding potential for blockage were reached by comparing this likely range of debris loadings with FTDL values. Figures B-1 through B-69 present these values for each parametric case and each accident sequence in the form of dashed box. Section 3.4 describes how this metric was calculated. Cases in which the range of expected debris exceeded FTDL values were assumed **very likely** to fail. Alternately, cases in which the range of expected debris was lower than FTDL values were assumed **unlikely** to fail. Intermediate cases were assigned **likely** and **possible** grades.

Range of Predicted Screen Head Loss. The favorable and unfavorable estimates for debris loadings were coupled with a head-loss model to obtain "favorable" and "unfavorable" estimates for head loss across the sump screen. Judgments regarding the potential for blockage were reached by comparing this likely range of head loss with the failure criterion. For example, a parametric case in which both favorable and unfavorable head-loss estimates far exceed the $NPSH_{Margin}$ is more likely to fail because failure in this case cannot be attributed to "conservative" assumptions used in the licensee estimates of $NPSH_{Margin}$[22].

[22]Typically licensee estimates for $NPSH_{Margin}$ are based on conservative assumptions regarding containment overpressure and coolant temperature. If ΔH_f predictions are only slightly higher than the $NPSH_{Margin}$, one could conclude that the failure is a reflection of "conservative" assumptions. This comparison provides insights on a case-by-case basis to address this uncertainty.

3.2 Insulation Debris Generation

Most, if not all, of the RCS piping and auxiliary piping (e.g., service water piping) in PWRs is insulated. Estimating insulation debris generation from a LOCA is complicated by many factors, including, but not limited to, the following.

1. The spatial arrangement of piping systems and equipment that can serve both as targets and as locations of high-energy breaks

2. The spatial distribution of insulation types and thickness

3. The relative potential of breaks occurring in various sizes of pipes and piping locations such as walls and elbows

4. The unknown destruction response of each insulation type and of concrete and coatings to a two-phase depressurization jet

5. The unknown range and shape of a two-phase depressurization jet in the presence of obstacles such as concrete structures and adjacent piping

6. The exact location, severity, and directionality of a given LOCA event

Items 1 and 2 can be addressed with plant-specific spatial data and complete insulation inventories. The fidelity of estimates for items 3 and 4 can be addressed, in part, through exhaustive testing and analysis of in-service piping. However, many features of an accident scenario, such as items 5 and 6, will always retain a high degree of variability[23] that resists deterministic evaluation and requires bounding or stochastic analysis. Each of these complications is compounded in the present parametric analysis of recirculation-sump blockage potential by the wide variations in plant geometry, the variety of types and applications of various thermal insulations, and the incomplete knowledge of their spatial locations in any given plant. In particular, the best information currently available regarding insulation types in most plants is a rough estimate of volumetric proportion such as 80% RMI, 15% cal-sil, and 5% fiber.

To address the many complexities of debris generation, the CASINOVA computer model was developed in support of the ongoing GSI-191 program. This tool allows stochastic sampling of break locations and parametric investigation of issues such as the importance of jet direction, range, and shape on debris volumes. At the heart of this model are CAD data describing the relative spatial locations of piping systems, equipment, and insulation applications. Complete spatial data for two volunteer plants are available for comparison. Both volunteer plants have a Westinghouse four-loop RCS. The first is an ice condenser containment, and the second is a large dry containment. Given the spatial data in electronic form, damage zones can be mapped at any number of break locations, and the range of debris volumes can be estimated for each insulation type. Although simplistic, the CASINOVA simulation provides a wealth of information regarding the spatial correlation of piping systems, insulation types, and potential damage volumes.

Simulations of debris generation currently are performed assuming spherical ZOIs surrounding each break that completely destroy all insulation types out to a radius equal to 12 diameters (12D) of the broken pipe. These breaks are located uniformly along pipes of every size that can be considered high-energy lines (i.e., $\cong$ 500 psi or higher) capable of producing a jet when broken. In the present evaluations, the CASINOVA model simulated approximately 1350 break locations. Figure 3-3 shows the

[23] BWR experience suggests that this uncertainty may overwhelm any other uncertainties.

level of detail incorporated in the CASINOVA simulation of a volunteer plant. Insulation on large tanks and pipes is subdivided into panels as shown in the figure, and all insulated pipes are divided into discrete segments representing point insulation sources that can be enveloped by a damage zone. The large sphere in the lower right-hand corner of Fig. 3-3 identifies the ZOI surrounding a large pipe break.

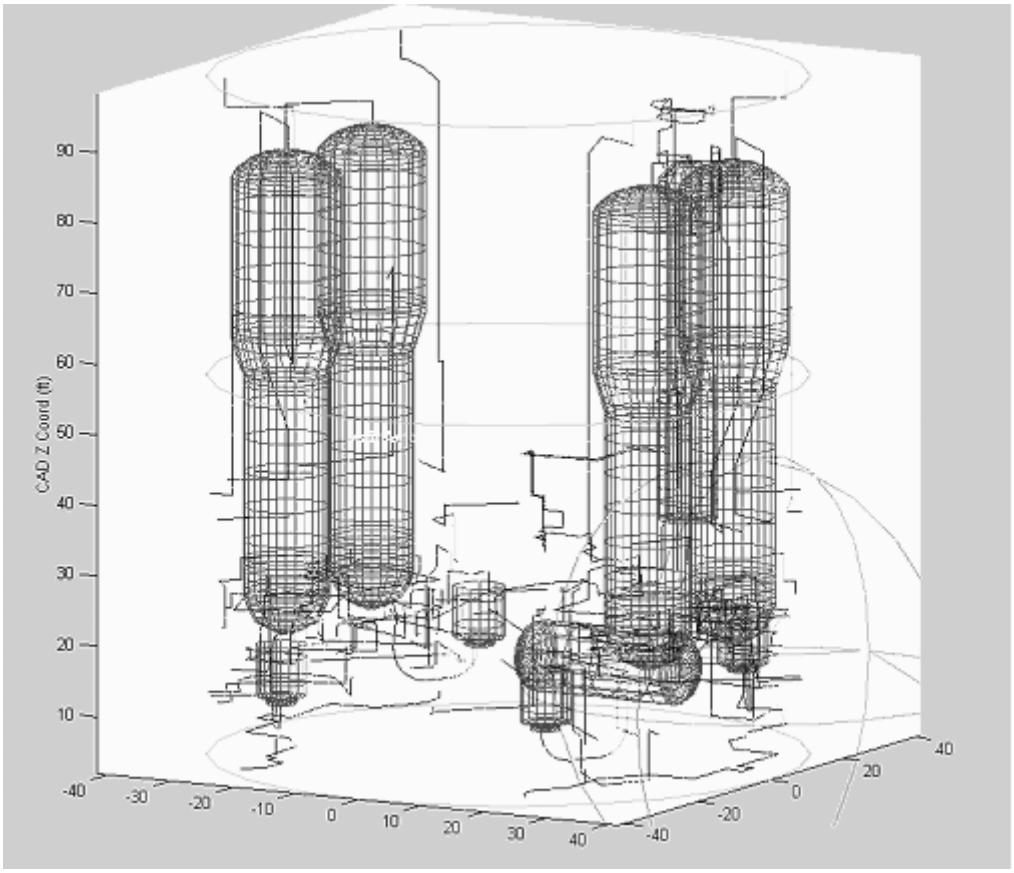

Fig. 3-3. Graphic of Volunteer Plant Piping and Equipment Data Imported to the CASINOVA Simulation Model.

The assumption of 12D damage zones for debris generation is based on engineering interpretations of high-pressure destruction testing performed (1) for the BWR Strainer Blockage Study [Zigler, 1995] using single-phase steam and air-jet surrogates and (2) in conjunction with the ongoing GSI-191 test program using 1400-psi, 310°C, two-phase water jets. Single-phase air jets were found to inflict significant damage to fibrous insulation types at a distance of 60D. Because of variability in the potential offset and separation of the broken pipe ends, LOCA jets traditionally have been assumed capable of damage to all insulation within a sphere of equivalent radius. Recent GSI-191 tests using two-phase water jets have exhibited damage to cal-sil and fiber insulation greater than previously measured in terms of both damage distances and fraction of finer fragments generated. This testing indicates that use of 12D spheres is a reasonable approximation for fibrous and cal-sil insulation debris generation.

Because complete, plant-specific information is not available, several important assumptions must be made for the present parametric analyses to apply high-fidelity volunteer-plant data in a generic way.

1. The lengths, sizes and complexity of piping and equipment present in the volunteer plants are representative of all PWR designs. This assumption extends to the relative proportion of piping sizes.
2. The thickness of an insulation application is proportional to the piping size, or the equipment circumference and is roughly the same regardless of the insulation type.
3. The thickness of insulation applications and the reactor systems to which they are applied in the volunteer plants are representative of typical applications of thermal insulation throughout the industry.
4. Where volumetric fractions of several insulation types have been provided, they can be assumed distributed in those proportions homogeneously throughout the containment.

The applicability of the first and third assumptions can be addressed only by compiling more plant-specific models of spatial data. If CAD models of a plant already exist, it is relatively easy to import these data to the CASINOVA simulation. The validity of the second assumption was confirmed by comparing the thicknesses of various types of insulation applied to pipes of comparable size in different plants.

The fourth assumption (regarding homogeneity of insulation types) is thought to be the most limiting condition of the present parametric analysis. Careful inspection of detailed insulation layout data available for six USI A-43 plants and two GSI-191 volunteer plants confirms that this assumption is not accurate for most regions of their containment. Preferential application of fiber insulation to smaller pipes and auxiliary pipes is more common, whereas RMI is used primarily on large components such as the reactor vessel and steam generators. This spatial dependency of the insulation application means that the fiber on small pipes is more likely to be affected by breaks in small pipes. Thus, the local proportion of fiber near a small break may be much higher than the containment-averaged proportion (This finding is also consistent with the GSI-191 database [NEI, 1997]). Although the assumption of homogeneity guarantees that each insulation type is represented in every postulated break, it may de-emphasize the potentially higher volumes of "problematic insulation" that could actually be generated by a break in a specific location of the plant. The potential spatial correlation between insulation types and break locations that may exist in a plant were not addressed in the parametric analyses because only approximate volumetric proportions were provided in the industry survey. As a result, it is possible that the risk of sump failure following a SLOCA may have been underestimated for some plants. Because large breaks already generate and transport large quantities of debris, this issue is not likely to affect the assessment of the potential for sump failure for LLOCAs.

The limitations of assuming homogeneous insulation types were mitigated in the following way. First, distributions of possible debris volumes were constructed for the volunteer plants by examining all possible breaks in pipes of three size ranges. Pipes between 2 and 4 in. in diameter represent small breaks.[24] Pipes between 4 and 6 in. in diameter represent medium breaks. All pipes greater than 6 in. in diameter represent large breaks. Figure 3-4 shows the frequency distribution (histogram) of insulation-debris volumes that can be generated in volunteer plant 1 from large-pipe breaks if all insulation types suffer equal damage to a spherical radius of 12D. Figure 3-5 presents the same data in a cumulative format. For example, 50% (fraction of 0.5) of all breaks will generate 250 ft^3 of debris or less for large-break LOCAs.

Second, the 95^{th} percentile was selected as a representative debris volume for each of the three break sizes, and finally, the homogenized composition factors were applied to estimate the volume of debris for each insulation type. Use of the 95^{th} percentile as an upper estimate avoids the extreme conservatism of reporting the debris volume of the single worst break, but it compensates for potential

[24] The choice of 2 in. to 4 in. was made based on the volunteer plant definition of an SLOCA. These results are equally applicable to a postulated 2-in.-equivalent break in a larger pipe. It should be noted that when 2-in.-equivalent breaks are postulated in the hot leg and cold leg (e.g., 2-in. circular hole in the hot leg), they generate significantly larger amounts of debris.

spatial correlations that cannot be assessed in the parametric study. Table 3-4 summarizes the statistics of the debris-generation simulations. Although debris-volume estimates derived from only two volunteer-plants are used for all cases, they are the best surrogates available for the parametric analysis of industry-wide vulnerability to sump blockage.

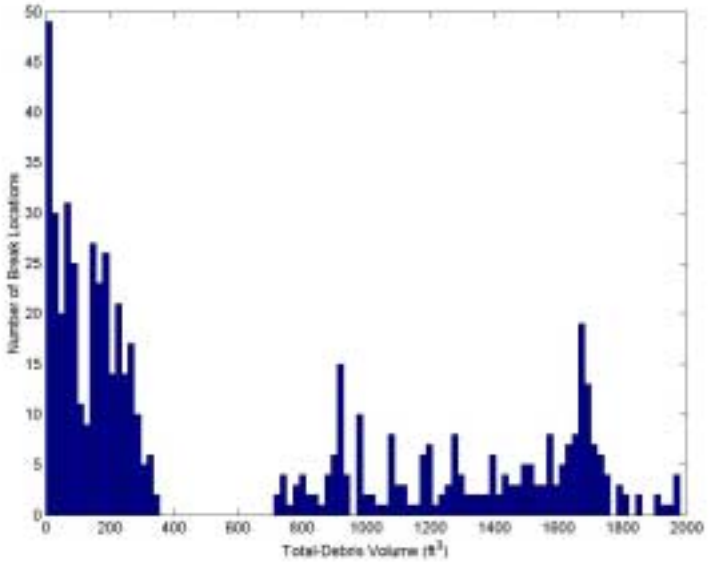

Fig. 3-4. Frequency Distribution of Possible Breaks from Large-Pipe Breaks in Volunteer Plant 1.

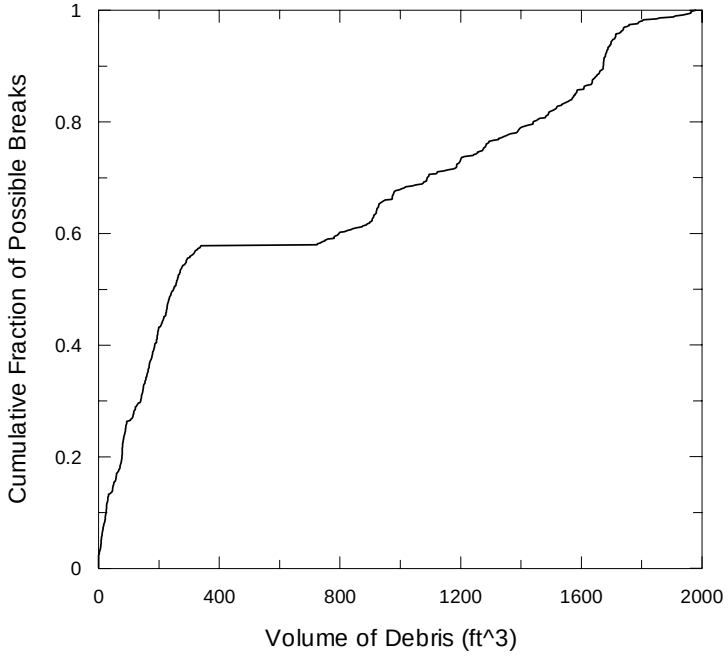

Fig. 3-5. Cumulative Distribution of Debris Volumes for LLOCA Occurring in Volunteer Plant 1.

Table 3-4. Summary of Debris-Generation Simulations for Three Break Sizes.

		Debris Volume (ft^3)		
Break Size	Diameter Range (in)	5^{th} %-ile	50^{th} %-ile	95^{th} %-ile
SLOCA	$2 < d \leq 4$	1	4	25
MLOCA	$4 < d \leq 6$	8	18	40
LLOCA	$6 < d$	20	250	1700

Table 3-5 cites other estimates of LOCA debris volumes that have been reported in the literature for several PWR power plants [Kolbe, 1982]. The total debris volumes summed over all insulation types agree well with the CASINOVA value of 1700 ft^3 for the 95^{th} percentile of volumes that can be generated from large breaks in volunteer plant 1. This table provides confirmation that LOCAs can damage a significant fraction of the insulation present in the containment, and it offers a quality assurance check that the CASINOVA simulation is properly calculating volumes for all other break sizes. For reference, there is approximately 7200 ft^3 of insulation in the containment of volunteer plant 1 distributed by volume as 21% fiber, 46% particulate, and 33% RMI.

Table 3-5. Comparison Debris Volumes for Limiting Breaks in Several PWRs [Kolbe, 1982].

Plant	Break	RMI ft^3	Fiber ft^3	Cal-Sil ft^3	Total ft^3
Salem 1 (W-Dry)	Hot Leg	391	353	0	744
	Cold Leg	**598**	**685**	**0**	**1283**
ANO 1 (CE-Dry)	**Main Steam Line**	**726**	**0**	**1157**	**1883**
Maine Yankee (CE-Dry)	**Main Steam Line**	**0**	**66**	**785**	**851**
(No Longer Operating)	Hot Leg 1	0	49	246	295
	Hot Leg 2 or Crossover 1	0	41	384	425
	Crossover 2	0	86	317	403
	Cold Leg	0	53	50	103
	Pressurizer (6-in line)	0	26	7	33
Sequoyah 2 (W-Ice)	Pressurizer (6-in line)	31	0	0	31
	Hot Leg	751	0	0	751
	Coolant Pump	241	0	0	241
	Steam Generator 4	141	0	0	141
	Steam Generator 1	852	0	0	852
	Loop Closure	**1419**	**0**	**0**	**1419**
Prairie Island 1 (W-Dry)	Main Steam Line	1149	40	0	1189
	Feedwater	316	40	0	356
	Hot Leg	1099	40	0	1139
	Cold Leg	338	0	0	338
	Crossover	**1341**	**40**	**0**	**1381**

3.3 Debris Transport

Table 3-6 lists the "favorable" and "unfavorable" transport fractions used in the present study. Note that these values are based on consideration of generation, washdown, and pool transport of "transportable" forms of fibrous debris only. Neither the "favorable" nor the "unfavorable" values listed in the table considered the potential for transport of large pieces[25] or the potential for increased transport in containments that have specific features that might enhance transport (e.g., a horizontal sump screen with no curb and an exposed sump location). In keeping with the philosophy of comparing required transport with the FTDL, it is felt that a case capable of failing when applying the "favorable" transport fraction is very likely to fail. On the other hand, cases that did not fail when assessed using "unfavorable" estimates may still fail if one were to include other mechanisms of transport (e.g., exposed sump transport).

Table 3-6. "Favorable" and "Unfavorable" Estimates for Debris Transport Fraction.

Transport Conditions	Favorable Estimate	Unfavorable Estimate
SLOCA with Sprays Inactive	5%	10%
SLOCA with Sprays Active All MLOCAs and LLOCAs	10%	25%

The underlying assumptions that form the basis for these transport fractions are as follows.

- Based on BWROG and GSI-191 debris generation experimental data, it is assumed that **not** all the insulation contained in the ZOI would be generated into "transportable" form. It is assumed that approximately 33% of the insulation would be generated into smaller "transportable" forms.[26] The other 67% is assumed to be generated in the form of partially torn blankets or large pieces that would sink to bottom of the pool. A part of this debris would erode when subjected to falling break water flow. Current analyses assumed that about 50% of the debris might be generated in the transportable form.

- The generated insulation fragments would be transported and distributed throughout the containment by the jets. Only a fraction of this debris would be deposited directly into the pool. The rest of the insulation would not be added to the pool if CS was not activated. The fraction added to the pool would be higher for the SLOCA and MLOCA because vapor flow velocities in the containment are expected to be low.

- Only a fraction of the debris added to the pool formed on the containment floor would be transported to the sump screen. Several experiments have been carried out to establish a defensible minimum value that can be used in the parametric evaluations [LANL, 2001c; LANL, 2001d]. Findings from these experiments were used in the transport fraction estimates.

[25] As noted below, large pieces stay afloat for up to 30 min following a LOCA. The density of a dry blanket is only 2.3 lb/ft^3. These pieces could be easily transported toward the sump and deposit on the sump screen.

[26] Ongoing debris generation experiments suggest that up to 50% of the debris may be in transportable form. This finding applies to both cal-sil and fiberglass insulation. Thus, 33% presents a reasonable estimate considering that not all insulation is arranged as in the configurations tested.

Early considerations of containment pool debris transport focused on the sliding and tumbling properties of debris pieces along the floor, and an extensive test program was pursued to measure the threshold velocities required for motion of various debris sizes. A draft report is available that describes this series of separate-effects tests [Maji, 2000]. In summary, the following was found.

1. Flocks of loosely attached fiberglass debris could remain suspended and move to the sump screen at flume-averaged velocities as low as 0.05 ft/s. These flocks (referred to as Size Class 1 and 2 in NUREG/CR-6224 [Zigler, 1995]) can be maintained in suspension for hours with small amounts of turbulence.

2. Fiberglass insulation fragments (sizes between 1/2 and 1 in.) that have settled to the floor will begin to tumble and slide with a depth-averaged flow of approximately 0.12 ft/s. These fragments can also remain in suspension for prolonged periods of time. Furthermore, these fragments can easily degrade into finer fragments when subjected to turbulent mixing flows.

3. RMI shreds are much less mobile and can be de-emphasized as a transport concern except for horizontal sump screens with no curbing that are located near to or are exposed to the break.

4. Cal-sil in fragmented form easily dissolves in hot water and transports as a suspended particulate up to physical diameters approaching 1/2 in. As confirmed by recent testing and shown in Fig. 3-5, the combination of cal-sil and minimal amounts of fiber form a very effective filter capable of inducing significant head losses across a sump screen. Also, cal-sil fragments by themselves can accumulate on the sump screen, even without the presence of fiberglass. Such deposition coupled with hot water induces very large pressure drops.

5. As-manufactured fiberglass blankets and RMI cassettes initially float on water and take between 15 and 30 min to sink. Therefore, their transport could not be ruled out for exposed sumps, especially for sumps with horizontal sump screens.

A series of tests was designed and specifically carried out in the three-dimensional (3-D) tank facility to obtain further data on debris transportability. Some of the important conclusions, as used in this study, are as follows.

1. Although floor-level transport is still an important consideration for determining maximum possible transport fractions, tests show significant transport of individual fibers and small clusters of fibers. These materials can be easily washed down by sprays (or small films of draining water). This testing can be viewed as (a) supporting a transport fraction of 10% under conditions expected to exist in the containment following a LOCA (including an SLOCA) or (b) failing to preclude this level of transport as a possibility. This material tends to deposit uniformly over a vertical or horizontal screen in very thin layers, and continued collection of this material has been observed to continue at a gradually decreasing rate for as long as 5 h.[27]

2. Real fractions of transport could be very large depending on spray actuation, sump flow and location, and orientation of the sump. Transport fractions in excess of 0.75 were measured for fibrous shreds when they were subjected to flow conditions representative of conditions expected to exist in the containment following an LLOCA.

[27] Decreasing collection rates for most tests suggest that a finite amount of initial source material is being slowly filtered from a finite pool of water, but other tests that combine threshold floor velocities with splashing water that penetrates to the pool bottom suggest that migration and turbulent degradation can be an important long-term source of finely divided fibers.

Fig. 3-6. Screen of 1/8-in. Mesh Opening Obstructed by Cal-Sil (Small Yellow Lumps) and Fiberglass (Uniform Translucent Mat). Close Inspection Reveals Very Small to Microscopic Cal-Sil Granules Imbedded in a Complex Fiber Mat. The Broken Bed to the Right of the Photo Was Damaged During Screen Removal. Nominal Fiber Thickness is 1/10-in.

3.4 Debris Accumulation and Buildup

Ongoing GSI-191 tests have shown that debris accumulation and buildup on a sump screen depends strongly on the orientation of the sump screen (i.e., vertical, horizontal, or slanted), approach velocity, and debris type. For debris type and sizes of present interest (i.e., small fragments of cal-sil and fiberglass), GSI-191 developed an extensive database for vertical screens and a limited database for horizontal screens. These experiments are being continued to gather additional data. The important experimental findings (to date) are as follows.

1. Fine debris tends to build up uniformly on vertical or horizontal screens. This trend is shown in Figs. 3-6 and 3-7. In both cases, small volumes of fine fibrous (nominal thickness of 1/10-in.) and cal-sil insulation were introduced into the flume and allowed to accumulate naturally on the screen.

2. Heavier debris builds up preferentially from bottom to top on vertical screens and uniformly in the case of horizontal sumps. Although curbs have an effect on debris accumulation, their effect is minimal when approach velocities are high (0.25 ft/s).

3. Very small approach velocities (<0.05 ft/s) are sufficient to keep a piece of fiberglass debris attached to a vertical sump screen. Buildup of thicker (1 to 2 in.) fiber beds would be necessary to induce the high head losses necessary to overwhelm the $NPSH_{Margin}$. However, fibrous debris readily detaches from the screen when flow through the screen is terminated.

4. Fibrous debris buildup in the presence of cal-sil is very similar to buildup in its absence (see Fig. 3-6). However, debris beds made up of cal-sil and fiber behave differently. Very small quantities of fibrous debris may induce very large pressure drops if cal-sil is present. In fact, a very thin bed could induce large pressure drops. For example, the bed shown in Fig. 3-6 caused a head loss in excess of 1 ft-water (and still increasing when the experiment was terminated[28]). However, upon termination of flow, the debris remained intact on the screen instead of crumbling as noted in the case of pure fiber beds.

Fig. 3-7. Thin Fiber Bed Beginning to Build on a Vertical Screen of 1/4-in. Mesh Opening.

Based on these findings, it was concluded that the fibrous and particulate debris of present interest would accumulate uniformly on the screen. However, two questions remained.

1. Would such fine fragments be capable of bridging relatively larger (¼-in.) screen mesh openings?
2. Would a 1/8-in.-thick[29] bed be able to filter debris and induce head loss?

Experiments were conducted to address these issues, and the findings are as follows.

[28] The experiment was terminated because a temporary arrangement was used to perform these 'quick-look' experiments. There was a concern that this screen may fail. Besides, head-loss measurement was not part of present set of experiments.

[29] Previous testing [Zigler, 1995] has shown that fiber beds spanning a regular mesh are vulnerable to localized collapse under very high pressures, so some minimum thickness will be needed to maintain mechanical integrity while supporting the imbedded particulate. NUREG/CR-6224 stated that fiber beds can survive approximately 50 ft of water per inch of thickness; so to withstand a nominal $NPSH_{Margin}$ of 6 ft, our analyses assumed that 1/8-in.-thick fiber beds would be necessary. This finding is based on test data obtained for 1/8-in.-mesh-opening BWR strainers. Confirmation of this finding for ¼-in. screens was necessary.

1. Fiber beds as thin as 1/8 in. can filter significant quantities of cal-sil and induce high head losses. However, significant head loss can occur for much thinner layers, especially when combined with cal-sil (see Fig. 3-6). The assumption that a full 1/8-in.-thick fiber bed is required for failure is certainly a favorable assumption for plants with a small $NPSH_{Margin}$ or with partially submerged screens where thin beds do not have to support an extreme head loss to reach the sump failure criterion. This assumption can be used to estimate FTDL for fibrous debris.

2. Figure 3-7 shows the initial growth of a fiber bed on a 1/4-in.-mesh screen. Note how individual fibers are able to stretch across the corners of the mesh and gradually reduce the effective opening. At this point of bed development, the solid patches of fiber represent the larger flocks of debris that were suspended in the water flow. After several minutes, the fiber mat becomes contiguous, causes significant head loss, and is virtually indistinguishable from similar beds formed on 1/8-in.-mesh screens.

3.5 Head-Loss Modeling and Assumptions

Detailed head-loss calculations were performed for each parametric case. The primary objective of these calculations was to define all combinations of particulate and fiber that can fail the required sump-performance conditions. Of special interest are (a) the minimum volume of fiber in combination with particulate debris needed to fail the sump and (b) the minimum volume of fiber needed to fail the sump in the absence of particulates. A secondary objective was to estimate the range of expected screen head loss for each parametric case.

To meet this objective, head-loss calculations were performed for a very large number of fiber volumes and particulate masses combined uniformly on each wetted sump-screen area. In some cases, the wetted area was estimated from the pool depth, the screen height, and the reported screen area. Head-loss correlations that predict the differential pressure drop per unit thickness of the debris bed were adopted from previous studies performed in support of the BWR strainer-blockage study [Zigler, 1995]. These correlations predict pressure drop as a function of the water-flow velocity and the debris-bed characteristics for a uniform bed with no significant edge effects. Thus, a head-loss estimate can be made for any combination of particulate and fiber debris. As explained above, both favorable and unfavorable values were defined for each parameter. For example, if a case required both Kaowool and Nukon as the fibrous component of a mixed debris bed, the head-loss characteristics of Kaowool were adopted for the unfavorable calculation (larger pressure drop per unit thickness) and the head-loss characteristics of Nukon were adopted for the favorable calculation (smaller pressure drop per unit thickness).

The strainer head losses associated with a debris bed composed of both fibrous insulation and particulate debris depends on the type of particulate within the bed, as well as on the type of fibrous debris. Several types of particulate debris would likely be available within PWR containments for transport to the sump screen. First, the destruction of certain types of insulation and fire barrier materials, such as cal-sil, would likely result in substantial quantities of particulate debris. Other types of particulate debris include: resident dust and dirt, concrete dust from erosion in the break jet, failed containment coatings, and Zn and Al precipitation byproducts. The characteristics affecting head-loss performance are unique for each type of particulate and are not well known for most types.

Comparisons of the "bump-up" factors associated with each particulate type validated assumptions made in the parametric study for the treatment of particulate debris[30]. Bump-up factors are defined as

[30] Note that "bump-up" factors were not used in the head loss calculations. This discussion is provided only to illustrate the relative contribution to head loss when different types of particulate are introduced to a fibrous debris bed.

the ratio of the head loss with particulate in the fiber bed to the head loss without particulate for the same flow conditions. Bump-up factors were determined from the URG gravity head-loss tests [BWROG, 1998] by dividing the head loss associated with a given quantity of particulate and fiber by the head loss for a similar test without particulate. Note that (1) these tests were all conducted in one test facility using the same test procedures so that the only substantial difference was the type of particulate, (2) all tests that were compared had a particulate-to-fiber mass ratio of approximately 1, and (3) the thickness of the fiber debris bed was approximately 2 in. Bump-up factors determined in this manner for several particulate types are compared in Fig. 3-8.

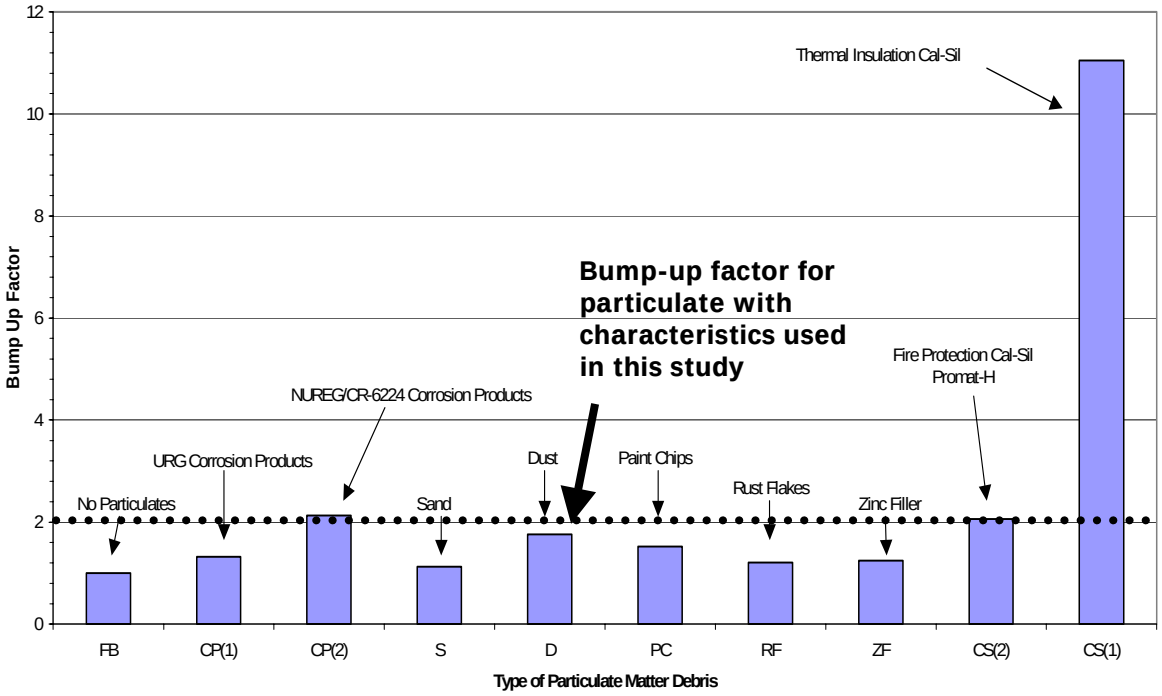

Fig. 3-8. Comparison of Particulate Bump-Up Factors.

The types of particulate examined in the gravity head-loss tests included corrosion products, sand, concrete dust, paint chips, rust flakes, zinc filler, and two types of cal-sil. Figure 3-8 shows that most types of particulates tested caused similar magnitudes of head loss; i.e., the bump-up factors ranged from 1 to 2. Note that the factors for the corrosion product tests documented in NUREG/CR-6224 are comparable to the factors for corrosion products determined from the gravity head-loss tests. The notable exception was particulate formed from the thermal insulation cal-sil. Its bump-up factor was approximately 11. Furthermore, cal-sil bump-up factors determined from other test data suggest that the factors could reach as high as 50 for thin debris beds.

High cal-sil bump-up factors mean that cal-sil insulation debris will produce much higher head losses than comparable quantities of other types of particulate. However in this parametric study, cal-sil and all other microporous insulation debris were treated as a generic particulate. This means that the effect of cal-sil insulation debris in all head-loss calculations was underestimated in favor of reduced sump-blockage potential. This very favorable assumption was partly compensated for in the final vulnerability assignment by shifting cases with large amounts of cal-sil and designations of **possible** up one grade to

likely[31]. Comprehensive head-loss testing of typical PWR insulation types currently is being planned as an important part of the continuing GSI-191 PWR Sump Blockage Study. This testing is critical for the quantification and public dissemination of information that characterizes the behavior of these insulations when combined in a debris bed.

Pressure drop across a mixed debris bed is a function of the water velocity through the screen, the composition of the debris, and the thickness of the bed. Head losses were computed for each parametric case over a wide range of fiber volumes and particulate masses present in the bed to generate a head-loss response surface similar to that shown in Fig. 3-9. This figure shows the favorable range of head loss (vertical axis) that is characteristic of Nukon fiber beds on the sump screen of parametric case 17 (discussed in Section 4). Each combination of debris creates a unique pressure drop that may be less than or greater than the failure condition ΔH_f, which can be represented for this plant by a horizontal plane slicing through the surface at a height of 1.1 ft of water. Figure 3-10 presents a close-up view of the same response surface that has been limited to an upper range equal to ΔH_f. All debris beds that fall in the region defined by the upper plateau create unacceptable head loss; debris combinations that lie in the corner "notch" can still meet the required flow condition. Note that the three vertices of the acceptable performance region are defined by the debris combinations of (a) minimum fiber volume (0.59 ft^3) with zero particulate, (b) minimum fiber volume with minimum particulate loading required to meet the failure threshold (2.1 lb), and (c) zero particulate and the minimum fiber loading required to meet the failure threshold (3.24 ft^3).

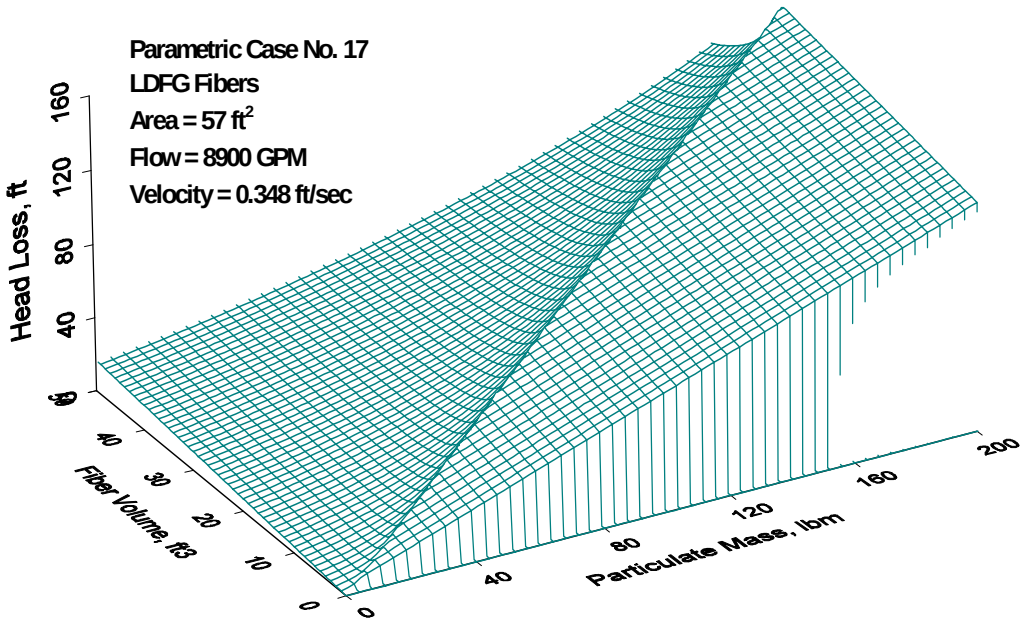

Fig. 3-9. Head-Loss Response Surface for Parametric Case 17.

[31] Similar adjustments were made for other qualitative grades (e.g., likely to very likely) as well. See Section 5 for further details.

Any combination of debris that lies on the contour of the failure condition will be referred to as an FTDL. This collection of points forms the failure-threshold function that is shown in Fig. 3-11 for SLOCA conditions in Case 17 for both favorable and unfavorable debris head-loss characteristics. Debris combinations that lie to the right of the curves will induce unacceptable head losses; combinations to the left will meet the ΔH_f performance criterion. The vertical line shared by both the favorable and unfavorable conditions simply emphasizes that any particulate mass above the threshold value corresponding to the minimum assumed fiber volume will cause excessive head loss. The box formed of dashed lines near the upper center of the figure delineates the approximate range of particulate and fiber loadings that might be expected to form on the screen. These ranges account for the generation and transport fractions in the manner described in Secs 3.2 and 3.3. For this case, all expected debris loadings lie in the failure region, and blockage is rated as **likely**, but for many of the parametric cases, the failure-threshold conditions intersect the range of expected. This implies that blockage is **possible**, and that plant features must be examined to identify any additional concerns.

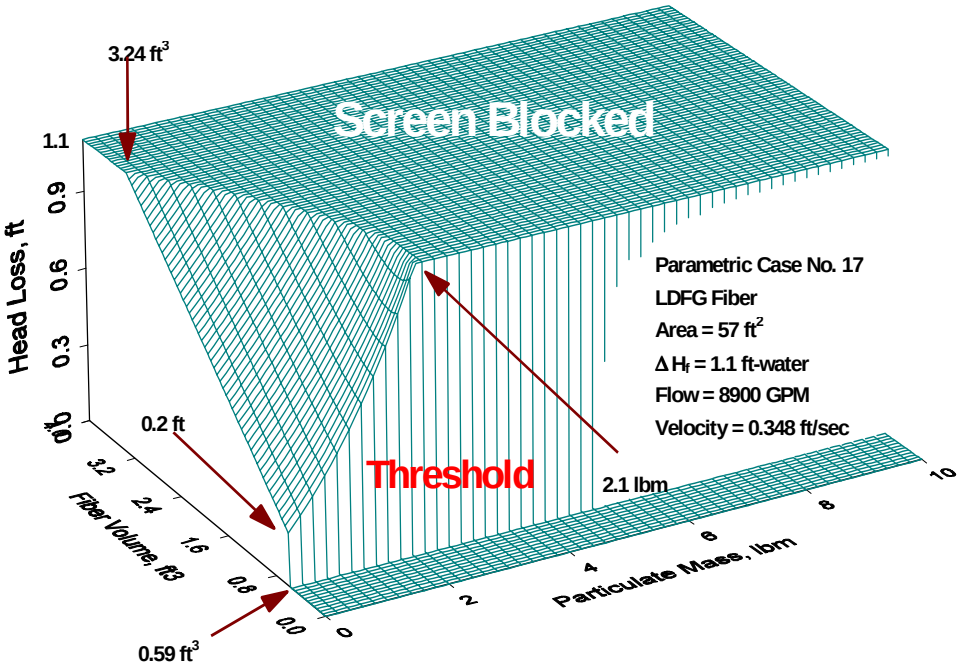

Fig. 3-10. Close-Up View of Head Loss Response Surface for Parametric Case 17.

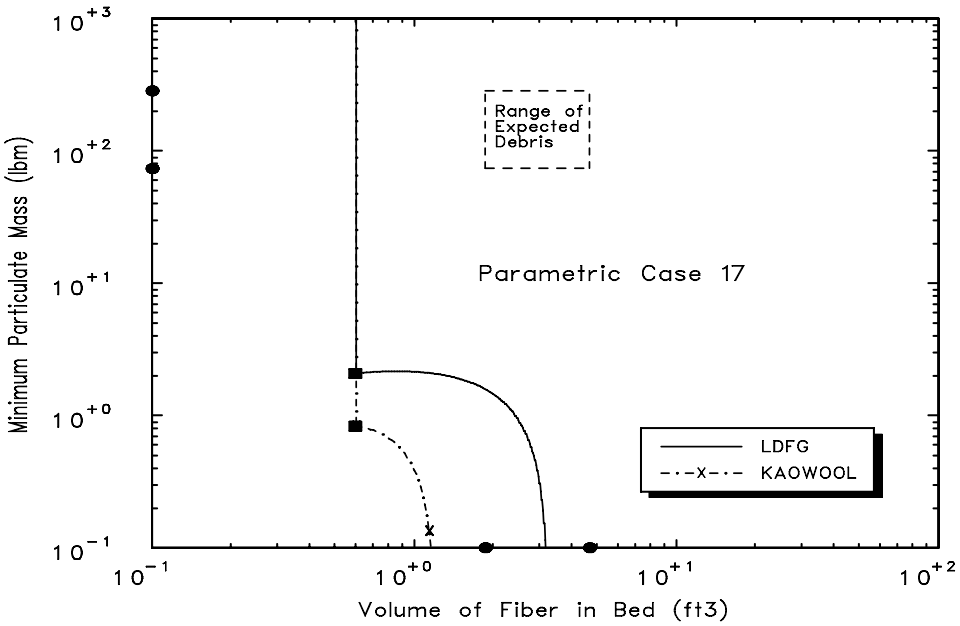

Fig. 3-11. Failure-Threshold Functions for Case 17 under SLOCA Conditions and Both Favorable (LDFG) and Unfavorable (Kaowool) Head-Loss Characteristics

Appendix B includes figures similar to Fig. 3-11 for all 69 parametric cases under both favorable and unfavorable head-loss assumptions for four flow conditions corresponding to SLOCA, MLOCA, LLOCA. Recall that the wetted screen area and the volumetric flow requirements together determine the face-averaged flow velocity of water approaching the screen. Summaries of these calculations and explanations of trends observed across the industry are presented in Sec. 5.0.

4.0 SAMPLE PARAMETRIC CALCULATION

Parametric calculations were performed for 69 cases to examine the potential for blockage of the sump screens by LOCA-generated debris. The parametric calculation approach and assumptions were discussed in Sec. 3. The results and limitations of these calculations are presented for all parametric calculations in Sec. 5. In this section, the calculation for one parametric case is presented to more completely illustrate the calculational approach. Parametric Case 17 was randomly chosen for demonstration purposes. Although Parametric Case 17 was chosen to closely represent a PWR unit (based on the unit's response to the Industry Survey and the unit's response to NRC GL 97-04 [US NRC, 1997]), it is possible that several differences exist between the data used in this analysis and the actual plant data. Therefore, these results, by themselves, should not be used to judge the susceptibility of a particular plant unit.

4.1 Description of the Parametric Case

The parameters used for the Case 17 calculation are listed in Table 4-1. As shown, the characteristics of this parametric case include both a relatively small sump-screen area and relatively large quantities of fibrous and cal-sil insulations; each is an indicator of likely screen blockage in the event of LOCA-generated debris. The following ECCS features characterize this parametric case.

- The safety injection (HPSI) pumps have an $NPSH_{Margin}$ of 13 ft-water; this value is significantly higher than that for RHR pumps or the CS pump in the recirculation mode (1.1 ft-water).[32] This is typical of most (but not all) operating PWRs. The $NPSH_{Margin}$ estimate assumes containment overpressurization.

- The plant has one of the smallest containments (10^6 ft^3 of free volume) and a CS actuation set point of 5.9 psig. Once again, several such PWR containments exist, and in all these cases, MELCOR calculations suggest that CS actuation is most likely even after a 2-in. line break.[33] Assuming that the CS pumps would actuate following a LOCA, the minimum recirculation flow (HPSI+CS flow) is approximately 8900 gpm, and maximum flow can reach 15,100 gpm. These values compare reasonably well with most of the operating PWRs in recirculation mode.

- The plant RCS is insulated with fiberglass, Kaowool, and jacketed cal-sil. The insulation on the other piping is not known and likely consists of fiberglass. Once again, this is typical of most operating plants. That is, inventories of insulations on non-RCS piping are not well accounted for in the survey.

- The screen hole size is 0.178 in.; which is larger than the median industry value but compares well with several plants.

[32]The plant IPE states that HPSI (three out of three pumps operating) is enough to make up for break flow following an LLOCA or SLOCA during recirculation mode. However, CS or RHR pumps would be necessary for decay heat removal.

[33]Sensitivity analyses examined the following possibilities for this case where a signal would isolate the chilled water supply to the fan coolers: aligning CCW for heat removal (an operator action not part of EOPs) and degraded fan-cooler performance caused by a fine layer of debris buildup.

Table 4-1. Plant Parameters Used in the Sample "Parametric-Case" Calculation.

Plant Parameter	Value
Sump-Screen Area	57 ft^2
NPSH Margin	1.1 ft-water CS and RHR 13 ft-water for HPSI
ECCS Pump Flow Rates (sprays on) SLOCA ECCS Flow (assuming CS) All ECCS Flow	 8,900 gpm 15,100 gpm
Sprays Activation Pressure	5 psig CS actuation likely for 2-in. line because containment volume is 10^6 ft^3 (relatively small)
Containment Free Area	Net area 6740 ft^2 Narrowest channel close to the strainer is 9 ft wide. Assuming that the6 ft water height in this channel flow area in the close proximity is about 60 ft^2; results in about 0.4 ft/s.
Fan Cooler	Not safety class.
Pool Levels At Switchover Maximum Height	 5.4 ft (@20 min) 6.78 ft (@24 min)
Sump Submergence	Completely submerged both at switchover and later. Base plant uses "cylindrical" basket strainers arranged vertically on the floor.
Sump Location	Remote
Sump-Screen Orientation	Vertical with respect to approaching flow
Sump-Screen Approach Velocity	SLOCA ECCS = 0.35 ft/s, All ECCS = 0.59 ft/s
Sump-Screen Clearance	0.178 in.
Insulation Types	Fiberglass blankets Kaowool blankets Jacketed cal-sil
Relative Fractions of Insulation Fibrous (fiberglass and Kaowool) Cal-Sil	 74.6% 25.4%

4.2 Minimum Debris Necessary to Induce Sump Failure

The failure threshold debris loading was obtained using the following steps.

Step #1. Define failure criterion.
Step #2. Define types of debris that might accumulate on the sump screen. This should include both fibrous and non-fibrous debris.
Step #3. Determine threshold debris loadings by inversing head-loss correlation (see Sec. 5.2 for further discussion).

Sump Failure Criterion

Because the sump screen would be completely submerged during the recirculation phase of ECCS core cooling, neither the screen area nor ΔH_f was limited by pool height, as was the case for several of the parametric cases. The sump failure criterion in this case is determined as follows for each system.

- *Containment Spray: ΔH across sump > 1.1 ft-water*
- *RHR: ΔH across sump > 1.1 ft-water*
- *HPSI: ΔH across sump screen > 13 ft-water*

The RHR heat exchangers are usually aligned with the LPSI system, which also acts as the RHR system during normal shutdown. When used as part of ECCS, the LPSI (RHR) system provides the necessary injection during the injection phase, but upon receiving a switchover signal, the RHR system is isolated and core make up is provided by HPSI only. Although, the operator can and may realign RHR to also provide reactor vessel makeup, it is not part of the licensing basis $NPSH_{Margin}$ estimates. The licensing basis estimates [US NRC, 1997] assume that only HPSI would be providing makeup water at a flow rate of approximately 1500 gpm (three pumps on two trains) and the CS system will provide for decay heat removal. At least one of the CS pumps must operate at full capacity to maintain sump water below the temperature used to estimate $NPSH_{Margin}$ for these pumps. Note also that the plant on which this parametric case is based takes limited credit for containment overpressure and/or sump water subcooling. These values were derived from containment modeling analyses.

Debris Sources and Types Used in Head Loss Estimation

This parametric case assumes that the piping is insulated by either fibrous or cal-sil insulation. The fibrous insulation was one of two types, either fiberglass or Kaowool; therefore, the fibrous debris formed on the screen could consist of either one of these types or a mixture of the two types. For this calculation, the fiberglass was represented by LDFG properties (typical of Nukon and Thermal Wrap). Because Kaowool is known to cause significantly larger head losses than LDFG, assuming Kaowool represented a less favorable assumption than assuming LDFG. Cal-sil was considered only as a particulate filtered by the fibrous debris bed. This was a favorable assumption because ongoing GSI-191 experiments have shown that cal-sil can itself accumulate on screens with clearances exceeding 1/8 in. and cause much more severe head losses than predicted by simply treating it as a particulate.

In addition to LOCA-generated insulation debris, other types of debris could accumulate. This debris could include dirt, dust, concrete dust, paint chips and particulate, corrosion products, and miscellaneous materials left inside the containment, such as duct tape and plastic tags. The LOCA jet would likely generate some of this debris, such as paint chips or concrete dust. For the parametric study, a generic composition of particulate with the approximate characteristics of dirt was assumed. The mass of miscellaneous particulate in containment was assumed to range from 100 to 500 lb. Applying the transport fraction leads to a range of particulate in the screen debris of 10 to 125 lb.

In summary, the head-loss analysis assumed the following.

- A fibrous layer would form on the strainer surface through accumulation of fibrous debris that is generated by LOCA jets and transported thereafter by recirculating water. "Favorable" analyses assumed that these fibers would consist of LDFG fibers, whereas Kaowool fibers were used in the "unfavorable" analyses.
- Head loss could be caused by fibers themselves and by filtration of particulate debris by the fiber bed. These particulates would include substantial quantities of cal-sil and miscellaneous particulates. The head loss is estimated assuming that all particulates are made of "dirt", which is a favorable assumption because BWROG studies have clearly shown that cal-sil results in very high head losses compared with dirt, dust, or any other particulate material (See Sec. 3 for discussion).

Threshold Quantities

The minimum mass of particulate needed for a specified fiber volume to reach the sump failure criterion (ΔH_f) was determined for various LOCAs in Figs. 4-1 through 4-4. Figures 4-1 through 4-3 present these threshold values for the CS system. Figure 4-4 presents these values for a SLOCA and blockage of the HPSI system. In all these figures, the minimum particulate mass is shown for both LDFG and Kaowool fibers. The following conclusions can be drawn from these figures.

- The inflection points of these figures (also denoted by square points) show that the screen in parametric case 17 could be blocked effectively with as little as 0.59 ft^3 of LDFG insulation debris.[34] This quantity of fibrous debris coupled with 2.1 lb of particulate debris is sufficient to reach the sump failure criterion (ΔH_f) for CS following a SLOCA. Even lower quantities of fiberglass and particulates would block the CS following a LLOCA. On the other hand, a larger quantity of particulate debris would be necessary to block the HPSI system. Specifically, a combination of 0.59 ft^3 of fiber and 21 lb of particulate debris will cause the sump failure criterion (ΔH_f) to be exceeded for the HPSI system.

- These figures also show that 3.24 ft^3 of LDFG debris and no particulate would be sufficient to reach the sump failure criterion (ΔH_f) for CS following a SLOCA.

- Note that in each case, the quantity of Kaowool necessary to reach the sump failure criterion (ΔH_f) is less than that calculated for LDFG.

In all these figures, a dashed square indicates the quantity of debris expected to reach the sump. The following section describes how these estimates were obtained for parametric case 17.

[34]With less fiber than this minimum, the fiber would not effectively filter the particulate from the flow stream.

4.3 Likely Quantity of Debris Expected to Accumulate on the Sump

The quantity of debris that likely will accumulate on the sump screen was estimated following the steps below.

1. Estimate the quantity of debris generated by the LOCA. This estimate should include insulation and non-insulation debris (e.g., concrete dust).

2. Estimate the quantity of debris that would be transported to the close proximity of the sump screen. This estimate is obtained by multiplying the quantity generated by the transport fraction.

Quantity of Insulation Debris Generated

A simple model was used to estimate the quantity of debris generated. This model (a) assumes that postulated SLOCA, MLOCA, and LLOCA[35] events would generate approximately 25 ft^3, 40 ft^3, and 1700 ft^3 of insulation, respectively, and (b) proportions that volume according to the containment-averaged fractions of different insulations present in the containment. For parametric case 17, where 74.6% was fibrous and 25.4% was cal-sil, the volumes of debris generated are shown in Table 4-2.

The basis for these assumptions and the associated uncertainties is discussed in Sec. 3.

Quantity of Non-Insulation Debris Generated

The only debris sources (other than insulation) considered in the present calculation are "miscellaneous particulates." A "generic value" of 100 to 500 lb was used in these calculations, where "favorable" estimates are based on a particulate mass of 100 lb and "unfavorable" estimates are based on 500 lb. These miscellaneous particulate estimates are to account for the following potential debris sources.

- *Dust and Dirt*. The BWROG URG suggests a "generic" value of 150 lb for this category. Given that PWRs have larger surface areas, quantities in excess of 150 lb are possible. See Sec. 3 for dust-loading estimates.

- *Precipitants*. All PWR containments have large exposed aluminum and zinc surfaces. Hot, high-pH borated water reacts with such surfaces and generates hydrogen and particulates with a median size of 10 microns.

- *Paint Dust*. Jet interactions with the paint could produce large volumes of paint dust as demonstrated by Heissdampfreaktor (HDR) tests. BWROG URG proposed a generic estimate of 85 lb.

- *Fire Barrier Materials*. Pabco rigid panel (approximately 200 ft^3) is used as the fire barrier material. Whether this material is susceptible to debris generation is not known. If it is comparable to Marinite, ongoing debris generation tests indicate that very little debris would be generated (unless the material is subjected to high radiation aging for long time, in which some debris generation is likely).

[35]The LLOCA contribution for case 17 also was estimated assuming reported debris to be on RCS piping. This special case resulted in 300 ft^3. This special case was run because Plant 17 reported only fibrous and cal-sil debris inventory in the containment. The rest is not included in the plant survey. This does not change the outcome.

- *Filter Materials and Other Miscellaneous Fibers*. The filters used are fiberglass, high-efficiency particulate air (HEPA) filters, and charcoal filters. None of these are located inside the missile shield; all are located in the annulus region. Potential for generation is probably minimal.

- *Failed Paint Coatings*. Approximately 200,000 ft^2 of steel and concrete surfaces are coated in the plant that formed the basis for parametric case 17. Use of the SRS results suggests that up to 25 ft^3 of paint debris may be generated by "failure" of a 1- to 2-mil-thick top layer during a LOCA.

Table 4-2. Estimates for Parametric Case 17 Insulation Debris Generation.

Break Size	Debris Generated (ft^3)		Miscellaneous Debris (lb)	
	Fibrous	Cal-Sil	Favorable	Unfavorable
SLOCA	18.7	6.4	100	500
MLOCA	29.8	10.2	100	500
LLOCA	1270	432	100	500

Debris Transport Fraction

The transport of LOCA-generated debris from the point of generation to the sump screen is also a very difficult and complex problem. For the parametric study, a simple approach was used to gain insights into the relative effect of debris transport on the potential for PWR sump screen blockage. Reasonable transport fractions were assumed to determine the quantities of insulation debris on the screen. The transport fractions are shown in Table 4-3 for conditions considered favorable and unfavorable to debris transport. These transport fractions are supported by the following characteristics for Parametric Case 17.

- Velocity in the annulus as compared with the transport velocities of the debris of interest
- Sump location with respect to spray drainage

Numerous experiments confirm these transport fractions.

Table 4-3. Estimates for Parametric Case 17 Debris Transport Fractions.

Transport Conditions	Favorable Estimate	Unfavorable Estimate
SLOCA with Sprays Inactive	5%	10%
SLOCA with Sprays Active All MLOCAs and LLOCAs	10%	25%

Debris Accumulation and Head Loss

The debris-generation quantities in Table 4-2 and the transport fractions in Table 4-3 determined the ranges of masses of debris expected to accumulate on the screen following a LOCA. These quantities are shown in Table 4-4. Note that cal-sil is listed in mass units to reflect that it was treated as a particulate (the density of cal-sil is nominally about 100 lb/ft^3).

The debris was assumed to be uniformly mixed and evenly spread across the screen. This assumption is supported by the following characteristics for parametric case 17.

- At a flow rate of 8,900 gpm, the screen approach velocity is 0.35 ft/s.

- At such high approach velocities, both cal-sil and fibrous insulation are found (experimentally) to form uniform beds. Beds as low as 0.1 in. tended to be uniform. Such uniform beds were built on screens with clearances of up to 1/4 in. (see the discussions in Sec. 3).

Table 4-4. Estimates for Parametric Case 17 Insulation Debris Accumulated on Screen.

Break Size	Range of Debris Accumulated	
	Favorable	Unfavorable
SLOCA	Fiber: 1.9 ft^3 Cal-Sil: 64 lb Misc.: 10 lb	Fiber: 4.7 ft^3 Cal-Sil: 159 lb Misc.: 125 lb
MLOCA	Fiber: 3.0 ft^3 Cal-Sil: 102 lb Misc.: 10 lb	Fiber: 7.5 ft^3 Cal-Sil: 254 lb Misc.: 125 lb
LLOCA	Fiber: 127 ft^3 Cal-Sil: 4320 lb Misc.: 10 lb	Fiber: 317 ft^3 Cal-Sil: 10800 lb Misc.: 125 lb

4.4 Sump Loss Potential

The values shown in Table 4-4 are plotted as the dashed box in Figs. 4-1 through 4-4. As demonstrated in these three figures, the boxes of expected debris ranges were far in excess of the minimum particulate masses needed to block the screen. It was judged **very likely** that the screens in parametric case 17 will be blocked by debris following a LOCA. This judgment also considers the effects of uncertainties, such as the unknown accident progression for a SLOCA and variability in the actual amount of debris generated.

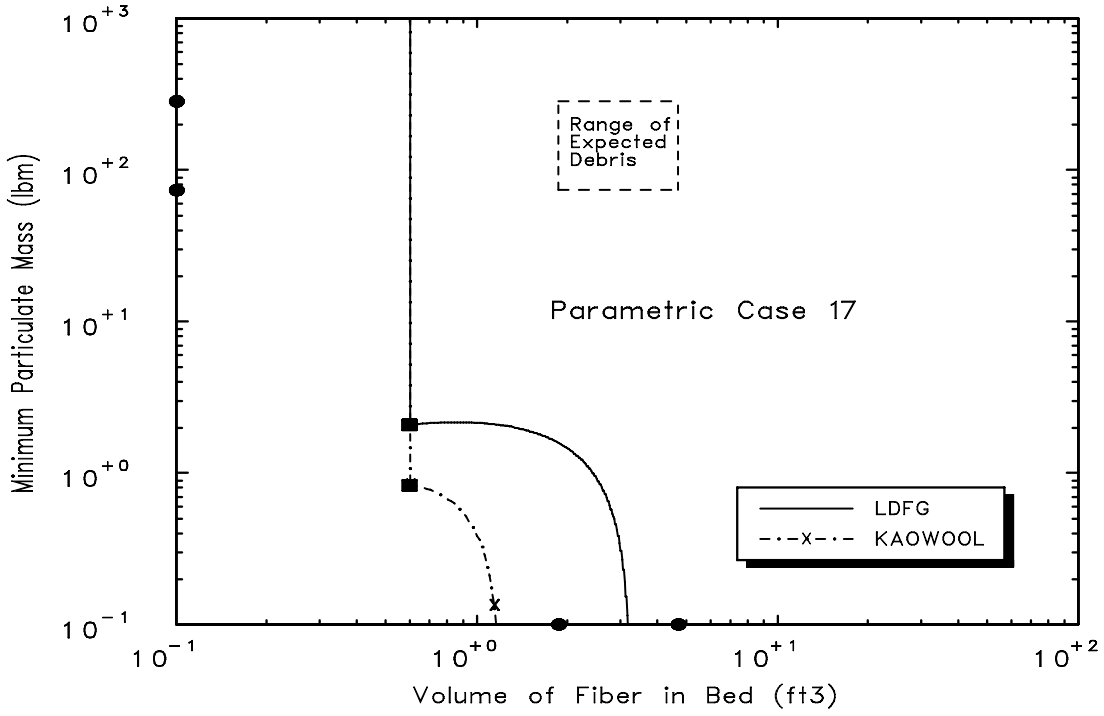

Fig. 4-1. Minimum Debris Loading Necessary for CS Failure Following an SLOCA.

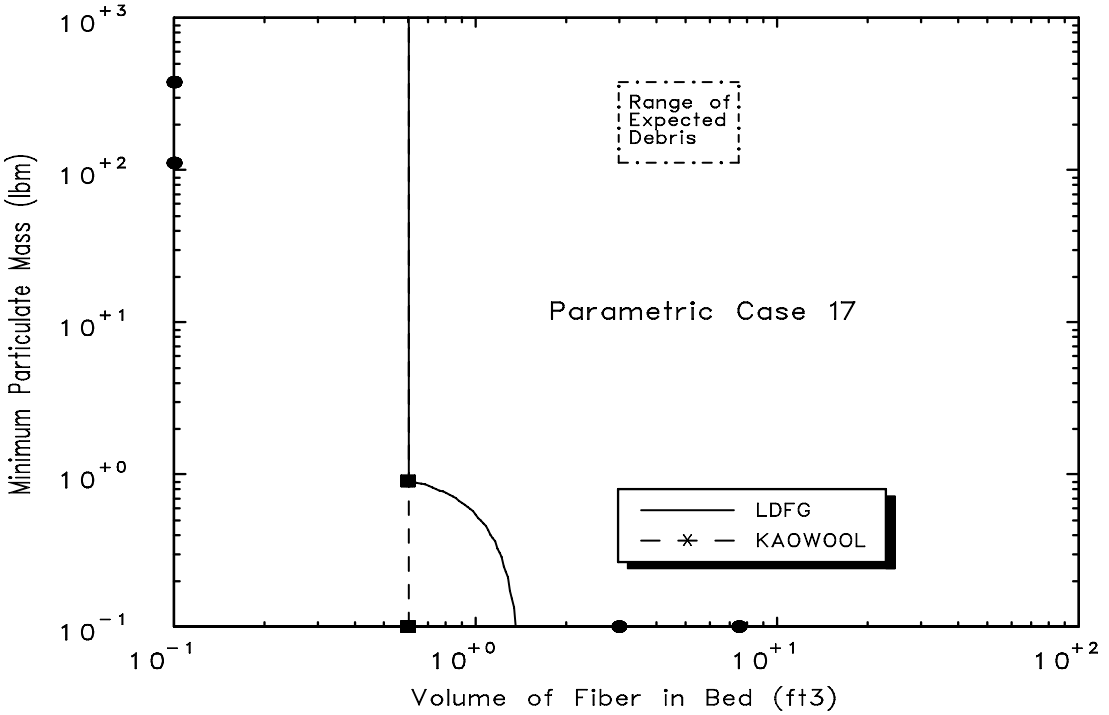

Fig. 4-2. Minimum Debris Loading Necessary for CS Failure following an MLOCA.

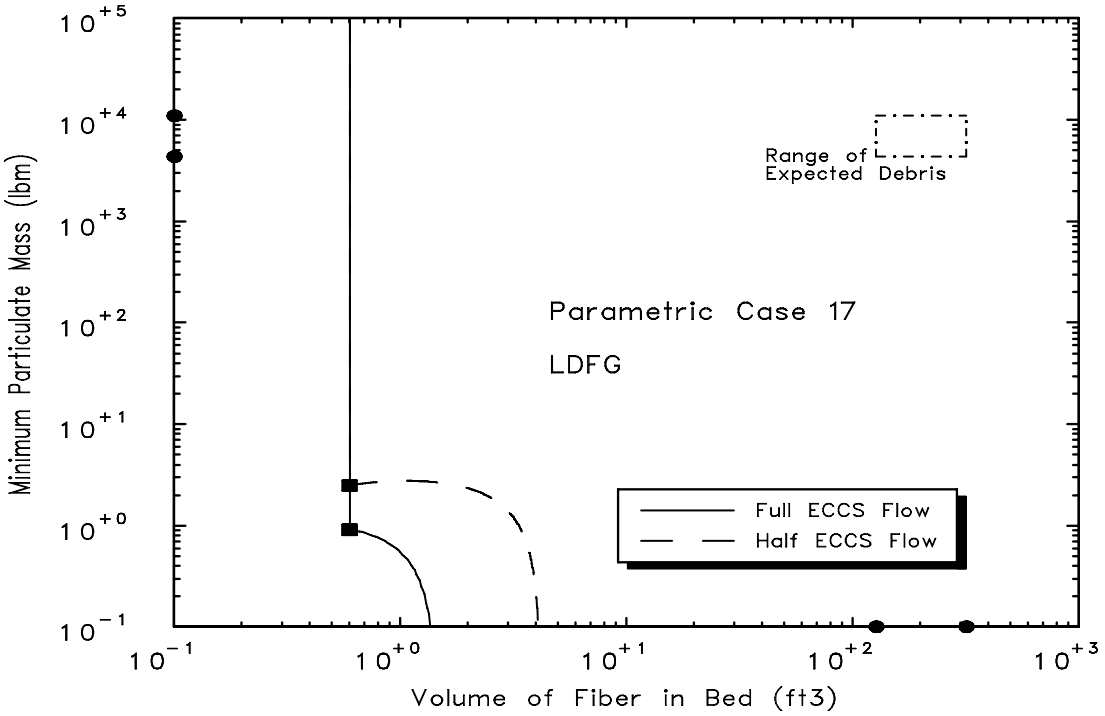

Fig. 4-3. Minimum Debris Loading Necessary for CS Failure following an LLOCA.

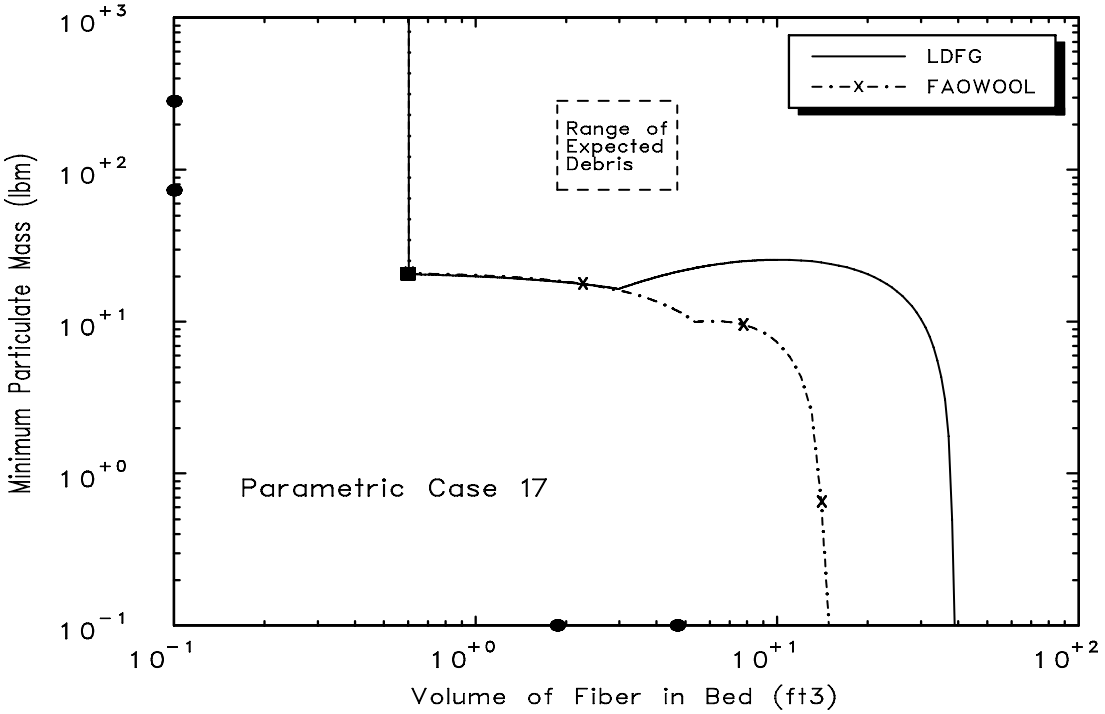

Fig. 4-4. Minimum Debris Loading Necessary for an SLOCA with HPSI Failure.

For parametric case 17, the fraction of the ZOI debris volume subsequently transported to the sump screen that would result in screen blockage was determined to be minimal. These minimum transport fractions are shown in Fig. 4-5 for each of the systems and break scenarios studied. Transport of less than 4% of the ZOI fibrous debris following a SLOCA may result in a FDTL on the sump screen. Because more debris would be generated following a MLOCA or LLOCA, the transport fractions for these events that result in the failure-threshold debris loading were even lower. The largest particulate transport fraction of 3.2% was for the HPSI system. It was higher than the corresponding SLOCA transport fraction of 0.3% for the CS system because the 13 ft-water ΔH_f for the HPSI was much higher than the 1.1 ft-water ΔH_f for the CS. In other words, it would take substantially more particulate mass to overcome the higher ΔH_f. However, even for the HPSI, the transport fractions needed to reach the ΔH_f were all relatively small.

Yet another way to look at the severity of the potential problem in parametric case 17 was to calculate the predicted head losses for both the estimated favorable and unfavorable debris screen loadings. These debris quantities are shown in Figs. 4-2, 4-3, and 4-4 for an SLOCA, MLOCA, and LLOCA, respectively. Specifically, the lower left corners of the dashed boxes represent the favorable conditions and the upper right corners represent the unfavorable conditions. These head losses are shown in Fig. 4-6. It is easily shown that these head losses all greatly exceeded the ΔH_f. In fact, most of these calculated head losses exceeded the recognized validity range of the head-loss correlation, but it must be concluded that the screen would very likely be blocked by all of these debris loadings.

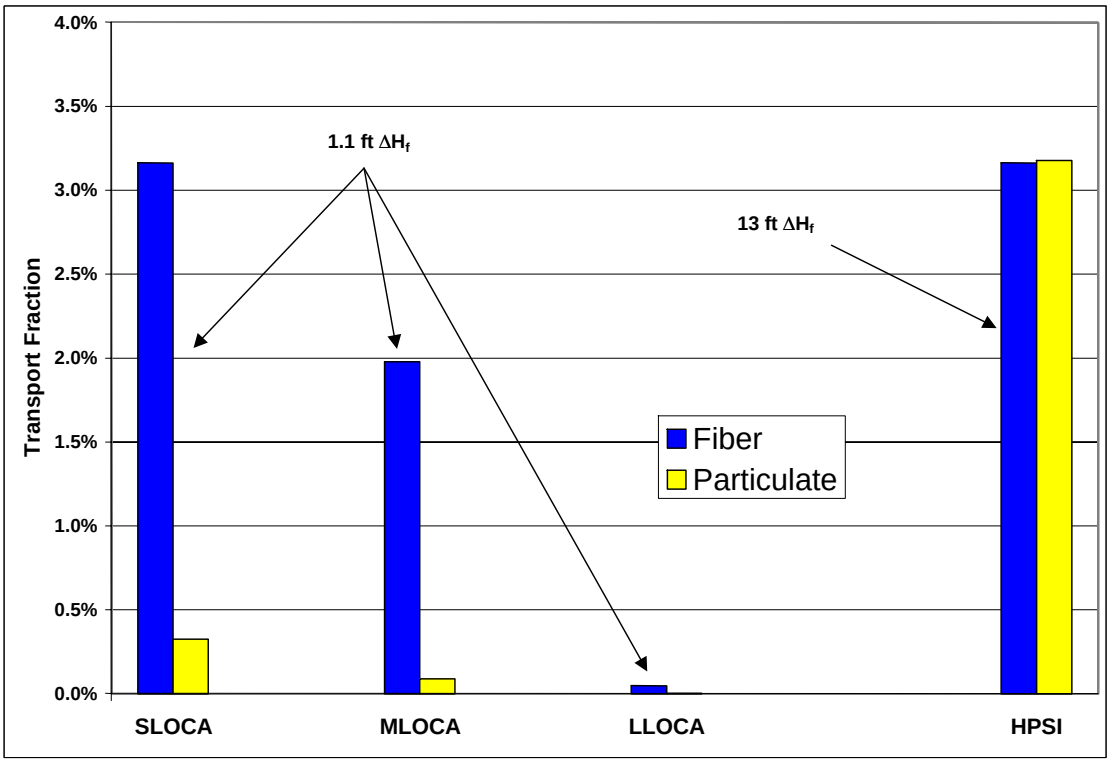

Fig. 4-5. Minimum Transport Fraction for Fiber and Particulate Debris.

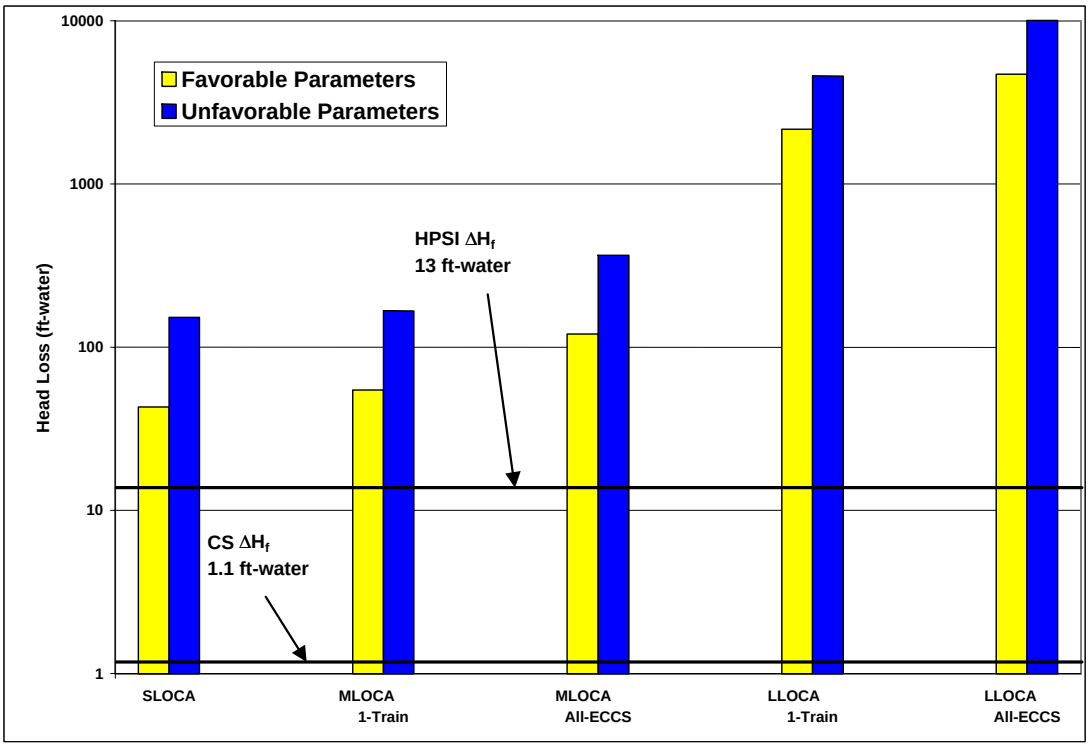

Fig. 4-6. Likely Pressure Drop across the Screen Caused by Debris Accumulation.

5.0 RESULTS OF THE PARAMETRIC CALCULATIONS

As explained in Sec. 1, each operating power plant was represented by a parametric case study using the best available information. In brief, each case was examined following the step-by-step procedure discussed in Sec. 4 to assess their individual vulnerability to sump blockage. Final determinations of the blockage potential for each case were expressed with a qualitative grade of **unlikely**, **possible**, **likely**, and **very likely**. The results of the parametric evaluations are presented and explained in this section. The input data that formed the bases for these evaluations are presented in Appendix A, and specific results for each parametric case are provided in Appendix B.

5.1 Description of the Parametric Case Set

As previously noted, central to each parametric case study is the best available physical description of an actual PWR. Within resource constraints, every attempt was made to base these parametric cases on the 69 operating PWRs, as described below.

- To the extent feasible, actual plant information was collected from available sources such as licensee responses to NRC GL 97-04 [US NRC, 1997], the GSI-191 Industry Survey [NEI, 1997], and plant UFSARs.

- Where sufficient information from these sources could not be obtained or the information included in those sources was incomplete, one of two options was undertaken. In the preferred option, sources such as NRC website data, the report "Overview and Comparison of US Commercial Nuclear Power Plants" [US NRC, 1990], or NUREGs developed as part of the USI A-43 study[36] [Serkiz, 1985; Wysocki, 1982; Wysocki, 1983; Kolbe, 1982; Weigand, 1982] were used to compile data that could be confirmed with either NRC or plant information sources.[37] Alternatively, data from units of similar type and vintage were adopted as surrogates for plant-specific descriptions.

Table 5-1 provides values for many of the important parameters that define each parametric case; a more detailed set of tables is included in Appendix A. The following general conclusions can be drawn regarding the accuracy and fidelity of the data presented in this table.

- Typically, information with high fidelity was available for the following parameters: (a) ECCS and CS flow rates following large- and medium-break LOCAs, (b) $NPSH_{Margin}$ for each pumping system, (c) time to ECCS switchover following large and medium LOCAs, (d) expected water levels on the containment floor at the time of ECCS switchover, (e) containment-averaged volumetric fraction of insulation in each insulation type, and (f) recirculation-sump geometry and containment-layout information. For these factors, parametric variations addressed issues such as the comparison between a single operational ECCS train and nominal full-flow plant performance.

- Information describing the accident progression following an SLOCA was not readily available in any of the official plant documents. Of particular interest was the status of CS following a SLOCA and the net flow through the recirculation sump. This gap in understanding of the SLOCA accident progression is a reflection of two facts: (a) the SLOCA (and MLOCA for that matter) has

[36]NUREGs from the USI A-43 study provided very valuable data. However, insulation information from these sources appears to be outdated because many plants continue to replace insulation with other types as needed.
[37]Insulation vendors confirmed the insulation data in some cases.

not been part of DBA or licensing-basis safety evaluations and (b) considerable variability exists between licensees in their ECCS and CS responses to SLOCAs. To overcome this gap, a series of RCS and containment simulations was carried out with the objective of determining the range of "favorable" and "unfavorable" conditions that could exist in the containment following a postulated SLOCA.

- Insulation information was available to the required detail for only two GSI-191 volunteer plants and six USI A-43 plants [Serkiz, 1985]. For the rest of the plants, available insulation information included (a) the types of insulation present on the RCS piping and (b) either the quantities of each type present in containment or the volumetric fraction of the total insulation belonging to each type. This information is not sufficient to perform precise debris-generation estimates because the locations of each insulation type in containment are not known. In fact, some of the plant estimates for even the volumetric fraction are tenuous. This is a reflection of the fact that licensees have not tracked rigorously the type(s), location(s), or quantities of different insulations in the containment[38]. Because only rough estimates of insulation composition were available, this generic assessment places more emphasis on estimating failure-threshold debris loadings than on estimating the quantities of debris generated and transported. Although the latter estimates also were used in determining the relative likelihood of plant blockage, they are just two of the many factors that were examined parametrically.

Despite some of these limitations, the case studies do serve their central purpose of providing a set of parametric samples that closely represent US PWRs. Therefore, the parametric analyses provide a reasonable representation of the magnitude of the sump-blockage problem, and the results can be used to gain valuable and defensible insights into the safety significance of this issue to the industry.

[38] This situation is very similar to the BWR experience at the onset of BWR study.

Table 5-1. Important Parameters that Define Parametric Case Studies.

Case	Reported Sump Screen Area	Reported NPSH Margin	Full ECCS Flow	Cont. Spray Act. Set-point	Switchover Pool Height	Maximum Pool Height	Height of Sump Screen	Sump Submergence	Sump Location	Open Cont. Floor Area	Sump Screen Hole Size	Fibrous Insulation	Reflective Metallic Insulation	Micro (Cal Sil) Insulation	Other Insulations
Units	ft^2	ft-water	GPM	psig	ft	ft	ft	-	-	ft^2	inch	%	%	%	%
1	42.4	10.02	7600	30	5.3	5.5	6	Partial	exposed	NR	0.125	yes	yes	yes	0
2	260	5	18424	18.2	2.24	4.7	6.25	Partial	remote	7400	0.115	13.4	85.7	0.9	0
3	210	3.8	19740	8.5	4.5	11	4.5	Fully	remote	13000	0.09	20.0	80.0	0	0
4	135	1.7	18416	2.9	5.5	14	NR	NR	NR	7000	0.204	50	50	<1	<<1
5	51.31	8.2	10000	NR	2.93	4.75	1	Fully	int. exp.	7500	0.25	yes	yes	yes	0
6	66	9	15600	2.9	NR	NR	5.25	Fully	int. exp.	NR	0.250	21	33	46	0
7	12.67	4.3	14200	20	0.82	6.1	1.5	At Max	NR	11682	0.152	0	100	0	0
8	135	1.7	18416	2.9	5.5	14	NR	NR	NR	7000	0.204	50	50	<1	<<1
9	11.64	2.6	14200	21.5	3.5	9.41	0	Fully	remote	15077	0.12	100.0	0	0	0
10	104	1.9	16000	14	1.92	7.5	3.5	At Max	int. exp.	10823	0.3	yes	yes	yes	yes
11	229	3	10498	4.75	5.25	5.25	3.5	Fully	exposed	10300	0.224	80.0	0	20.0	0
12	93.2	NR	7600	NR	5.33	6.89	below	Fully	NR	8497	0.25	yes	yes	0	0
13	214.4	NR	10000	30	1.74	5.89	below	Fully	remote	10415	0.125	9.0	91.0	0	0
14	204	0.96	10720	30	6	9.18	4.75	Fully	exposed	7700	0.132	17.4	67.5	15.2	0
15	368	0.54	14200	18	3.84	4.14	2.2	Fully	NR	11948	0.097	100	0	0	0
16	229	3	10498	4.75	5.25	5.25	3.5	Fully	exposed	10300	0.224	80.0	0	20.0	0
17	57	1.1	15100	5	5.4	6.78	3.5	Fully	remote	6740	0.1783	74.6	0	25.4	0
18	28.4	9.26	15600	2.81	2.5	13.2	3	At Max	exposed	4530	0.25	0	100	0	0
19	36.1	3.3	10300	22	2.1	4.1	below	Fully	int. exp.	NR	0.125	36.0	10.0	39.3	14.7
20	11.64	2.6	14200	21.5	3.5	9.41	0	Fully	remote	15077	0.12	100.0	0	0	0
21	225	7.35	16000	3	5.43	11.45	5	Fully	remote	NR	0.078	85	15	0	0
22	85.4	4.2	10498	25	1.5	5.5	0	Fully	NR	NR	0.221	yes	yes	yes	0
23	260	5	18424	18.2	2.24	4.7	6.25	Partial	remote	7400	0.115	13.4	85.7	0.9	0
24	12.67	4.3	14200	20	0.82	6.1	1.5	At Max	NR	11682	0.152	0	100	0	0
25	414	3.5	17400	9.5	3.6	NR	3	Fully	remote	NR	0.25	yes	yes	0	0
26	93	1.5	10720	10	4.27	4.27	below	Fully	exposed	8700	0.12	20.0	75.0	5.0	0
27	392	0.9	19920	27	2.12	4.41	8.667	Partial	remote	NR	0.125	yes	yes	0	yes
28	134	1.1	17500	25.3	3.67	5.5	3.75	At Max	remote	6273	0.125	55.0	30.0	15.0	0
29	12.67	4.3	14200	20	0.82	6.1	1.5	At Max	NR	11682	0.152	0	100	0	0
30	127.93	3.6	11836	22	2.73	5.42	5	At Max	int. exp.	3775	0.125	1	50	48	1
31	12.67	4.3	14200	20	0.82	6.1	1.5	At Max	NR	11682	0.152	0	100	0	0
32	168	0.7	12100	13.05	0.9	6.1	6.25	Partial	exposed	10464	0.1197	65.0	30.0	5.0	0
33	692	0.9	10008	27	1.9	4.5	7	Partial	NR	12300	0.25	yes	yes	yes	NR
34	51	13	7600	23	3.25	8.5	2.75	Fully	int. exp.	4690	NR	3.7	96.3	0	0
35	62.75	8.2	10000	NR	2.93	4.75	1	Fully	int. exp.	7500	0.25	yes	yes	yes	0
36	86.4	1.3	11000	30	4	7	below	Fully	remote	10714	0.25	50.0	30.0	0	20.0
37	158	0.83	10000	10.3	0.7	4.7	5	Partial	exposed	10545	0.75	35.0	60.0	5.0	0
38	210	3.8	19740	8.5	4.5	11	4.5	Fully	remote	13000	0.09	20.0	80.0	0	0
39	318	NR	12114	10	3	7.3	3	Fully	int. exp.	9500	0.125	40.0	60.0	0	0
40	201	0.9	15960	8	5.8	9.9	5	Fully	remote	9843	0.094	10	75	15	0
41	330	5.25	15600	3	7	21	6	Fully	NR	1710	0.12	60.0	40.0	0	0
42	134	3.9	17500	25.3	3.67	5.5	3.75	At Max	remote	6273	0.125	55.0	30.0	15.0	0
43	127.93	3.6	11836	22	2.73	5.42	5	At Max	int. exp.	3775	0.125	1	50	48	1
44	37.5	1.3	17610	27	3.5	9.5	2.5	Fully	int. exp.	9460	0.12	0.5	80.0	0.0	19.5
45	70	0	9625	3.7	3.5	6.83	0	Fully	NR	7497	0.132	yes	yes	yes	0
46	571	1.07	15330	NR	2.13	2.25	0	Fully	int. exp.	NR	0.25	87.0	10.0	3.0	0
47	48	0.97	13314	24	1.75	3.5	0	Fully	int. exp.	13265	0.25	31.9	8.9	42.2	17.0
48	168	0.7	12100	13.05	0.9	6.1	6.25	Partial	exposed	10464	0.1197	65.0	30.0	5.0	0
49	187.2	1.7	15600	3	8.52	14.42	8	Fully	exposed	4033	0.25	0	95.0	0	5.0
50	330	5.25	15600	3	7	21	6	Fully	NR	1710	0.12	20.0	80.0	0	0
51	150	0.62	17050	8.6	7	11.5	7	Fully	remote	7700	0.1875	9.3	31.7	59.0	0
52	210	3.8	19740	8.5	4.5	11	4.5	Fully	remote	13000	0.09	20.0	80.0	0	0
53	66	9	15600	2.9	NR	NR	5.25	Fully	int. exp.	NR	0.250	21	33	46	0
54	42.4	10.02	7600	30	5.3	5.5	6	Partial	exposed	NR	0.125	yes	yes	yes	0
55	115.4	1.01	10480	9.48	4.59	7.6	0	Fully	exposed	9310	0.09375	yes	yes	yes	0
56	37.5	1.3	17610	27	3.5	9.5	2.5	Fully	int. exp.	9460	0.12	0.5	80.0	0.0	19.5
57	39.62	17	9200	23	3.5	8	5.083	At Max	int. exp.	4930	1	1	61	38	0
58	NR	15.1	15900	8	NR	NR	NR	NR	NR	NR	NR	NR	NR	NR	NR
59	158	0.83	10000	10.3	0.7	4.7	5	Partial	exposed	10545	0.75	35.0	60.0	5.0	0
60	108	5.6	5600	28	2.78	5.4	below	Fully	exposed	6000	0.1875	44.5	6.4	12.7	36.4
61	51	13	7600	23	3.25	8.5	2.75	Fully	int. exp.	4690	NR	3.7	96.3	0	0
62	104	1.9	16000	14	1.92	7.5	3.5	At Max	int. exp.	10823	0.3	yes	yes	yes	yes
63	93	1.5	10720	10	4.27	4.27	below	Fully	exposed	8700	0.12	20.0	75.0	5.0	0
64	28.4	9.26	15600	2.81	2.5	13.2	3	At Max	exposed	4530	0.25	0	100	0	0
65	93	1.5	10720	10	4.27	4.27	below	Fully	exposed	8700	0.12	20.0	75.0	5.0	0
66	224	0.6	15800	8	5.8	9.9	5	Fully	remote	11318	NR	0	80	20	0
67	414	3.5	17400	9.5	3.6	NR	3	Fully	remote	NR	0.25	yes	yes	0	0
68	370	2.1	15300	NR	0.5	2.75	0	Fully	int. exp.	NR	0.25	15.0	60.0	25.0	0
69	125	2.4	11000	23	2	6.7	2	Fully	NR	8832	0.25	2.0	98.0	0	0

5.2 Failure-Threshold Debris Loadings

For each parametric case, the quantity of debris that would be necessary to cause sump-screen blockage of a magnitude sufficient to affect the performance of the ECCS and/or CS pumps was calculated following the steps described below. The results from each of these steps are discussed in the following subsections.

1. Define the failure criterion, ΔH_f, in terms of pressure loss across the screen. This failure criterion was based either on $NPSH_{Margin}$ or on pool depth as described in Sec. 1.

2. Compile a list of insulations that may be potentially present on the sump screen and identify the appropriate head-loss correlations for each type when they are present on the screen individually and in combination with other debris.

3. Estimate the debris quantities required to induce failure by iteratively solving debris-bed head-loss correlations taken from NUREG/CR-6224. In other words, the amount of debris needed on the screen was determined by solving the head-loss correlations with the failure criterion, ΔH_f, assumed as the pressure drop. This step defined all combinations of fiber and particulate that could result in an assumed failure of the sump as a result of excessive pressure drop across *each* screen defined in the parametric case studies. Results from these comprehensive calculations are presented graphically in Appendix B.

5.2.1 Definition of Sump Failure Criteria

The GSI-191 Industry Survey [NEI, 1997] queried each plant licensee for information about (see Fig. 5-1)

1. the height of water on the containment floor at the time of switchover following a postulated LOCA (Question 1a in survey) and
2. the height of the top of the sump screen measured from the containment floor (Question 3c in survey).

The responses were compared to identify those sumps that are expected to be fully submerged for the duration of the recirculation phase (i.e., Response 3c < Response 1a) and those that are expected to be only partially submerged (i.e., Response 3c > Response 1a). See Fig. 1-1 for schematics of submerged and partially submerged sumps.

Submerged Sumps

For completely submerged sumps, failure of the ECCS or CS was assumed to occur when sump-screen head loss exceeded the $NPSH_{Margin}$ for that pump. While applying this general criterion, some simplifications were made to address several interdependencies between various pumping systems.

- Some reactors depend on HPSI systems for core decay-heat removal during an SLOCA (e.g., a 2-in. break) and on the CS system for heat rejection from the sump. In these reactors, the HPSI pumps typically have a higher $NPSH_{Margin}$ (~10 ft) than the CS pumps (1 to 5 ft). Because the margins are so different for these systems, it is not clear what failure criterion should be used. As a first-order approximation, core damage could be assumed when the HPSI-pump $NPSH_{Margin}$ is lost. However, this approximation may not be accurate because loss of the CS system could permit the sump-water temperature to exceed the maximum temperature assumed in the HPSI-pump $NPSH_{Margin}$ calculation. The present study assumed that sump failure occurs when head loss across the screen exceeds the $NPSH_{Margin}$ of *either* of these systems. This assumption is only

important for an SLOCA in some large containments, and it has little or no effect on the outcome of the MLOCA and LLOCA sequences.

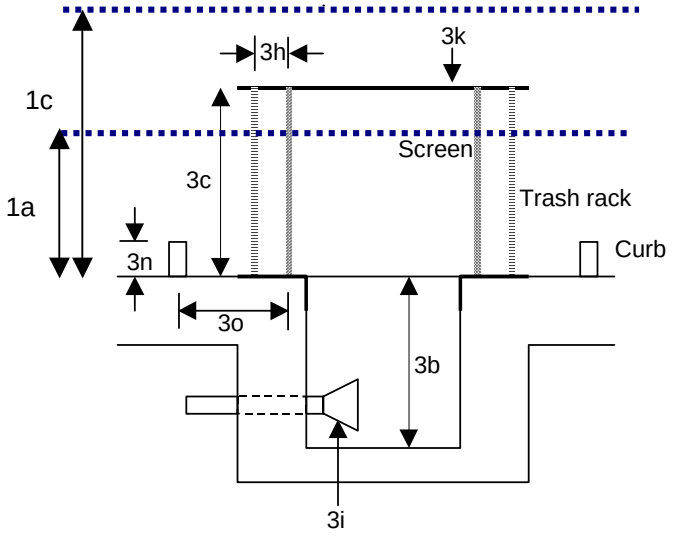

Question #	Information
3a	No. of cont. sumps
3b	Sump depth
3c	Height above floor
3d	Whether it has screen
3e	Screen area
3f	Screen hole size
3g	Trash rack status
3h	Dist. between trash rack and screen
3l	Trash rack area
3j	Trash rack hole size
3k	Solid plate
3l	Vortex suppressor
3m	Debris curb
3n	Debris curb height
3o	Dist. between debris curb and screen
1a	Height of water pool on containment floor at time of switchover
1c	Maximum height of water pool on the containment floor

Fig. 5-1. Illustration of Sump Parameters Queried in the GSI-191 Industry Survey.

- In the case of sub-atmospheric containments, inside recirculation pumps switch on within minutes after an LLOCA or MLOCA. During this time, the containment pool is very turbulent and debris is expected to be in suspension. As a result, these pumps may fail from debris blockage long before ECCS switchover occurs. Again, it is not clear what head-loss criterion should be used to determine success or failure. Sensitivity analyses suggest that this is not a major issue because both the inside recirculation pumps and the LPSI/CS pumps have approximately the same $NPSH_{Margin}$. The present study assumed sump failure when screen head losses exceeded the LPSI $NPSH_{Margin}$.

- Parametric analyses for all break sizes used NPSH margins estimated by the licensees for LLOCA flow conditions, and their calculations credit sources of water that would not be available for a MLOCA or SLOCA. Examples of these sources include water from accumulators and from the RCS inventory. As a result, the NPSH margins available following an SLOCA and MLOCA may actually be lower than the favorable values adopted here. However, it is likely that other conservatisms in the licensee estimates (e.g., no containment overpressure credit) partially compensate for these differences.

Partially Submerged Sumps

In the case of partially submerged sumps, failure was assumed if the screen head loss exceeded either (a) the $NPSH_{Margin}$ defined as discussed above or (b) 1/2 the pool height reported in response to Question 1(a) of the Industry Survey. A set of the parametric cases with screens that are only partially submerged at ECCS switchover and whose failure criteria are limited by the pool depth rather than by the $NPSH_{Margin}$ is shown in Fig. 5-2. Each case is described by a group of three vertical bars. The first bar shows the limiting $NPSH_{Margin}$ reported in the survey; the second bar shows the failure criterion, ΔH_f, that would be assumed for the parametric case if the pool were at maximum depth; and the third bar shows the failure criterion that would be assumed for the pool depth at ECCS switchover. Failure criteria for *all* parametric calculations were defined based on the pool depth at switchover (third bar for these

cases) because any significant debris transport will occur during recirculation at this depth and because maximum pool depths may only be reached much later in the accident sequence. It is clear from Fig. 5-2 that a partially submerged sump is much more vulnerable to failure by blockage than if the same screen is fully submerged.

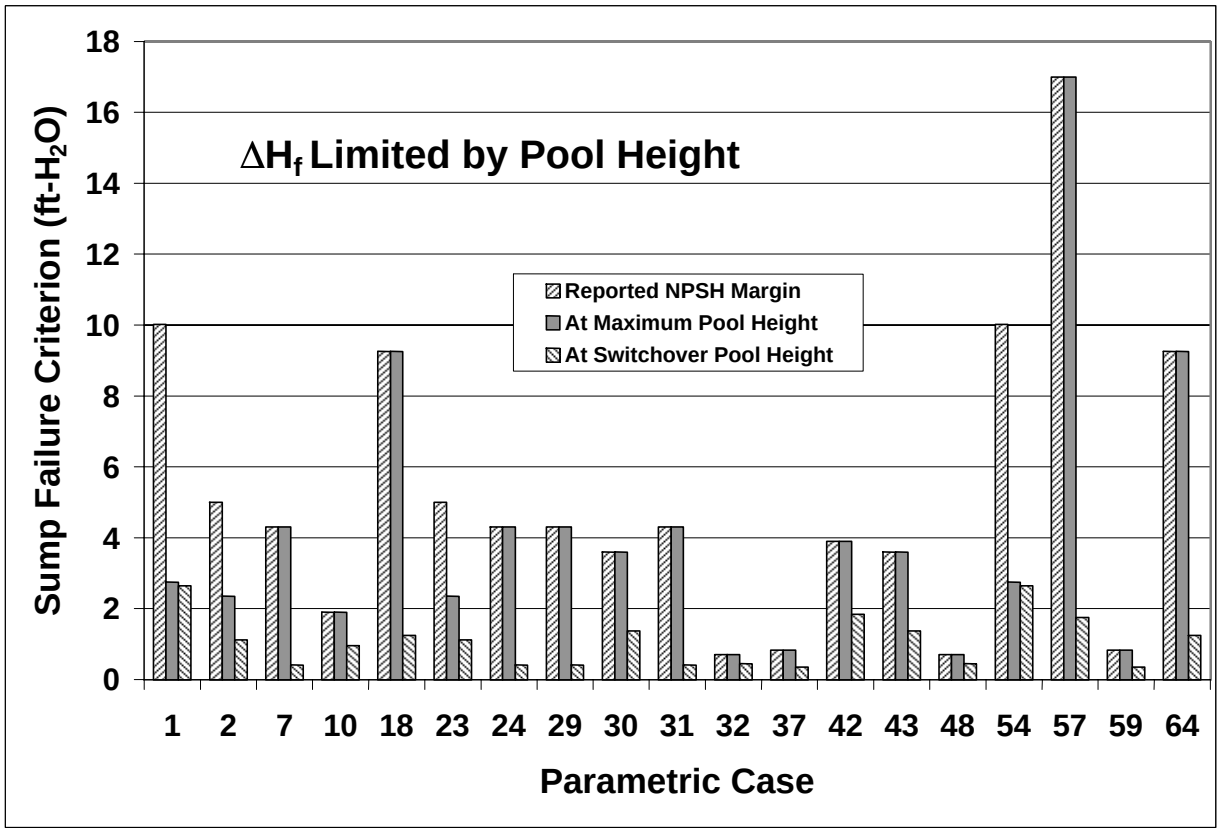

Figure 5-2. Effect of Partial Sump-Screen Submergence on Sump Failure Criterion.

Full or partial screen submergence also affects the area available for debris deposition, and it determines the water velocity through the screen for a constant volumetric flow rate. The screen area covered by the pool will be referred to as the "wetted" screen area. Larger wetted areas reduce the concern for blockage because (1) the screen-surface water velocities are lower, which reduces both debris transport and debris-bed head loss and (2) larger screens can accommodate more debris for the same thickness of bed. Wetted areas for all parametric cases with screens partially submerged at ECCS switchover are shown in Fig. 5-3. Again, each case is described by a group of three bars as defined for Fig. 5-2. Note that 13 of 25 cases transition from partially submerged to fully submerged as the pool fills to maximum depth (bars 2 and 3 equal) and that several plants reported screen areas that will never be covered by water (bar 1 > bar 2).

Wetted screen area and the assumed sump failure criterion, ΔH_f, are both important metrics used to determine the potential for debris blockage. Typically, both lower wetted area and lower available head increase the concern. Figure 5-4 plots the values assumed for these parameters in each case study. Note that many of the points represent multiple cases with nearly equivalent sump conditions.

This figure demonstrates that numerous parametric cases have combinations of low ΔH_f *and* small screen area and that most cases have failure conditions of less than 6 ft-water and screen areas less than 200 ft^2.

5.2.2 Types of Debris Expected to Reach the Sump

Information regarding the types of debris present in containment was used in the head-loss model to estimate FTDLs for each case. Table 5-1 provides the proportions of each insulation type that were assumed to be present in the containment. As explained in Sec. 3, any debris generated and transported to the screen was assumed to have the same proportional composition. This implies that the insulation is distributed homogeneously throughout the containment when, in fact, important spatial dependencies have been observed in the detailed volunteer-plant data. A generic debris type referred to here as "particulate" augments the reported insulation list. This type is used to represent particulate debris that is expected to be either present in the containment at the time of a LOCA or generated during the course of the LOCA progression. Reasonable particulate loadings on the sump screen range from 10 to 125 lbm.

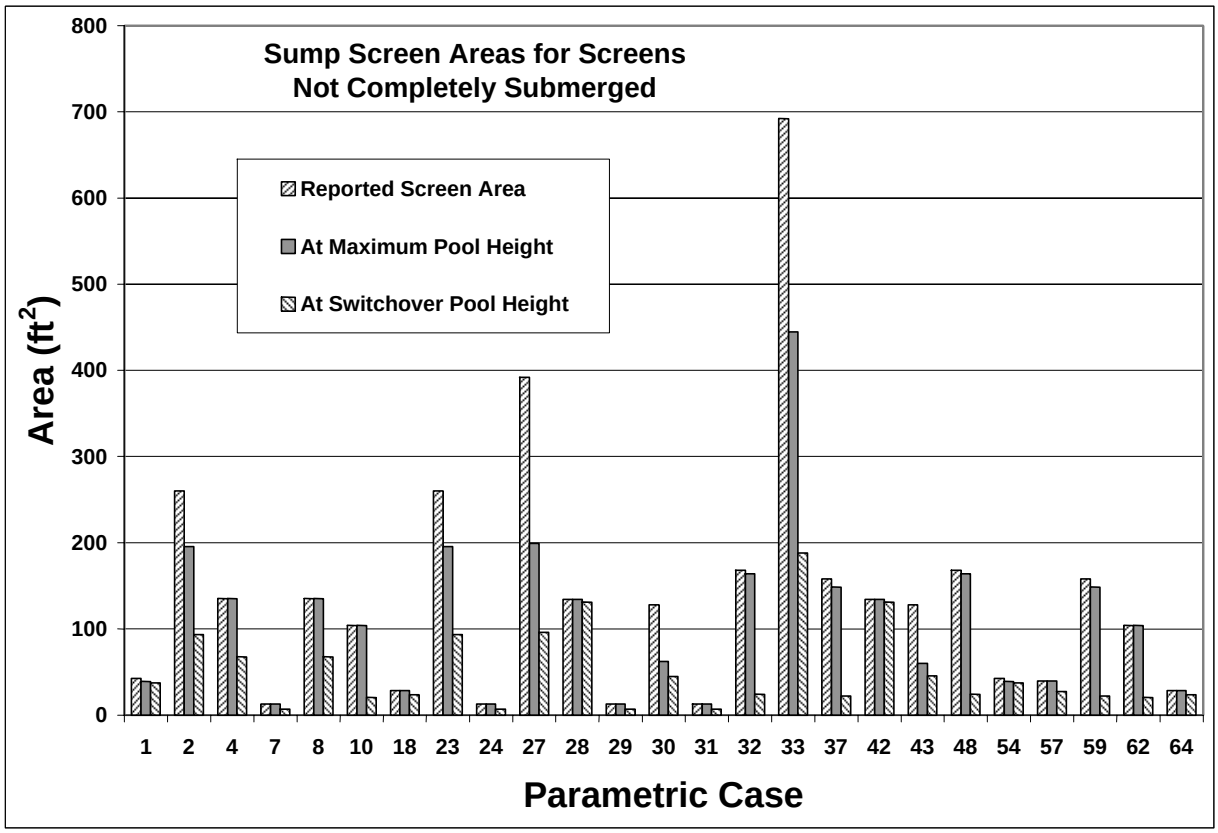

Fig. 5-3. Impact of Pool Submergence on Sump Screen Area.

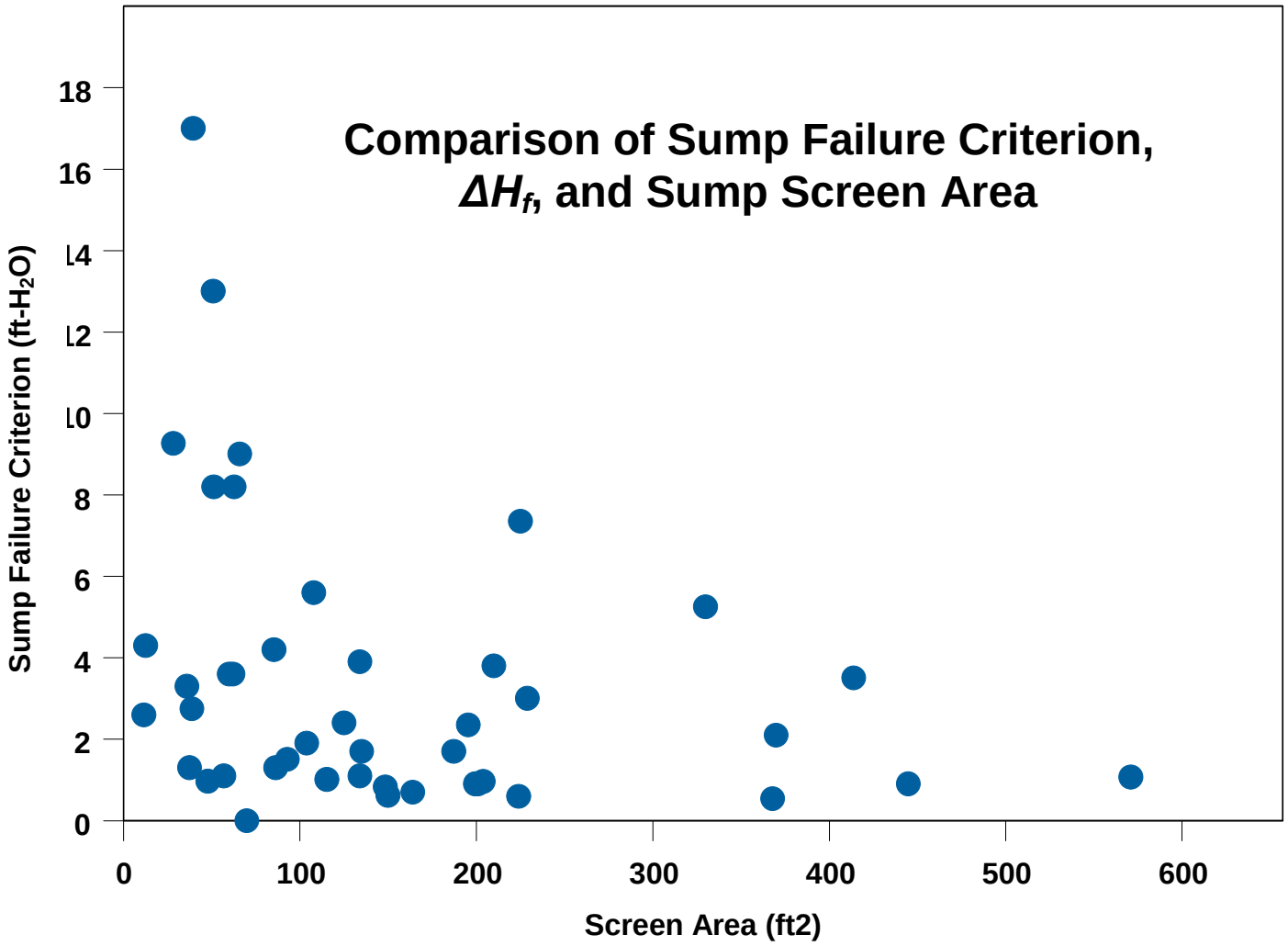

Fig. 5-4. Comparison of Sump Failure Criteria and Sump Screen Areas for All Parametric Cases.

5.2.3 Failure-Threshold RMI Debris Loading

For each parametric case, the threshold stainless-steel[39] RMI quantity needed on the screen to induce sump failure is shown in Fig. 5-5 for both an SLOCA (dark bars in back) and an LLOCA (light bars in front). Also plotted on the figure are the estimated volumes (from Table 3-3) of insulation that may be damaged by the corresponding ZOI (assuming an insulation composition of 100% RMI) and the quantities of foil expected to be separated from the cassettes.[40] Note that the amount of RMI debris needed to block the sump is always greater for an SLOCA than for an LLOCA because the recirculation flow velocities are lower, and thus, the debris bed must be thicker to cause the same head loss. Case number 45 is unique because it has such a low $NPSH_{Margin}$ that very small amounts of debris will fail the sump (bar not shown in figure).

For an LLOCA, failure-threshold RMI debris volumes range between 1 ft^3 and 3 x 10^4 ft^3. Considering that the maximum quantity of RMI-foil shreds generated in a LLOCA ZOI would be approximately 560 ft^3, blockage by RMI debris is unlikely for most parametric cases unless the transport fraction to the sump exceeds about 0.18 (100 ft^3/560 ft^3). Several additional arguments eliminate many of the remaining cases.

(1) Few have large proportions of RMI insulation in containment.
(2) The ZOI may be smaller for some RMI types than the 12D zone assumed here, so the volume of RMI debris may be overestimated.
(3) Bulk flow velocities in excess of 0.4 ft/s would be necessary to transport RMI debris on the floor, making RMI one of the least transportable debris types expected in containment.
(4) Screen approach velocities in excess of 1 ft/s are required for upward movement of debris near a curb [Maji, 2000].

For an SLOCA, the above arguments are even more severe, and only a very small subset of the parametric cases needs to be examined for potential RMI blockage. This subset may include cases 45, 32, 37, 48, and 59.

Realistically, plant susceptibility to RMI debris is unlikely to be an industry-wide concern and is probably only valid for a small subset of the parametric cases that have (a) large volumes of RMI insulation, (b) exposed sump locations with horizontal screens at or below floor level, and (c) no curbing surrounding the sump.

---

[39] The GSI-191 survey suggests that PWRs exclusively used stainless-steel RMI on the primary piping. A few plants used aluminum RMI on the reactor vessel, but that is not a major source of debris in the present evaluations. Therefore, the analyses and conclusions stated here should not be extrapolated to all types of RMI.

[40] Debris generation testing has shown that approximately 33% of damaged cassettes are reduced to shredded foil [BWRORG, 1998].

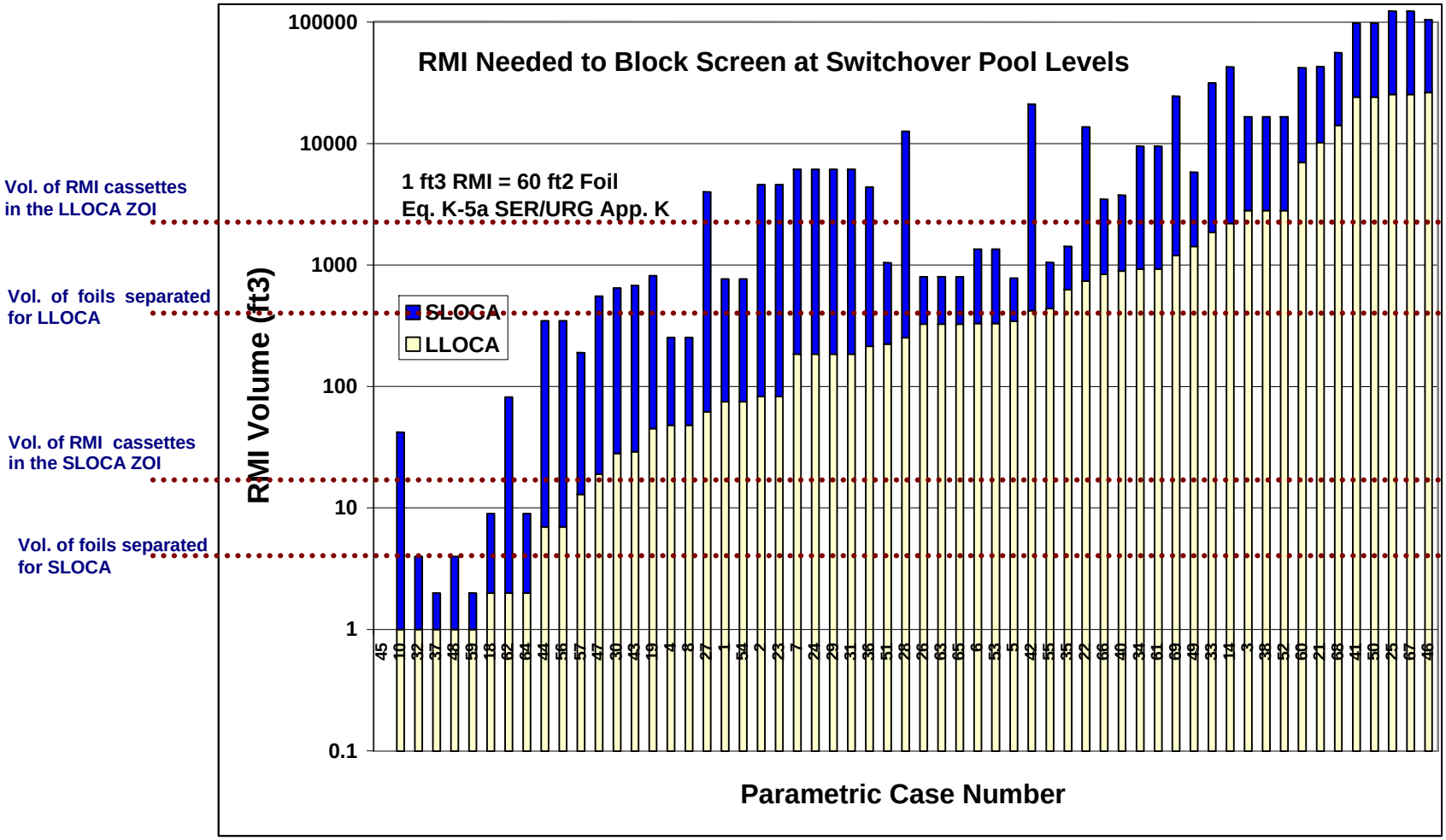

Fig. 5-5. Failure-Threshold RMI Debris Loading for Each Parametric Case.

5.2.4 Threshold Quantities for Fiber and Particulate Accumulation

For each parametric case, the threshold fiber and particulate quantities necessary to induce blockage were calculated. Appendix B presents these results graphically, and this section provides a summary of the findings.

Testing and calculations confirm that blockage can occur in one of two ways.

1. The first and most likely means for blockage involves formation of a thin fibrous bed on the screen, which then filters incoming particulates. Tests performed as part of the BWROG study demonstrated that beds with a nominal thickness of 1/8 in. could filter significant fractions of debris approaching the strainer and induce large differential pressure drops.[41] The filtration of particulates by thin layers of fiber (the "thin-bed effect") is the most limiting mechanism for sump blockage for many plants, especially following an SLOCA because (a) relatively small quantities of fibers are necessary to build a 1/8-in.-thick debris layer on the screen surface, (b) large quantities of particulate debris are already present in containment in the form of resident dirt and dust, and (c) significant quantities of particulate debris can be generated as a result of a LOCA.

2. The second mechanism for blockage involves formation of a thick-cake fiber layer on the surface with minimal particulates present. Tests performed as part of the BWROG study demonstrated that substantial head losses can be induced by pure fiber beds. Pure fiber beds are not realistic for a PWR LOCA accident scenario given the resident dust and the potential to damage particulate insulation types, but they are included in this discussion to demonstrate that blockage concerns are not driven solely by the presence of particulates.

Recent preliminary tests suggest that a screen clearance of 1/8 in. also can be obstructed by cal-sil granules alone without the presence of a fiber mat for enhanced filtration. Further testing is required to determine the sump conditions under which this blockage mechanism may be a concern, so it was not considered in the parametric analyses. Thus, if the minimum fiber needed for a 1/8-in. bed is not present, the sump was assumed to function adequately with any mass of particulate loading.

Figure 5-6 provides estimates for the volume of fibrous debris needed to build a 1/8-in.-thick contiguous debris bed on the wetted screen surface. For most parametric cases, this is the minimum quantity of fiber that would be necessary to cause sump failure if it were combined with a sufficient mass of particulate. Cases with large, partially submerged screen areas can accommodate more fiber as the water level rises (dark bars in background). Note that at switchover pool levels, over half of the cases can tolerate less than 1 ft^3 of fiber debris if sufficient particulate is present in the pool. Figure 5-7 presents the associated particulate masses necessary to cause sump failure in combination with the minimum fiber volume. Note that the first nine cases can fail on the minimum fiber loading alone without any contribution from particulates, and over half of the cases can fail with less than 50 lb of particulate on the minimum fiber bed, even for SLOCA flow conditions.

Figures 5-8 and 5-9 present, respectively, the cumulative distributions of the same data that are presented in Figs. 5-6 and 5-7. The cumulative distribution of minimum fiber volume (Fig. 5-8) simply shows the total number of parametric cases with minimum fiber volumes less than or equal to any value of interest. The cumulative distribution of failure-threshold particulate mass is similar except that ranges

[41] The ongoing GSI-191 study performed several tests to confirm the validity of this assumption for PWRs where some sump screens are oriented vertically and in some cases the screen clearance is as large as ¼ in. Section 3 discusses the experimental findings, which essentially are (a) uniform and contiguous LDFG debris layers can form at nominal thicknesses as low as 1/10 in., (b) these beds can filter significant quantities of cal-sil and other particulate debris, and (c) filtration can cause large pressure drops across an obstructed screen.

are provided to illustrate the number of cases that would fail at a given particulate loading under both favorable and unfavorable head-loss conditions.

From these two cumulative plots, the following conclusions can be drawn.

1. The minimum amount of fibrous debris necessary to cause sump failure varies from 0.25 ft^3 to 6 ft^3. This range is a direct reflection of variability in sump-screen areas across the PWR population. As shown in Fig. 5-8, transport and accumulation of approximately 1/2 ft^3 of fibrous material would be sufficient to raise blockage concerns for approximately 20 parametric cases; this number reaches 40 when the fiber volume is increased to 1 ft^3. As discussed in later sections, these are very small volumes compared with the quantity of debris that might be generated following a LOCA.

2. The failure-threshold particulate debris mass ranged from 2 lb to 175 lb for a LLOCA and from 5 lb to 300 lb for an SLOCA. For each break size, the ranges are a strong function of the variability in screen areas, and the difference between the two break sizes is caused primarily by the different recirculation water demands of the two accident scenarios. As shown in Fig. 5-9, a particulate loading of approximately 10 to 20 lb is adequate to meet the sump failure criteria for about 30 of the parametric cases, even following an SLOCA.

In summary, calculations of head loss for mixed debris beds on the sump screens of each parametric case indicate that the potential for blockage by a combination of fibrous and particulate debris is high. Because of the very small quantities of debris required in many cases to exceed the sump failure criteria, careful consideration of the potential fiber and particulate debris sources is needed.[42]

[42]In this context, it should be recognized that several of the BWR precursor events in the U.S. involved miscellaneous fiber sources such as air-handling-unit (AHU) filters.

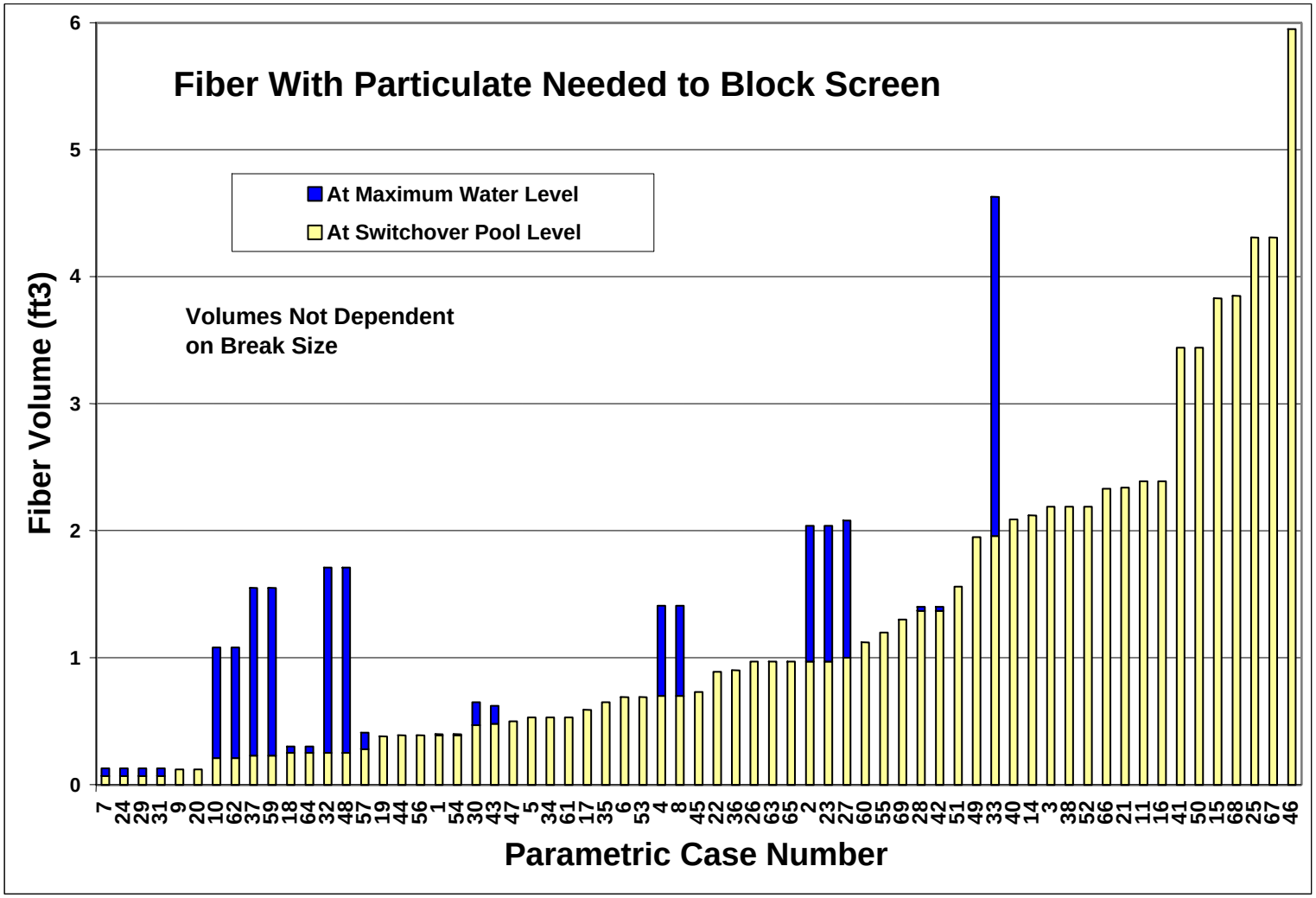

Fig. 5-6. Failure-Threshold Fiber Debris Loading for Each Parametric Case.

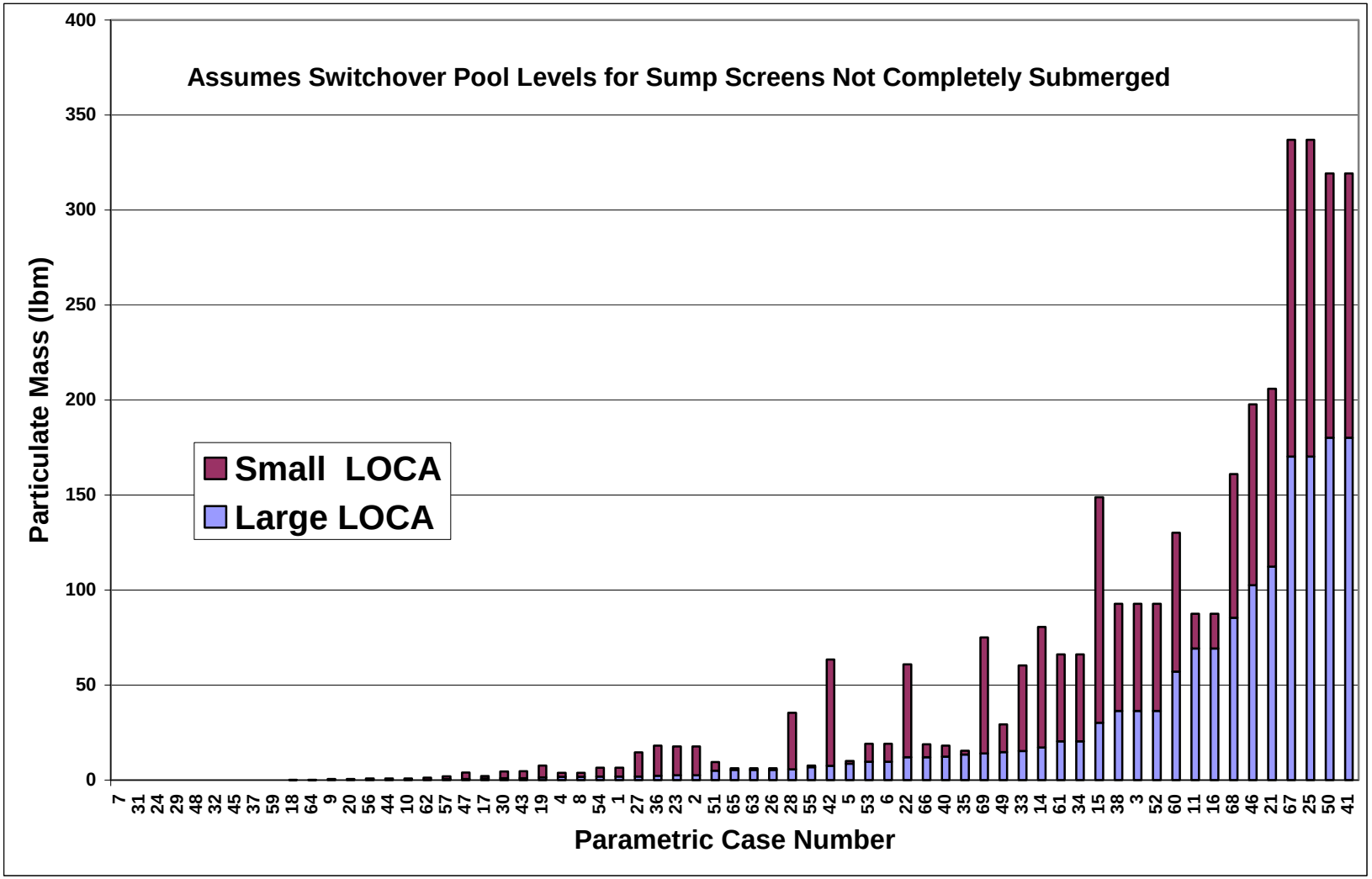

Fig. 5-7. Failure-Threshold Particulate Debris Loading for Each Parametric Case.

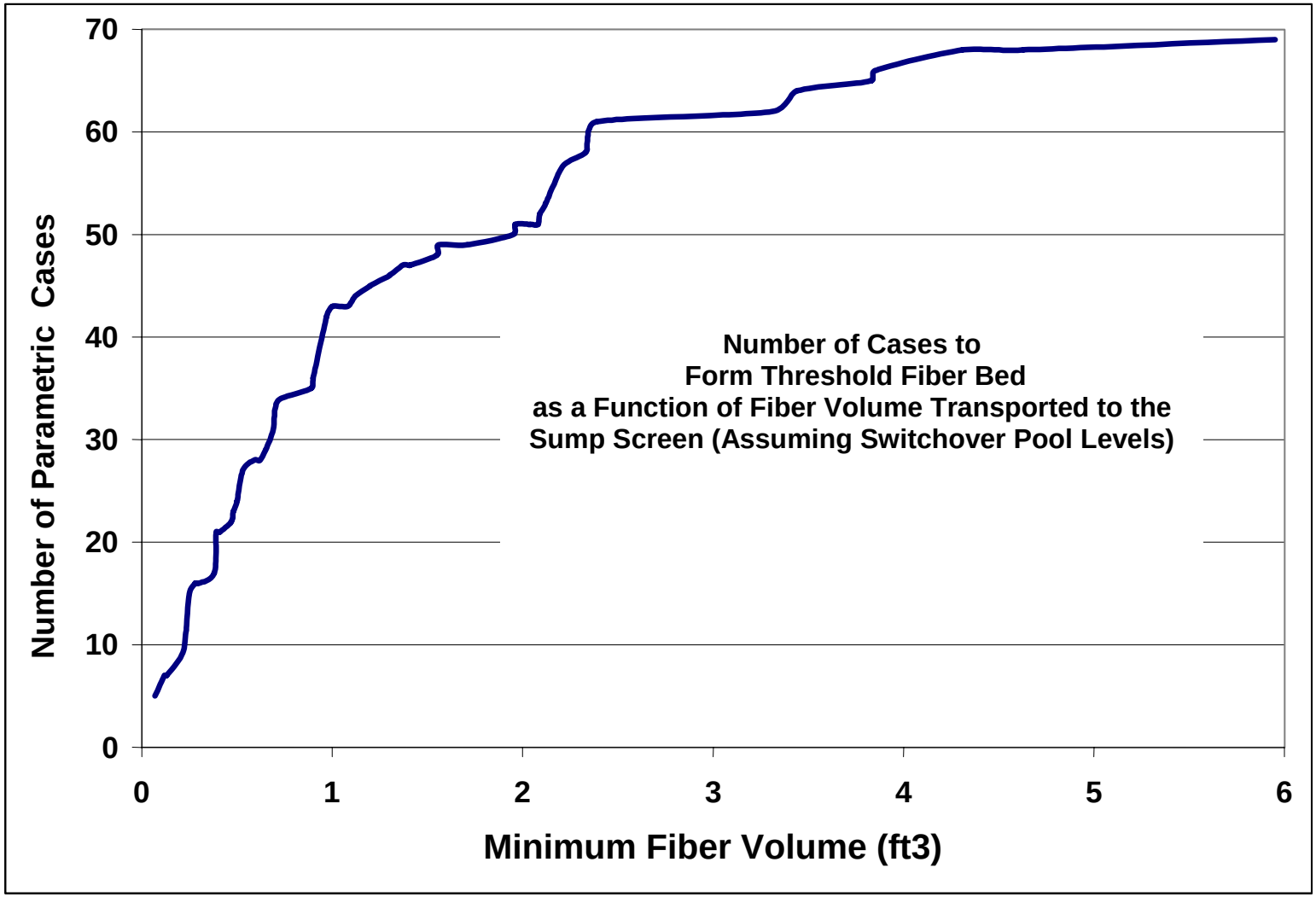

Fig. 5-8. Cumulative Distribution of Failure-Threshold Fiber Volume.

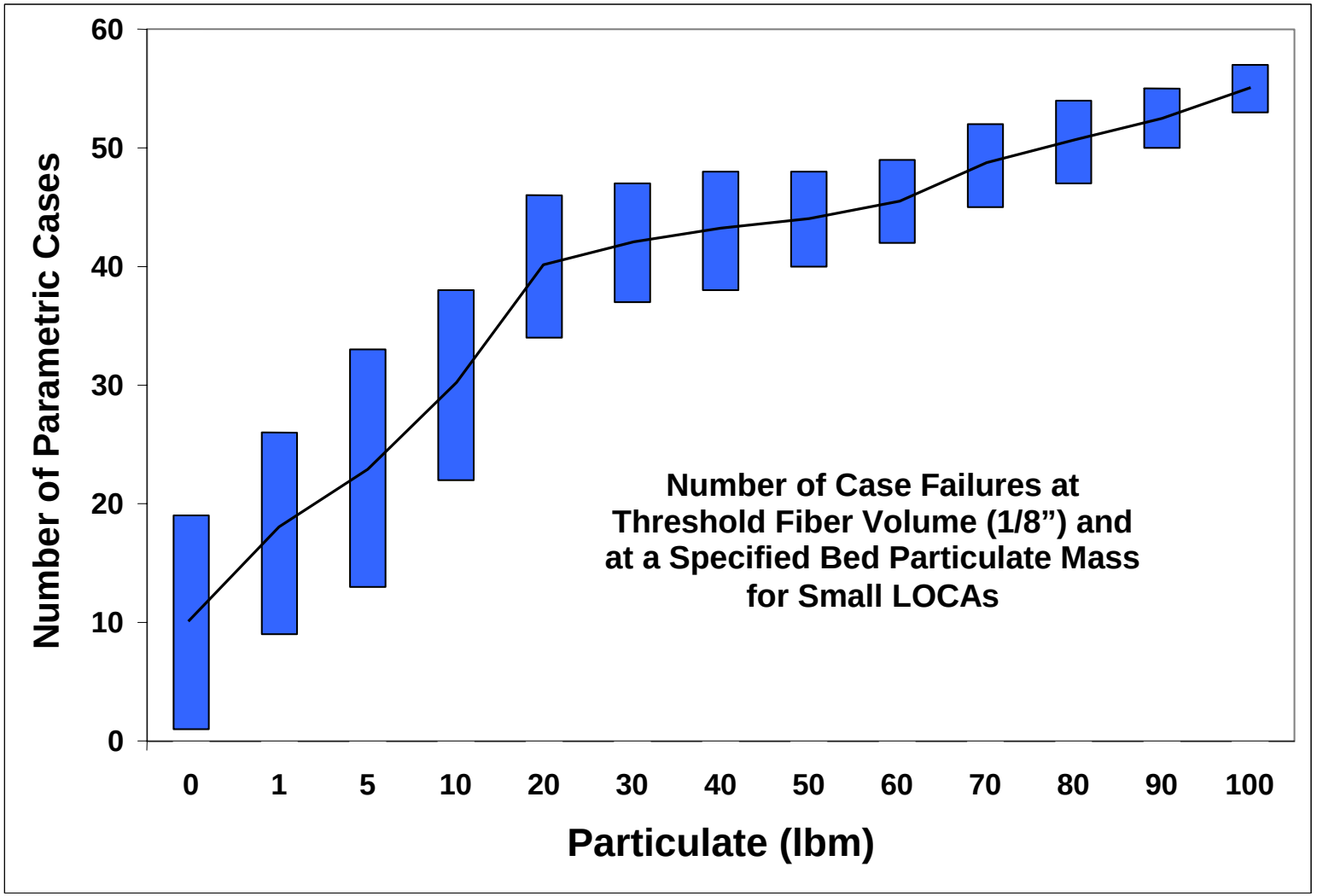

Fig. 5-9. Cumulative Distribution of Failure-Threshold Particulate Mass Corresponding to an SLOCA.

5.3 Quantity of Debris Expected to Accumulate at the Sump

Sources of Debris and Estimates for Volumes

Table 5-2 presents "generic" estimates for the quantity of insulation contained in the ZOI for each of the postulated break sizes. It should be noted that these values are not "bounding" estimates,[43] but rather are 95th percentile values as shown in Table 3-2. Section 3 provides further calculational bases for these estimates. In addition to debris generated by a break jet, there may be a significant inventory of dust and dirt in containment that represents an additional source of particulate debris. Table 5-2 includes a range of reasonable estimates of this inventory that are based on considerations of total surface area and dust-layer thickness.

Table 5-2. "Generic" Estimates of Insulation and Noninsulation Debris Volumes.

Break Size	Insulation Debris ZOI Inventory (ft^3)	Miscellaneous Particulate Debris in Containment (lbm)	
		Favorable	Unfavorable
SLOCA	25	100	500
MLOCA	40	100	500
LLOCA	1700	100	500

The next and final step in estimating the insulation debris source term is to proportion the ZOI volumes given in Table 5-2 according to the insulation fractions. Containment-averaged insulation fractions were provided by the licensees as part of the GSI-191 survey (Questions 5c and 5d). The following uncertainties exist in the debris generation estimates.

1. The ZOI estimates are based on interpretations of very preliminary debris generation test data obtained for cal-sil and preformed fiberglass blankets.

2. Case studies for the GSI-191 plants have shown that a majority of SLOCAs generate debris volumes substantially lower than the 25 ft^3 assumed above; however, the higher value was chosen to compensate for the fact that proportioning the ZOI volume by the insulation fractions tends to underestimate the quantity of fibrous or cal-sil debris generated because these insulation types are typically located on smaller pipes. Thus, the local proportion of fiber near a small break may be much higher than the containment-averaged proportion. This is not a major issue for the LLOCA or MLOCA, where sufficiently large quantities of debris are generated by most breaks and the ZOIs are, in general, large enough to envelop a large portion of the insulation in containment.

3. The only debris source other than insulation that was credited in the present calculation was "miscellaneous particulates." A "generic range" of 100 lb to 500 lb was used with a "favorable" estimate of 100 lb and an "unfavorable" estimate of 500 lb. DBA models for zinc and aluminum oxidation and paint dust inventories from the SRS study indicate a potential for the generation of significantly higher quantities of particulate.

[43] Limiting debris volumes were estimated as 28 ft^3, 50 ft^3, and 1900 ft^3 for the SLOCA, MLCOA, and LLOCA, respectively.

Minimum Transport Fraction

Another metric that is very useful to judge the relative potential for sump blockage is the minimum transport fraction required for failure. This figure of merit is a measure of the smallest fraction of debris present in the ZOI that would have to be transported to the sump screen before the FTDL is attained. This parameter is defined as

Min Transport Fraction = Threshold Debris Volume / Generated Debris Volume.

Figures 5-10 through 5-15 present the estimated minimum transport fractions for fibrous and particulate debris corresponding to LLOCA and SLOCA breaks. Figures 5-10 and 5-11 present SLOCA failure-threshold transport fractions for each parametric case for fiber and particulate, respectively. Figure 5-12 presents the minimum LLOCA particulate transport fraction for each case, but minimum fiber transport fractions for LLOCA were not illustrated because they were lower than 10% for all parametric cases. Figures 13 through 15 present the corresponding information in a cumulative format so that it is convenient to read the number of plants affected by transport fractions up to any value of interest. For example, Fig. 5-13 shows that sumps would fail in a SLOCA for 15 of the 60 parametric cases that contain fibrous insulation if the fiber transport fraction reaches 0.1 (10%). Further examination of these figures suggests the following conclusions.

- Very small fractions of the fiber debris generated (i.e., ZOI insulation volume) coupled with very small fractions of resident particulates would be necessary to cause blockage following a LLOCA. As shown in the cumulative distribution plots, 10% transport is sufficient to block the sump screens of virtually all the parametric cases in which fibrous insulation is present.

- Minimum sump-failure transport fractions for an SLOCA are higher than those for an LLOCA and in some cases reach nearly 100%. This is a reflection of the fact that SLOCAs have small ZOIs and lower recirculation flow rates. (Another issue is that HPSI systems generally tended to have larger $NPSH_{Margins}$).

Debris Transport:

Assessments over all parametric cases of the minimum transport fraction required to induce sump failure facilitate a comparison between the transport fractions of concern (minimum required for failure) and the transport fractions that are plausible under various accident scenarios. For example, if all parametric cases required that 90% of the generated debris be transported to the screen before failure occurred, then the industry-wide vulnerability would be very low because very few transport mechanisms are that efficient and the FTDLs would never be reached. However, a significant number of parametric cases were found to be vulnerable to transport fractions below 10%. Variability in the accident scenarios (particularly for SLOCAs) and limitations in the ability to predict detailed debris transport phenomena make it impossible to prove that transport fractions of 10% cannot occur. Recent transport testing has demonstrated that transport fractions of up to 25% are possible for some configurations of sump location, debris location and flow rates. Therefore, the favorable and unfavorable fractions defined in Table 5-3 were selected as reasonable values to use in this study. Section 3 discussed the fidelity of these estimated transport fractions in greater detail.

Table 5-3. Transport Fractions Used in the Parametric Study.

Transport Conditions	Favorable Transport Conditions	Unfavorable Transport Conditions
SLOCA with sprays inactive	5%	10%
SLOCA with sprays active All MLOCAs and LLOCAs where sprays would automatically activate	10%	25%

Debris Accumulation

The debris generation quantities and the transport fractions in Table 5-3 determine the ranges of debris masses expected to accumulate on the screen following a LOCA. These quantities are shown in Tables 5-4 and 5-5 for fiber and particulate debris, respectively. Note that cal-sil is listed in mass units to indicate that it was treated as a particulate. (The density of cal-sil is nominally about 100 lb/ft^3). Parametric case-specific plots in Appendix B compare the ranges of debris that might accumulate on the screen with the ranges necessary to cause sump failure.

Head Loss

All debris reaching the sump was assumed to be uniformly mixed and evenly spread across the screen. This assumption was validated for several different approach velocities and screen orientations as described in Sec. 3.

Head loss estimates were based on the research and experience associated with the resolution of the BWR strainer blockage issue. For fibrous debris beds, the NUREG/CR-6224 correlation was used. This correlation has been verified for (a) fibrous debris of different types (e.g., Nukon, ThermalWrap, or Kaowool) and (b) miscellaneous particulates (e.g., sludge). This correlation has not been validated for application with cal-sil debris or for use with some other types of miscellaneous debris. As shown in Sec. 3, this approach considerably underpredicts the effect of cal-sil by as much as an order of magnitude.

Table 5-6 presents the head-loss estimates obtained under favorable assumptions and unfavorable assumptions for the SLOCA, MLOCA, and LLOCA for all parametric cases.

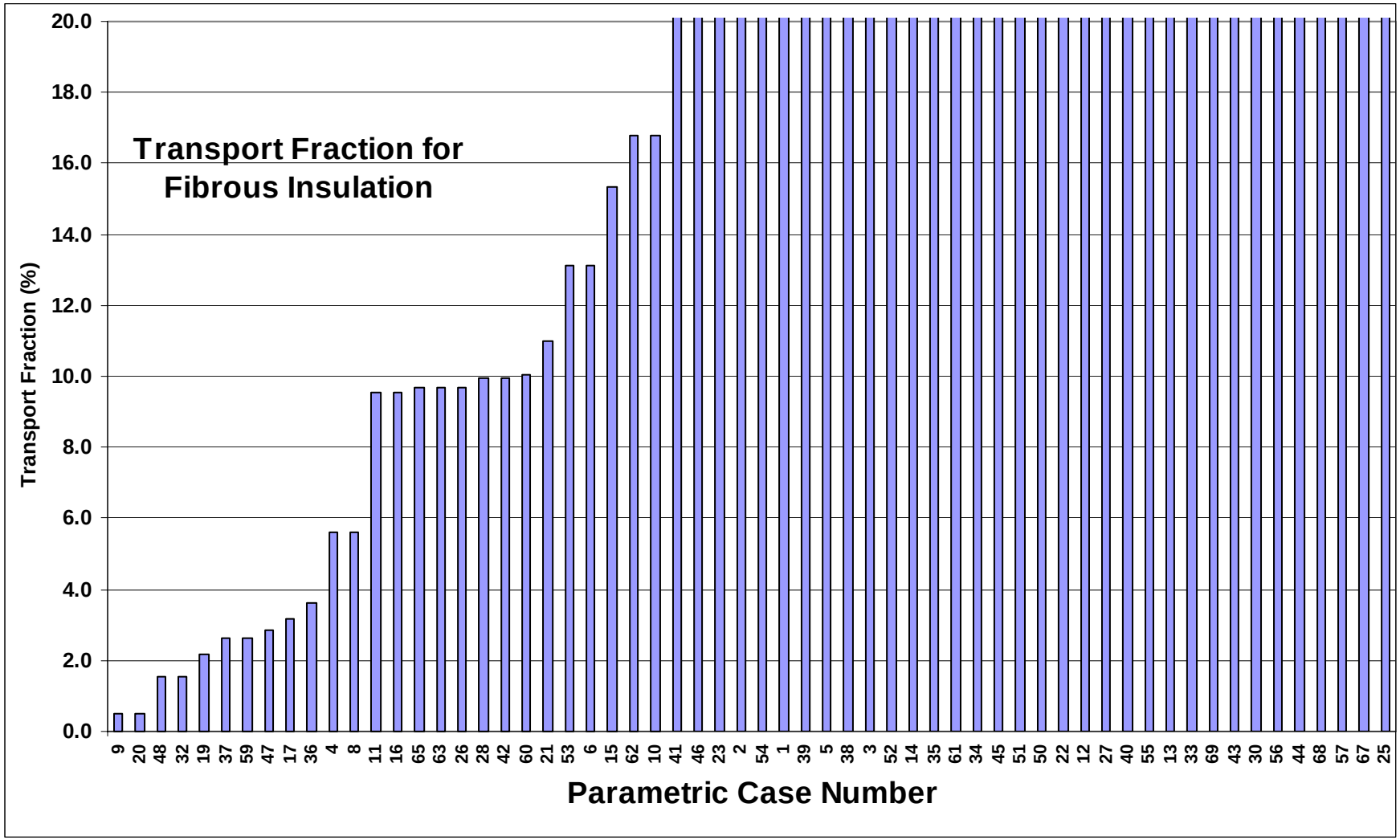

Fig. 5-10. Transport Fraction for Minimum Fibrous Insulation Volume for SLOCA.

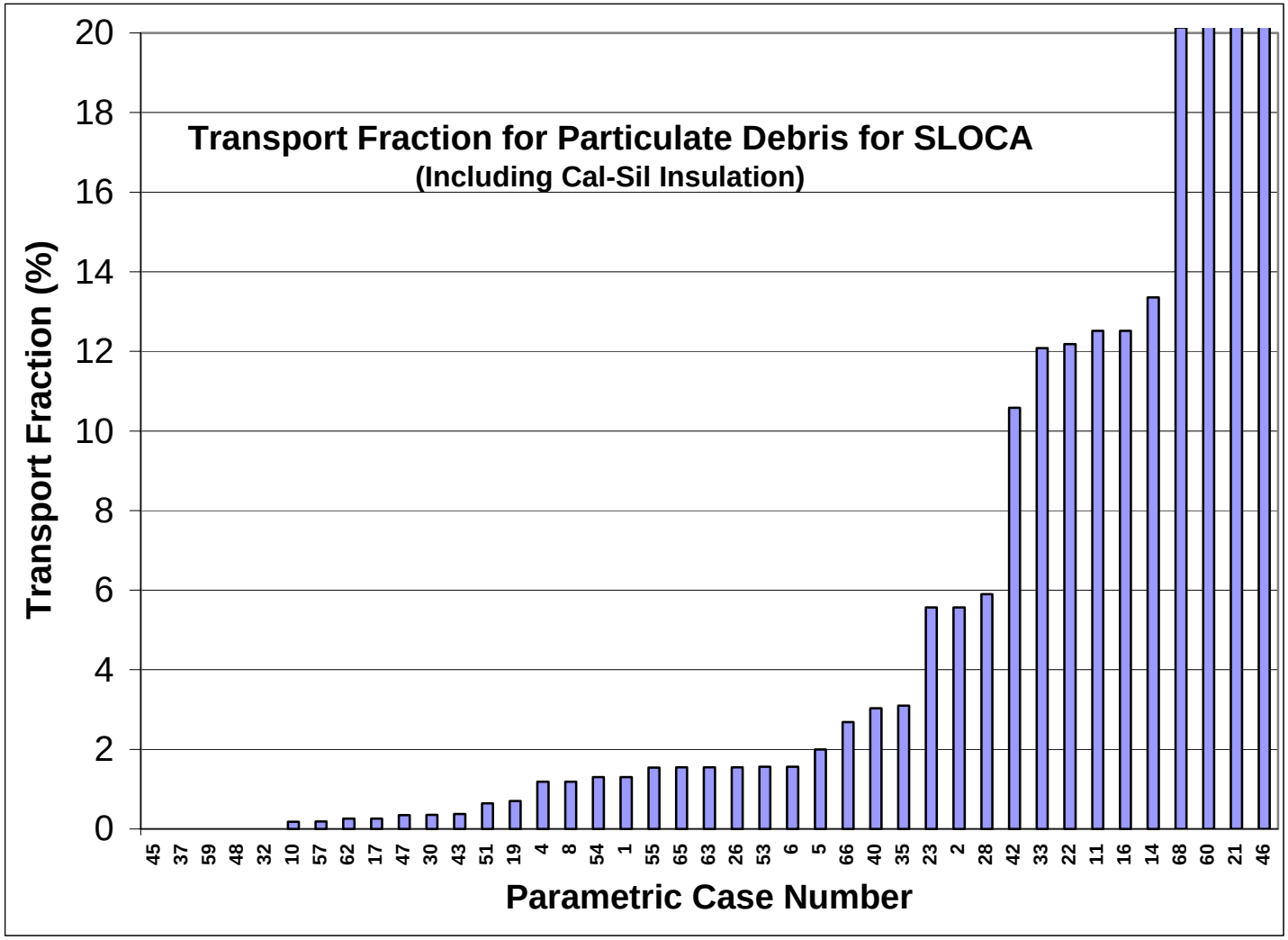

Fig. 5-11. Minimum Transport Fraction for Particulate Debris Corresponding to SLOCA.

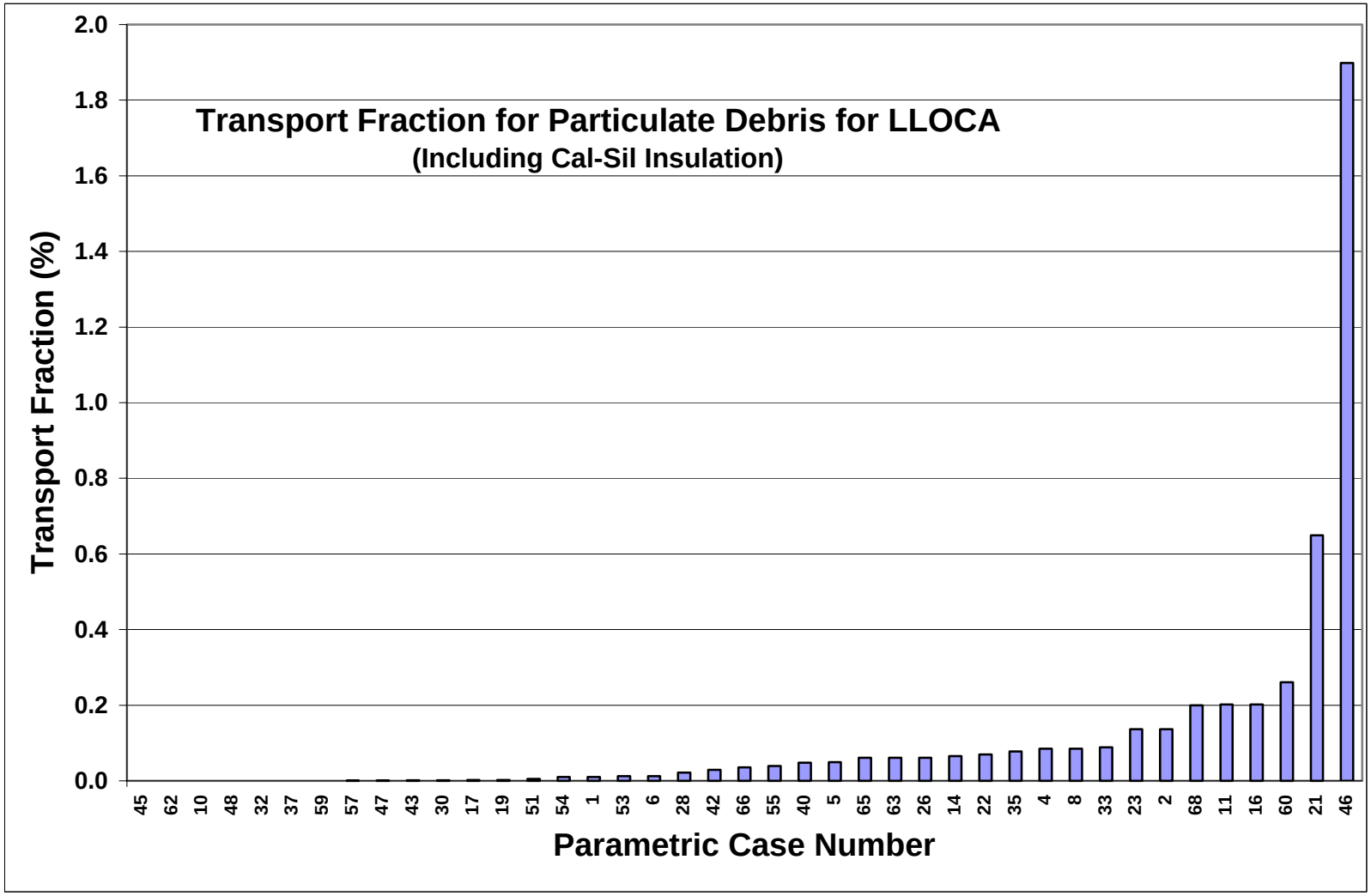

Fig. 5-12. Minimum Transport Fraction for Particulate Debris Corresponding to LLOCA.

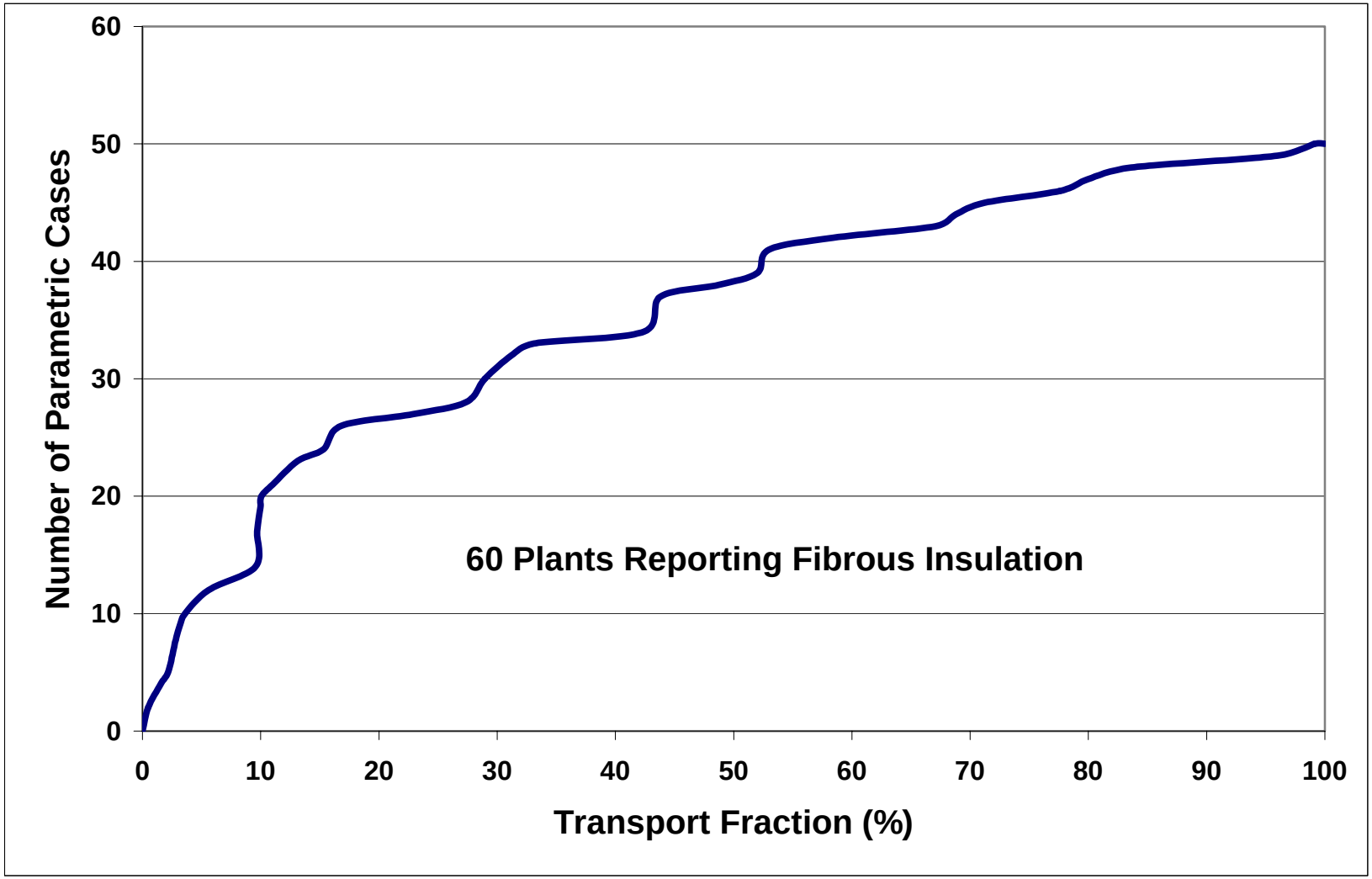

Fig. 5-13. Cumulative Distribution of Minimum Transport Fraction for Fibrous Insulation for SLOCA.

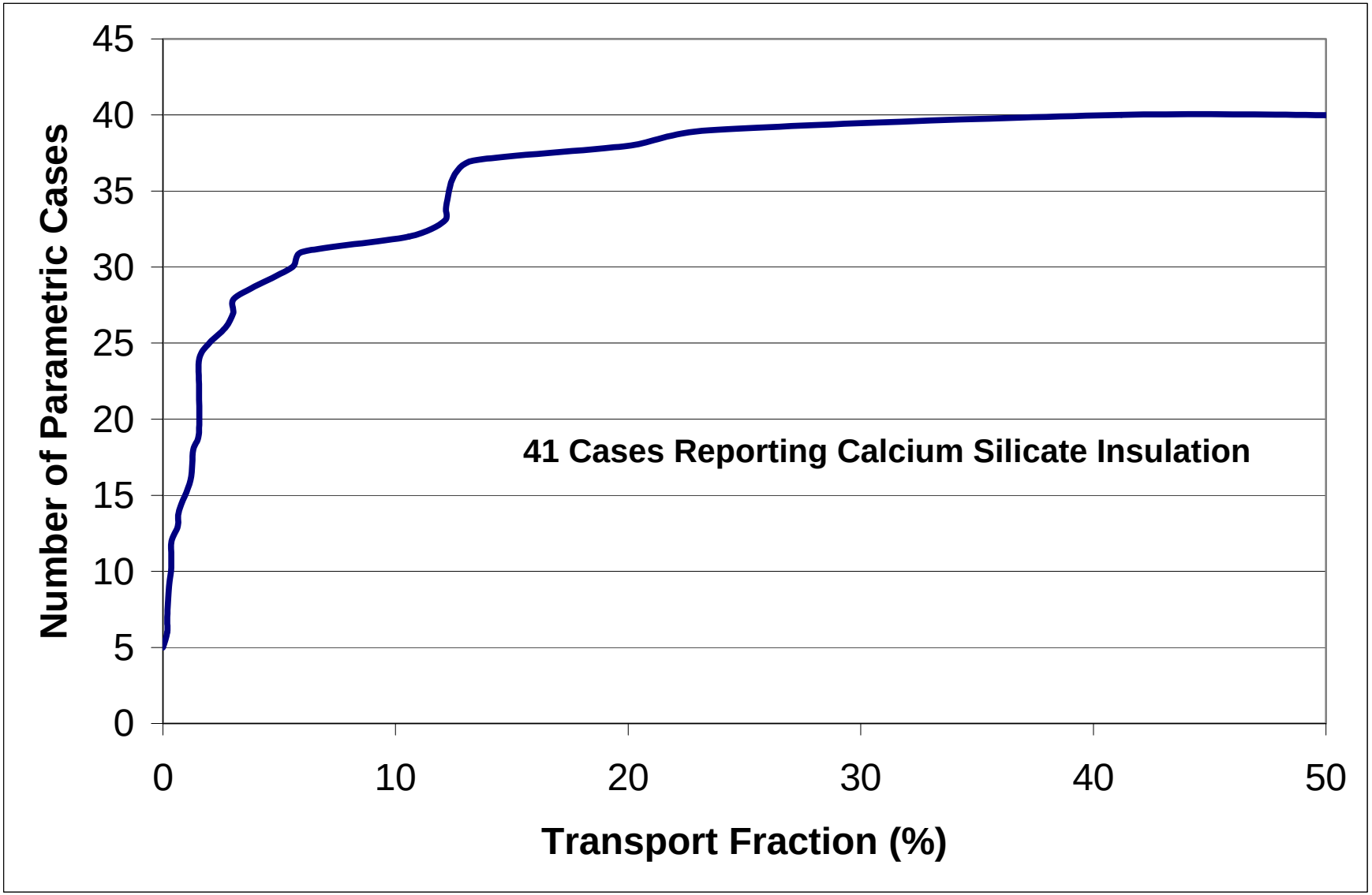

Fig. 5-14. Cumulative Distribution of Minimum Transport Fraction for Particulates Corresponding to SLOCA.

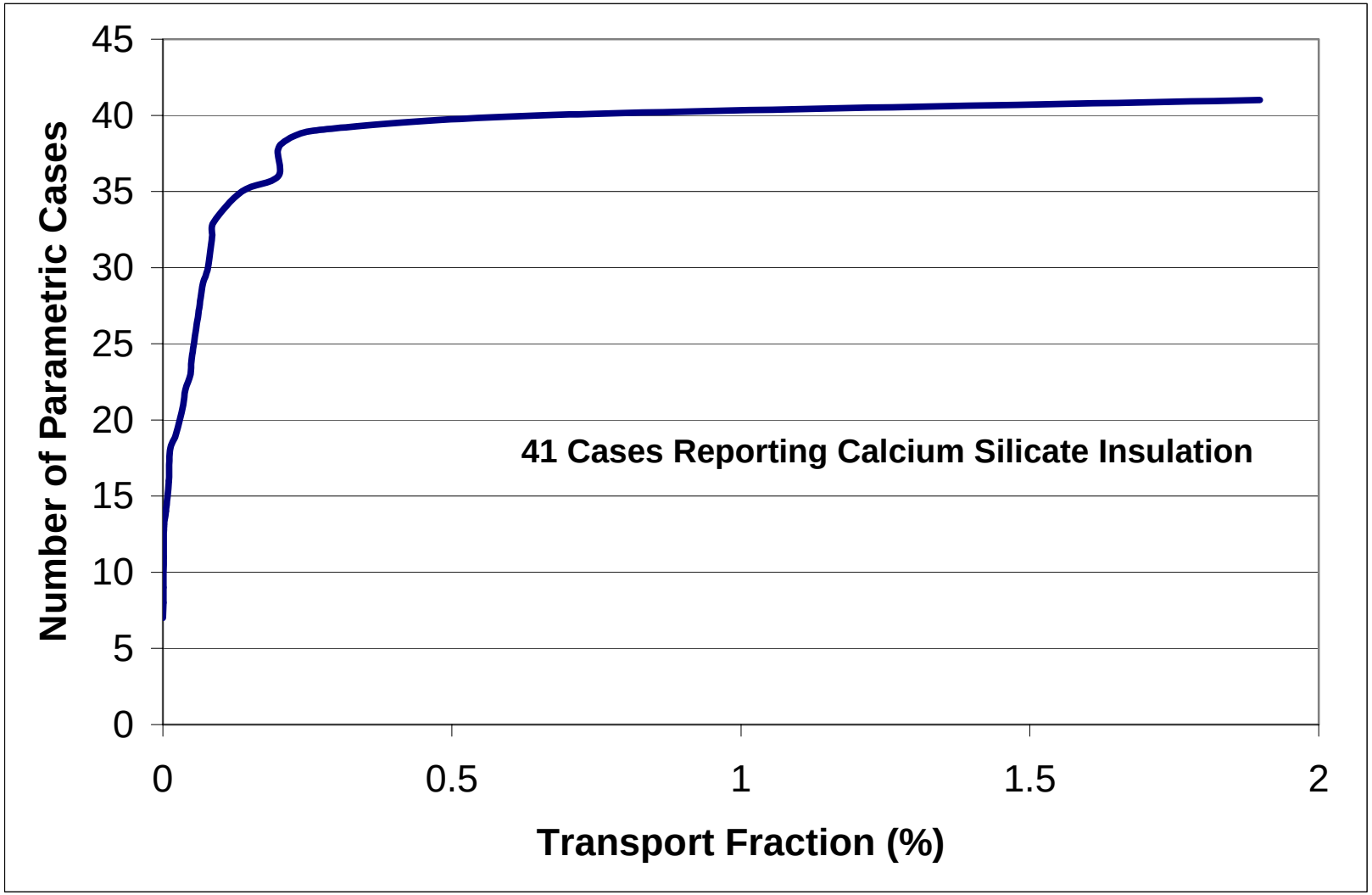

Fig. 5-15. Cumulative Distribution of Minimum Transport Fraction for Particulate Corresponding to LLOCA.

Table 5-4. Fiber Debris Volumes on Screen (ft^3).

	SLOCA		MLOCA		LLOCA	
Case	Favorable	Unfavorable	Favorable	Unfavorable	Favorable	Unfavorable
1	0.06	1.25	0.2	5	8.5	212.5
2	0.17	0.34	0.54	1.34	22.78	56.95
3	0.5	1.25	0.8	2	34	85
4	1.25	3.12	2	5	85	212.5
5	0.12	3.12	0.2	5	8.5	212.5
6	0.52	1.31	0.84	2.1	35.7	89.25
7	0	0	0	0	0	0
8	1.25	3.12	2	5	85	212.5
9	1.25	2.5	4	10	170	425
10	0.06	1.25	0.2	5	8.5	212.5
11	2.5	6.25	3.2	8	136	340
12	0.12	6.19	0.2	9.9	8.5	420.75
13	0.11	0.23	0.36	0.9	15.3	38.25
14	0.22	0.44	0.7	1.74	29.58	73.95
15	1.25	2.5	4	10	170	425
16	2.5	6.25	3.2	8	136	340
17	1.87	4.66	2.98	7.46	126.82	317.05
18	0	0	0	0	0	0
19	0.88	1.75	1.44	3.6	61.2	153
20	1.25	2.5	4	10	170	425
21	2.12	5.31	3.4	8.5	144.5	361.25
22	1	2	3.2	8	136	340
23	0.17	0.34	0.54	1.34	22.78	56.95
24	0	0	0	0	0	0
25	0.12	6.19	0.2	9.9	8.5	420.75
26	1	2.5	1.6	4	34	85
27	0.06	2.48	0.2	9.9	8.5	420.75
28	0.69	1.38	2.2	5.5	93.5	233.75
29	0	0	0	0	0	0
30	0.01	0.03	0.04	0.1	1.7	4.25
31	0	0	0	0	0	0
32	1.62	4.06	2.6	6.5	110.5	276.25
33	0.06	1.25	0.2	5	8.5	212.5

Table 5-4. Fiber Debris Volumes on Screen (ft^3) (cont)

	SLOCA		MLOCA		LLOCA	
Case	Favorable	Unfavorable	Favorable	Unfavorable	Favorable	Unfavorable
34	0.05	0.09	0.15	0.37	6.29	15.73
35	0.12	3.12	0.2	5	8.5	212.5
36	1.25	2.5	2	5	85	212.5
37	0.88	2.19	1.4	3.5	59.5	148.75
38	0.5	1.25	0.8	2	34	85
39	1	2.5	1.6	4	68	170
40	0.25	0.62	0.4	1	17	42.5
41	1.5	3.75	2.4	6	102	255
42	0.69	1.38	2.2	5.5	93.5	233.75
43	0.01	0.03	0.04	0.1	1.7	4.25
44	0.01	0.01	0.02	0.05	0.85	2.12
45	0.12	3.12	0.2	5	8.5	212.5
46	2.17	5.44	3.48	8.7	147.9	369.75
47	0.88	1.75	1.28	3.19	54.23	135.57
48	1.62	4.06	2.6	6.5	110.5	276.25
49	0	0	0	0	0	0
50	0.5	1.25	0.8	2	34	85
51	0.23	0.58	0.37	0.93	15.81	39.53
52	0.5	1.25	0.8	2	34	85
53	0.52	1.31	0.84	2.1	35.7	89.25
54	0.06	1.25	0.2	5	8.5	212.5
55	0.12	3.12	0.2	5	8.5	212.5
56	0.01	0.01	0.02	0.05	0.85	2.12
57	0.01	0.03	0.04	0.1	1.7	4.25
58	0.12	5	0.2	8	8.5	340
59	0.88	2.19	1.4	3.5	59.5	148.75
60	0.56	1.11	1.78	4.45	75.65	189.12
61	0.05	0.09	0.15	0.37	6.29	15.73
62	0.06	1.25	0.2	5	8.5	212.5
63	1	2.5	1.6	4	34	85
64	0	0	0	0	0	0
65	1	2.5	1.6	4	34	85
66	0	0	0	0	0	0
67	0.12	6.19	0.2	9.9	8.5	420.75
68	0.38	0.94	0.6	1.5	25.5	63.75
69	0.03	0.05	0.08	0.2	3.4	8.5

Table 5-5. Particulate Insulation Debris Mass on Screen (lb).

	SLOCA		MLOCA		LLOCA	
Case	Favorable	Unfavorable	Favorable	Unfavorable	Favorable	Unfavorable
1	12	122	40	490	1700	20825
2	1	2	4	9	153	382
3	0	0	0	0	0	0
4	0	0	0	0	0	0
5	25	306	40	490	1700	20825
6	115	288	184	460	7820	19550
7	0	0	0	0	0	0
8	0	0	0	0	0	0
9	0	0	0	0	0	0
10	12	122	40	490	1700	20825
11	50	125	80	200	3400	8500
12	0	0	0	0	0	0
13	0	0	0	0	0	0
14	19	38	61	152	2584	6460
15	0	0	0	0	0	0
16	50	125	80	200	3400	8500
17	64	159	102	254	4318	10795
18	0	0	0	0	0	0
19	38	75	157	393	6681	16702
20	0	0	0	0	0	0
21	0	0	0	0	0	0
22	25	50	80	200	3400	8500
23	1	2	4	9	153	382
24	0	0	0	0	0	0
25	0	0	0	0	0	0
26	12	31	20	50	850	2125
27	0	0	0	0	0	0
28	19	38	60	150	2550	6375
29	0	0	0	0	0	0
30	60	120	192	480	8160	20400
31	0	0	0	0	0	0
32	12	31	20	50	850	2125
33	12	122	40	490	1700	20825

Note: Only contribution from cal-sil particulate. Miscellaneous particulate contribution is determined using information in Tables 5-1 and 5-2.

Table 5-5. Particulate Insulation Debris Mass on Screen (lb) (cont).

	SLOCA		MLOCA		LLOCA	
Case	Favorable	Unfavorable	Favorable	Unfavorable	Favorable	Unfavorable
34	0	0	0	0	0	0
35	25	306	40	490	1700	20825
36	0	0	0	0	0	0
37	12	31	20	50	850	2125
38	0	0	0	0	0	0
39	0	0	0	0	0	0
40	38	94	60	150	2550	6375
41	0	0	0	0	0	0
42	19	38	60	150	2550	6375
43	60	120	192	480	8160	20400
44	0	0	0	0	0	0
45	25	306	40	490	1700	20825
46	8	19	12	30	510	1275
47	38	75	169	422	7174	17935
48	12	31	20	50	850	2125
49	0	0	0	0	0	0
50	0	0	0	0	0	0
51	147	369	236	590	10030	25075
52	0	0	0	0	0	0
53	115	288	184	460	7820	19550
54	12	122	40	490	1700	20825
55	25	306	40	490	1700	20825
56	0	0	0	0	0	0
57	48	95	152	380	6460	16150
58	25	125	40	200	1700	8500
59	12	31	20	50	850	2125
60	16	32	51	127	2159	5398
61	0	0	0	0	0	0
62	12	122	40	490	1700	20825
63	12	31	20	50	850	2125
64	0	0	0	0	0	0
65	12	31	20	50	850	2125
66	50	125	80	200	3400	8500
67	0	0	0	0	0	0
68	62	156	100	250	4250	10625
69	0	0	0	0	0	0

Note: Only contribution from cal-sil particulate. Miscellaneous particulate contribution is determined using information in Tables 5-1 and 5-2.

Table 5-6. Difference Between Calculated Head Loss and Failure Criterion for Favorable and Unfavorable Conditions (ft).

		SLOCA		MLOCA				LLOCA			
		Single Flow		Half-Flow		Full-Flow		Half-Flow		Full-Flow	
Case	Failure Criterion	Fav.	Unfav.	Fav.	Unfav.	Fav.	Unfav.	Fav.	Unfav.	Fav.	Unfav.
1	2.65	Uncertain	>>50	Uncertain	>>50	Uncertain	>>50	>>50	>>50	>>50	>>50
2	1.12	-1.1	-1.1	-1.1	29	-1.1	>>50	44.3	>>50	>>50	>>50
3	3.8	-3.8	-3.8	-3.8	-3.8	-3.8	-3.8	-3.1	27.7	-2	>>50
4	1.7	3.4	45.7	2.8	>>50	11.2	>>50	20	>>50	>>50	>>50
5	8.2	Uncertain	>>50	Uncertain	>>50	Uncertain	>>50	>>50	>>50	>>50	>>50
6	9	Cal-Sil	>>50	>>50	>>50	>>50	>>50	>>50	>>50	>>50	>>50
7	0.41	-0.4	-0.4	-0.4	-0.4	-0.4	-0.4	-0.4	-0.4	-0.4	-0.4
8	1.7	3.4	45.7	2.8	>>50	11.2	>>50	20	>>50	>>50	>>50
9	2.6	20.5	>>50	>>50	>>50	>>50	>>50	>>50	>>50	>>50	>>50
10	0.96	Uncertain	>>50	Uncertain	>>50	Uncertain	>>50	>>50	>>50	>>50	>>50
11	3	Cal-Sil	4.7	Cal-Sil	2.8	0.9	8.9	>>50	>>50	>>50	>>50
12	0	Uncertain	35.7	Uncertain	16.8	Uncertain	34.6	5.1	>>50	12.3	>>50
13	0	0	0	0	0	0	0	0.2	1.3	0.4	3.3
14	0.96	-1	-1	-1	-1	-1	-1	>>50	>>50	>>50	>>50
15	0.54	-0.5	-0.5	-0.5	1	-0.4	2.5	0	1	0.7	3.3
16	3	Cal-Sil	4.7	Cal-Sil	2.8	0.9	8.9	>>50	>>50	>>50	>>50
17	1.1	43	>>50	>>50	>>50	>>50	>>50	>>50	>>50	>>50	>>50
18	1.25	-1.2	-1.2	-1.2	-1.2	-1.2	-1.2	-1.2	-1.2	-1.2	-1.2
19	3.3	13.6	41.9	>>50	>>50	>>50	>>50	>>50	>>50	>>50	>>50
20	2.6	20.5	>>50	>>50	>>50	>>50	>>50	>>50	>>50	>>50	>>50
21	7.35	-7.3	-1.7	-7.2	-1.6	-6.9	4.5	-5.8	45.7	-3.2	>>50
22	4.2	Uncertain	2.1	10	39.1	25.4	>>50	>>50	>>50	>>50	>>50
23	1.12	-1.1	-1.1	-1.1	29	-1.1	>>50	44.3	>>50	>>50	>>50
24	0.41	-0.4	-0.4	-0.4	-0.4	-0.4	-0.4	-0.4	-0.4	-0.4	-0.4
25	3.5	-3.5	-2.1	-3.5	-2.1	-3.5	-0.6	-3.4	0	-3.4	5.4
26	1.5	3.8	29	2.7	17.7	7.2	38.6	>>50	>>50	>>50	>>50
27	0.9	-0.9	2.1	-0.9	31.8	-0.9	>>50	1.1	>>50	4.5	>>50
28	1.1	-1.1	1.2	6.7	24.3	15.2	>>50	>>50	>>50	>>50	>>50
29	0.41	-0.4	-0.4	-0.4	-0.4	-0.4	-0.4	-0.4	-0.4	-0.4	-0.4
30	1.37	Cal-Sil	Cal-Sil	Cal-Sil	Cal-Sil	Cal-Sil	Cal-Sil	>>50	>>50	>>50	>>50
31	0.41	-0.4	-0.4	-0.4	-0.4	-0.4	-0.4	-0.4	-0.4	-0.4	-0.4
32	0.45	>>50	>>50	>>50	>>50	>>50	>>50	>>50	>>50	>>50	>>50
33	0.9	Uncertain	Uncertain	Uncertain	16	Uncertain	33.5	48	>>50	>>50	>>50

Note: Several cases that had insufficient fiber to form a debris bed or did not exceed the failure criterion also had large amounts of cal-sil applied preferentially to small pipes. Technically, these cases should receive an entry of <zero, but they are annotated with the entry 'Cal-Sil' as a reminder of potential concern. Similarly, cases with zero head loss and poorly defined insulation compositions were annotated with the entry "Uncertain" to indicate that major uncertainties exist.

Table 5-6. Difference Between Calculated Head Loss and Failure Criterion for Favorable and Unfavorable Conditions (ft) (cont)

		SLOCA		MLOCA				LLOCA			
		Single Flow		Half-Flow		Full-Flow		Half-Flow		Full-Flow	
Case	Failure Criterion	Fav.	Unfav.	Fav.	Unfav.	Fav.	Unfav.	Fav.	Unfav.	Fav.	Unfav.
34	13	-13	-13	-13	-13	-13	-13	-10.9	>>50	-7.3	>>50
35	8.2	Uncertain	>>50	Uncertain	>>50	Uncertain	>>50	>>50	>>50	>>50	>>50
36	1.3	-1	2.3	0.8	18.6	3	40.5	12.7	42	37.7	>>50
37	0.35	>>50	>>50	>>50	>>50	>>50	>>50	>>50	>>50	>>50	>>50
38	3.8	-3.8	-3.8	-3.8	-3.8	-3.8	-3.8	-3.1	27.7	-2	>>50
39	0	0	0	0	1.6	0	3.2	0.2	0.9	0.6	2.4
40	0.9	-0.9	-0.9	-0.9	-0.9	-0.9	-0.9	>>50	>>50	>>50	>>50
41	5.25	-5.2	-3.4	-5.2	-2.9	-5.2	-0.5	-4.8	9.3	-4.1	38.1
42	1.84	-1.8	0.4	5.9	23.6	14.5	>>50	>>50	>>50	>>50	>>50
43	1.37	Cal-Sil	Cal-Sil	Cal-Sil	Cal-Sil	Cal-Sil	Cal-Sil	>>50	>>50	>>50	>>50
44	1.3	-1.3	-1.3	-1.3	-1.3	-1.3	-1.3	21.4	>>50	>>50	>>50
45	0	Uncertain	>>50	Uncertain	>>50	Uncertain	>>50	>>50	>>50	>>50	>>50
46	1.07	-1.1	-1.1	-1.1	-0.3	-1.1	0.5	0	3.1	1.4	9.4
47	0.97	8.4	25	>>50	>>50	>>50	>>50	>>50	>>50	>>50	>>50
48	0.45	>>50	>>50	>>50	>>50	>>50	>>50	>>50	>>50	>>50	>>50
49	1.7	-1.7	-1.7	-1.7	-1.7	-1.7	-1.7	-1.7	-1.7	-1.7	-1.7
50	5.25	-5.2	-5.2	-5.2	-5.2	-5.2	-5.2	-5.1	1.1	-4.8	14.9
51	0.62	Cal-Sil	Cal-Sil	Cal-Sil	Cal-Sil	Cal-Sil	Cal-Sil	>>50	>>50	>>50	>>50
52	3.8	-3.8	-3.8	-3.8	-3.8	-3.8	-3.8	-3.1	27.7	-2	>>50
53	9	Cal-Sil	>>50	>>50	>>50	>>50	>>50	>>50	>>50	>>50	>>50
54	2.65	Uncertain	>>50	Uncertain	>>50	Uncertain	>>50	>>50	>>50	>>50	>>50
55	1.01	Uncertain	>>50	Uncertain	46.4	Uncertain	>>50	>>50	>>50	>>50	>>50
56	1.3	-1.3	-1.3	-1.3	-1.3	-1.3	-1.3	21.4	>>50	>>50	>>50
57	1.75	Cal-Sil	Cal-Sil	Cal-Sil	Cal-Sil	Cal-Sil	Cal-Sil	>>50	>>50	>>50	>>50
58	0	>>50	>>50	>>50	>>50	>>50	>>50	>>50	>>50	>>50	>>50
59	0.35	>>50	>>50	>>50	>>50	>>50	>>50	>>50	>>50	>>50	>>50
60	5.6	-5.6	-5.6	-2.7	5.6	0.3	17.2	>>50	>>50	>>50	>>50
61	13	-13	-13	-13	-13	-13	-13	-10.9	>>50	-7.3	>>50
62	1.9	Uncertain	>>50	Uncertain	>>50	Uncertain	>>50	>>50	>>50	>>50	>>50
63	1.5	3.8	29	2.7	17.7	7.2	38.6	>>50	>>50	>>50	>>50
64	1.25	-1.2	-1.2	-1.2	-1.2	-1.2	-1.2	-1.2	-1.2	-1.2	-1.2
65	1.5	3.8	29	2.7	17.7	7.2	38.6	>>50	>>50	>>50	>>50
66	0.6	Cal-Sil	Cal-Sil	Cal-Sil	Cal-Sil	Cal-Sil	Cal-Sil	-0.6	-0.6	-0.6	-0.6
67	3.5	-3.5	-2.1	-3.5	-2.1	-3.5	-0.6	-3.4	0	-3.4	5.4
68	2.1	Cal-Sil	Cal-Sil	Cal-Sil	Cal-Sil	Cal-Sil	Cal-Sil	45.7	>>50	>>50	>>50
69	2.4	-2.4	-2.4	-2.4	-2.4	-2.4	-2.4	-2	7.6	-1.4	18.3

Note: Several cases that had insufficient fiber to form a debris bed or did not exceed the failure criterion also had large amounts of cal-sil applied preferentially to small pipes. Technically, these cases should receive an entry of <zero, but they are annotated with the entry 'Cal-Sil' as a reminder of potential concern. Similarly, cases with zero head loss and poorly defined insulation compositions were annotated with the entry "Uncertain" to indicate that major uncertainties exist.

5.4 Sump-Blockage Likelihood

The analyses described above were used to draw conclusions regarding sump-blockage likelihood. The final list is provided in Table 5-7. The qualitative grades were assigned by comparing the debris accumulated on the sump screen with that necessary for sump failure. Appendix B provides this comparison for each parametric case and for each accident sequence. The following criteria were generally applied.

1. A **very likely** grade was assigned when debris accumulated on the sump screen under 'favorable' transport conditions exceeded the FTDL. In Appendix B, corresponding figures would have the dashed box indicating "range of transported debris" located to the right of the solid line indicating "failure threshold debris loading." The corresponding head-loss entry in Table 5-6 would be larger than the $NPSH_{Margin}$ (or alternately ½-pool height).

2. An **unlikely** grade was assigned when debris accumulated on the sump screen under 'unfavorable' transport conditions were lower than the FTDL. In Appendix B, corresponding figures would have the dashed box indicating "range of transported debris" located to the left of the solid line indicating "failure threshold debris loading." The corresponding head-loss entry in Table 5-6 would be zero (because no head-loss calculations were performed for these cases).

3. For all other cases (or sequences), the qualitative grades **likely** and **possible** were assigned. A variety of qualitative rationales was used to distinguish between these two cases, including plant and sump design features and types and locations of debris. In all these cases, the dashed box in the Appendix B figures intersected the solid line, indicating that the favorable estimates for debris transported are lower than threshold values, but unfavorable estimates exceeded threshold values.

After determining a qualitative grade for each case using the method described above, one additional step was required before a final qualitative grade was assigned. There were certain factors that were identified for each of the parametric calculations that would certainly make the vulnerability assessment "worse" than that one would assign based on review of the Appendix B figures alone. No methodology was identified that would allow consideration of these factors in the numeric calculations that were performed to generate the figures in Appendix B. For example, as described in Section 3.5, cal-sil debris was treated in the calculations as if it was a "generic particulate." That is, the contribution of cal-sil debris to total head loss across the sump screen was calculated as if it were common particulate material, such as dirt or dust. However, previous experimental programs have provided overwhelming evidence to suggest that the effect of cal-sil may be to increase head loss by a factor of 5-10 more than that of a more "generic" particulate. Therefore, qualitative assessments were made for specific cases that increased the vulnerability ranking (e.g., from **possible** to **likely**) based on these types of considerations. Table 5-8 shows the dominant factors that were considered for making these qualitative judgments.

It should be noted that the qualitative ranking provided above is not intended to imply an estimate of frequency for a sump blockage event but rather is best interpreted as the comparative concern placed on groups of cases with similar ranking. For example, cases with ratings of **very likely** are found to have the following general characteristics.

1. A significant fraction of the containment inventory of insulation is made up of fibrous materials and/or cal-sil.

2. The sump-screen area and $NPSH_{Margin}$ (or pool height) are such that the FTDLs and minimum transport fractions are very small. These plants generally generated and transported significantly larger quantities than necessary for sump failure. Finally, the estimates for head loss far exceeded the failure criterion.

Cases with ratings of **unlikely** are found to have the following general characteristics.

1. A very small fraction of the containment inventory of insulation is made up of fibrous materials. Most of the insulation is in the form of RMI and foam-type insulations. These types of debris are less likely to be transported, and when accumulated, they would not result in significant head loss.

The rating of unlikely should be interpreted judiciously because it is based almost entirely on the assumption that amount of fibrous insulation in that containment is insignificant. These data should be validated further before screening these cases from further considerations.

Other important findings of the parametric study can be summarized as follows.

- Accumulation of very large quantities of RMI fragments would be necessary to induce sump failure by the assumed head-loss criteria. The potential for sump failure as a result of transport of RMI debris was found to be **unlikely** for all parametric cases except 3 (3 out of 69) that have unique sump features. It is concluded that the industry-wide potential for sump failure as a result of LOCA-generated RMI debris alone is very low.

- Transport and accumulation of small quantities of fibrous and particulate debris is sufficient to cause sump failure by the assumed head-loss criteria. Approximately ½ ft^3 of fibrous insulation combined with only 10 lb of particulates would be sufficient to raise sump blockage concerns for a significant number of parametric cases (30 out of 69). This finding is a direct reflection of the fact that a significant number of PWR units have sump screen areas less than 100 ft^2 and NPSH margins less than 4 ft-water.

- Postulated small, medium, and large breaks in the RCS piping could generate more than 25 ft^3, 40 ft^3, and 1700 ft^3 of insulation debris, respectively. Only a small fraction of this insulation may actually be composed of transportable, problematic debris.[†] Nevertheless, transport of only 5% of the damaged volume is sufficient to raise ECCS operability concerns for a significant number of the parametric cases in this study.

- In numerous parametric cases, the estimated quantities of debris reaching the sump (evaluated using both favorable and unfavorable assumptions) far exceeded the threshold values necessary to induce sump failure. The actual number of parametric cases where failure was predicted varied depending on the break size. In general, an LLOCA tended to generate and transport substantially larger quantities than the FTDLs. Although estimates for the quantity of debris transported following an SLOCA depended strongly on assumptions related to CS actuation, a small subset of parametric cases were capable of transporting quantities of debris sufficient for failure even without sprays. In these parametric cases, recirculation sumps are located inside the missile shield and have special features such as horizontal screens at or below the containment floor level.

[†]Transportable problematic debris includes small fragments of fiber and particulates (such as fiberglass and cal-sil) that can move readily to the sump and induce large pressure drops when they accumulate on the screen.

- For many parametric cases, head-loss estimates (evaluated using both favorable and unfavorable assumptions) exceeded the $NPSH_{Margin}$ for the ECCS and/or CS pump(s). Typically, head-loss estimates following a LLOCA were much larger than the $NPSH_{Margin}$. This finding eliminates the need to perform numerous sensitivity analyses to examine whether the blockage is a reflection of 'conservative' assumptions made while calculating the $NPSH_{Margin}$. (For example, if the head-loss estimates were to be only 1 or 2 ft above the $NPSH_{Margin}$, it could be argued that the blockage concern is purely a reflection of conservative assumptions that are part of any plant $NPSH_{Margin}$ calculations).

Table 5-7. Results of Parametric Evaluations Regarding Potential for Blockage.

ID	SLOCA	MLOCA	LLOCA	ID	SLOCA	MLOCA	LLOCA
1	Likely+	Very Likely+	Very Likely	36	Very Likely+	Very Likely	Very Likely
2	Unlikely	Possible	Very Likely	37	Very Likely	Very Likely	Very Likely
3	Unlikely	Unlikely	Likely	38	Unlikely	Unlikely	Likely
4	Very Likely	Very Likely	Very Likely	39	Unlikely	Possible	Very Likely
5	Very Likely+	Very Likely+	Very Likely	40	Unlikely	Unlikely	Very Likely
6	Likely	Very Likely	Very Likely	41	Unlikely	Unlikely	Likely
7*	Unlikely	Unlikely	Unlikely	42	Likely+	Very Likely	Very Likely
8	Very Likely	Very Likely	Very Likely	43	Unlikely	Unlikely	Very Likely
9	Very Likely	Very Likely	Very Likely	44	Unlikely	Unlikely	Very Likely
10	Very Likely+	Very Likely+	Very Likely	45	Very Likely+	Very Likely+	Very Likely
11	Very Likely+	Very Likely+	Very Likely	46	Unlikely	Possible	Very Likely
12	Possible	Very Likely+	Very Likely	47	Very Likely	Very Likely	Very Likely
13	Unlikely	Unlikely	Very Likely	48	Very Likely	Very Likely	Very Likely
14	Unlikely	Unlikely	Very Likely	49*	Unlikely	Unlikely	Unlikely
15	Unlikely	Likely	Very Likely	50	Unlikely	Unlikely	Possible
16	Very Likely+	Very Likely+	Very Likely	51	Very Likely+	Very Likely+	Very Likely+
17	Very Likely	Very Likely	Very Likely	52	Unlikely	Unlikely	Likely
18*	Unlikely	Unlikely	Unlikely	53	Likely	Very Likely	Very Likely
19	Very Likely	Very Likely	Very Likely	54	Likely+	Likely	Very Likely
20	Very Likely	Very Likely	Very Likely	55	Possible	Likely+	Very Likely
21	Unlikely	Possible	Likely	56	Unlikely	Unlikely	Very Likely
22	Very Likely+	Very Likely	Very Likely	57	Unlikely	Unlikely	Very Likely
23	Unlikely	Possible	Very Likely	58	Very Likely	Very Likely	Very Likely
24*	Unlikely	Unlikely	Unlikely	59	Very Likely	Very Likely	Very Likely
25	Possible+	Possible+	Very Likely	60	Unlikely	Likely	Very Likely
26	Very Likely	Very Likely	Very Likely	61	Unlikely	Unlikely	Likely
27	Likely+	Likely	Very Likely	62	Very Likely+	Very Likely+	Very Likely
28	Likely+	Very Likely	Very Likely	63	Very Likely	Very Likely	Very Likely
29*	Unlikely	Unlikely	Unlikely	64*	Unlikely	Unlikely	Unlikely
30	Possible+	Unlikely	Very Likely	65	Very Likely	Very Likely	Very Likely
31*	Unlikely	Unlikely	Unlikely	66*	Unlikely	Unlikely	Unlikely
32	Very Likely	Very Likely	Very Likely	67	Unlikely	Unlikely	Very Likely+
33	Unlikely	Likely+	Very Likely	68	Unlikely	Unlikely	Very Likely
34	Unlikely	Unlikely	Very Likely+	69	Unlikely	Unlikely	Likely
35	Very Likely+	Very Likely+	Very Likely				

Tally	SLOCA	MLOCA	LLOCA
Very Likely	25	31	53
Likely	7	6	7
Possible	4	6	1
Unlikely	33	26	8

* Zero-Fiber Plant
+ Ranking Elevated due to Factors Not Considered in Calculations

Table 5-8. Factors Not Considered in Parametric Calculations.

Case	Insulation Quantity Not Reported	Insulation Fractions Not Reported	Significant Cal-Sil (>5%)	High Approach Velocity	Exposed Sump	Sprays Expected for SLOCA
1	x	x	unknown	L	x	
2	x			L		
3	x					x
4	x			L		x
5	x	x	unknown	L		x
6	x		x (>40%)	S, M, L	x	x
7	x			S, M, L		
8	x			L		x
9	x			S, M, L		
10	x	x	unknown	M, L		
11	x		x (>20%)		x	x
12	x	x				x
13						
14			X		x	
15	x					
16	x		x (>20%)		x	x
17			x (>20%)	S, M, L		x
18	x			S, M, L	x	x
19			x (>30%)	M, L		
20	x			S, M, L		
21	x					x
22	x	x	Unknown			
23	x			L		
24	x			S, M, L		
25	x	x				x
26	x		X		x	x
27	x	x		L		
28	x		X			
29	x			S, M, L		
30	x		x (>40%)	M, L		
31	x			S, M, L		
32	x		X	M, L	x	x
33	x	x	Unknown			

Table 5-8. Factors Not Considered in Parametric Calculations (cont).

Case	Insulation Quantity Not Reported	Insulation Fractions Not Reported	Significant Cal-Sil (>5%)	High Approach Velocity	Exposed Sump	Sprays Expected for SLOCA
34				L		
35	x	x	Unknown	L		x
36	x			L		
37	x		X	S, M, L	x	x
38	x					x
39						x
40	x		X			x
41	x					x
42	x		X			
43	x		x (>40%)	M, L		
44				M, L		
45	x	x	Unknown		x	x
46	x					x
47			x (>40%)	M, L		
48	x		X	M, L	x	x
49	x					x
50	x					x
51			x (>50%)			x
52	x					x
53	x		x (>40%)	S, M, L		x
54	x	x	Unknown	L		
55	x	x	Unknown		x	x
56				M, L		
57	x		x (>30%)	M, L		
58	x	x	Unknown	?		x
59	x		X	S, M, L		x
60	x		X			
61				L		
62	x	x	Unknown	M, L		
63	x		X		x	x
64	x			S, M, L	x	x
65	x		X			x
66	x		x (>20%)			x
67	x	x				x
68	x		x (>20%)			x
69	x					

6.0 REFERENCES

BWROG, 1998 — BWR Owners' Group, "Utility Resolution Guide for ECCS Suction Strainer Blockage," NEDO-32686-A, October 1998.

Kolbe, 1982 — Kolbe, R. and E. Gahan, "Survey of Insulation Used in Nuclear Power Plants and the Potential for Debris Generation," NUREG/CR-2403, SAND82-0927, Burns and Roe, Inc. & Sandia National Laboratories, May 1982.

LANL, 2001a — Rao, D.V. et al., "GSI-191: Summary and Analysis of US Pressurized Water Reactor Industry Survey Responses and Responses to GL 97-04," LA-UR-XXXX, DRAFT, Los Alamos National Laboratory (Planned for Release September 2001).

LANL, 2001b — Ross, K.W. et al., "GSI-191: Thermal-Hydraulic Response of PWR Reactor Coolant System and Containments to Selected Accident Sequences," LA-UR-XXXX, DRAFT, Los Alamos National Laboratory (Planned for Release September 2001).

LANL, 2001c — Letellier, B.C. et al., "GSI-191: Integrated Debris Transport Tests in Water Using Simulated Containment Floor Geometries," LA-UR-XXXX, DRAFT, Los Alamos National Laboratory (Planned for Release October 2001).

LANL, 2001d — Letellier, B.C. et al., "GSI-191: Separate Effects Characterization of Debris Transport in Water," LA-UR-XXXX, DRAFT, Los Alamos National Laboratory (Planned for Release October 2001).

LANL, 2001e — Rao, D.V., "GSI-191: Debris Generation Test Summary," LA-CP-XXXX, DRAFT, Los Alamos National Laboratory (Proprietary Data: Planned for Limited Release October 2001).

LANL, 2001f — Darby, J. et al., "GSI-191: Technical Approach for Risk Assessment of PWR Sump-Screen Blockage," LA-UR-XXXX, DRAFT, Los Alamos National Laboratory (Planned for Release October 2001).

Lockheed, 1995 — Lockheed Idaho Technologies Co., "RELAP5/MOD3 Code Manual," Volumes I through VII, NUREG/CR-5535, Rev. 1, Idaho National Engineering Laboratory, June 1995.

Maji, 2000 — Maji, A. K., et al., "GSI-191: PWR Sump Debris Transport Testing, Transport Characteristics of Selected Thermal Insulations," University of New Mexico & Los Alamos National Laboratory, September 2000 (Draft).

NEI, 1997 — NEI, "Results of Industry Survey on PWR Design and Operations," Compiled Database of Plant Responses, Nuclear Energy Institute, June 1997.

Serkiz, 1985 — Serkiz, A. W., "USI A-43 Regulatory Analysis," NUREG/CR-0869, Rev. 1, Office of Nuclear Reactor Regulation, U.S. Nuclear Regulatory Commission, October 1985.

Summers, 1994 — Summers, R. M., et al., "MELCOR Computer Code Manuals," Volumes 1 and 2, NUREG/CR-6119, SAND93-1285, Sandia National Laboratories, September 1994.

US NRC, 1990 — US NRC, "Overview and Comparison of U.S. Commercial Nuclear Power Plants Nuclear Power Plant System Source Book," NUREG/CR-5640, US Nuclear Regulatory Commission, September 1990.

US NRC, 1997 — US NRC, "Assurance of Sufficient Net Positive Suction Head for Emergency Core Cooling and Containment Heat Removal Pumps," NRC Generic Letter 97-04, US Nuclear Regulatory Commission, October 1997.

Weigand, 1982 — Weigand, G. G., et al., "A Parametric Study of Containment Emergency Sump Performance," NUREG/CR-2758, SAND82-0624, ARL-46-82, Sandia National Laboratories and Alden Research Laboratory, July 1982.

Wysocki, 1982 — Wysocki, J. and R. Kolbe, "Methodology for Evaluation of Insulation Debris Effects, Containment Emergency Sump Performance Unresolved Safety Issue A-43," NUREG/CR-2791, SAND82-7067, Burns and Roe, Inc. & Sandia National Laboratories, September 1982.

Wysocki, 1983 — Wysocki, J., "Probabilistic Assessment of Recirculation Sump Blockage Due to Loss of Coolant Accidents," NUREG/CR-3394, SAND83-7116, Sandia National Laboratories, July 1983.

Zigler, 1995 — Zigler, G., et al., "Parametric Study of the Potential for BWR ECCS Strainer Blockage Due to LOCA Generated Debris," NUREG/CR-6224, SEA No. 93-554-06-A:1, Science and Engineering Associates, Inc., October 1995.

APPENDIX A

DESCRIPTIVE DATA ASSUMED FOR EACH PARAMETRIC CASE

Table A-1(a) Plant Parameters for Parametric Study.

Parametric Case	Containment Type	Cont. Inside Diameter	Cont. Free Volume	Cont. Spray Act. Set Point	Switchover Pool Height	Switchover Time	Maximum Pool Height	Maximum Time to Switchover	Sump Location	Sump-Screen Hole Size
Units	-	ft	ft^3	psig	ft	min	ft	min	-	in.
1	Dry	105	?	30	5.3	30	5.5	65	exposed	0.125
2	Dry	135	2.980	18.2	2.24	9.59	4.7	18.37	remote	0.115
3	Dry	146	2.600	8.5	4.5	20	11	20	remote	0.09
4	Ice	115	?	2.9	5.5	20	14	58	?	0.204
5	Dry	116	1.550	?	2.93	15.2	4.75	43	int. exp.	0.25
6	Ice	115	?	2.9	?	?	?	?	int. exp.	0.250
7	Dry	140	2.900	20	0.82	13.23	6.1	15	?	0.152
8	Ice	115	?	2.9	5.5	20	14	58	?	0.204
9	Dry	140	2.700	21.5	3.5	35	9.41	63	remote	0.12
10	Dry	150	2.340	14	1.92	20	7.5	30	int. exp.	0.3
11	Dry	130	2.000	4.75	5.25	480	5.25	480	exposed	0.224
12	Dry	126	?	?	5.33	25	6.89	33	?	0.25
13	Dry	130	2.000	30	1.74	29.17	5.89	29.17	remote	0.125
14	Dry	116	2.090	30	6	25	9.18	25	exposed	0.132
15	Dry	140	2.700	18	3.84	21.3	4.14	25.9	?	0.097
16	Dry	130	2.000	4.75	5.25	480	5.25	480	exposed	0.224
17	Dry	110	1.050	5	5.4	20	6.78	24	remote	0.1783
18	Ice	106	?	2.81	2.5	30	13.2	60	exposed	0.25
19	Dry	135	2.610	22	2.1	13.3	4.1	166.1	int. exp.	0.125
20	Dry	140	2.700	21.5	3.5	35	9.41	63	remote	0.12
21	Dry	140	2.680	3	5.43	20	11.45	20	remote	0.078
22	Dry	130	2.100	25	1.5	25	5.5	52	?	0.221
23	Dry	135	2.980	18.2	2.24	9.59	4.7	18.37	remote	0.115
24	Dry	140	2.900	20	0.82	13.23	6.1	15	?	0.152
25	Dry	150	3.300	9.5	3.6	?	?	?	remote	0.25
26	Dry	116	1.910	10	4.27	30	4.27	30	exposed	0.12
27	Dry	135	2.500	27	2.12	14	4.41	26	remote	0.125
28	Dry	140	2.620	25.3	3.67	15	5.5	23	remote	0.125
29	Dry	140	2.900	20	0.82	13.23	6.1	15	?	0.152
30	Dry	140	2.630	22	2.73	14.4	5.42	57.5	int. exp.	0.125
31	Dry	140	2.900	20	0.82	13.23	6.1	15	?	0.152
32	Sub	126	?	13.05	0.9	3.42	6.1	89	exposed	0.1197
33	Dry	140	2.500	27	1.9	13	4.5	26	?	0.25
34	Dry	105	?	23	3.25	12	8.5	24	int. exp.	?
35	Dry	116	1.550	?	2.93	15.2	4.75	43	int. exp.	0.25
36	Dry	130	2.000	30	4	27	7	40	remote	0.25
37	Sub	126	1.800	10.3	0.7	2.2	4.7	73	exposed	0.75
38	Dry	146	2.600	8.5	4.5	20	11	20	remote	0.09

Table A-1(a) Plant Parameters for Parametric Study (cont).

Parametric Case	Containment Type	Cont. Inside Diameter	Cont. Free Volume	Cont. Spray Act. Set Point	Switchover Pool Height	Switchover Time	Maximum Pool Height	Maximum Time to Switchover	Sump Location	Sump-Screen Hole Size
Units	-	ft	ft^3	psig	ft	min	ft	min	-	in.
39	Dry	130	2.500	10	3	25	7.3	29	int. exp.	0.125
40	Sub	126	1.800	8	5.8	45	9.9	201	remote	0.094
41	Ice	115	1.220	3	7	20	21	100	?	0.12
42	Dry	140	2.620	25.3	3.67	15	5.5	23	remote	0.125
43	Dry	140	2.630	22	2.73	14.4	5.42	57.5	int. exp.	0.125
44	Dry	130	2.030	27	3.5	21.67	9.5	29	int. exp.	0.12
45	Dry	116	1.600	3.7	3.5	20	6.83	20	?	0.132
46	Dry	140	2.500	?	2.13	25.54	2.25	26	int. exp.	0.25
47	Dry	135	2.610	24	1.75	22.12	3.5	45	int. exp.	0.25
48	Sub	126	?	13.05	0.9	3.42	6.1	89	exposed	0.1197
49	Ice	115	?	3	8.52	10.2	14.42	15	exposed	0.25
50	Ice	115	1.220	3	7	20	21	100	?	0.12
51	Dry	116	1.780	8.6	7	30	11.5	30	remote	0.1875
52	Dry	146	2.600	8.5	4.5	20	11	20	remote	0.09
53	Ice	115	?	2.9	?	?	?	?	int. exp.	0.250
54	Dry	105	?	30	5.3	30	5.5	65	exposed	0.125
55	Dry	130	1.920	9.48	4.59	30	7.6	30	exposed	0.09375
56	Dry	130	2.030	27	3.5	21.67	9.5	29	int. exp.	0.12
57	Dry	108	?	23	3.5	12.4	8	30.9	int. exp.	1
58	Sub	140	1.030	8	?	?	?	?	?	?
59	Sub	126	1.800	10.3	0.7	2.2	4.7	73	exposed	0.75
60	Dry	105	0.997	28	2.78	43	5.4	43	exposed	0.1875
61	Dry	105	?	23	3.25	12	8.5	24	int. exp.	?
62	Dry	150	2.340	14	1.92	0.33	7.5	0.5	int. exp.	0.3
63	Dry	116	1.910	10	4.27	30	4.27	30	exposed	0.12
64	Ice	106	?	2.81	2.5	30	13.2	60	exposed	0.25
65	Dry	116	1.910	10	4.27	30	4.27	30	exposed	0.12
66	Sub	126	1.800	8	5.8	45	9.9	201	remote	?
67	Dry	150	3.300	9.5	3.6	?	?	?	remote	0.25
68	Dry	140	2.500	?	0.5	20	2.75		int. exp.	0.25
69	Dry	130	2.870	23	2	35	6.7	35	?	0.25

Table A-1(b) Additional Plant Parameters for Parametric Study.

Parametric Case	Total Screen Area	Height of Sump Screen	Area at Switchover	Area at Maximum Pool Depth	Reported NPSH Margin	Fibrous Insulation	Reflective Metallic Insulation	Part. (Cal-Sil) Insulation	Other Insulation	Dominant Fiber	Type of Other Insulation
Units	ft^2	ft	ft^2	ft^2	ft-water	%	%	%	%	-	-
1	42.4	6	37.5	38.9	10.02	yes	yes	yes	0	FG/Wool/Tmat	
2	260	6.25	93.2	195.5	5	13.4	85.7	0.9	0	Transco	
3	210	4.5	210	210	3.8	20.0	80.0	0	0	NUKON/Tmat	
4	135	?	67.5	135	1.7	50	50	<1	<<1	?	
5	51.31	1	51.31	51.31	8.2	yes	yes	yes	0	NUKON/Wool	
6	66	5.25	66	66	9	21	33	46	0	?	
7	12.67	1.5	6.93	12.67	4.3	0	100	0	0	?	
8	135	?	67.5	135	1.7	50	50	<1	<<1	?	
9	11.64	0	11.64	11.64	2.6	100.0	0	0	0	NUKON	
10	104	3.5	20.4	104	1.9	yes	yes	yes	yes	FG/Wool	Foam
11	229	3.5	229	229	3	80.0	0	20.0	0	FG/Wool/Tmat	
12	93.2	below	93.2	93.2		yes	yes	0	0	Temp Mat	
13	214.4	below	214.4	214.4		9.0	91.0	0	0	NUKON	
14	204	4.75	204	204	0.96	17.4	67.5	15.2	0	?	
15	368	2.2	368	368	0.54	100	0	0	0	NUKON	
16	229	3.5	229	229	3	80.0	0	20.0	0	FG/Wool/Tmat	
17	57	3.5	57	57	1.1	74.6	0	25.4	0	FG/Wool	
18	28.4	3	23.67	28.4	9.26	0	100	0	0	?	
19	36.1	below	36.1	36.1	3.3	36.0	10.0	39.3	14.7	Wool/FG	Gyp, Foam, Poly
20	11.64	0	11.64	11.64	2.6	100.0	0	0	0	NUKON	
21	225	5	225	225	7.35	85	15	0	0	FG/Tmat	
22	85.4	0	85.4	85.4	4.2	yes	yes	yes	0	FG/Wool/Tmat	
23	260	6.25	93.2	195.5	5	13.4	85.7	0.9	0	Transco	
24	12.67	1.5	6.93	12.67	4.3	0	100	0	0	?	
25	414	3	414	414	3.5	yes	yes	0	0	?	
26	93	below	93	93	1.5	20.0	75.0	5.0	0	FG/Wool	
27	392	8.667	95.9	199.5	0.9	yes	yes	0	yes	NUKON	
28	134	3.75	131.1	134	1.1	55.0	30.0	15.0	0	NUKON/Wool	
29	12.67	1.5	6.93	12.67	4.3	0	100	0	0	?	
30	127.93	5	44.94	62.1	3.6	1	50	48	1	?	
31	12.67	1.5	6.93	12.67	4.3	0	100	0	0	?	
32	168	6.25	24.2	164	0.7	65.0	30.0	5.0	0	FG/Wool	
33	692	7	187.8	444.9	0.9	yes	yes	yes	?	?	
34	51	2.75	51	51	13	3.7	96.3	0	0	?	
35	62.75	1	62.75	62.75	8.2	yes	yes	yes	0	NUKON/Wool	
36	86.4	below	86.4	86.4	1.3	50.0	30.0	0	20.0	NUKON/Wool	Neoprene
37	158	5	22.1	148.5	0.83	35.0	60.0	5.0	0	FG/Wool	

Table A-1(b) Additional Plant Parameters for Parametric Study (cont).

Parametric Case	Total Screen Area	Height of Sump Screen	Area at Switchover	Area at Maximum Pool Depth	Reported NPSH Margin	Fibrous Insulation	Reflective Metallic Insulation	Part. (Cal-Sil) Insulation	Other Insulation	Dominant Fiber	Type of Other Insulation
Units	ft^2	ft	ft^2	ft^2	ft-water	%	%	%	%	-	-
38	210	4.5	210	210	3.8	20.0	80.0	0	0	NUKON/Tmat	
39	318	3	318	318	?	40.0	60.0	0	0	NUKON/Tranco	
40	201	5	201	201	0.9	10	75	15	0	?	
41	330	6	330	330	5.25	60.0	40.0	0	0	?	Armaflex (Foam)
42	134	3.75	131.1	134	3.9	55.0	30.0	15.0	0	NUKON/Wool	
43	127.93	5	45.65	59.89	3.6	1	50	48	1	?	
44	37.5	2.5	37.5	37.5	1.3	0.5	80.0	0.0	19.5	Temp Mat	Foam
45	70	0	70	70	0	yes	yes	yes	0	FG/Wool	
46	571	0	571	571	1.07	87.0	10.0	3.0	0	NUKON/Wool	
47	48	0	48	48	0.97	31.9	8.9	42.2	17.0	Tmat/FG	Foam
48	168	6.25	24.2	164	0.7	65.0	30.0	5.0	0	FG/Wool	
49	187.2	8	187.2	187.2	1.7	0	95.0	0	5.0	?	
50	330	6	330	330	5.25	20.0	80.0	0	0	?	Armaflex (Foam)
51	150	7	150	150	0.62	9.3	31.7	59.0	0	?	
52	210	4.5	210	210	3.8	20.0	80.0	0	0	NUKON/Tmat	
53	66	5.25	66	66	9	21	33	46	0	?	
54	42.4	6	37.5	38.9	10.02	yes	yes	yes	0	FG/Wool/Tmat	
55	115.4	0	115.4	115.4	1.01	yes	yes	yes	0.0	NUKON/Wool	
56	37.5	2.5	37.5	37.5	1.3	0.5	80.0	0.0	19.5	Temp Mat	Foam
57	39.62	5.083	27.3	39.6	17	1	61	38	0	?	
58	?	?	?	?	15.1	?	?	?	?	?	
59	158	5	22.1	148.5	0.83	35.0	60.0	5.0	0	FG/Wool	
60	108	below	108	108	5.6	44.5	6.4	12.7	36.4	?	Vinycel (resin)
61	51	2.75	51	51	13	3.7	96.3	0	0	?	
62	104	3.5	20.4	104	1.9	yes	yes	yes	yes	FG/Wool	Foam
63	93	below	93	93	1.5	20.0	75.0	5.0	0	FG/Wool	
64	28.4	3	23.67	28.4	9.26	0	100	0	0	?	
65	93	below	93	93	1.5	20.0	75.0	5.0	0	FG/Wool	
66	224	5	224	224	0.6	0	80	20	0	?	
67	414	3	414	414	3.5	yes	yes	0	0	?	
68	370	0	370	370	2.1	15.0	60.0	25.0	0	NUKON/Wool	
69	125	2	125	125	2.4	2.0	98.0	0	0	NUKON	

Table A-2. Data Used in Calculation of Head Loss – ECCS/Screen Characteristics.

#	SLOCA Flow Rate (gpm)	Full Flow (gpm)	Fav. Screen Area (ft^2)	Unfav. Screen Area (ft^2)	Fav. ΔH_f (ft)	Unfav. ΔH_f (ft)
1	2500	7600	38.87	37.45	0	0
2	2500	18424	195.52	93.18	1.1	1.1
3	8900	19740	210.00	210.00	3.9	1.84
4	8900	18416	135.00	67.50	4.3	0.41
5	8900	10000	51.31	51.31	1.5	1.5
6	8900	15600	66.00	66.00	2.35	1.12
7	2500	14200	12.67	6.93	4.3	0.41
8	8900	18416	135.00	67.50	0.7	0.45
9	2500	14200	11.64	11.64	2.75	2.65
10	2500	16000	104.00	20.40	3.8	3.8
11	8900	10498	229.00	229.00	12	0
12	8900	7600	93.20	93.20	12	0
13	2500	10000	214.40	214.40	12	0
14	2500	10720	204.00	204.00	3.8	3.8
15	2500	14200	368.00	368.00	9	9
16	8900	10498	229.00	229.00	12	0
17	8900	15100	57.00	57.00	4.3	0.41
18	8900	15600	28.40	23.67	2.75	2.65
19	2500	10300	36.10	36.10	0.9	0.9
20	2500	14200	11.64	11.64	2.35	1.12
21	8900	16000	225.00	225.00	3.5	3.5
22	2500	10498	85.40	85.40	3.5	3.5
23	2500	18424	195.52	93.18	3	3
24	2500	14200	12.67	6.93	2.6	2.6
25	8900	17400	414.00	414.00	15.1	0
26	8900	10720	93.00	93.00	12	0
27	2500	19920	199.46	95.89	2.4	2.4
28	2500	17500	134.00	131.14	1.7	1.7
29	2500	14200	12.67	6.93	1.9	0.96
30	2500	11836	62.10	44.94	7.35	7.35
31	2500	14200	12.67	6.93	1.7	1.7
32	8900	12100	163.97	24.19	1.3	1.3
33	2500	10008	444.86	187.83	3	3
34	2500	7600	51.00	51.00	0.97	0.97
35	8900	10000	62.75	62.75	9.26	1.25

Table A-2. Data used in Calculation of Head Loss – ECCS/Screen Characteristics (cont).

#	SLOCA Flow Rate (gpm)	Full Flow (gpm)	Fav. Screen Area (ft^2)	Unfav. Screen Area (ft^2)	Fav. ΔH_f (ft)	Unfav. ΔH_f (ft)
36	2500	11000	86.40	86.40	9.26	1.25
37	8900	10000	148.52	22.12	13	13
38	8900	19740	210.00	210.00	5.25	5.25
39	8900	12114	318.00	318.00	12	0
40	8900	15960	201.00	201.00	9	9
41	8900	15600	330.00	330.00	0.54	0.54
42	2500	17500	134.00	131.14	5.25	5.25
43	2500	11836	59.89	45.65	2.6	2.6
44	2500	17610	37.50	37.50	4.3	0.41
45	8900	9625	70.00	70.00	0.9	0.9
46	8900	15330	571.00	571.00	5.6	5.6
47	2500	13314	48.00	48.00	1.5	1.5
48	8900	12100	163.97	24.19	8.2	8.2
49	8900	15600	187.20	187.20	2.1	2.1
50	8900	15600	330.00	330.00	0.96	0.96
51	8900	17050	150.00	150.00	1.7	1.7
52	8900	19740	210.00	210.00	3.6	1.37
53	8900	15600	66.00	66.00	4.2	4.2
54	2500	7600	38.87	37.45	1.3	1.3
55	8900	10480	115.40	115.40	0.9	0.9
56	2500	17610	37.50	37.50	1.1	1.1
57	2500	9200	39.62	27.28	3.6	1.37
58	8900	15900	800.00	10.00	13	0
59	8900	10000	148.52	22.12	1.9	1.9
60	2500	5600	108.00	108.00	0.7	0.45
61	2500	7600	51.00	51.00	1.07	1.07
62	2500	16000	104.00	20.40	0.62	0.62
63	8900	10720	93.00	93.00	3.8	3.8
64	8900	15600	28.40	23.67	1.01	1.01
65	8900	10720	93.00	93.00	0.83	0.35
66	8900	15800	224.00	224.00	8.2	8.2
67	8900	17400	414.00	414.00	17	1.75
68	8900	15300	370.00	370.00	0.83	0.35
69	2500	11000	125.00	125.00	3.3	3.3

Table A-3. Data Used in Calculation of Head Loss – Insulation Characteristics.

#	Favorable Fiber	Favorable RMI	Favorable Particulate	Unfav. Fiber	Unfav. RMI	Unfav. Particulate	Favorable Fiber Fab Density (lbm/ft^3)	Unfav. Fiber Fab Density (lbm/ft^3)	Favorable Fiber Mat Density (lbm/ft^3)	Unfav. Fiber Mat Density (lbm/ft^3)	Favorable Svf (ft^2/ft^3)	Unfav. Svf (ft^2/ft^3)
1	0.050	0.850	0.010	0.500	0.010	0.490	2.4	11.3	175	159	171000	137000
2	0.134	0.857	0.009	0.134	0.857	0.009	2.4	2.4	175	175	171000	171000
3	0.200	0.800	0.000	0.200	0.800	0.000	2.4	11.3	175	159	171000	137000
4	0.500	0.500	0.000	0.500	0.500	0.000	2.4	11.3	175	159	171000	137000
5	0.050	0.850	0.100	0.500	0.010	0.490	2.4	8.0	175	160	171000	96000
6	0.210	0.330	0.460	0.210	0.330	0.460	2.4	11.3	175	159	171000	137000
7	0.000	1.000	0.000	0.000	1.000	0.000	2.4	11.3	175	159	171000	137000
8	0.500	0.500	0.000	0.500	0.500	0.000	2.4	11.3	175	159	171000	137000
9	1.000	0.000	0.000	1.000	0.000	0.000	2.4	2.4	175	175	171000	171000
10	0.050	0.850	0.100	0.500	0.010	0.490	2.4	8.0	175	160	171000	96000
11	0.800	0.000	0.200	0.800	0.000	0.200	2.4	11.3	175	159	171000	137000
12	0.050	0.950	0.000	0.990	0.010	0.000	11.3	11.3	159	159	137000	137000
13	0.090	0.910	0.000	0.090	0.910	0.000	2.4	2.4	175	175	171000	171000
14	0.174	0.675	0.152	0.174	0.675	0.152	2.4	11.3	175	159	171000	137000
15	1.000	0.000	0.000	1.000	0.000	0.000	2.4	2.4	175	175	171000	171000
16	0.800	0.000	0.200	0.800	0.000	0.200	2.4	11.3	175	159	171000	137000
17	0.746	0.000	0.254	0.746	0.000	0.254	2.4	8.0	175	160	171000	96000
18	0.000	1.000	0.000	0.000	1.000	0.000	2.4	8.0	175	160	171000	96000
19	0.360	0.100	0.393	0.360	0.100	0.393	2.4	8.0	175	160	171000	96000
20	1.000	0.000	0.000	1.000	0.000	0.000	2.4	2.4	175	175	171000	171000
21	0.850	0.150	0.000	0.850	0.150	0.000	2.4	11.3	175	159	171000	137000
22	0.800	0.000	0.200	0.800	0.000	0.200	2.4	11.3	175	159	171000	137000
23	0.134	0.857	0.009	0.134	0.857	0.009	2.4	2.4	175	175	171000	171000
24	0.000	1.000	0.000	0.000	1.000	0.000	2.4	11.3	175	159	171000	137000

Table A-3 Data used in Calculation of Head Loss – Insulation Characteristics (cont.)

#	Favorable Fiber	Favorable RMI	Favorable Particulate	Unfav. Fiber	Unfav. RMI	Unfav. Particulate	Favorable Fiber Fab Density (lbm/ft^3)	Unfav. Fiber Fab Density (lbm/ft^3)	Favorable Fiber Mat Density (lbm/ft^3)	Unfav. Fiber Mat Density (lbm/ft^3)	Favorable Svf (ft^2/ft^3)	Unfav. Svf (ft^2/ft^3)
25	0.050	0.950	0.000	0.990	0.010	0.000	2.4	8.0	175	160	171000	96000
26	0.200	0.750	0.050	0.200	0.750	0.050	2.4	8.0	175	160	171000	96000
27	0.050	0.950	0.000	0.990	0.010	0.000	2.4	2.4	175	175	171000	171000
28	0.550	0.300	0.150	0.550	0.300	0.150	2.4	8.0	175	160	171000	96000
29	0.000	1.000	0.000	0.000	1.000	0.000	2.4	11.3	175	159	171000	137000
30	0.010	0.500	0.480	0.010	0.500	0.480	2.4	11.3	175	159	171000	137000
31	0.000	1.000	0.000	0.000	1.000	0.000	2.4	11.3	175	159	171000	137000
32	0.650	0.300	0.050	0.650	0.300	0.050	2.4	8.0	175	160	171000	96000
33	0.050	0.850	0.100	0.500	0.010	0.490	2.4	11.3	175	159	171000	137000
34	0.037	0.963	0.000	0.037	0.963	0.000	2.4	11.3	175	159	171000	137000
35	0.050	0.850	0.100	0.500	0.010	0.490	2.4	8.0	175	160	171000	96000
36	0.500	0.300	0.000	0.500	0.300	0.000	8.0	8.0	160	160	96000	96000
37	0.350	0.600	0.050	0.350	0.600	0.050	2.4	8.0	175	160	171000	96000
38	0.200	0.800	0.000	0.200	0.800	0.000	2.4	11.3	175	159	171000	137000
39	0.400	0.600	0.000	0.400	0.600	0.000	2.4	2.4	175	175	171000	171000
40	0.100	0.750	0.150	0.100	0.750	0.150	2.4	11.3	175	159	171000	137000
41	0.600	0.400	0.000	0.600	0.400	0.000	2.4	11.3	175	159	171000	137000
42	0.550	0.300	0.150	0.550	0.300	0.150	2.4	8.0	175	160	171000	96000
43	0.010	0.500	0.480	0.010	0.500	0.480	2.4	11.3	175	159	171000	137000
44	0.005	0.800	0.000	0.005	0.800	0.000	11.3	11.3	159	159	137000	137000
45	0.050	0.850	0.100	0.500	0.010	0.490	2.4	8.0	175	160	171000	96000
46	0.870	0.100	0.030	0.870	0.100	0.030	2.4	8.0	175	160	171000	96000
47	0.319	0.089	0.422	0.319	0.089	0.422	2.4	11.3	175	159	171000	137000
48	0.650	0.300	0.050	0.650	0.300	0.050	2.4	8.0	175	160	171000	96000
49	0.000	0.950	0.000	0.000	0.950	0.000	2.4	11.3	175	159	171000	137000

Table A-3 Data used in Calculation of Head Loss – Insulation Characteristics (cont.)

#	Fav. Fib	Fav. RMI	Fav. Mic	Unfav. Fib	Unfav. RMI	Unfav. Mic	Fav. Fiber Fab Den (lbm/ft3)	Unfav. Fiber Fab Den (lbm/ft3)	Fav. Fiber Mat Den (lbm/ft3)	Unfav. Fiber Mat Den (lbm/ft3)	Fav. Svf (ft2/ft3)	Unfav. Svf (ft2/ft3)
50	0.200	0.800	0.000	0.200	0.800	0.000	2.4	11.3	175	159	171000	137000
51	0.093	0.317	0.590	0.093	0.317	0.590	2.4	11.3	175	159	171000	137000
52	0.200	0.800	0.000	0.200	0.800	0.000	2.4	11.3	175	159	171000	137000
53	0.210	0.330	0.460	0.210	0.330	0.460	2.4	11.3	175	159	171000	137000
54	0.050	0.850	0.100	0.500	0.010	0.490	2.4	11.3	175	159	171000	137000
55	0.050	0.850	0.100	0.500	0.010	0.490	2.4	11.3	175	159	171000	137000
56	0.005	0.800	0.000	0.005	0.800	0.000	11.3	11.3	159	159	137000	137000
57	0.010	0.610	0.380	0.010	0.610	0.380	2.4	11.3	175	159	171000	137000
58	0.050	0.850	0.100	0.800	0.000	0.200	2.4	11.3	175	159	171000	137000
59	0.350	0.600	0.050	0.350	0.600	0.050	2.4	8.0	175	160	171000	96000
60	0.445	0.040	0.127	0.445	0.040	0.127	2.4	11.3	175	159	171000	137000
61	0.037	0.963	0.000	0.037	0.963	0.000	2.4	11.3	175	159	171000	137000
62	0.050	0.850	0.100	0.500	0.010	0.490	2.4	8.0	175	160	171000	96000
63	0.200	0.750	0.050	0.200	0.750	0.050	2.4	8.0	175	160	171000	96000
64	0.000	1.000	0.000	0.000	1.000	0.000	2.4	8.0	175	160	171000	96000
65	0.200	0.750	0.050	0.200	0.750	0.050	2.4	8.0	175	160	171000	96000
66	0.000	0.800	0.200	0.000	0.800	0.200	2.4	11.3	175	159	171000	137000
67	0.050	0.950	0.000	0.990	0.010	0.000	2.4	8.0	175	160	171000	96000
68	0.150	0.600	0.250	0.150	0.600	0.250	2.4	8.0	175	160	171000	96000
69	0.020	0.980	0.000	0.020	0.980	0.000	2.4	2.4	175	175	171000	171000

Table A-4. Determination of Screen Submerged Fraction/Area for Use in ΔH Calculations.

ID No.	Switchover		Maximum Pool		Total Screen Area (ft^2)	Height of Screen (ft)	Submerged Fraction		Submerged Area	
	Pool Height (ft)	Time (min)	Pool Height (ft)	Time (min)			Low	High	Unfav. Area (ft^2)	Fav. Area (ft^2)
1	5.3	30	5.5	65	42.4	6	0.88	0.92	37.5	38.9
2	2.24	9.59	4.7	18.37	260	6.25	0.36	0.75	93.2	195.5
3	4.5	20	11	20	210	4.5	1	1	210	210
4	5.5	20	14	58	135	Unknown	0.5	1	67.5	135
5	2.93	15.2	4.75	43	51.31	1	1	1	51.31	51.31
6	Unknown	Unknown	Unknown	Unknown	66	5.25	1	1	66.0	66.0
7	0.82	13.23	6.1	15	12.67	1.5	0.55	1	6.93	12.67
8	5.5	20	14	58	135	Unknown	0.5	1	67.5	135
9	3.5	35	9.41	63	11.64	0	1	1	11.64	11.64
10	1.92	20	7.5	30	104	3.5	0.55	1	20.4	104
11	5.25	480	5.25	480	229	3.5	1	1	229	229
12	5.33	25	6.89	33	93.2	below	1	1	93.2	93.2
13	1.74	29.17	5.89	29.17	214.4	below	1	1	214.4	214.4
14	6	25	9.18	25	204	4.75	1	1	204	204
15	3.84	21.3	4.14	25.9	368	2.2	1	1	368	368
16	5.25	480	5.25	480	229	3.5	1	1	229	229
17	5.4	20	6.78	24	57	3.5	1	1	57	57
18	2.5	30	13.2	60	28.4	3	0.83	1	23.67	28.4
19	2.1	13.3	4.1	166.1	36.1	below	1	1	36.1	36.1
20	3.5	35	9.41	63	11.64	0	1	1	11.64	11.64
21	5.43	20	11.45	20	225	5	1	1	225	225
22	1.5	25	5.5	52	85.4	0	1	1	85.4	85.4
23	2.24	9.59	4.7	18.37	260	6.25	0.36	0.75	93.2	195.5
24	0.82	13.23	6.1	15	12.67	1.5	0.55	1	6.93	12.67
25	3.6	Unknown	Unknown	Unknown	414	3	1	1	414	414
26	4.27	30	4.27	30	93	below	1	1	93	93
27	2.12	14	4.41	26	392	8.667	0.24	0.51	95.9	199.5
28	3.67	15	5.5	23	134	3.75	0.98	1	131.1	134
29	0.82	13.23	6.1	15	12.67	1.5	0.55	1	6.93	12.67
30	2.73	14.4	5.42	57.5	127.93	5	0.55	1	44.94	62.10
31	0.82	13.23	6.1	15	12.67	1.5	0.55	1	6.93	12.67
32	0.9	3.42	6.1	89	168	6.25	0.14	0.98	24.2	164.0
33	1.9	13	4.5	26	692	7	0.27	0.64	187.8	444.9
34	3.25	12	8.5	24	51	2.75	1	1	51	51
35	2.93	15.2	4.75	43	62.75	1	1	1	62.75	62.75

Table A-4. Determination of Screen Submerged Fraction/Area for Use in ΔH Calculations (cont).

ID No.	Switchover		Maximum Pool		Total Screen Area (ft^2)	Height of Screen (ft)	Submerged Fraction		Submerged Area	
	Pool Height (ft)	Time (min)	Pool Height (ft)	Time (min)			Low	High	Unfav. Area (ft^2)	Fav. Area (ft^2)
36	4	27	7	40	86.4	below	1	1	86.4	86.4
37	0.7	2.2	4.7	73	158	5	0.14	0.94	22.1	148.5
38	4.5	20	11	20	210	4.5	1	1	210	210
39	3	25	7.3	29	318	3	1	1	318	318
40	5.8	45	9.9	201	201	5	1	1	201	201
41	7	20	21	100	330	6	1	1	330	330
42	3.67	15	5.5	23	134	3.75	0.98	1	131.1	134
43	2.73	14.4	5.42	57.5	127.93	5	0.55	1	45.65	59.89
44	3.5	21.67	9.5	29	37.5	2.5	1	1	37.5	37.5
45	3.5	20	6.83	20	70	0	1	1	70	70
46	2.13	25.54	2.25	26	571	0	1.00	1.00	571.0	571.0
47	1.75	22.12	3.5	45	48	0	1	1	48	48
48	0.9	3.42	6.1	89	168	6.25	0.14	0.98	24.2	164.0
49	8.52	10.2	14.42	15	187.2	8	1	1	187.2	187.2
50	7	20	21	100	330	6	1	1	330	330
51	7	30	11.5	30	150	7	1	1	150	150
52	4.5	20	11	20	210	4.5	1	1	210	210
53	Unknown	Unknown	Unknown	Unknown	66	5.25	1	1	66.0	66.0
54	5.3	30	5.5	65	42.4	6	0.88	0.92	37.5	38.9
55	4.59	30	7.6	30	115.4	0	1	1	115.4	115.4
56	3.5	21.67	9.5	29	37.5	2.5	1	1	37.5	37.5
57	3.5	12.4	8	30.9	39.62	5.083	0.69	1	27.3	39.6
58	Unknown	Unknown	Unknown	Unknown	Unknown	Unknown	-	-	-	-
59	0.7	2.2	4.7	73	158	5	0.14	0.94	22.1	148.5
60	2.78	43	5.4	43	108	below	1	1	108	108
61	3.25	12	8.5	24	51	2.75	1	1	51	51
62	1.92	0.33	7.5	0.5	104	3.5	1	1	20.4	104
63	4.27	30	4.27	30	93	below	1	1	93	93
64	2.5	30	13.2	60	28.4	3	0.83	1	23.67	28.4
65	4.27	30	4.27	30	93	below	1	1	93	93
66	5.8	45	9.9	201	224	5	1	1	224	224
67	3.6	Unknown	Unknown	Unknown	414	3	1	1	414	414
68	0.5	20	2.75	Unknown	370	0	1.00	1.00	370.0	370.0
69	2	35	6.7	35	125	2	1	1	125	125

Note: Submerged fractions were estimated for parametric cases where data were not known.

Table A-5. Calculation of ΔH_f.

ID No.	Reported NPSH Margin (ft)	Switchover Pool Height (ft)	Screen Height (ft)	Min Calc	Favorable ΔH_f (ft)	Unfavorable ΔH_f (ft)
1	10.02	5.3	6	2.65	2.75	2.65
2	5	2.24	6.25	1.12	2.35	1.12
3	3.8	4.5	4.5	3.8	3.8	3.8
4	1.7	5.5	Unknown	1.7	1.7	1.7
5	8.2	2.93	1	8.2	8.2	8.2
6	9	Unknown	5.25	9	9	9
7	4.3	0.82	1.5	0.41	4.3	0.41
8	1.7	5.5	Unknown	1.7	1.7	1.7
9	2.6	3.5	0	2.6	2.6	2.6
10	1.9	1.92	3.5	0.96	1.9	0.96
11	3	5.25	3.5	3	3	3
12	None Reported	5.33	0	N.A.	12	0
13	None Reported	1.74	0	N.A.	12	0
14	0.96	6	4.75	0.96	0.96	0.96
15	0.54	3.84	2.2	0.54	0.54	0.54
16	3	5.25	3.5	3	3	3
17	1.1	5.4	3.5	1.1	1.1	1.1
18	9.26	2.5	3	1.25	9.26	1.25
19	3.3	2.1	0	3.3	3.3	3.3
20	2.6	3.5	0	2.6	2.6	2.6
21	7.35	5.43	5	7.35	7.35	7.35
22	4.2	1.5	0	4.2	4.2	4.2
23	5	2.24	6.25	1.12	2.35	1.12
24	4.3	0.82	1.5	0.41	4.3	0.41
25	3.5	3.6	3	3.5	3.5	3.5
26	1.5	4.27	below	1.5	1.5	1.5
27	0.9	2.12	8.667	0.9	0.9	0.9
28	1.1	3.67	3.75	1.1	1.1	1.1
29	4.3	0.82	1.5	0.41	4.3	0.41
30	3.6	2.73	5	1.365	3.6	1.37
31	4.3	0.82	1.5	0.41	4.3	0.41
32	0.7	0.9	6.25	0.45	0.7	0.45
33	0.9	1.9	7	0.9	0.9	0.9
34	13	3.25	2.75	13	13	13
35	8.2	2.93	1	8.2	8.2	8.2

Table A-5. Calculation of ΔH_f (cont).

ID No.	Reported NPSH Margin (ft)	Switchover Pool Height (ft)	Screen Height (ft)	Min Calc	Favorable ΔH_f (ft)	Unfavorable ΔH_f (ft)
36	1.3	4	below	1.3	1.3	1.3
37	0.83	0.7	5	0.35	0.83	0.35
38	3.8	4.5	4.5	3.8	3.8	3.8
39	None Reported	3	3	N.A.	12	0
40	0.9	5.8	5	0.9	0.9	0.9
41	5.25	7	6	5.25	5.25	5.25
42	3.9	3.67	3.75	1.835	3.9	1.84
43	3.6	2.73	5	1.365	3.6	1.37
44	1.3	3.5	2.5	1.3	1.3	1.3
45	0	3.5	0	0	0	0
46	1.07	2.13	0	1.07	1.07	1.07
47	0.97	1.75	0	0.97	0.97	0.97
48	0.7	0.9	6.25	0.45	0.7	0.45
49	1.7	8.52	8	1.7	1.7	1.7
50	5.25	7	6	5.25	5.25	5.25
51	0.62	7	7	0.62	0.62	0.62
52	3.8	4.5	4.5	3.8	3.8	3.8
53	9	Unknown	5.25	9	9	9
54	10.02	5.3	6	2.65	2.75	2.65
55	1.01	4.59	0	1.01	1.01	1.01
56	1.3	3.5	2.5	1.3	1.3	1.3
57	17	3.5	5.083	1.75	17	1.75
58	15.1	Unknown	Unknown	15.1	15.1	0
59	0.83	0.7	5	0.35	0.83	0.35
60	5.6	2.78	0	5.6	5.6	5.6
61	13	3.25	2.75	13	13	13
62	1.9	1.92	3.5	0.96	1.9	1.9
63	1.5	4.27	below	1.5	1.5	1.5
64	9.26	2.5	3	1.25	9.26	1.25
65	1.5	4.27	below	1.5	1.5	1.5
66	0.6	5.8	5	0.6	0.6	0.6
67	3.5	3.6	3	3.5	3.5	3.5
68	2.1	0.5	0	2.1	2.1	2.1
69	2.4	2	2	2.4	2.4	2.4

Notes:

1. Where no $NPSH_{Margin}$ was reported in the survey, values of 0 ft-H_20 and 12 ft-H_20 were assumed for minimum and maximum NPSH margin, respectively.

2. For fully submerged screens, ΔH_f was assumed to be equal to the reported $NPSH_{Margin}$. For partially submerged screens, ΔH_f was calculated to be the lesser of the reported $NPSH_{Margin}$ and half the pool height.

Table A-6. Screen Characteristics.

ID No.	Sump Location	Screen Hole Size (in.)	ID No.	Sump Location	Screen Hole Size (in.)
1	exposed	0.125	36	remote	0.25
2	remote	0.115	37	exposed	0.75
3	remote	0.09	38	remote	0.09
4	Unknown	0.204	39	int. exp.	0.125
5	int. exp.	0.25	40	remote	0.094
6	int. exp.	0.250	41	Unknown	0.12
7	Unknown	0.152	42	remote	0.125
8	Unknown	0.204	43	int. exp.	0.125
9	remote	0.12	44	int. exp.	0.12
10	int. exp.	0.3	45	Unknown	0.132
11	exposed	0.224	46	int. exp.	0.25
12	Unknown	0.25	47	int. exp.	0.25
13	remote	0.125	48	exposed	0.1197
14	exposed	0.132	49	exposed	0.25
15	Unknown	0.097	50	Unknown	0.12
16	exposed	0.224	51	remote	0.1875
17	remote	0.1783	52	remote	0.09
18	exposed	0.25	53	int. exp.	0.250
19	int. exp.	0.125	54	exposed	0.125
20	remote	0.12	55	exposed	0.09375
21	remote	0.078	56	int. exp.	0.12
22	Unknown	0.221	57	int. exp.	1
23	remote	0.115	58	Unknown	Unknown
24	Unknown	0.152	59	exposed	0.75
25	remote	0.25	60	exposed	0.1875
26	exposed	0.12	61	int. exp.	Unknown
27	remote	0.125	62	int. exp.	0.3
28	remote	0.125	63	exposed	0.12
29	Unknown	0.152	64	exposed	0.25
30	int. exp.	0.125	65	exposed	0.12
31	Unknown	0.152	66	remote	Unknown
32	exposed	0.1197	67	remote	0.25
33	Unknown	0.25	68	int. exp.	0.25
34	int. exp.	Unknown	69	Unknown	0.25
35	int. exp.	0.25			

APPENDIX B

FAILURE-THRESHOLD DEBRIS LOADING FOR EACH PARAMETRIC CASE

The minimum mass of particulate needed to cause blockage for a specified fiber volume was determined for

- each parameter case;
- the small-, medium-, and large-break scenarios;
- full-ECCS flow and half-ECCS flow (for MLOCA and LLOCA); and
- both favorable and unfavorable parameter values.

In addition, the range of expected debris generated and transported to the sump screen was compared with fiber/particulate debris combinations predicted to cause blockage. The results for each parameter case were combined into a set of four plots presented on a single page. Because so much input data and synthesized analysis is presented together in a generic format, these figures are, in some cases, relatively complex.

The first plot on each page (upper left) provides tabular data associated with that particular case. These data include the ranges (favorable to unfavorable conditions) of debris expected on the sump screen, the screen area, the $NPSH_{Margin}$, the small-break and full-ECCS flow rates. Also shown in the first plot are the fiber debris volumes and miscellaneous particulate mass plotted on a linear scale.

The second plot (upper right) on each page shows the results for the SLOCA scenario. Both the favorable (solid line) and unfavorable (dashed line) minimum-particulate-mass curves are plotted. Note the log-scales. For example, in parametric case 1, the primary difference between favorable and unfavorable conditions was the composition of insulation. The plant has fiber, RMI, and particulate insulation, but the relative fractions of each were not reported. In addition, the type of fiber was not reported. Therefore, favorable conditions assumed very little fiber and very little particulate insulation; i.e., most of the insulation was assumed to be RMI. Conversely, the unfavorable conditions assumed little RMI but equal quantities of fiber and particulate insulations. Further, the favorable conditions assumed the fiber was LDFG, such as Nukon, but the unfavorable conditions assumed the fibrous insulation was high-density fiberglass, such as Temp Mat. High-density fiberglass will cause a larger head loss than low-density fiberglass. As shown in the second plot for case 1, it would take substantially less particulate to block the screen for the unfavorable conditions than it would for the favorable conditions. The gap between the two curves provides some measure of the uncertainty associated with predicting blockage. The square symbol represents the threshold debris loadings needed to cause blockage, i.e., where induced head loss is equal to the sump failure criterion, ΔH_f. The volume of fiber at the squares is just sufficient to create a uniform 1/8-in. layer of fiber across the sump screen assumed for the associated parametric case. The plotted curves rise vertically at the square symbols indicating that without the threshold layer of fiber (fiber volume less than that of the threshold conditions), an unlimited mass of particulate would not cause blockage. This was a fundamental assumption common to all the head-loss calculations with regard to particulates.

The ranges of expected debris on the screen for the SLOCA are shown as a dashed-line box on the second plot, and the boundaries of the box are highlighted on the axes with the circle symbol. Note that the expected mass of particulate includes both particulate-insulation debris and miscellaneous particulate transported to the screen. The range of particulate for the SLOCA is printed near the top of the plot.

The third plot (lower left) on each page provides information similar to the second plot but for the MLOCA. Where only one flow rate was assumed for the SLOCA scenarios, two flow rates were assumed for the MLOCA and LLOCA scenarios, i.e., full ECCS flow and one-half of the total ECCS flow rate. This was intended to illustrate the effect of operating with one train of the ECCS instead of two trains of the ECCS. Therefore, the third plot has four minimum-particulate curves, i.e., favorable and unfavorable conditions at full- and half-ECCS flow.

The fourth plot (lower right) on each page shows the same information for the LLOCA as the third plot shows for the MLOCA. Actually, the minimum-particulate head-loss curves are the same for the MLOCA and LLOCA scenarios, but the expected debris ranges are substantially different.

When the figures are examined for each parametric case, it becomes evident that the sump failure curves for some plants intersect the dashed box defining the range of fibrous and particulate debris that may be expected to transport to the sump. All debris combinations within the box and to the right of the failure-threshold will induce head loss in excess of the sump failure criterion. For all debris combinations to the left of the failure threshold, the sump will continue to function as required. Thus, the proportion of the area in the expected-range box that lies to the right of the curve provides a rough indication of the sump failure potential for these intermediate cases. For example, in case 1, approximately 73% of all reasonable debris loadings would provide debris conditions leading to sump blockage following an SLOCA. Table B-1, listed at the end of the figures, provides this percentage for the SLOCA, MLOCA and LLOCA for each of the 69 parametric cases.

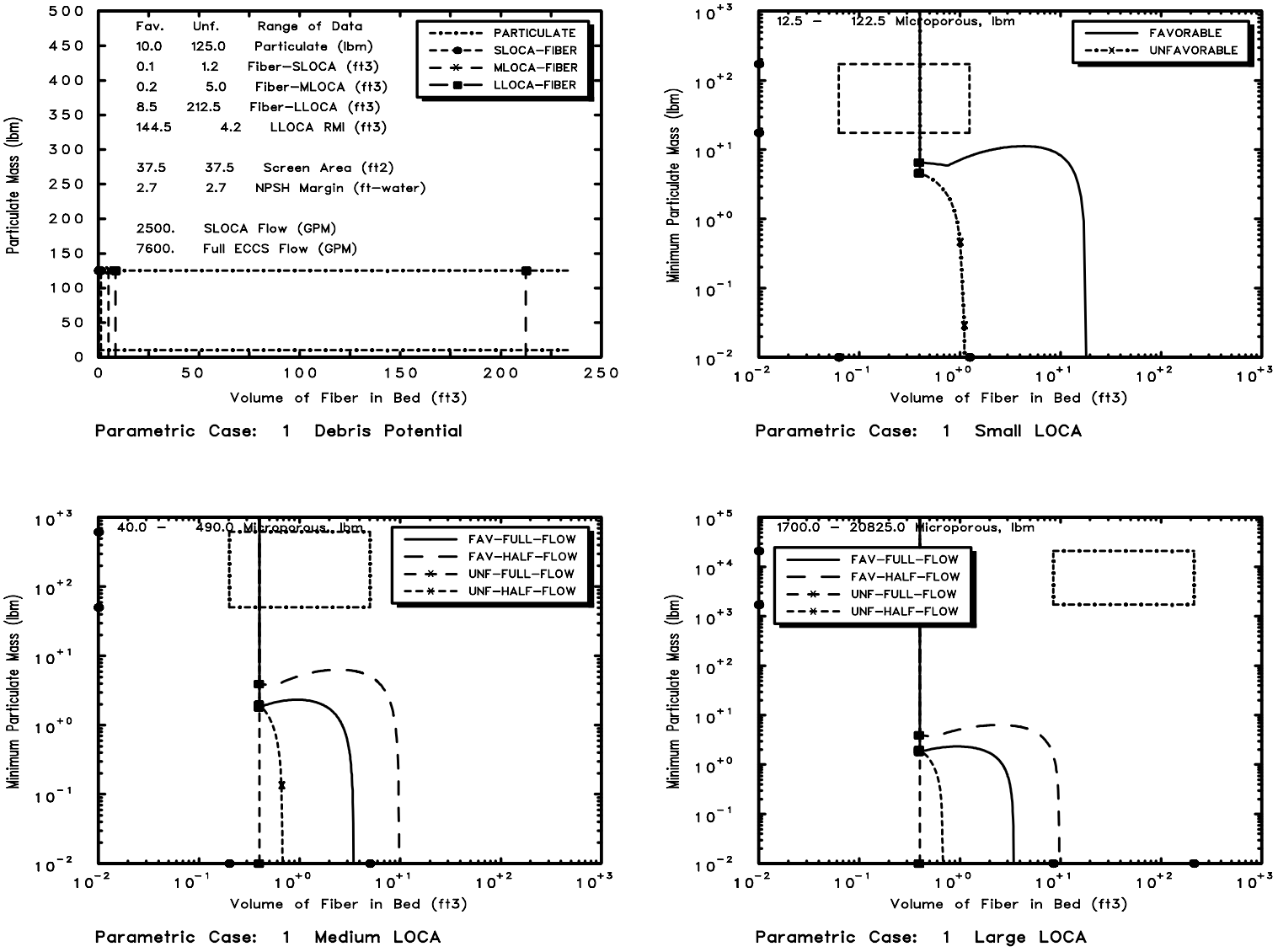

Fig. B-1. Parametric Case 1.

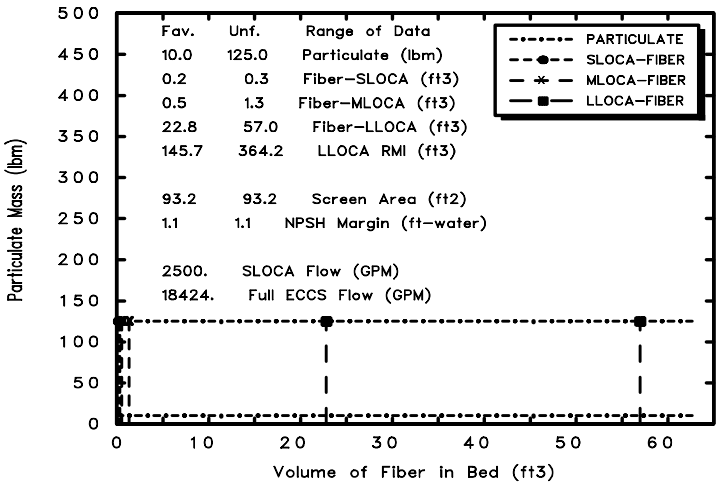

Parametric Case: 2 Debris Potential

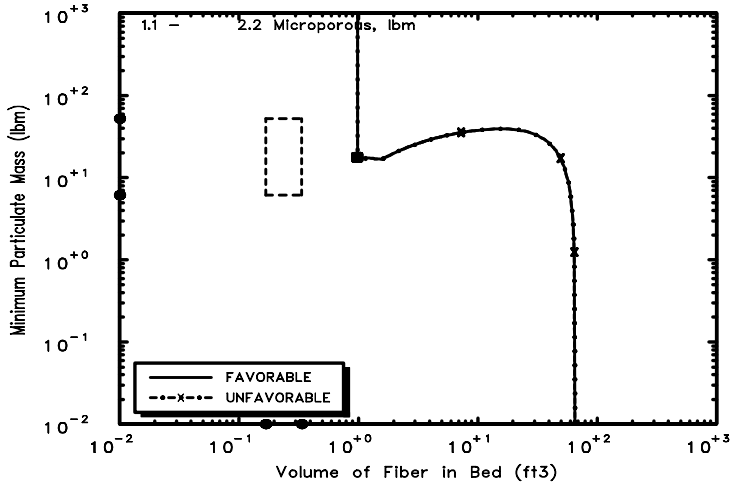

Parametric Case: 2 Small LOCA

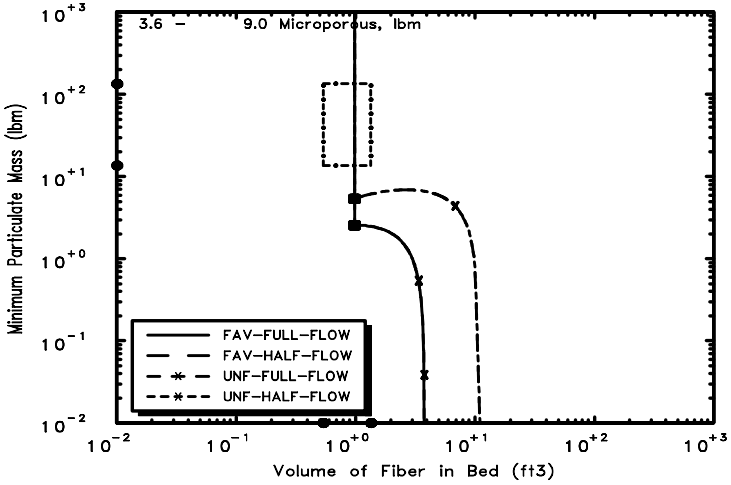

Parametric Case: 2 Medium LOCA

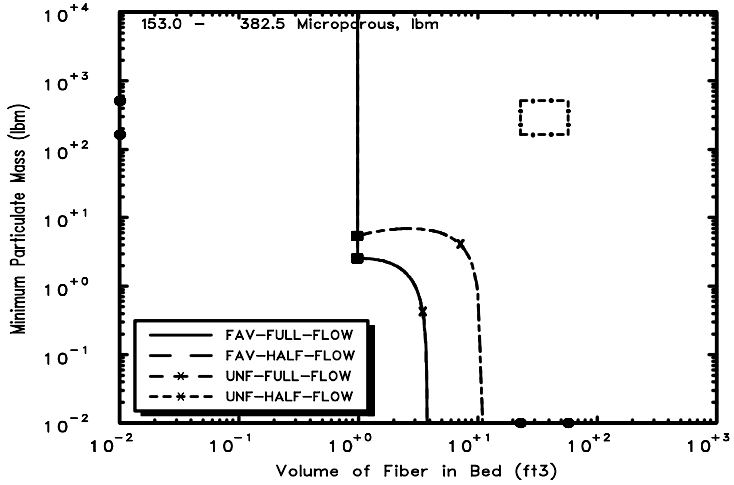

Parametric Case: 2 Large LOCA

Fig. B-2. Parametric Case 2.

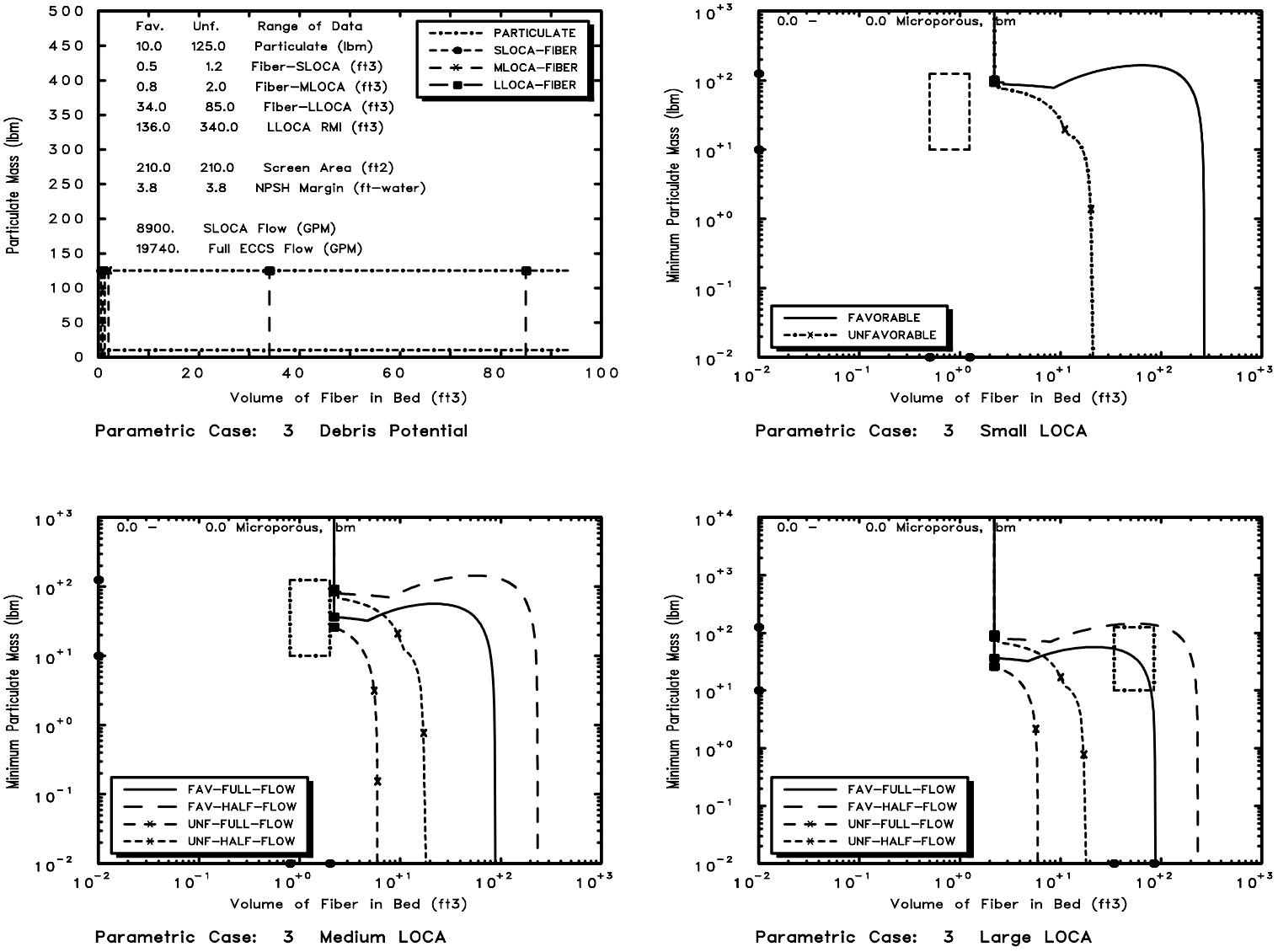

Fig. B-3. Parametric Case 3.

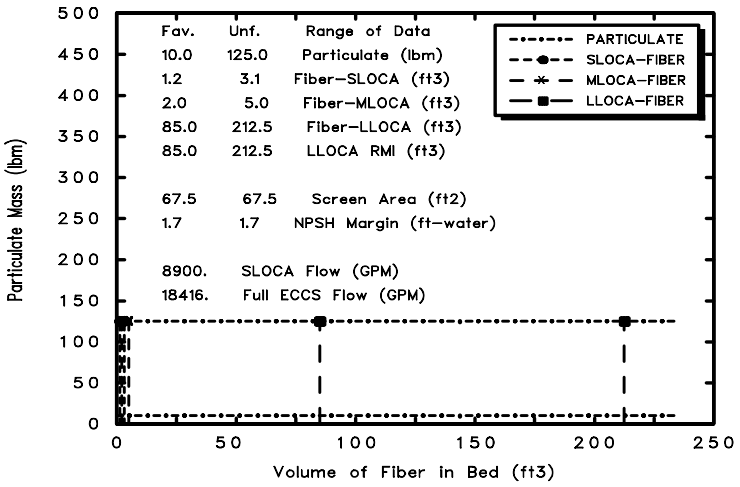

Parametric Case: 4 Debris Potential

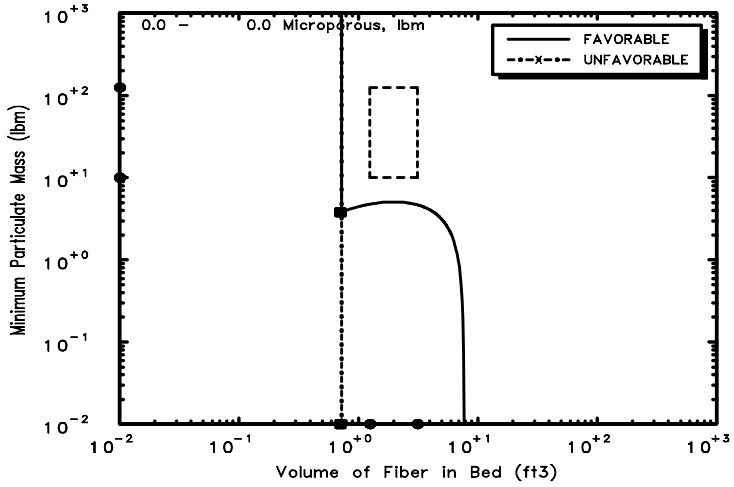

Parametric Case: 4 Small LOCA

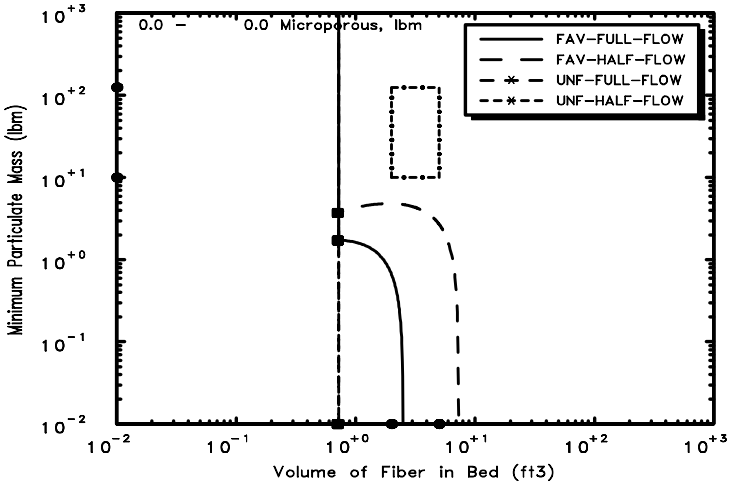

Parametric Case: 4 Medium LOCA

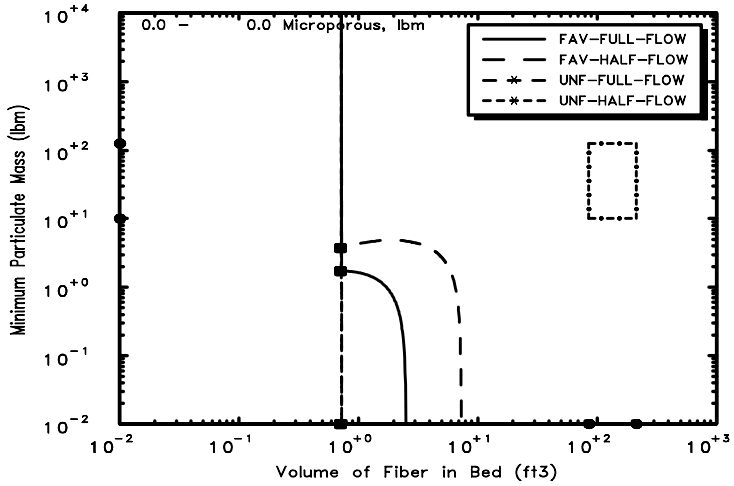

Parametric Case: 4 Large LOCA

Fig. B-4. Parametric Case 4.

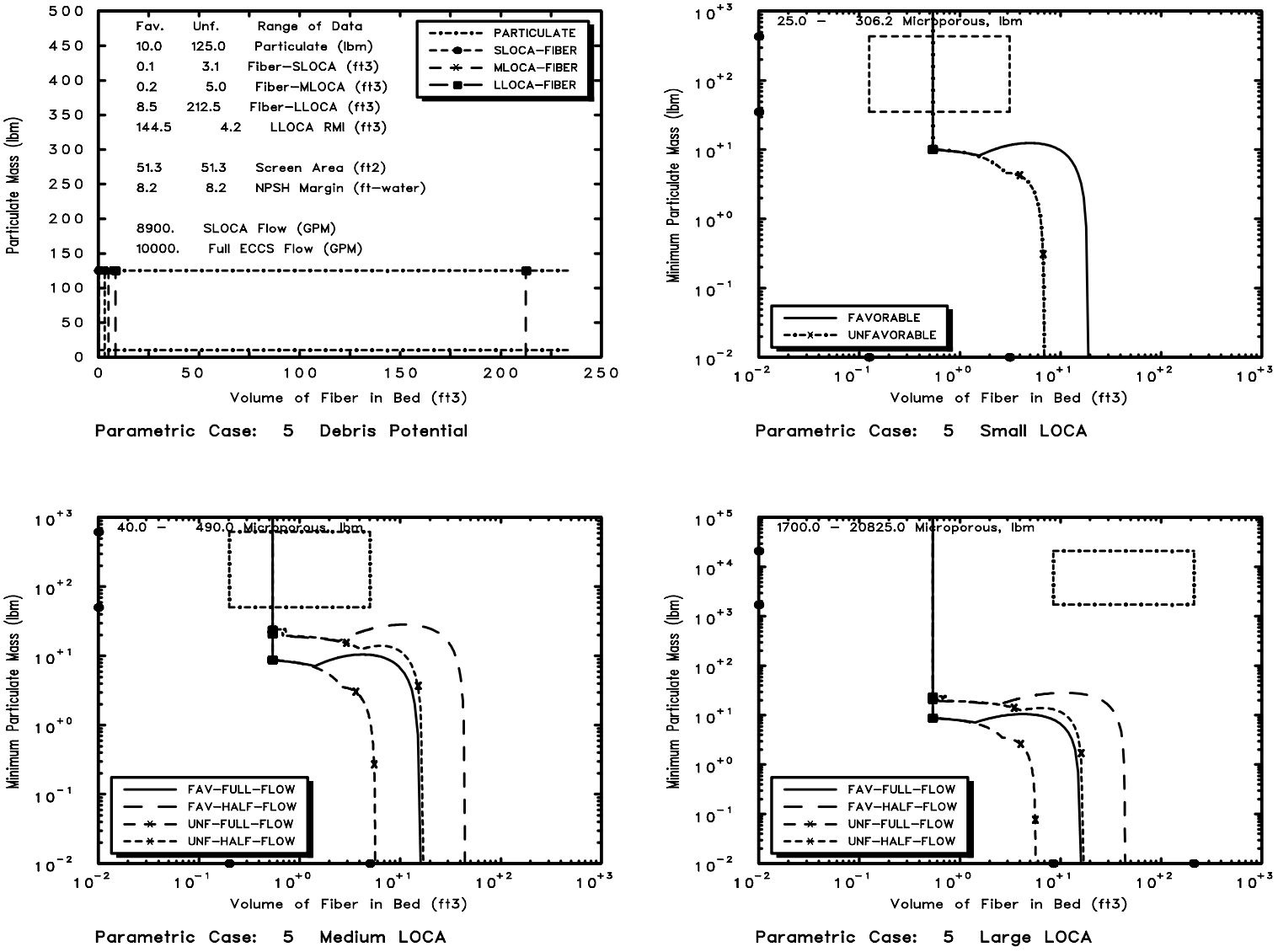

Fig. B-5. Parametric Case 5.

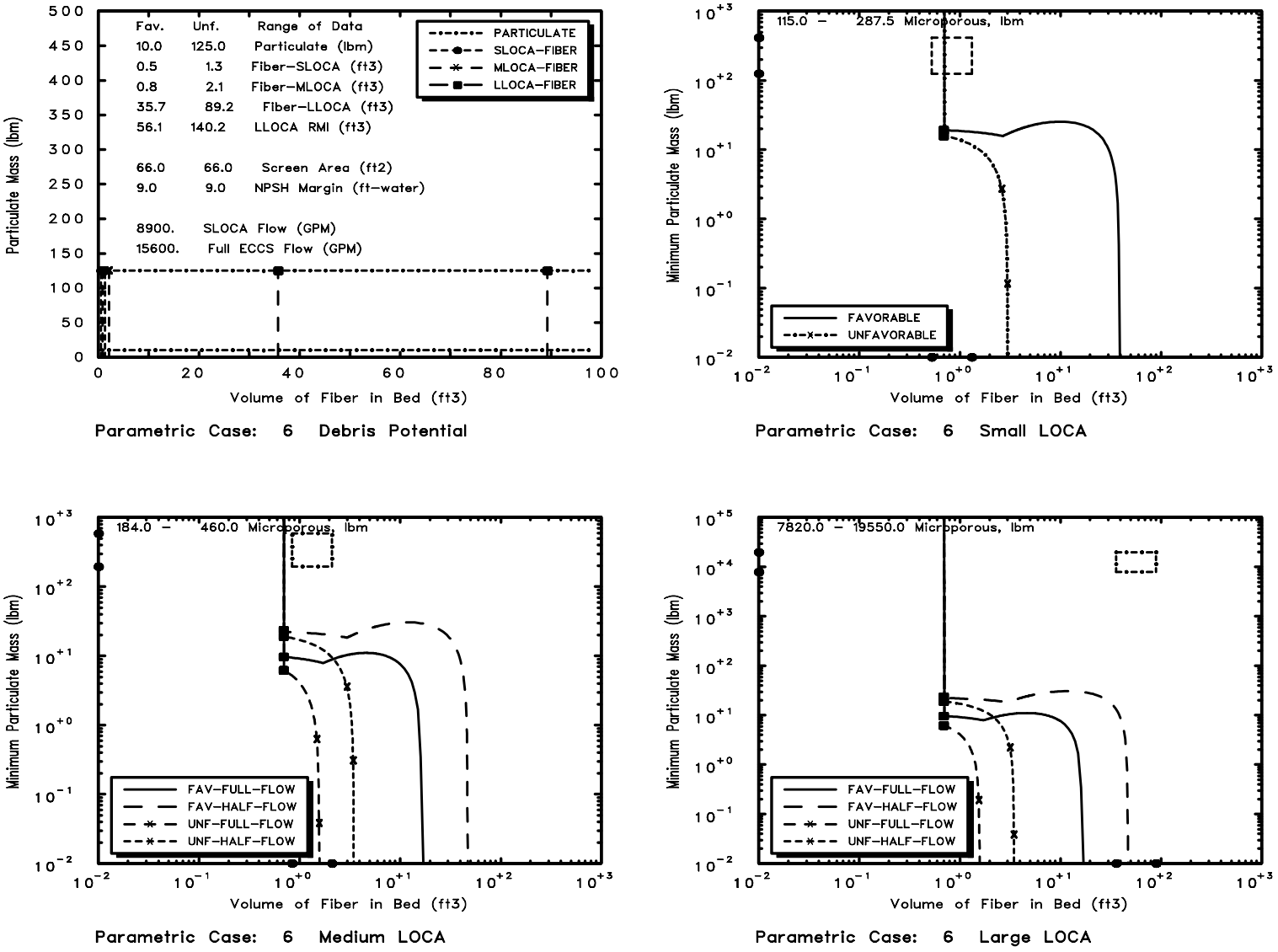

Fig. B-6. Parametric Case 6.

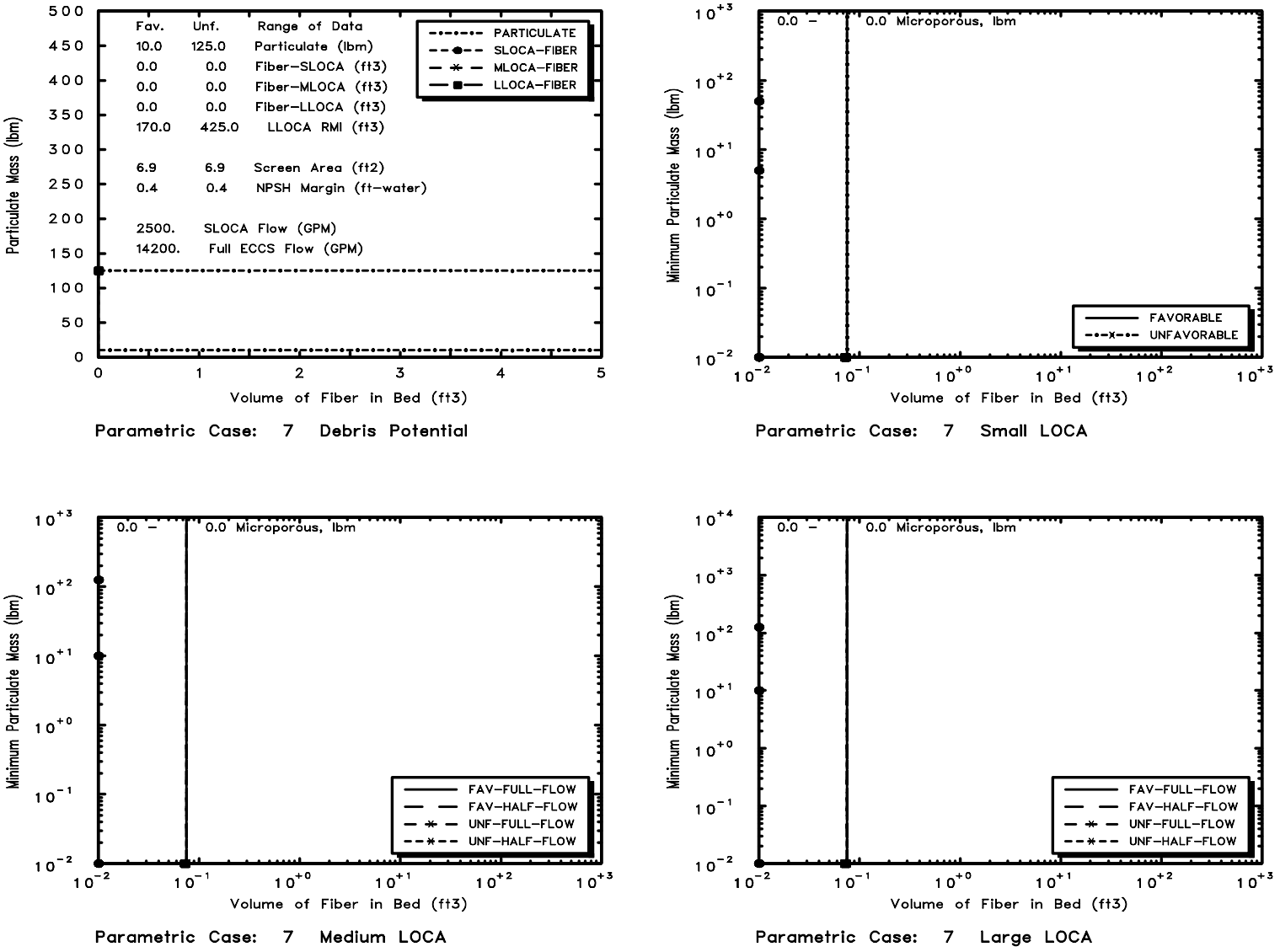

Fig. B-7. Parametric Case 7 (Note: No fiber in this case, so no debris boxes presented).

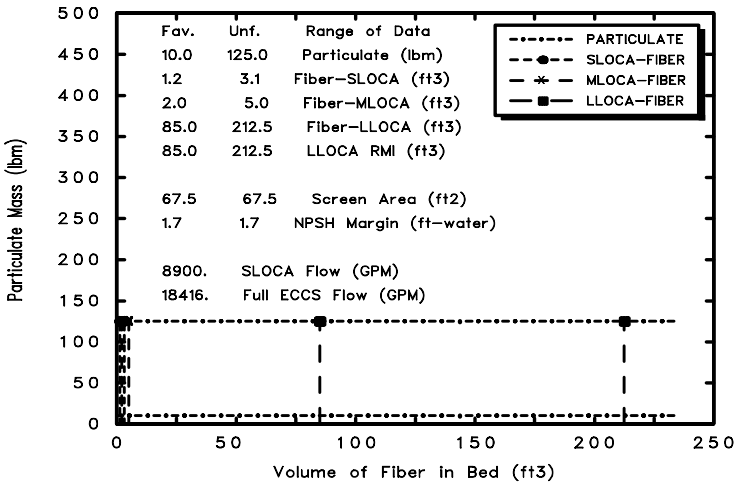

Parametric Case: 8 Debris Potential

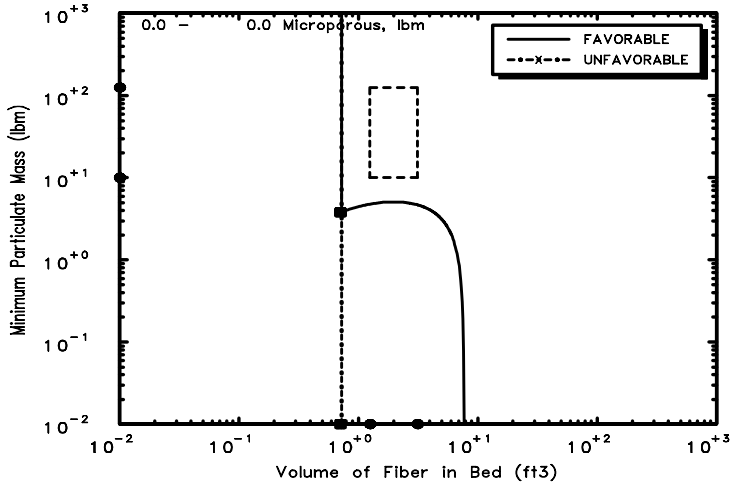

Parametric Case: 8 Small LOCA

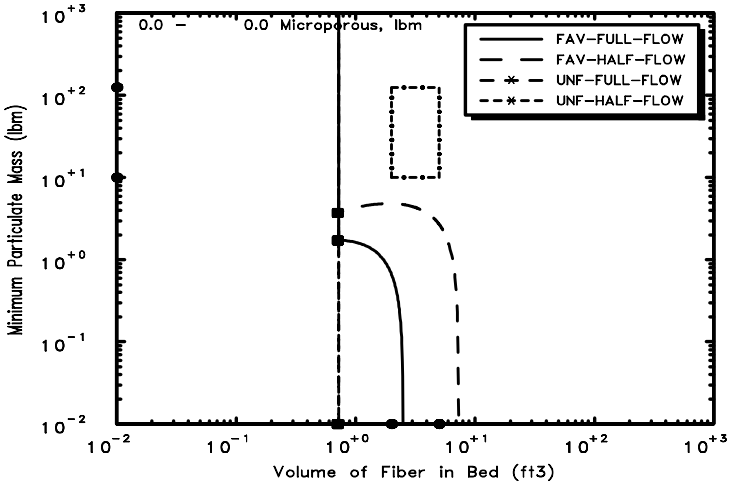

Parametric Case: 8 Medium LOCA

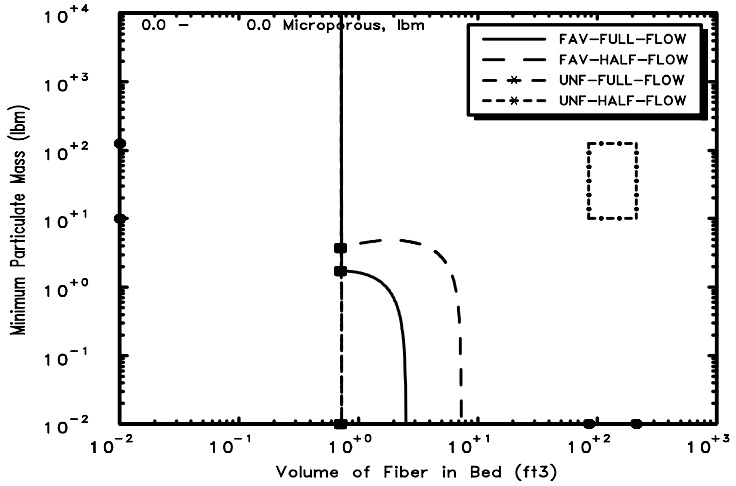

Parametric Case: 8 Large LOCA

Fig. B-8. Parametric Case 8.

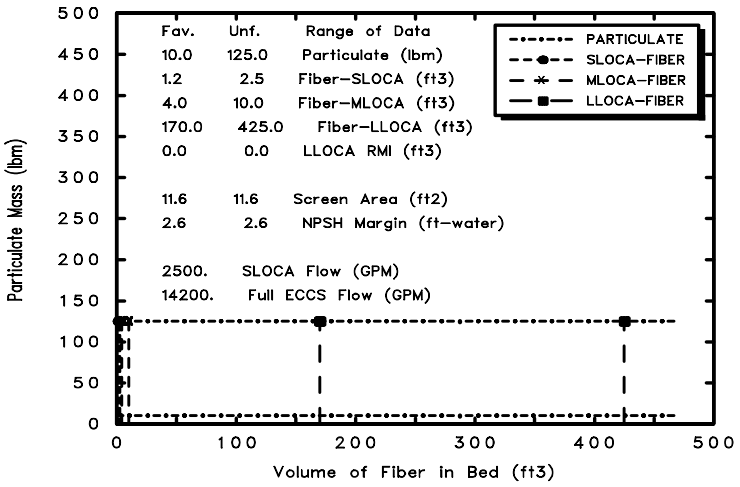

Parametric Case: 9 Debris Potential

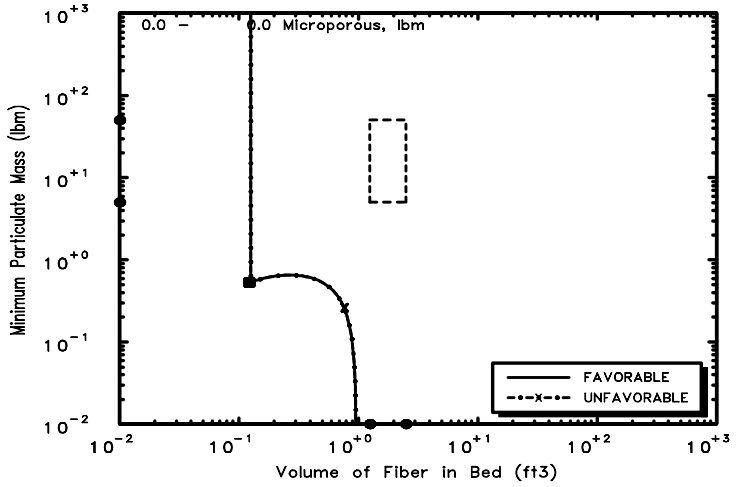

Parametric Case: 9 Small LOCA

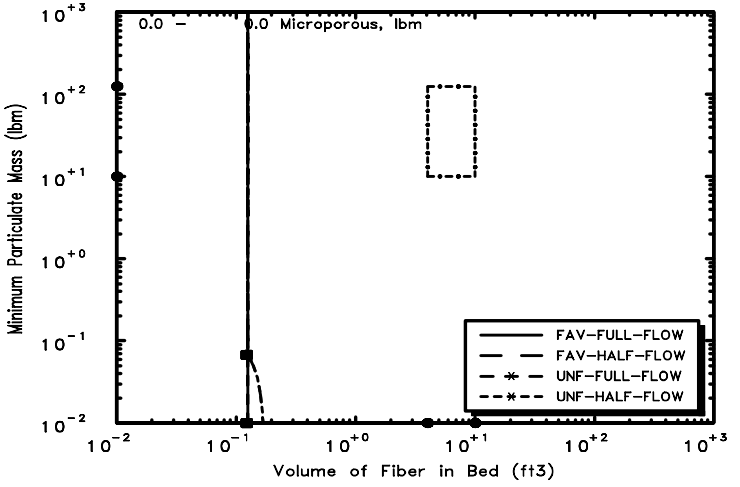

Parametric Case: 9 Medium LOCA

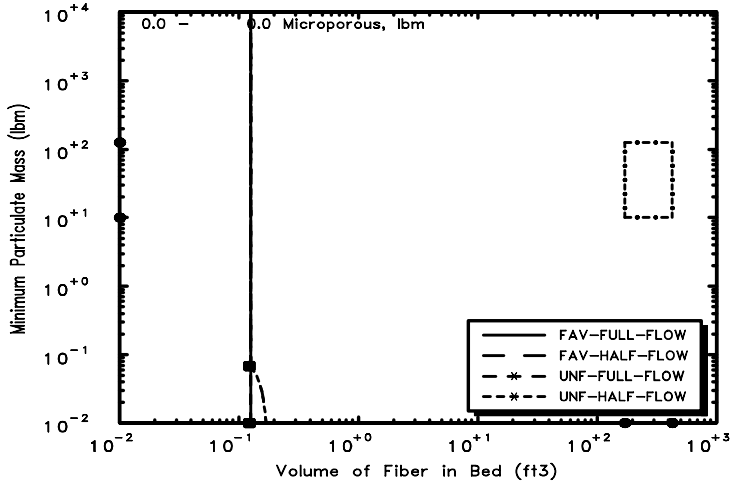

Parametric Case: 9 Large LOCA

Fig. B-9. Parametric Case 9.

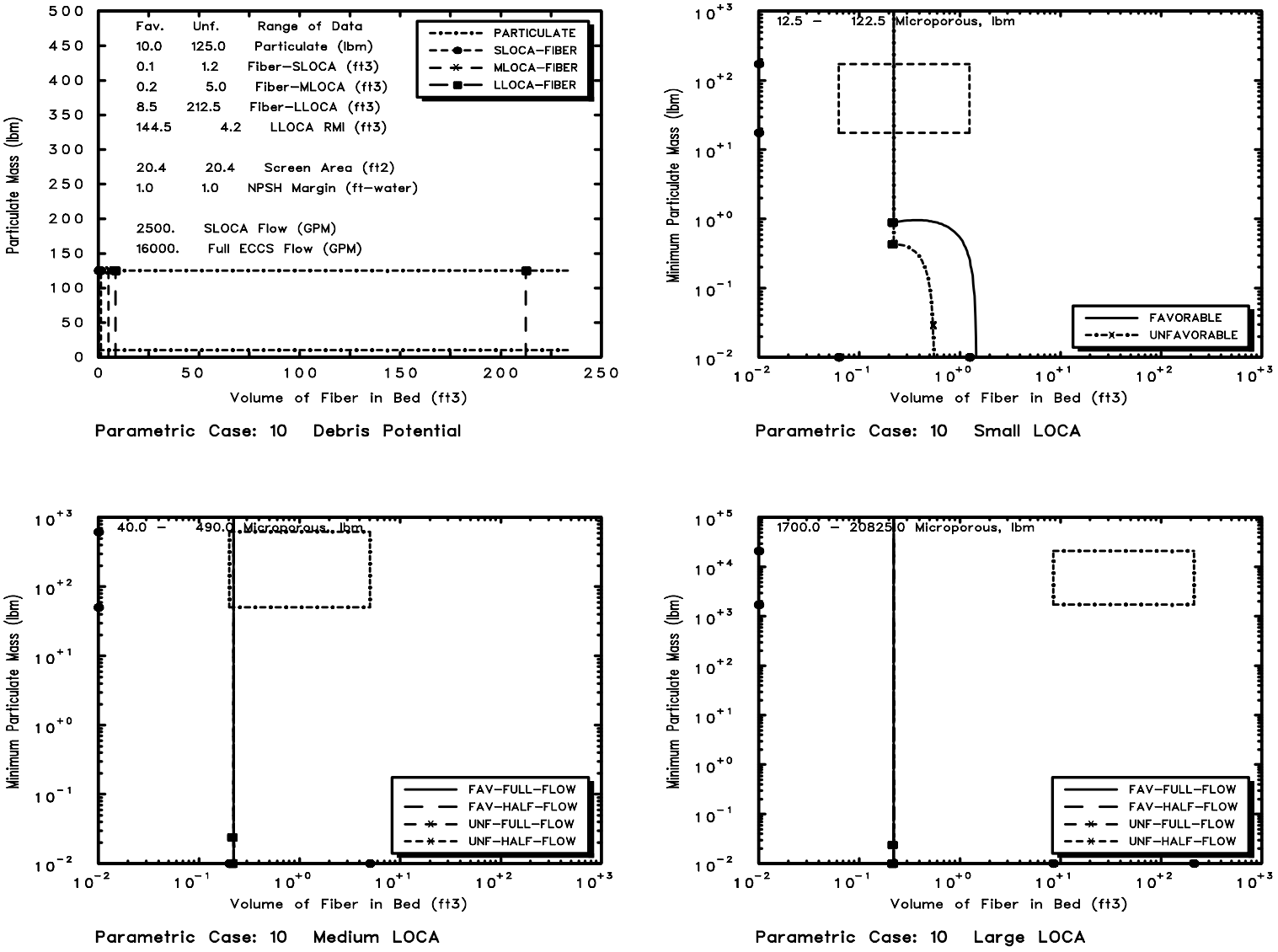

Fig. B-10. Parametric Case 10.

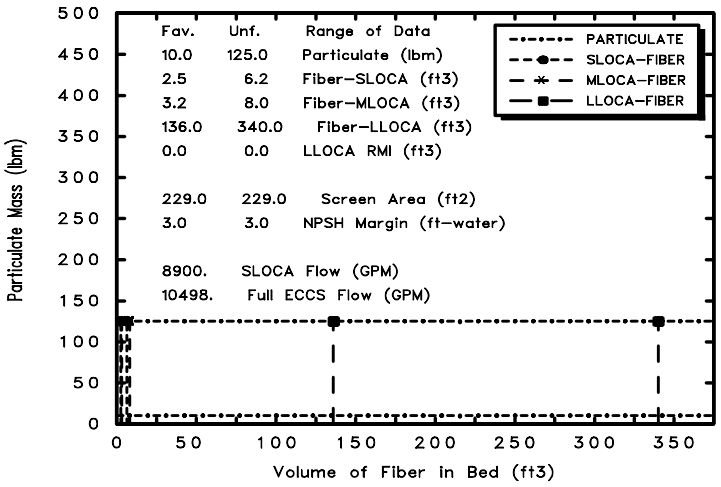

Parametric Case: 11 Debris Potential

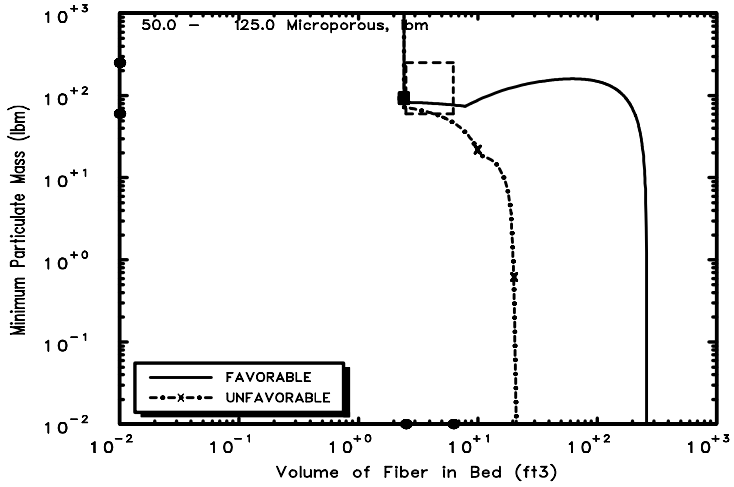

Parametric Case: 11 Small LOCA

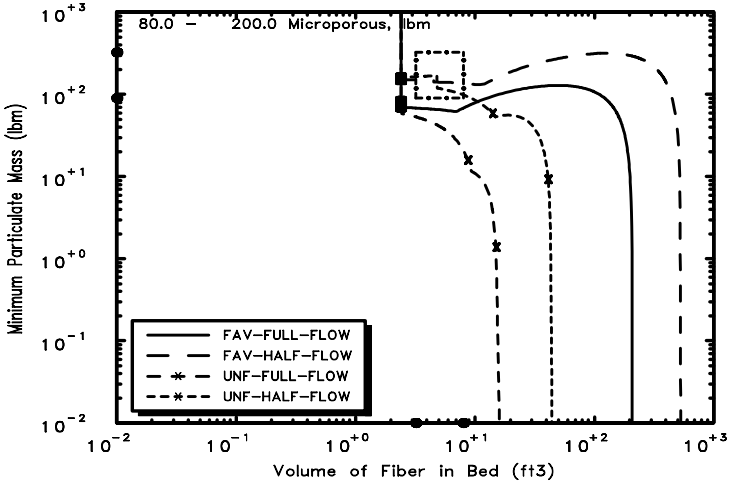

Parametric Case: 11 Medium LOCA

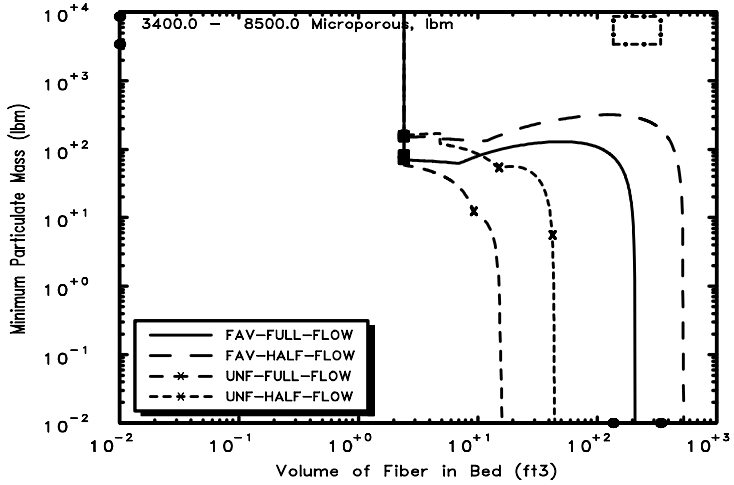

Parametric Case: 11 Large LOCA

Fig. B-11. Parametric Case 11.

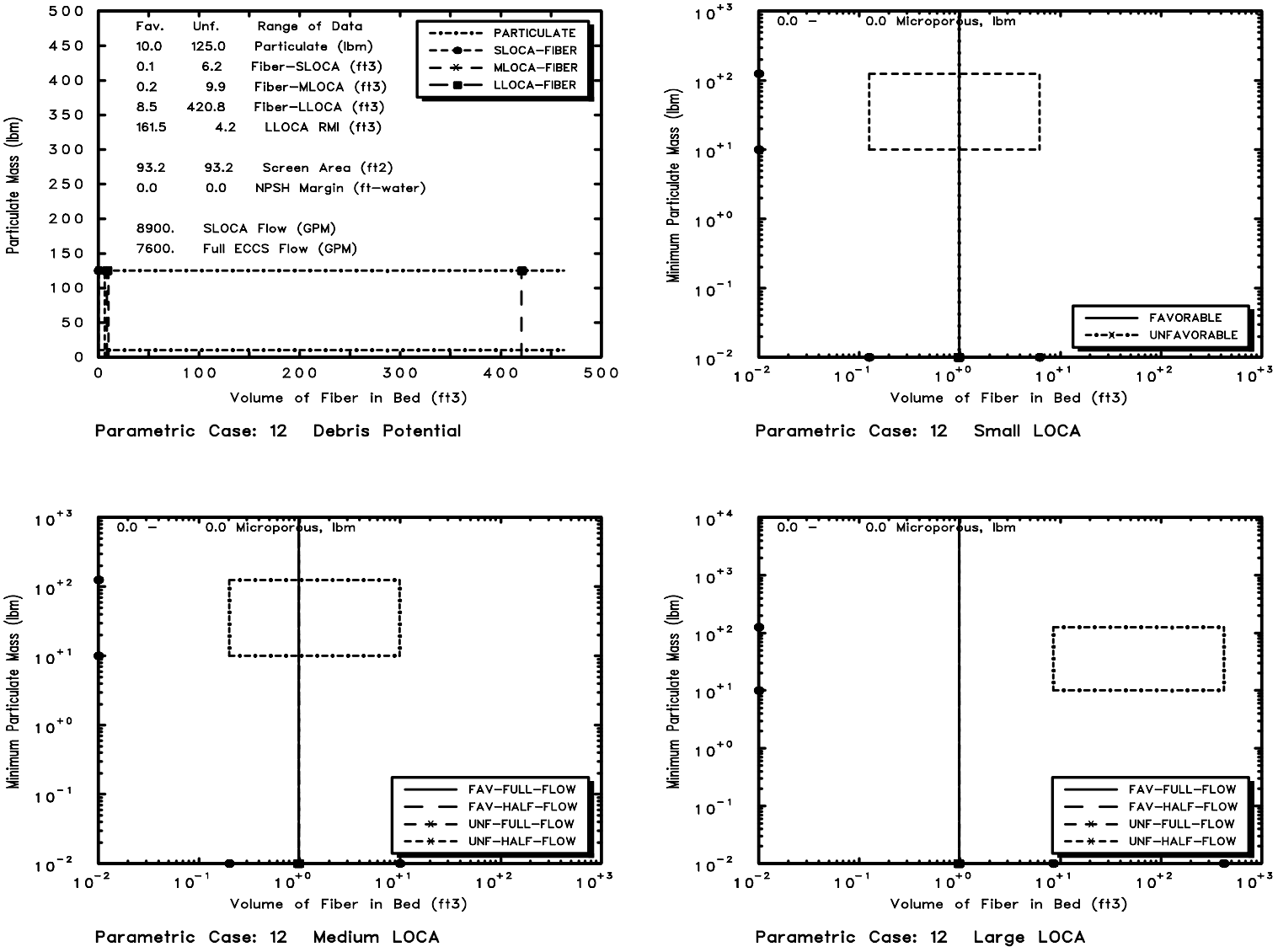

Fig. B-12. Parametric Case 12.

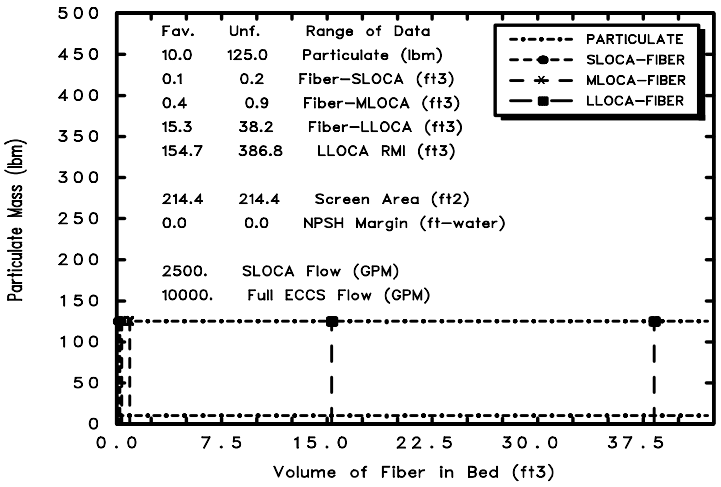

Parametric Case: 13 Debris Potential

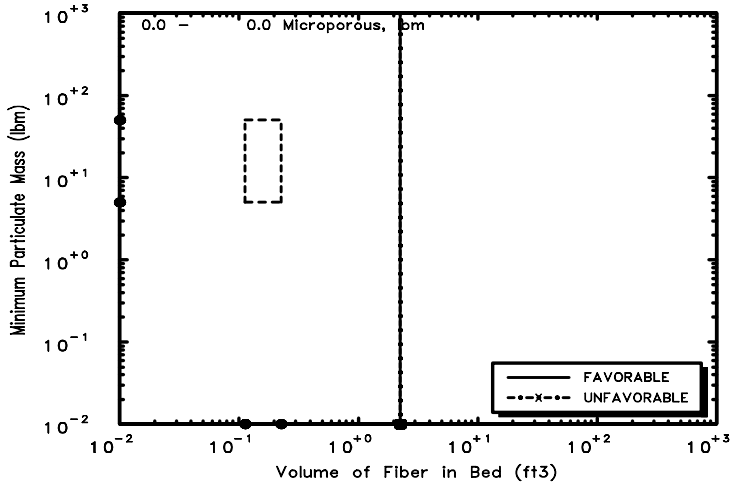

Parametric Case: 13 Small LOCA

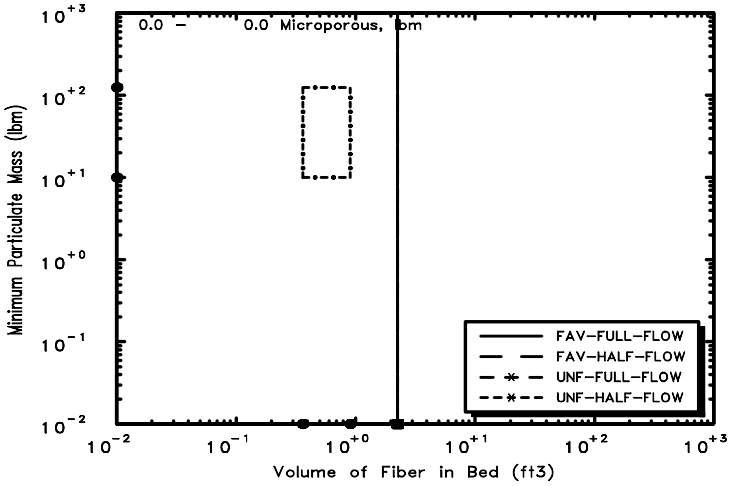

Parametric Case: 13 Medium LOCA

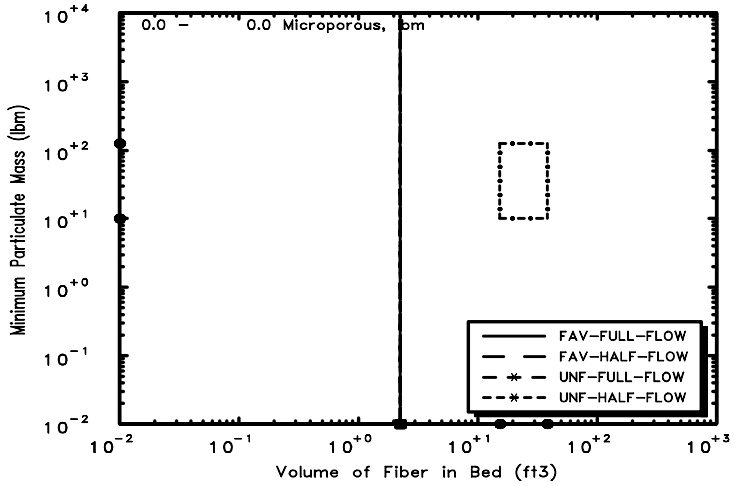

Parametric Case: 13 Large LOCA

Fig. B-13. Parametric Case 13.

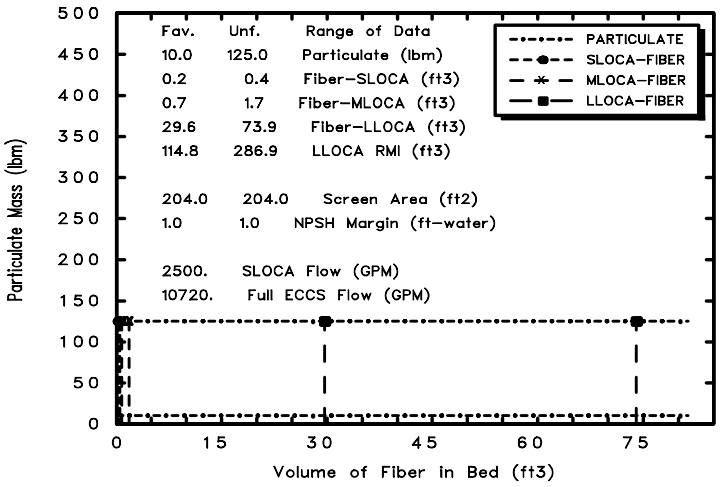

Parametric Case: 14 Debris Potential

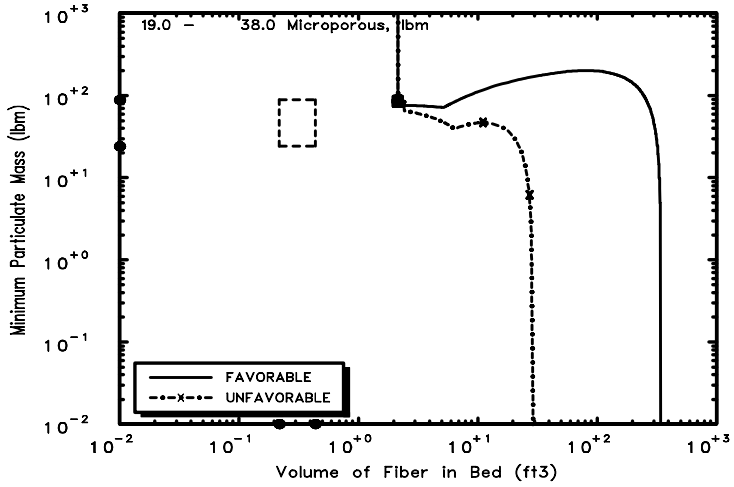

Parametric Case: 14 Small LOCA

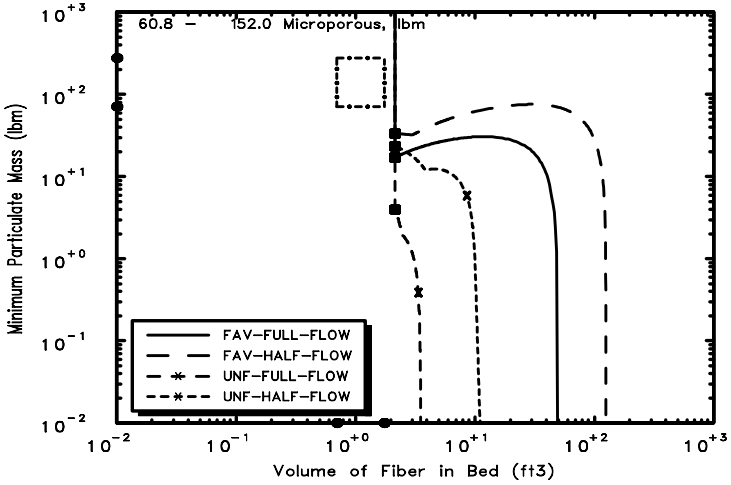

Parametric Case: 14 Medium LOCA

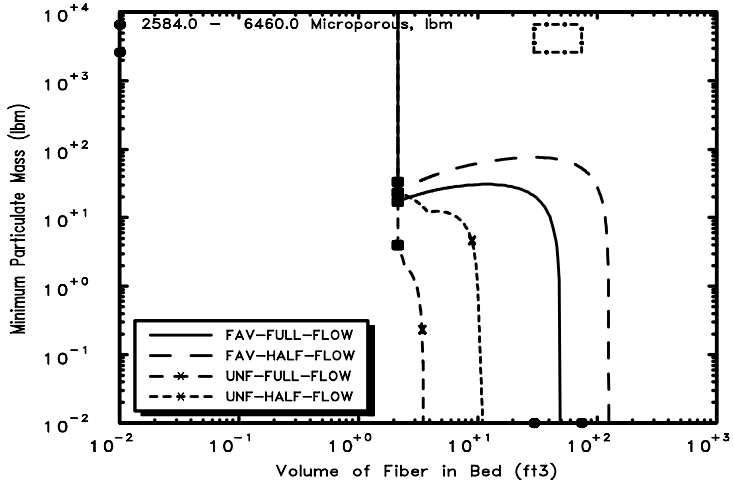

Parametric Case: 14 Large LOCA

Fig. B-14. Parametric Case 14.

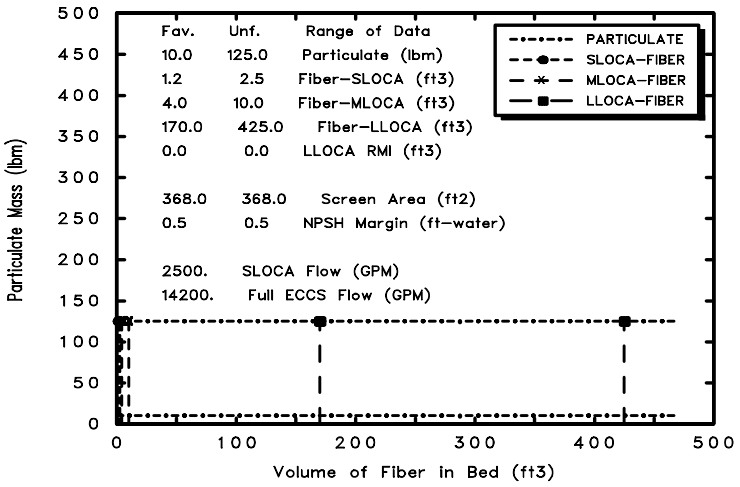

Parametric Case: 15 Debris Potential

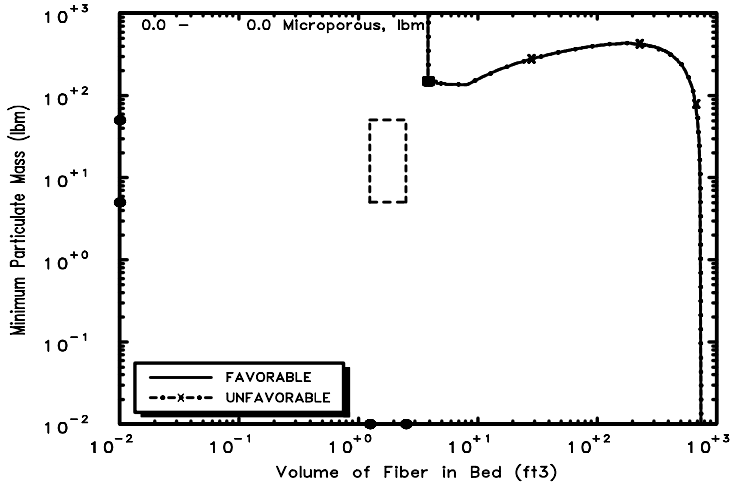

Parametric Case: 15 Small LOCA

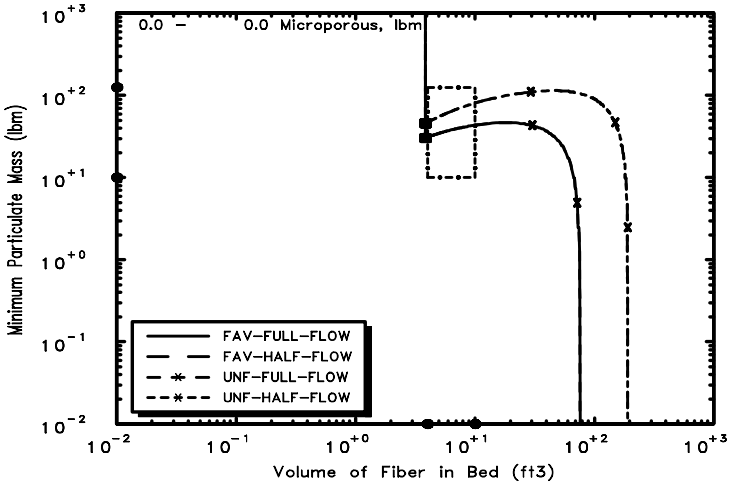

Parametric Case: 15 Medium LOCA

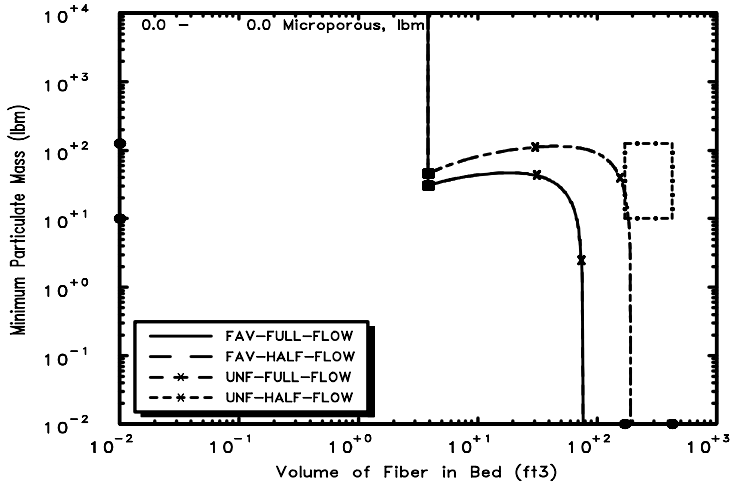

Parametric Case: 15 Large LOCA

Fig. B-15. Parametric Case 15.

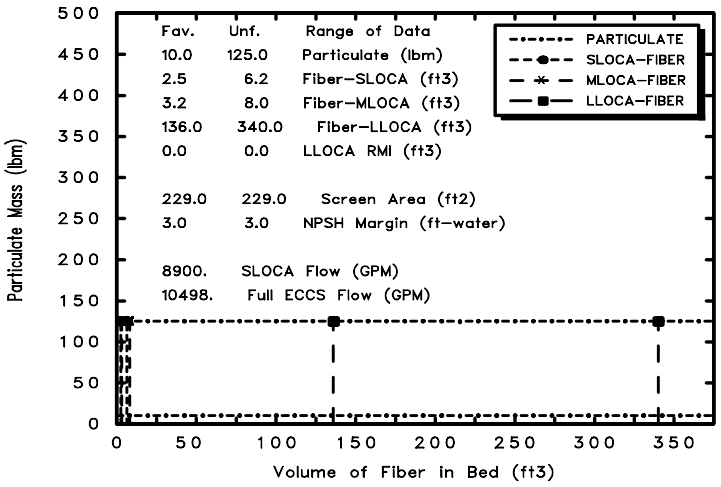

Parametric Case: 16 Debris Potential

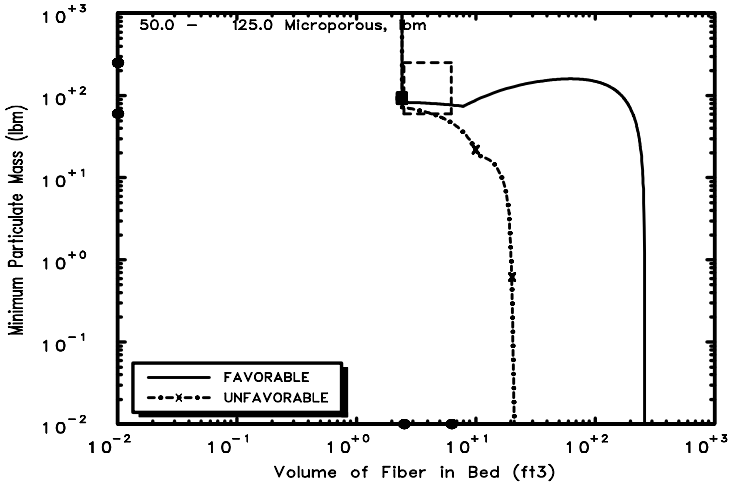

Parametric Case: 16 Small LOCA

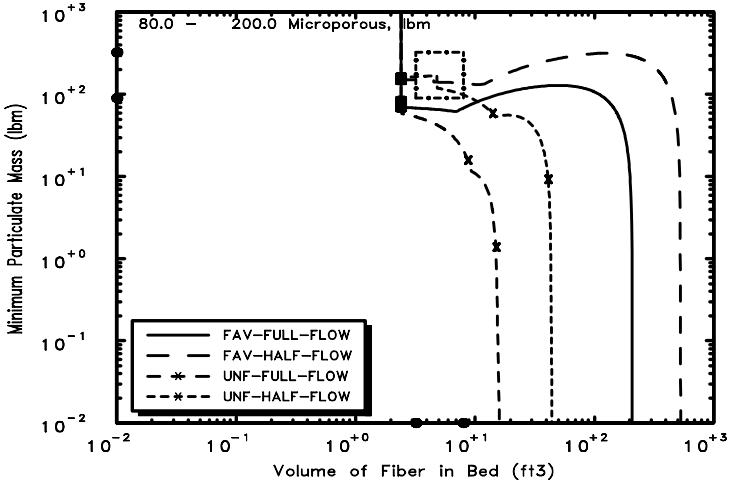

Parametric Case: 16 Medium LOCA

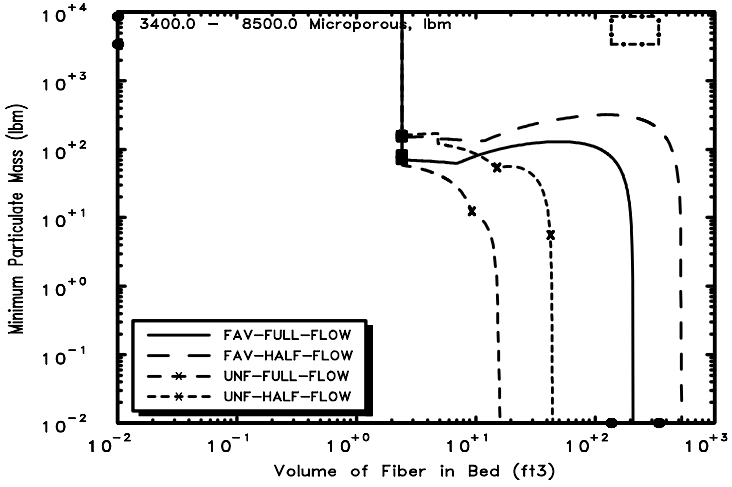

Parametric Case: 16 Large LOCA

Fig. B-16. Parametric Case 16.

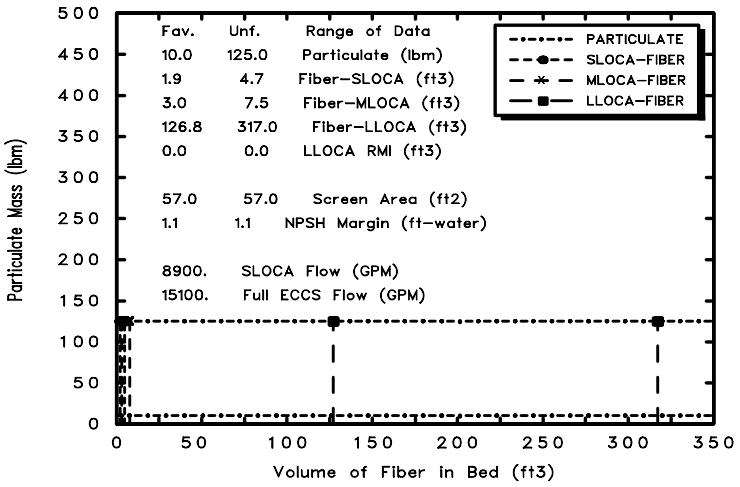

Parametric Case: 17 Debris Potential

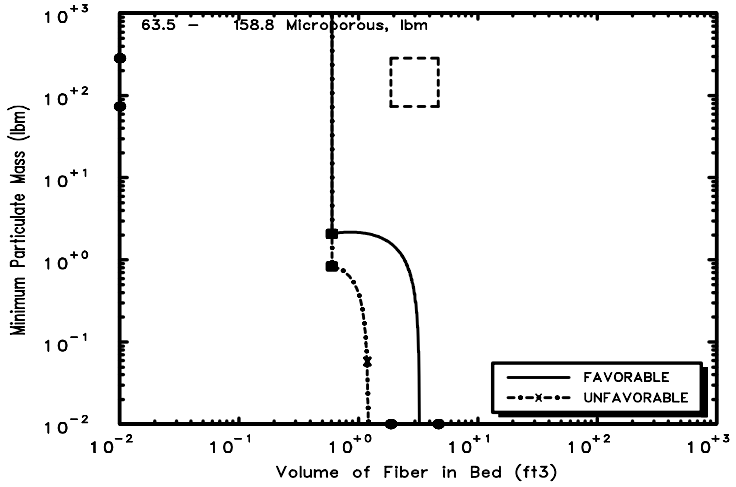

Parametric Case: 17 Small LOCA

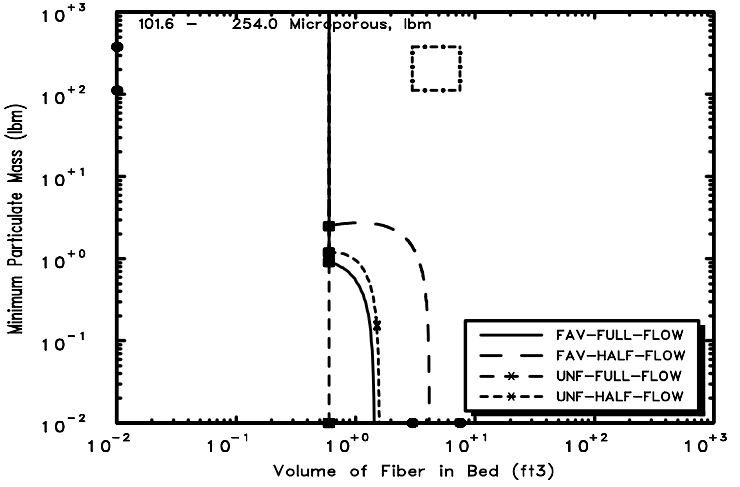

Parametric Case: 17 Medium LOCA

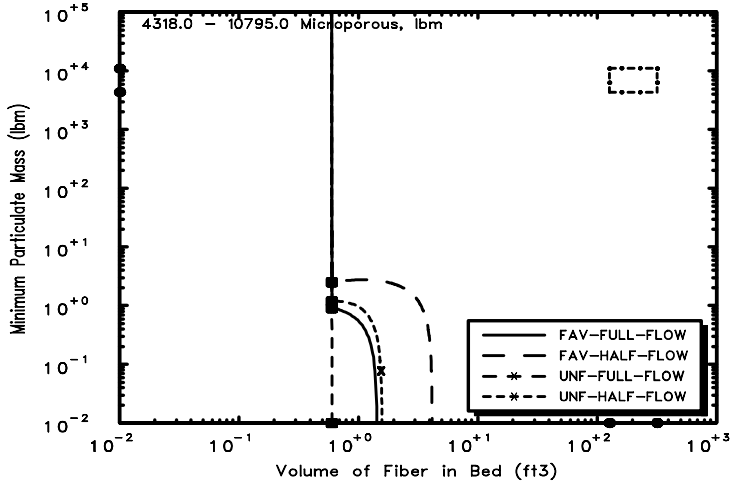

Parametric Case: 17 Large LOCA

Fig. B-17. Parametric Case 17.

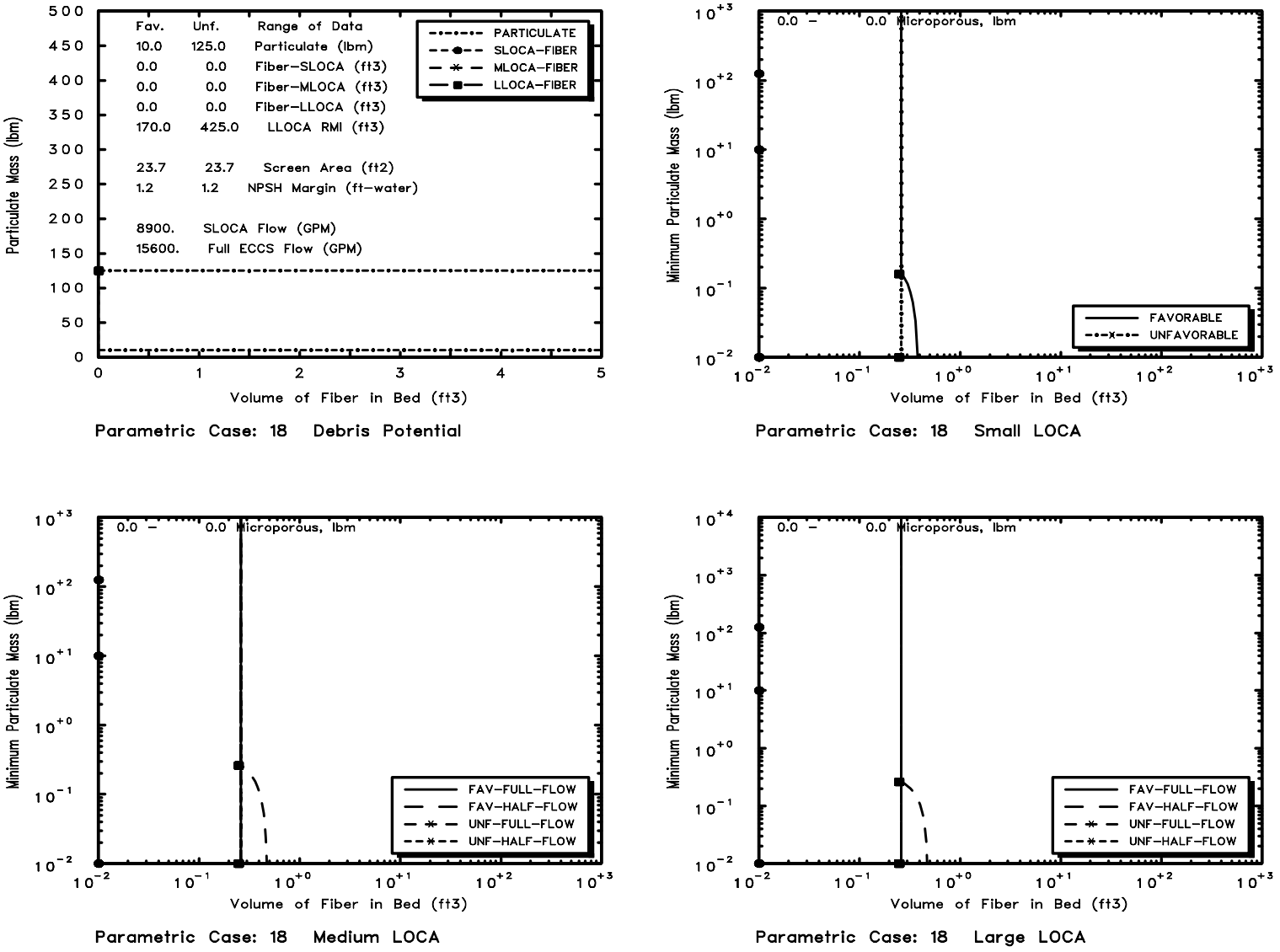

Fig. B-18. Parametric Case 18 (Note: No fiber in this case, so no debris boxes presented).

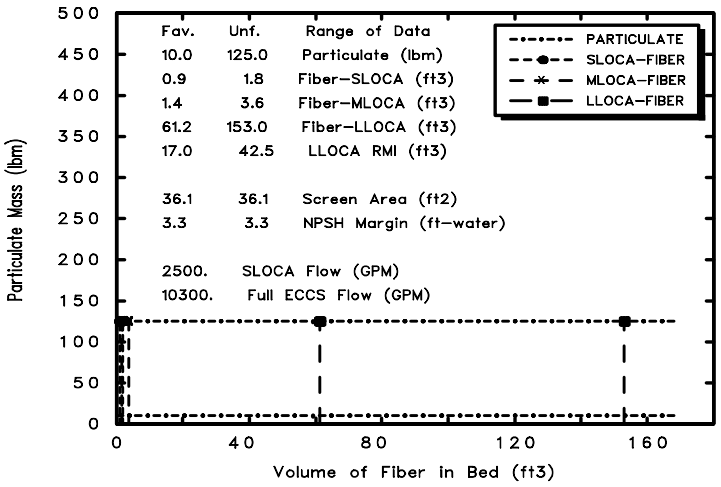

Parametric Case: 19 Debris Potential

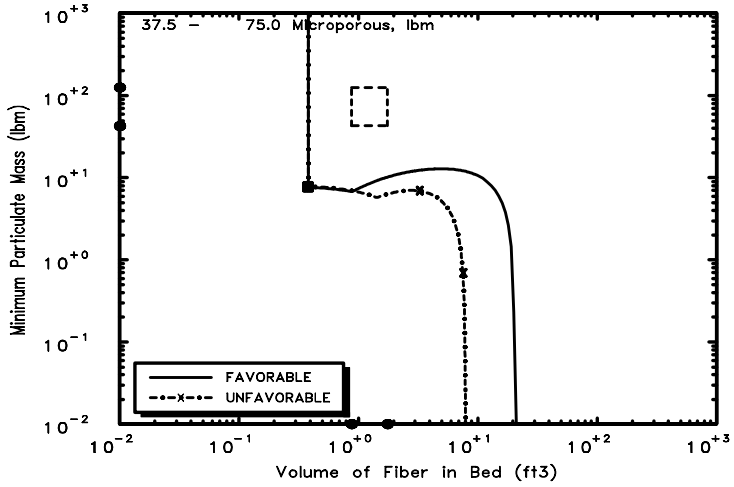

Parametric Case: 19 Small LOCA

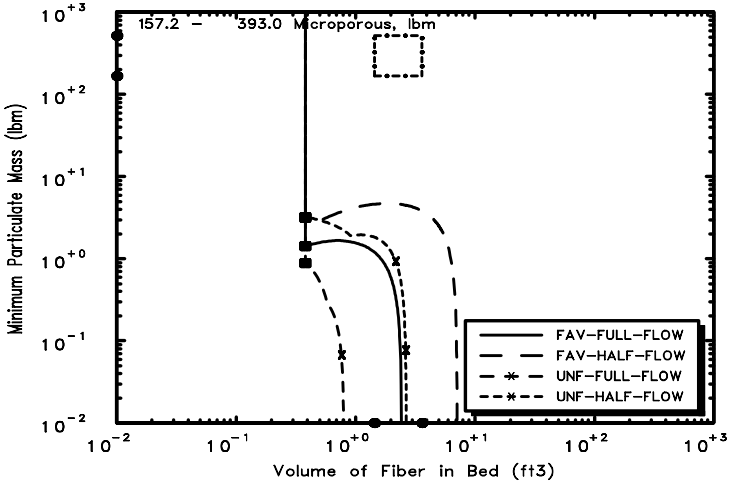

Parametric Case: 19 Medium LOCA

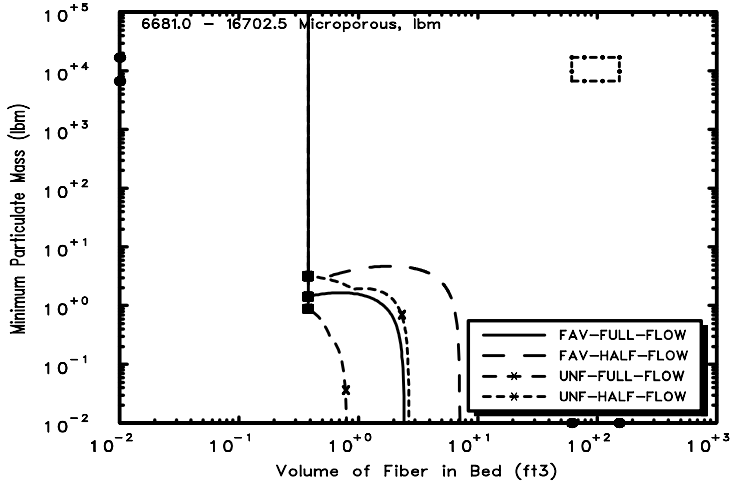

Parametric Case: 19 Large LOCA

Fig. B-19. Parametric Case 19.

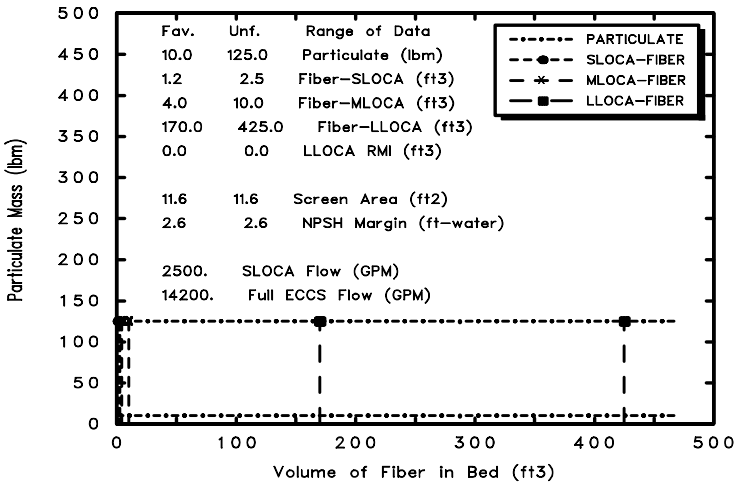

Parametric Case: 20 Debris Potential

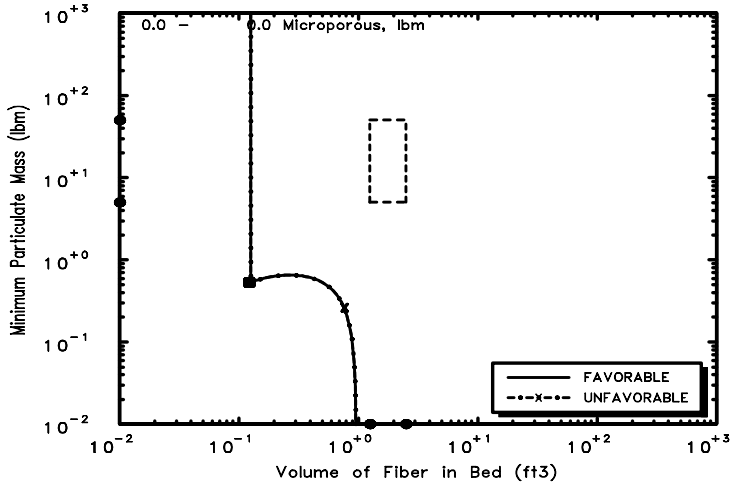

Parametric Case: 20 Small LOCA

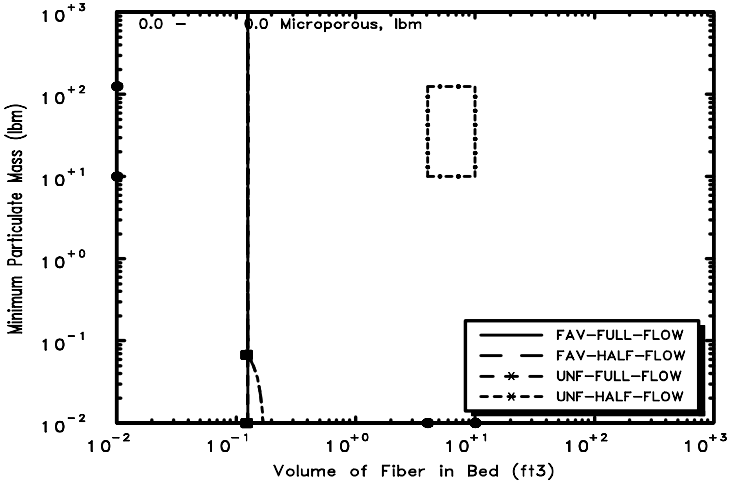

Parametric Case: 20 Medium LOCA

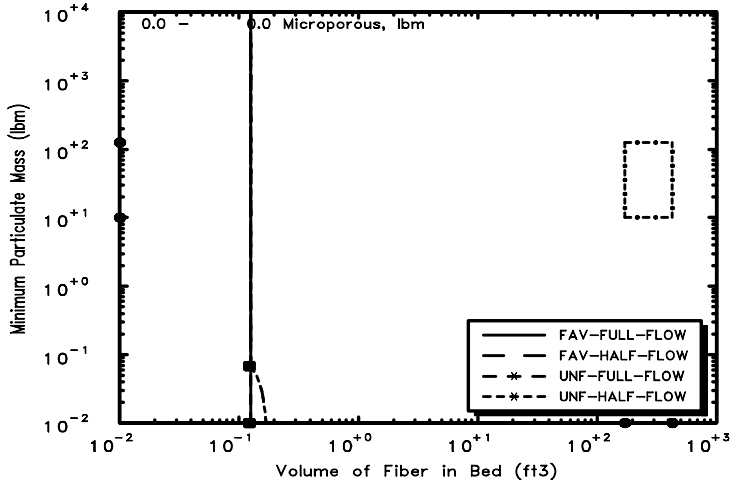

Parametric Case: 20 Large LOCA

Fig. B-20. Parametric Case 20.

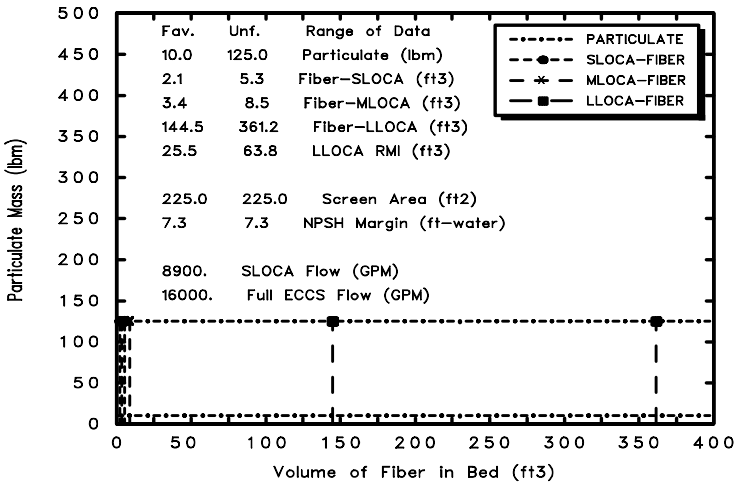

Parametric Case: 21 Debris Potential

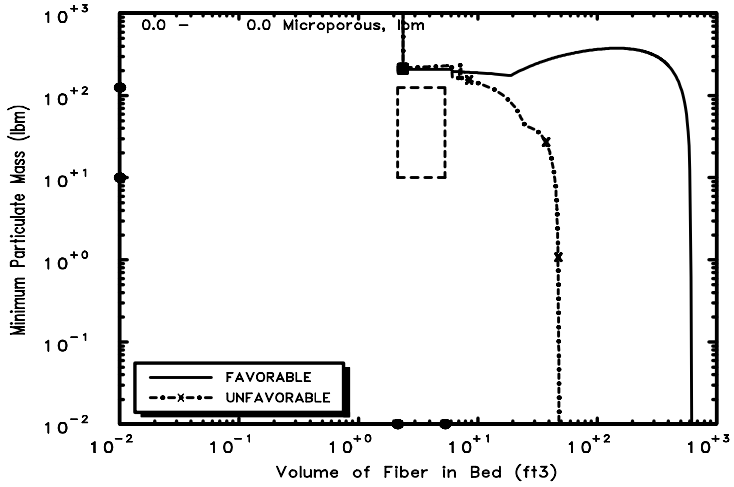

Parametric Case: 21 Small LOCA

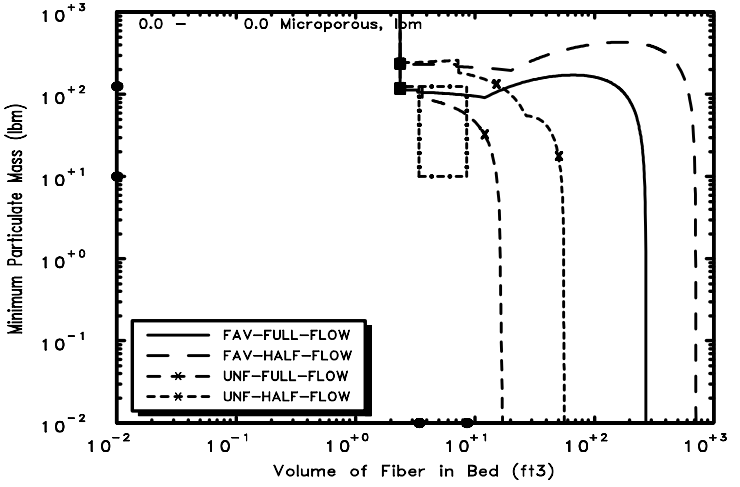

Parametric Case: 21 Medium LOCA

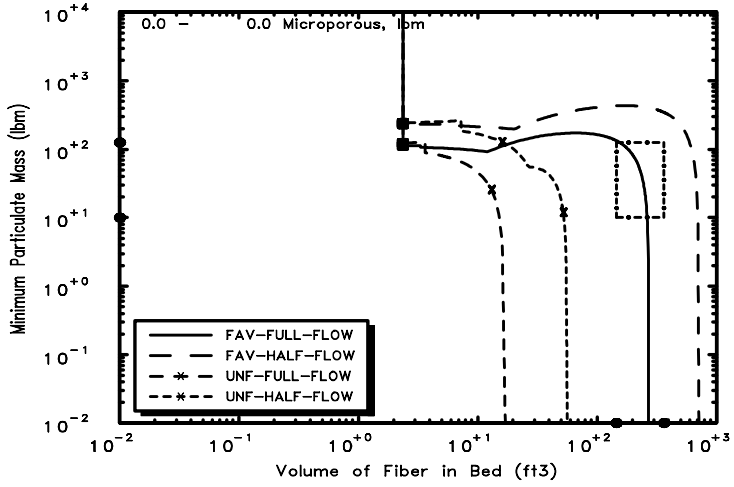

Parametric Case: 21 Large LOCA

Fig. B-21. Parametric Case 21.

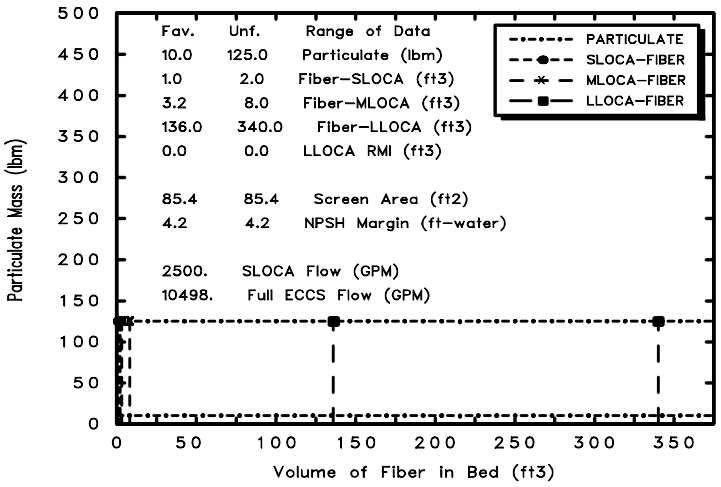

Parametric Case: 22 Debris Potential

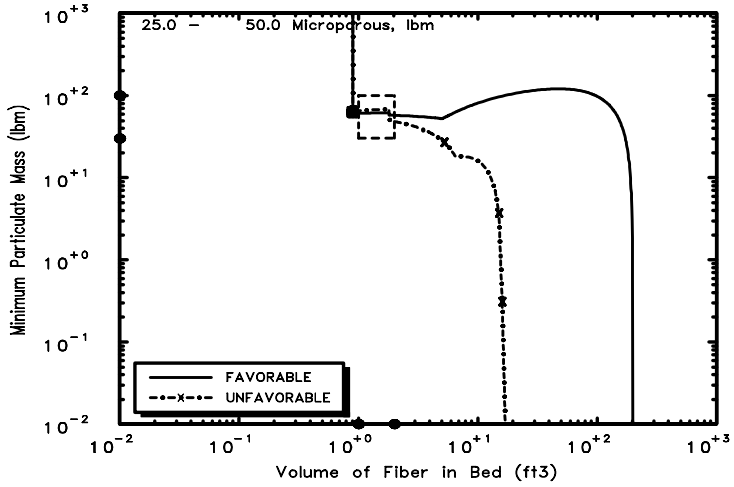

Parametric Case: 22 Small LOCA

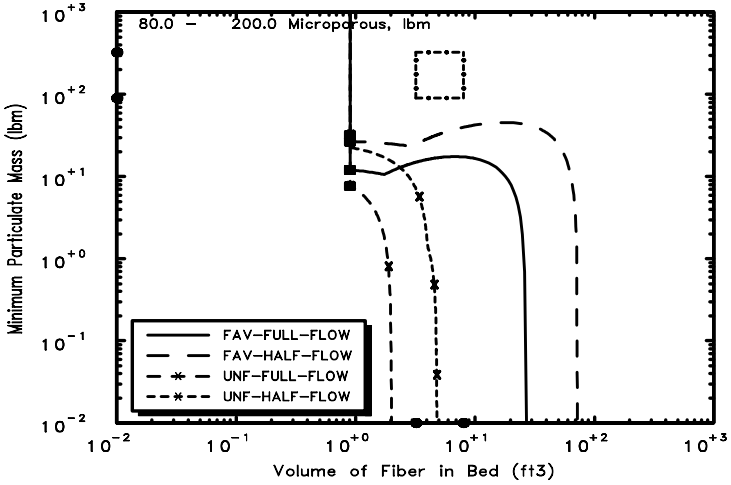

Parametric Case: 22 Medium LOCA

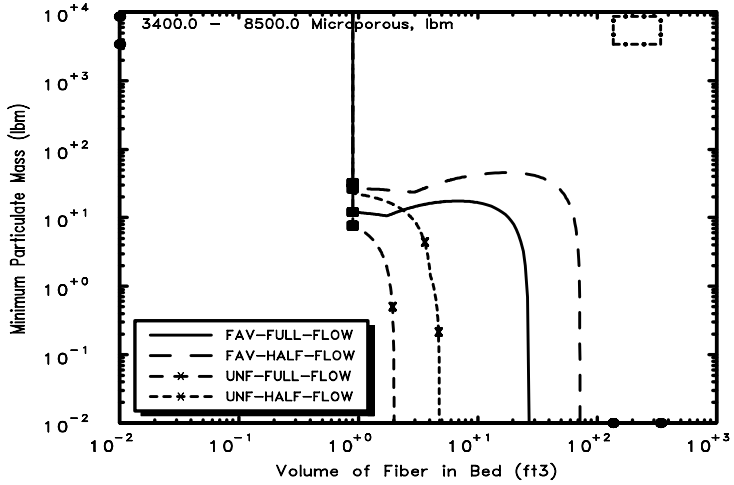

Parametric Case: 22 Large LOCA

Fig. B-22. Parametric Case 22.

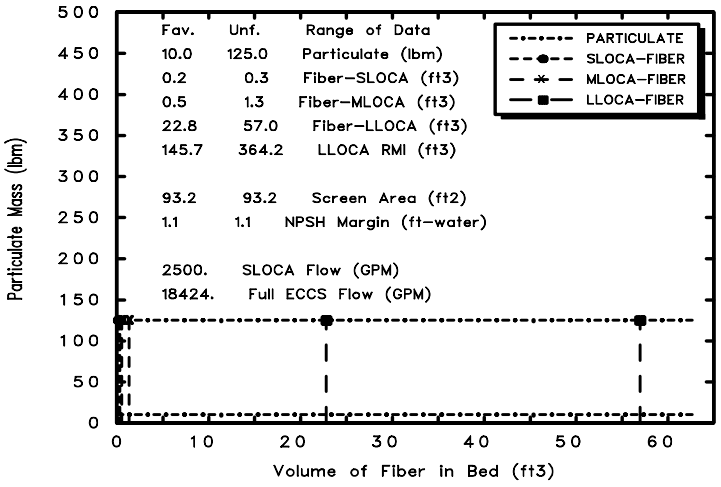

Parametric Case: 23 Debris Potential

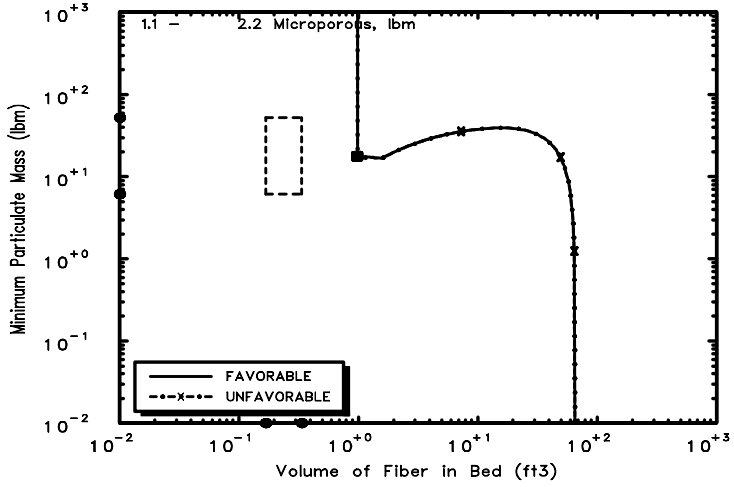

Parametric Case: 23 Small LOCA

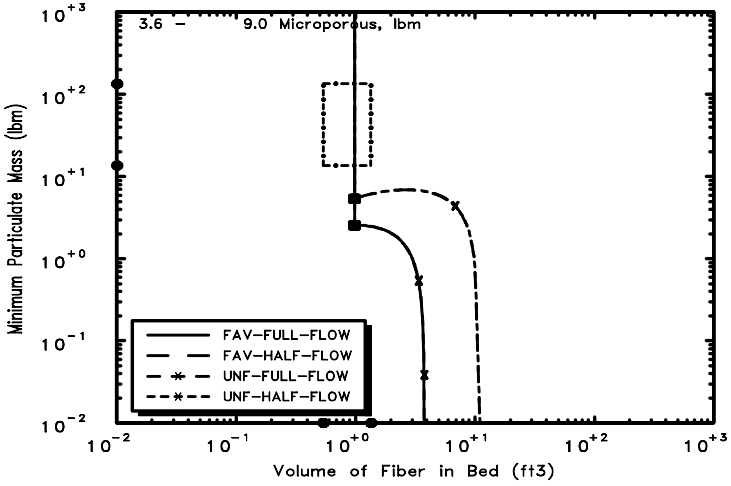

Parametric Case: 23 Medium LOCA

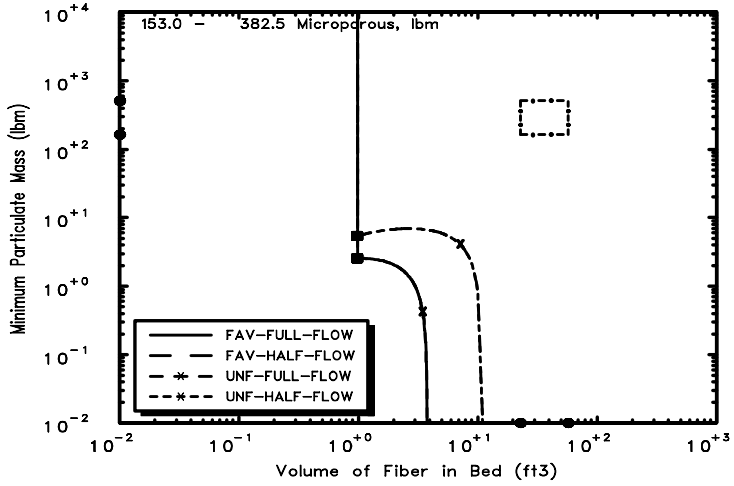

Parametric Case: 23 Large LOCA

Fig. B-23. Parametric Case 23.

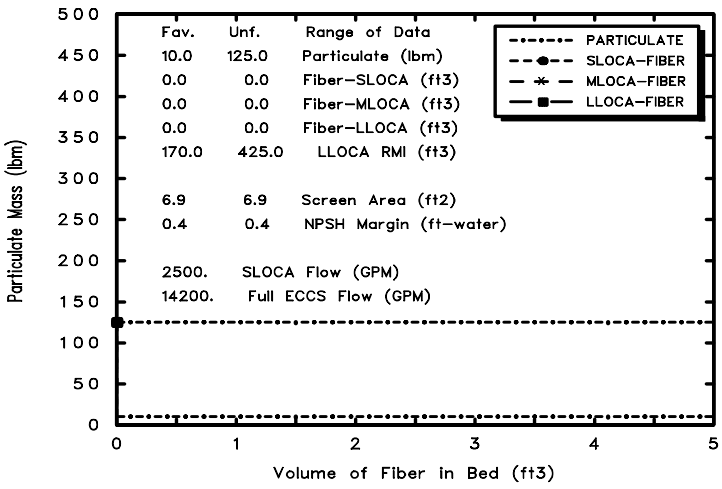

Parametric Case: 24 Debris Potential

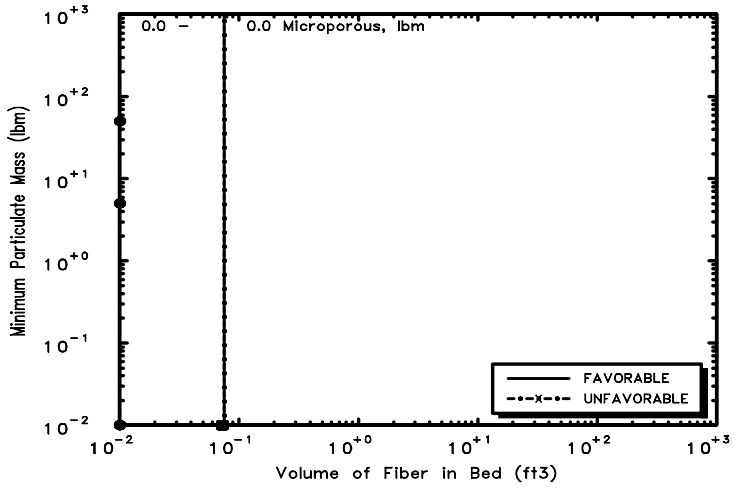

Parametric Case: 24 Small LOCA

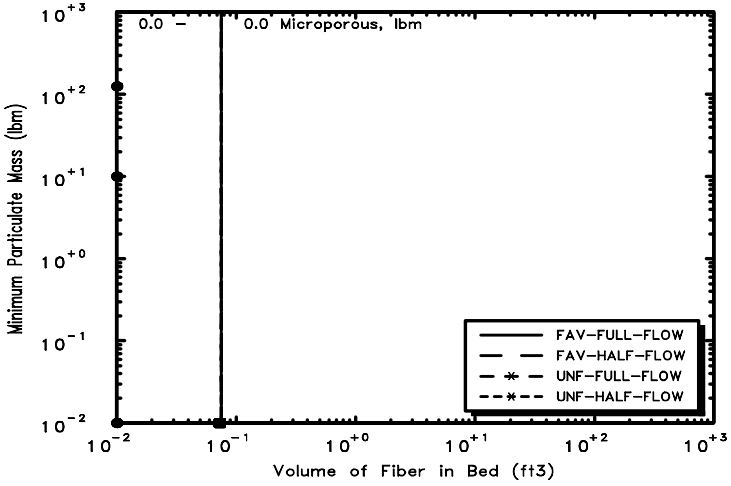

Parametric Case: 24 Medium LOCA

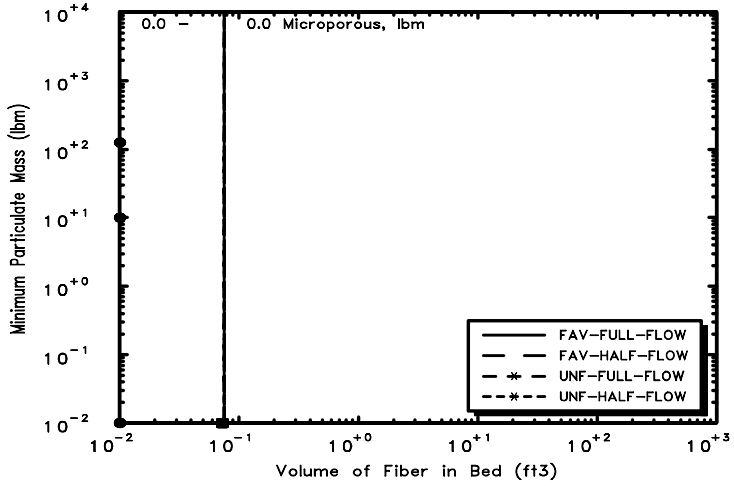

Parametric Case: 24 Large LOCA

Fig. B-24. Parametric Case 24 (Note: No fiber in this case, so no debris boxes presented).

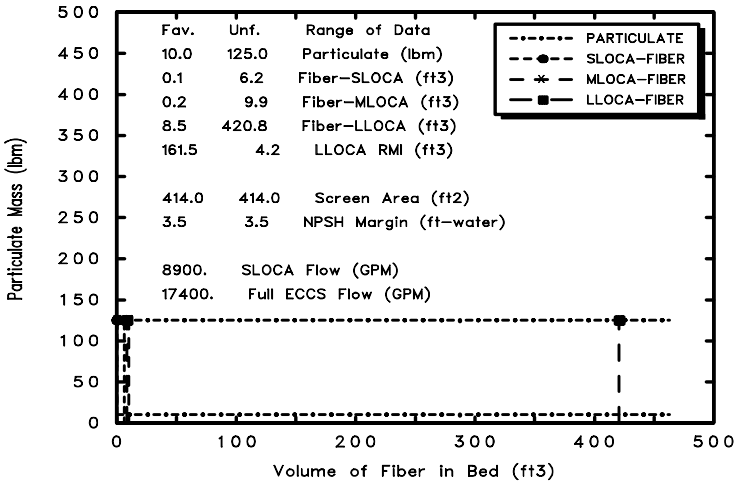

Parametric Case: 25 Debris Potential

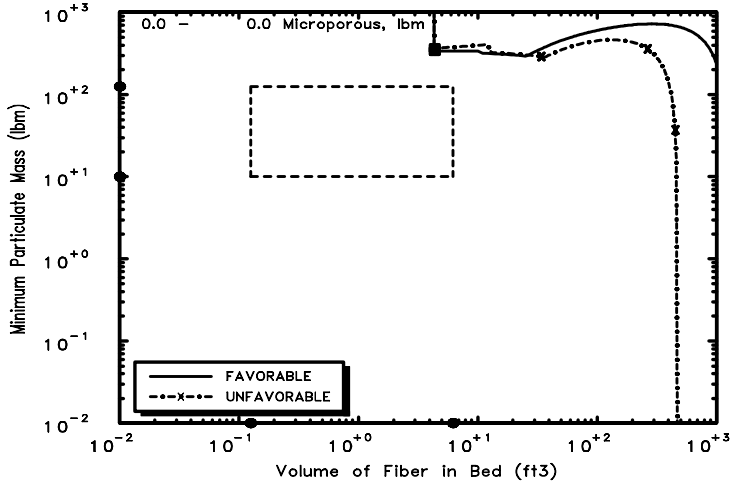

Parametric Case: 25 Small LOCA

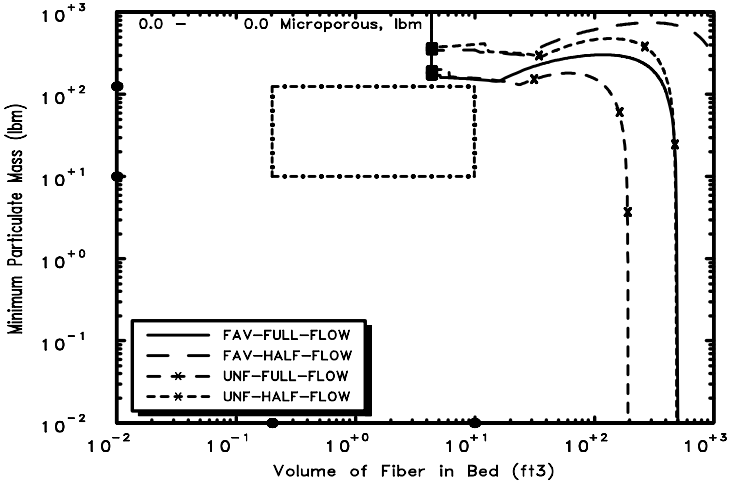

Parametric Case: 25 Medium LOCA

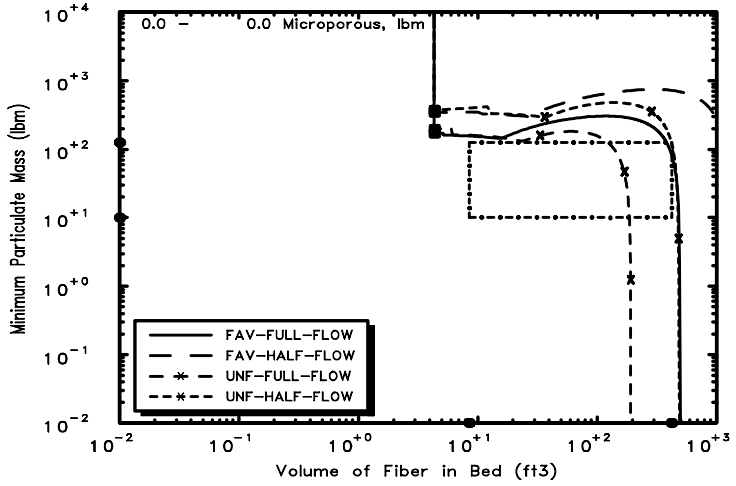

Parametric Case: 25 Large LOCA

Fig. B-25. Parametric Case 25.

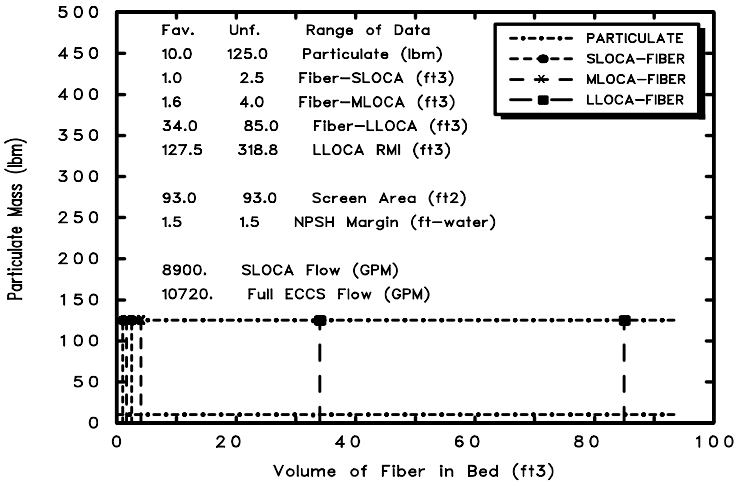

Parametric Case: 26 Debris Potential

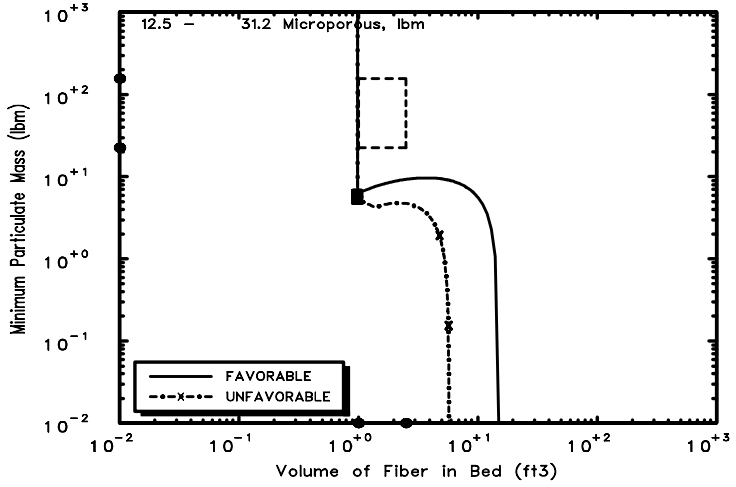

Parametric Case: 26 Small LOCA

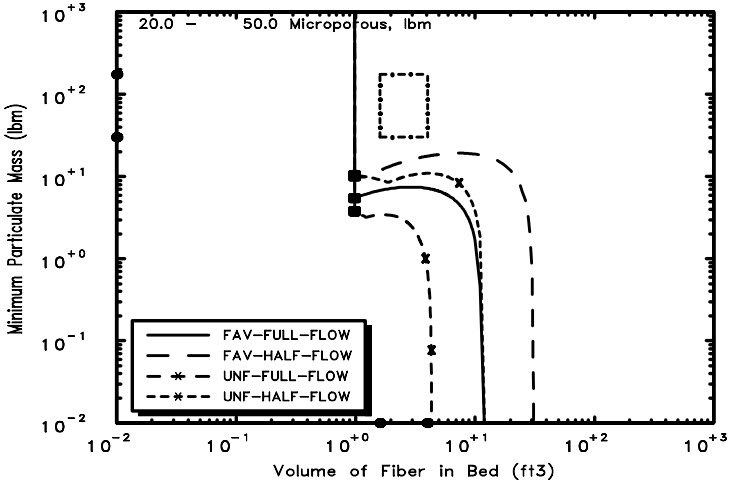

Parametric Case: 26 Medium LOCA

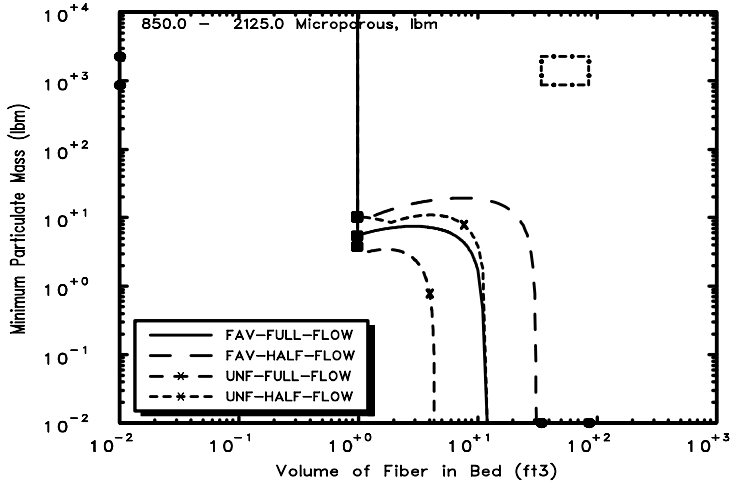

Parametric Case: 26 Large LOCA

Fig. B-26. Parametric Case 26.

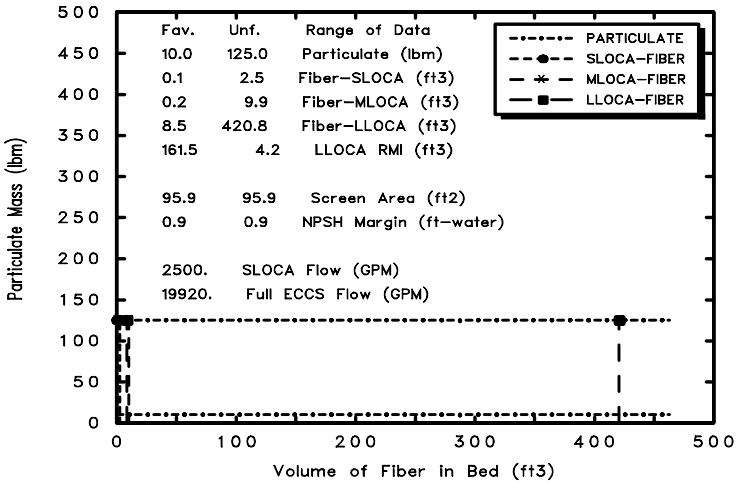

Parametric Case: 27 Debris Potential

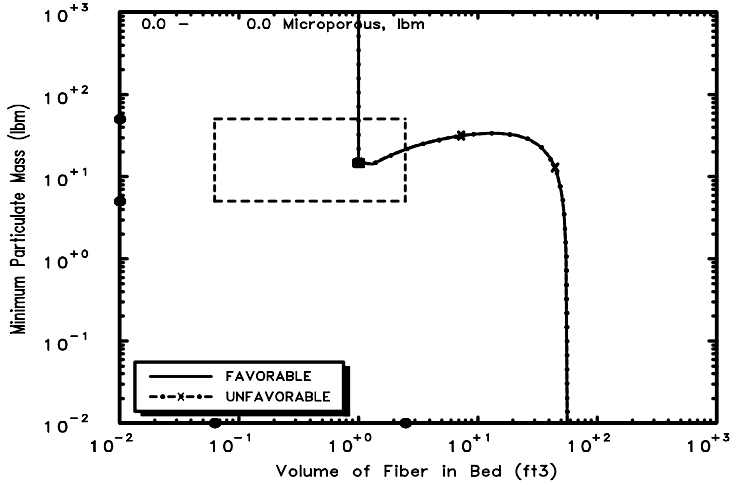

Parametric Case: 27 Small LOCA

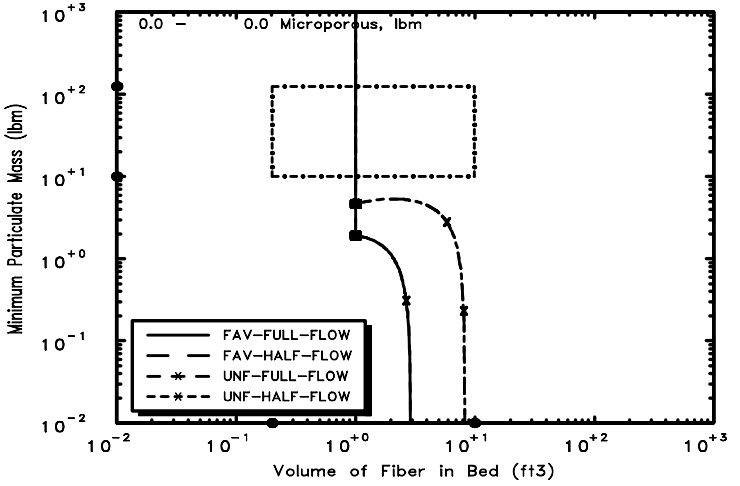

Parametric Case: 27 Medium LOCA

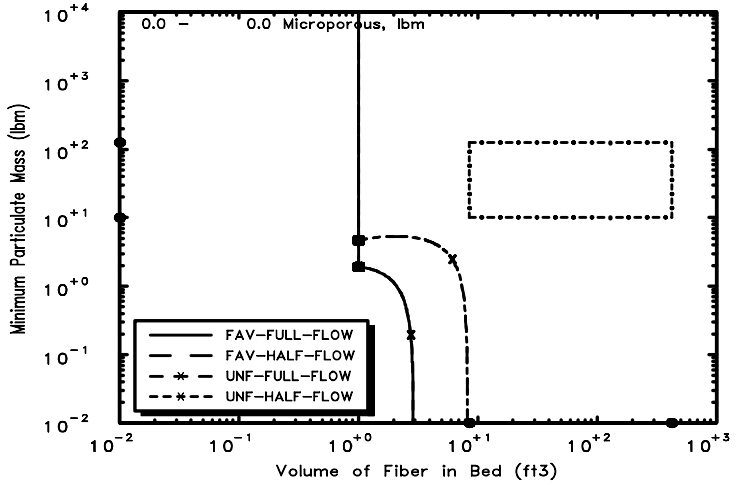

Parametric Case: 27 Large LOCA

Fig. B-27. Parametric Case 27.

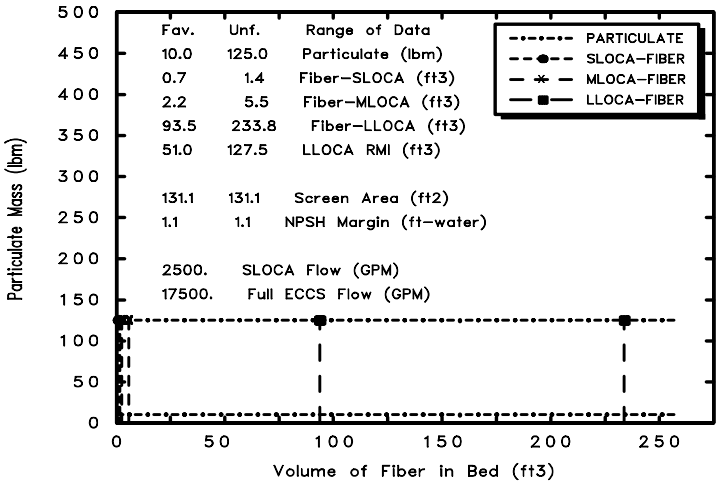

Parametric Case: 28 Debris Potential

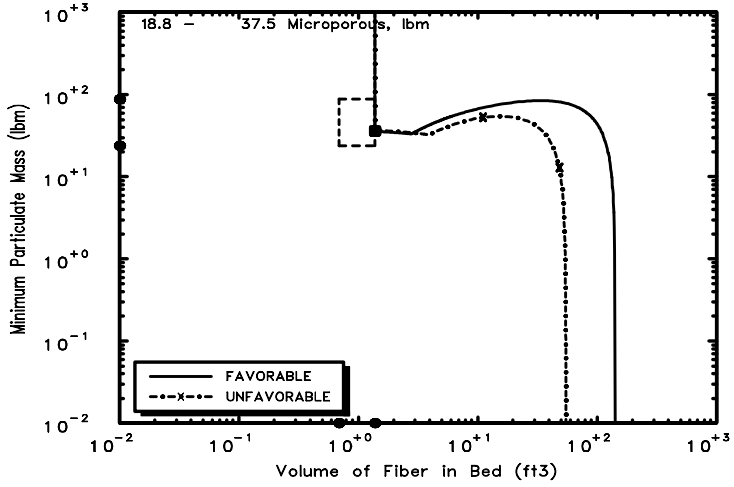

Parametric Case: 28 Small LOCA

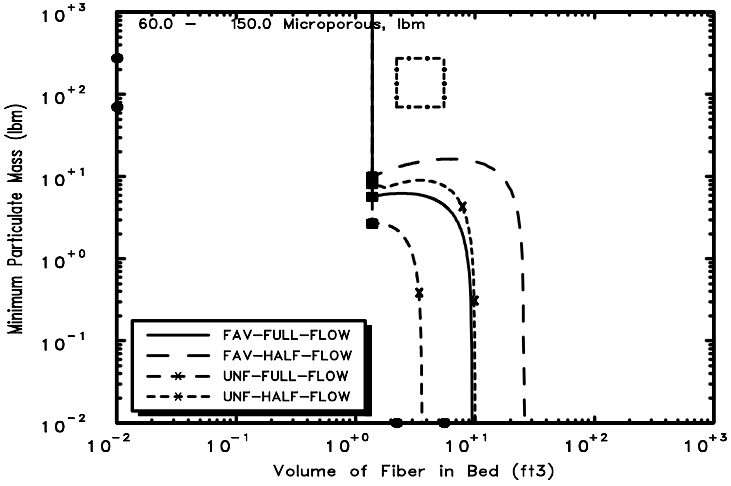

Parametric Case: 28 Medium LOCA

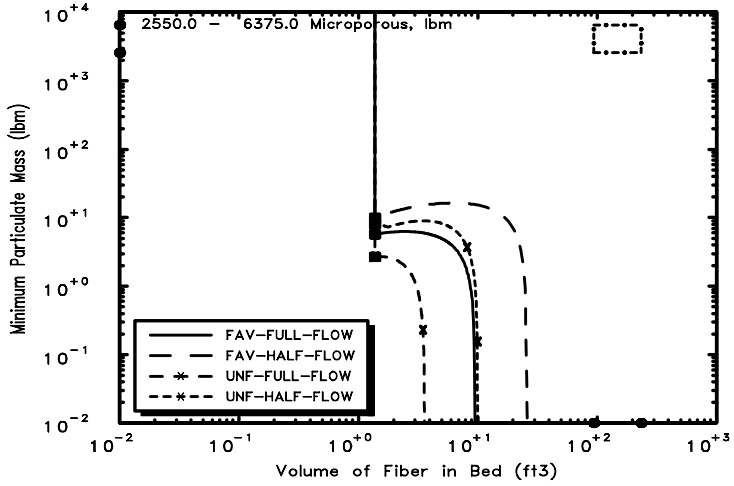

Parametric Case: 28 Large LOCA

Fig. B-28. Parametric Case 28.

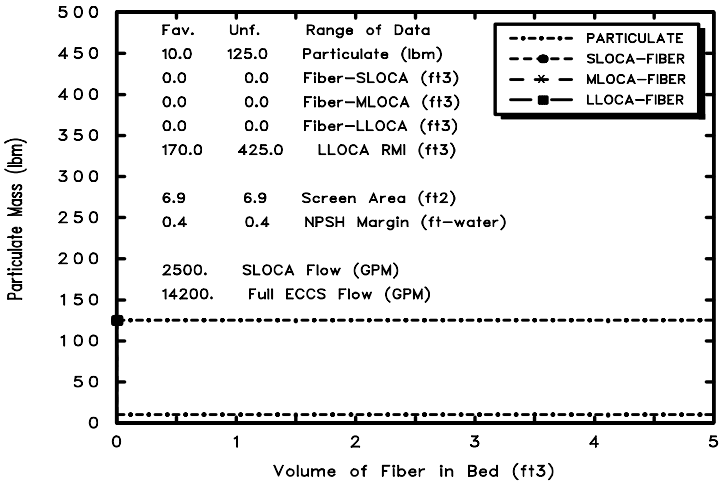

Parametric Case: 29 Debris Potential

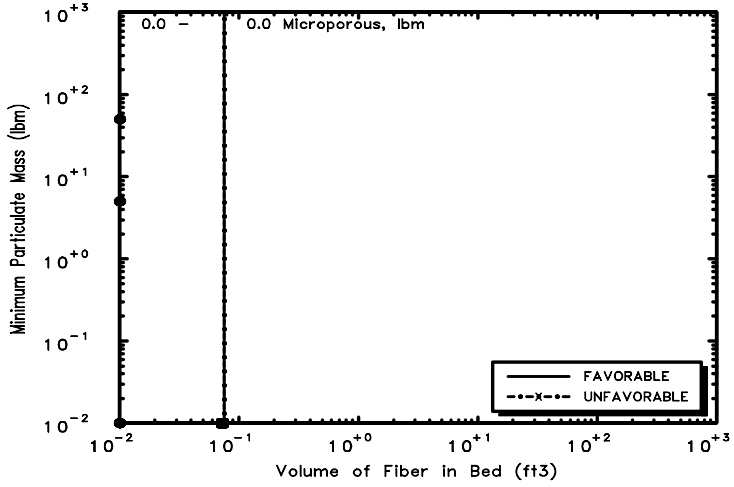

Parametric Case: 29 Small LOCA

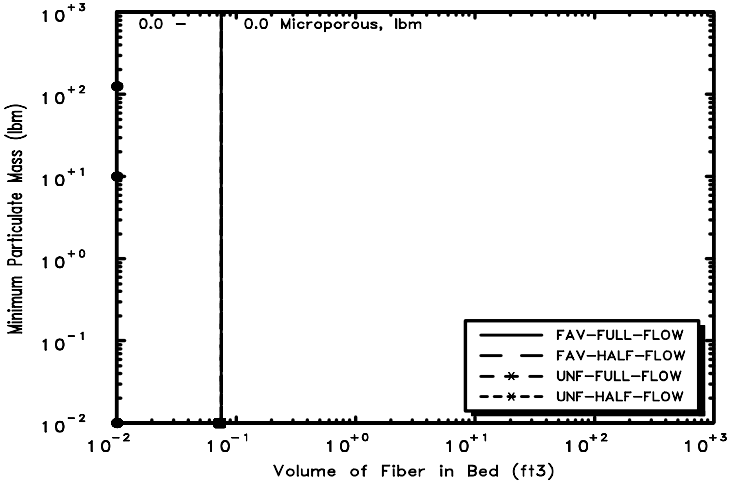

Parametric Case: 29 Medium LOCA

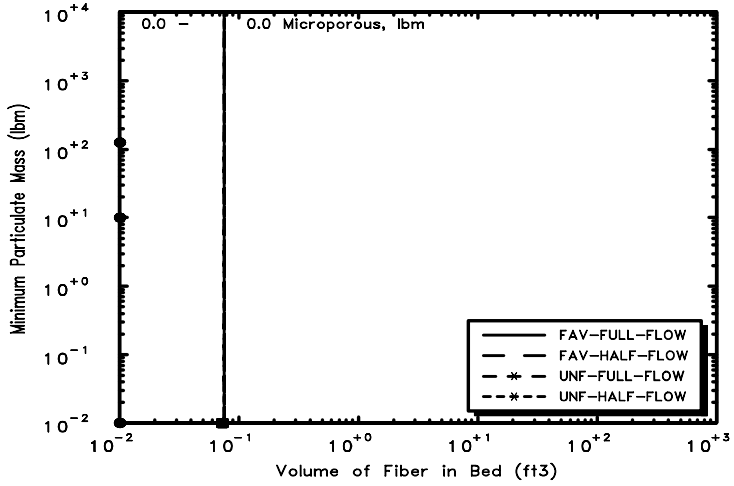

Parametric Case: 29 Large LOCA

Fig. B-29. Parametric Case 29 (Note: No fiber in this case, so no debris boxes presented).

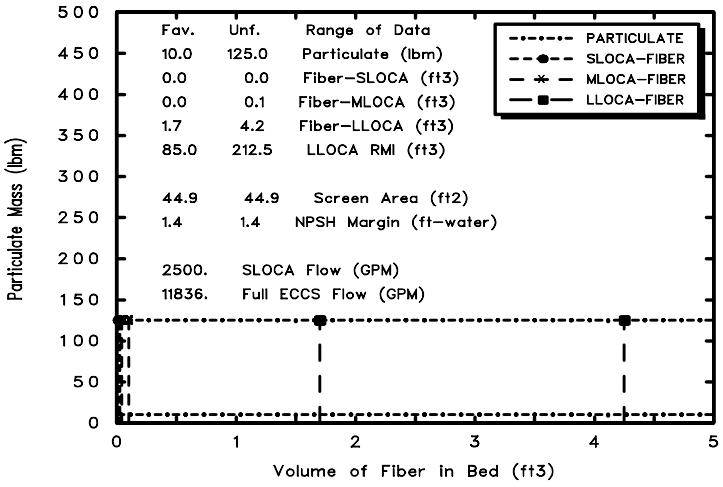

Parametric Case: 30 Debris Potential

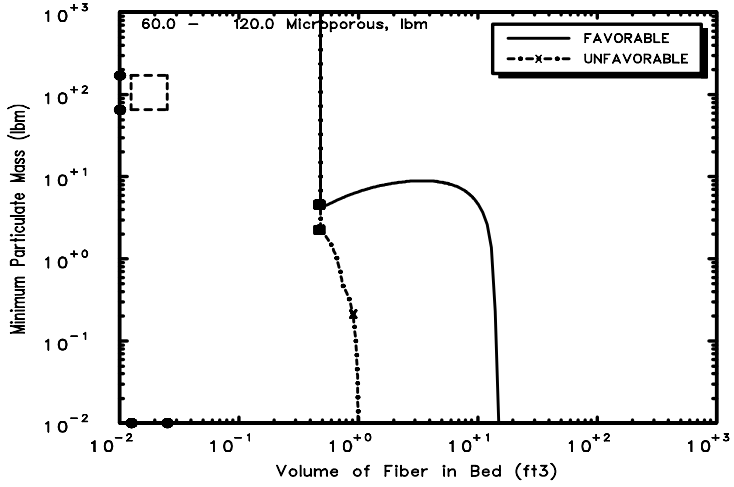

Parametric Case: 30 Small LOCA

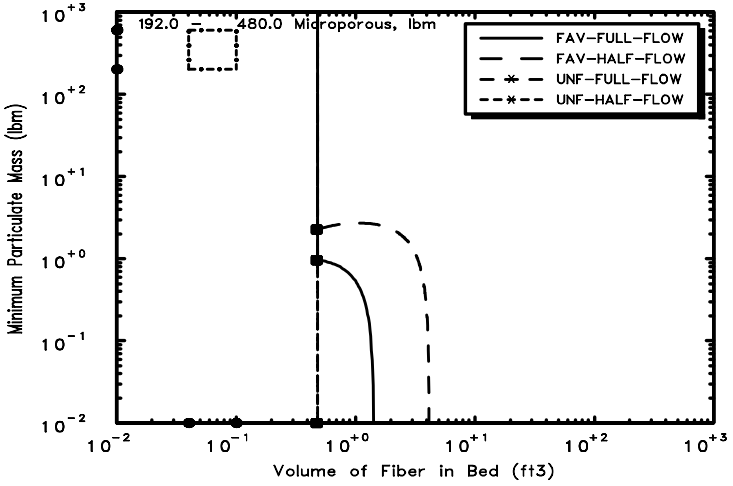

Parametric Case: 30 Medium LOCA

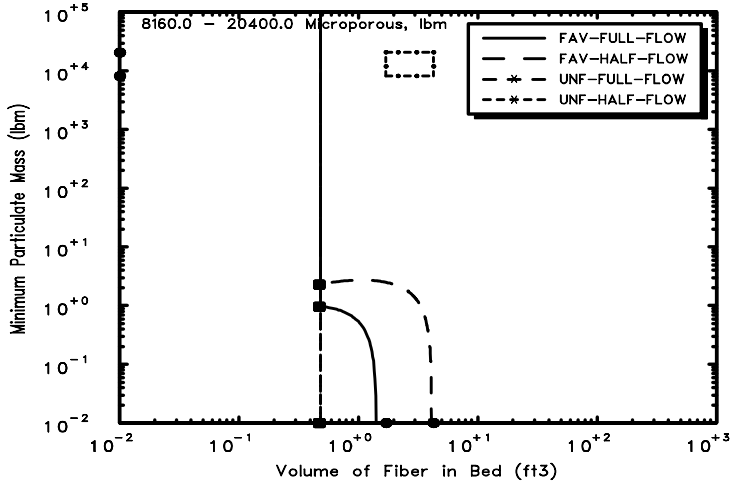

Parametric Case: 30 Large LOCA

Fig. B-30. Parametric Case 30.

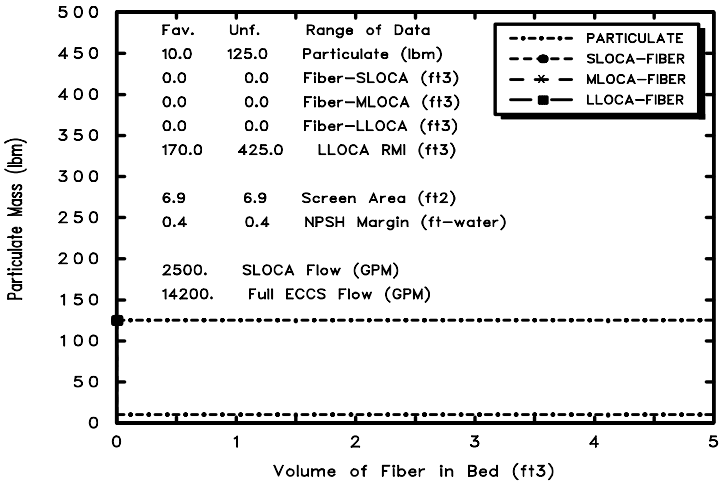

Parametric Case: 31 Debris Potential

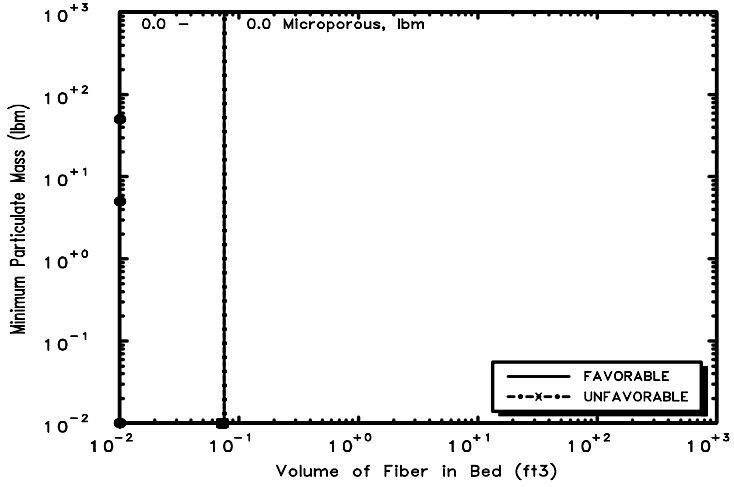

Parametric Case: 31 Small LOCA

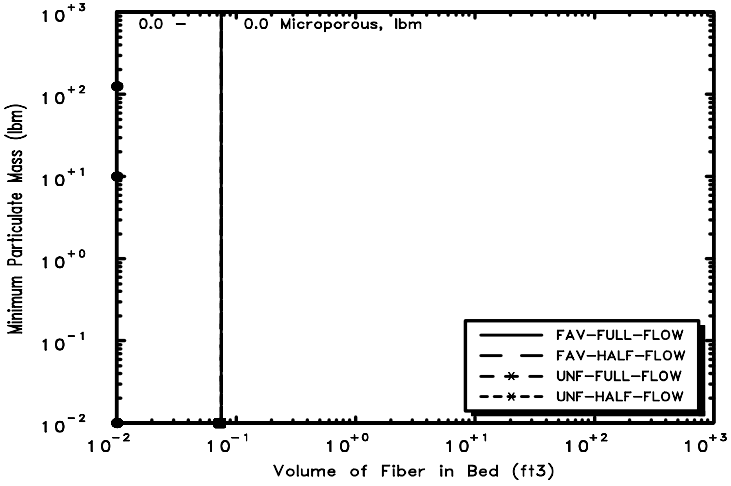

Parametric Case: 31 Medium LOCA

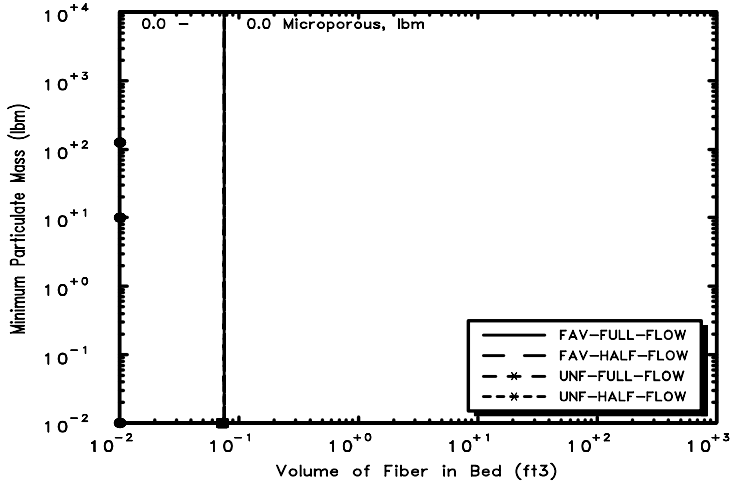

Parametric Case: 31 Large LOCA

Fig. B-31. Parametric Case 31 (Note: No fiber in this case, so no debris boxes presented).

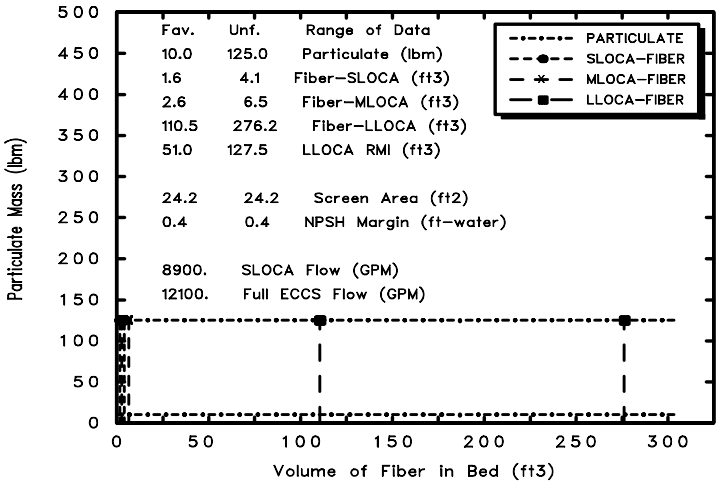

Parametric Case: 32 Debris Potential

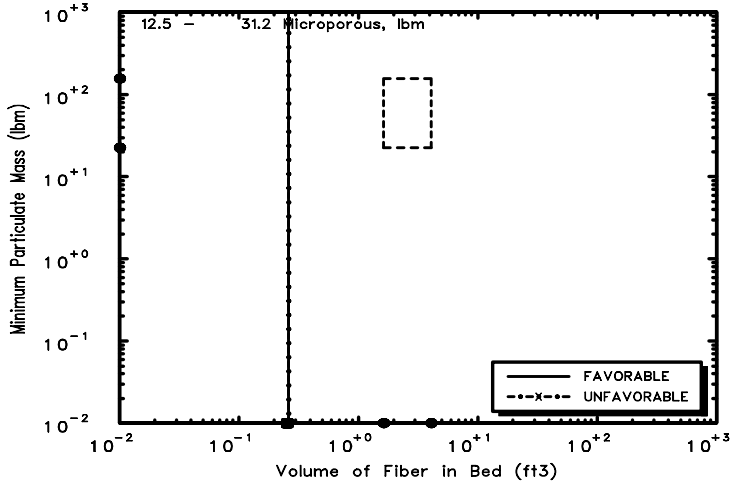

Parametric Case: 32 Small LOCA

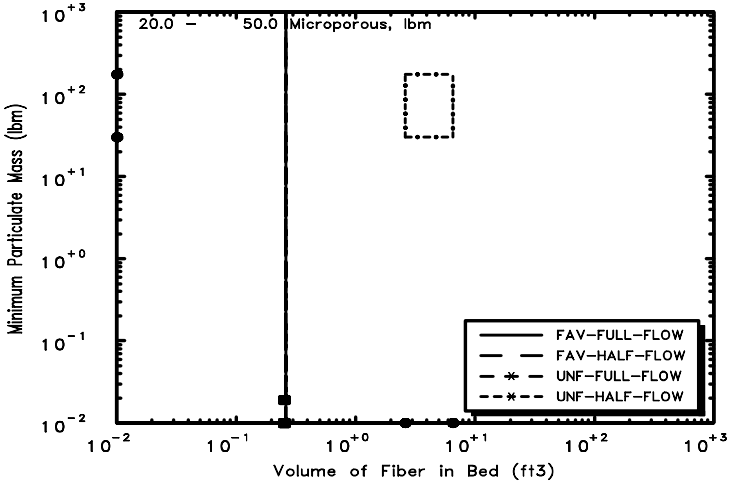

Parametric Case: 32 Medium LOCA

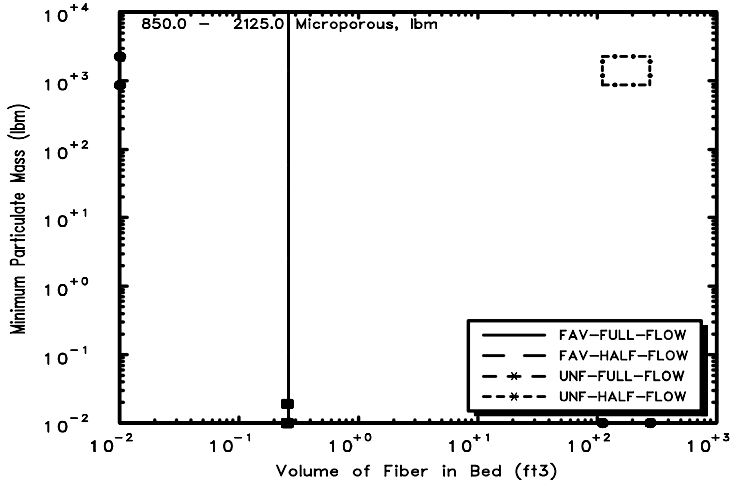

Parametric Case: 32 Large LOCA

Fig. B-32. Parametric Case 32.

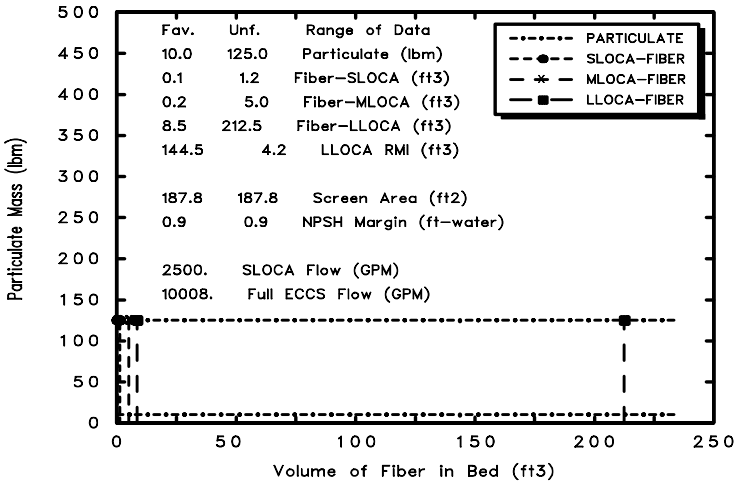

Parametric Case: 33 Debris Potential

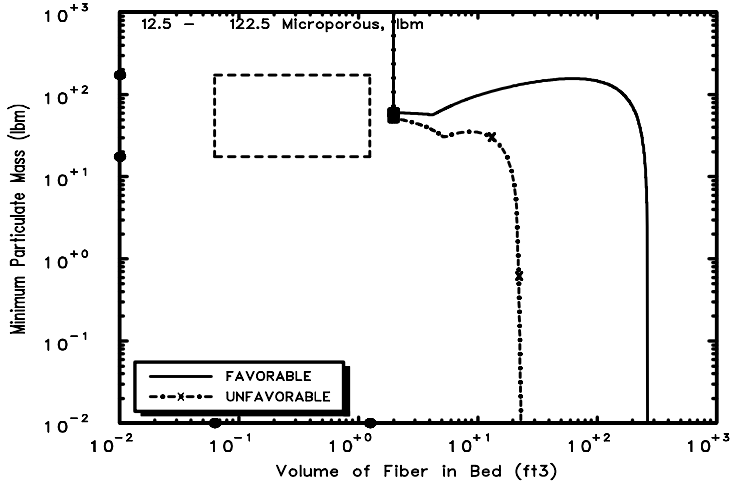

Parametric Case: 33 Small LOCA

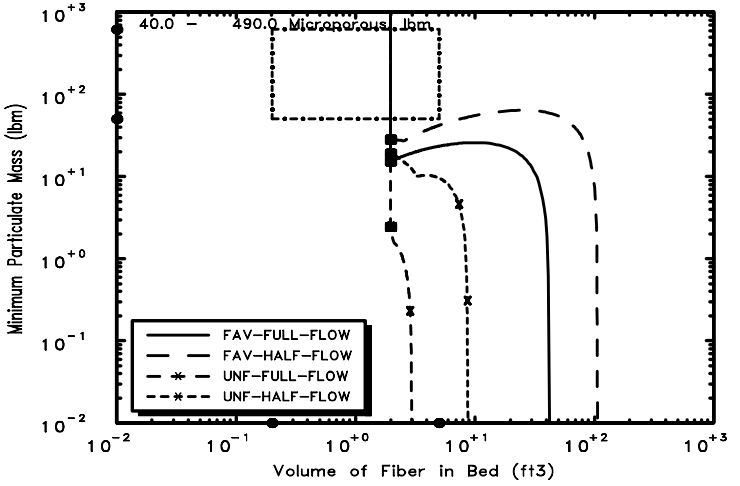

Parametric Case: 33 Medium LOCA

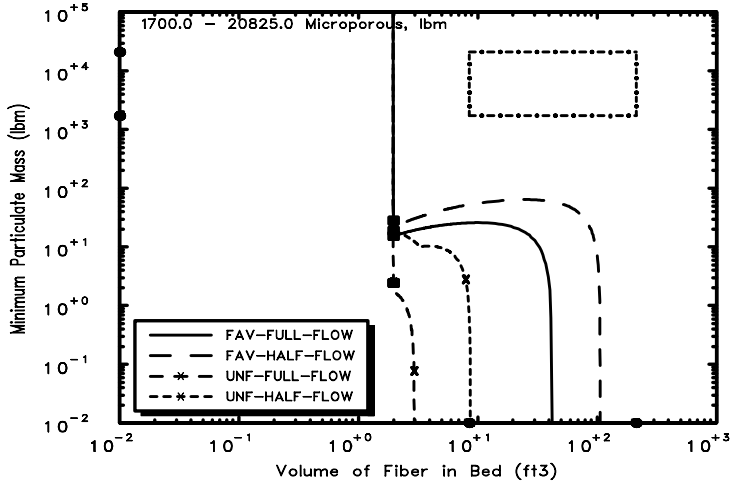

Parametric Case: 33 Large LOCA

Fig. B-33. Parametric Case 33.

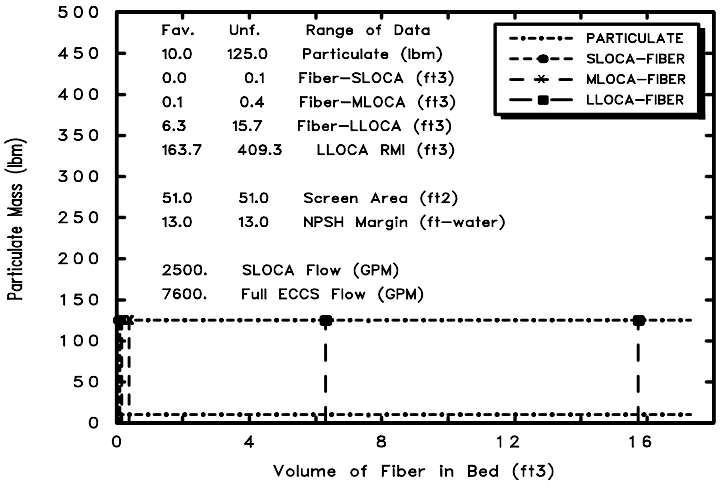

Parametric Case: 34 Debris Potential

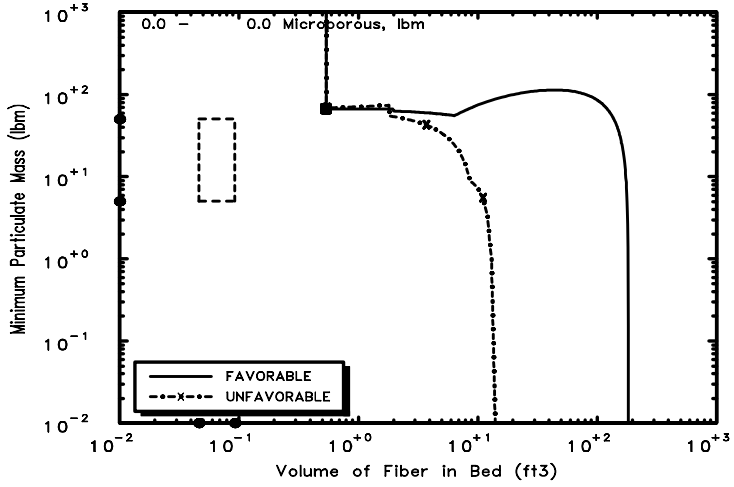

Parametric Case: 34 Small LOCA

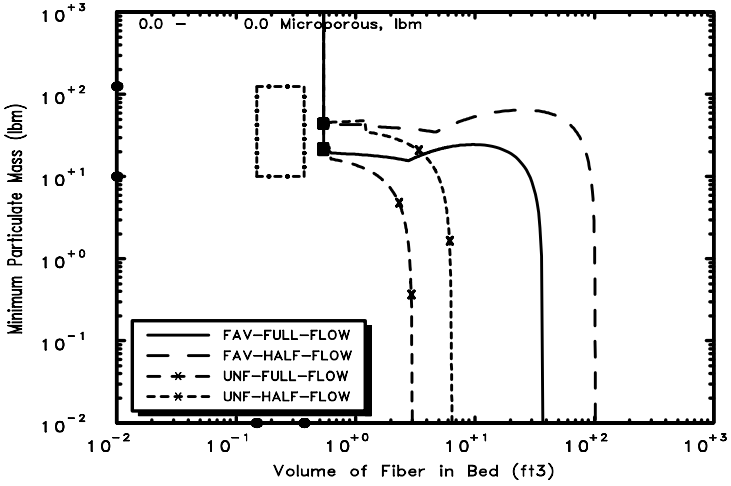

Parametric Case: 34 Medium LOCA

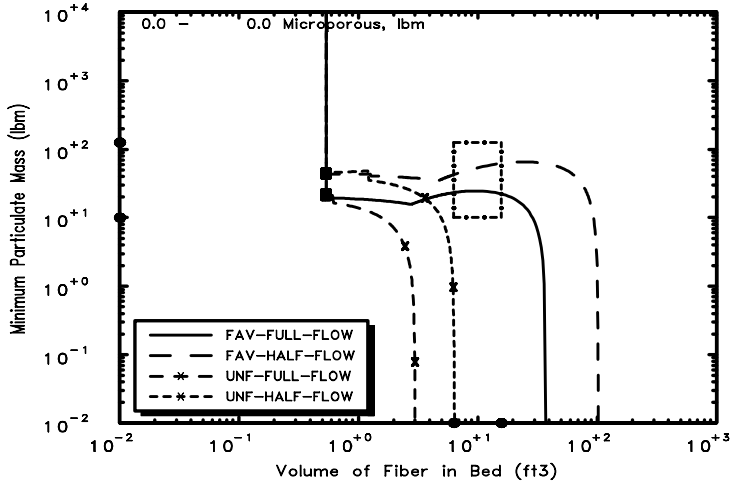

Parametric Case: 34 Large LOCA

Fig. B-34. Parametric Case 34.

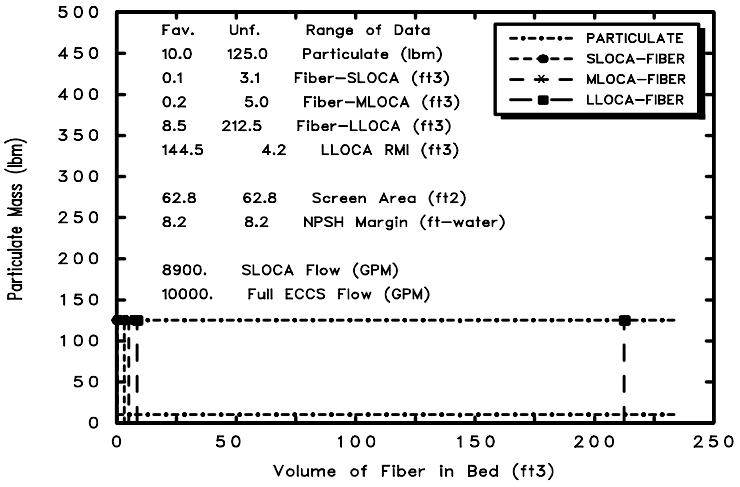

Parametric Case: 35 Debris Potential

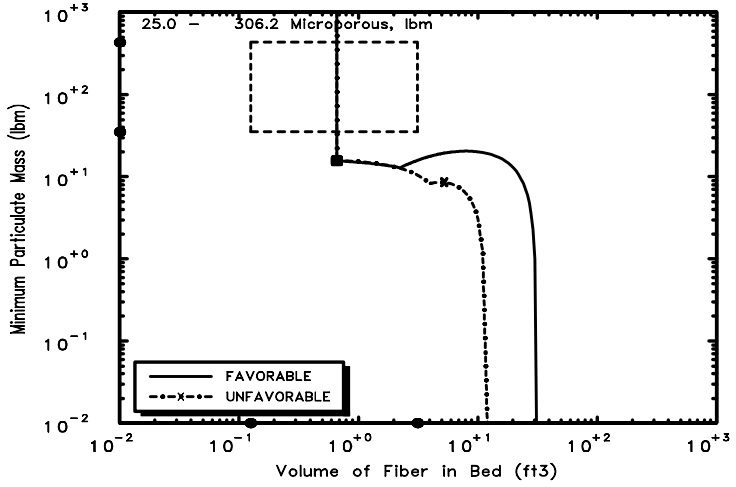

Parametric Case: 35 Small LOCA

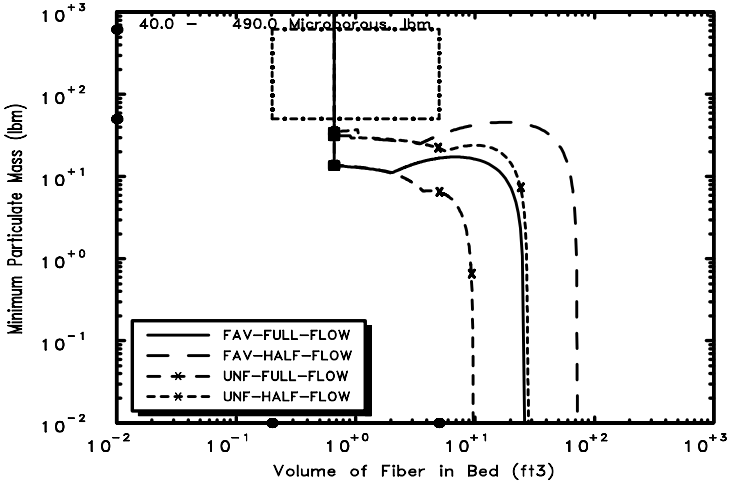

Parametric Case: 35 Medium LOCA

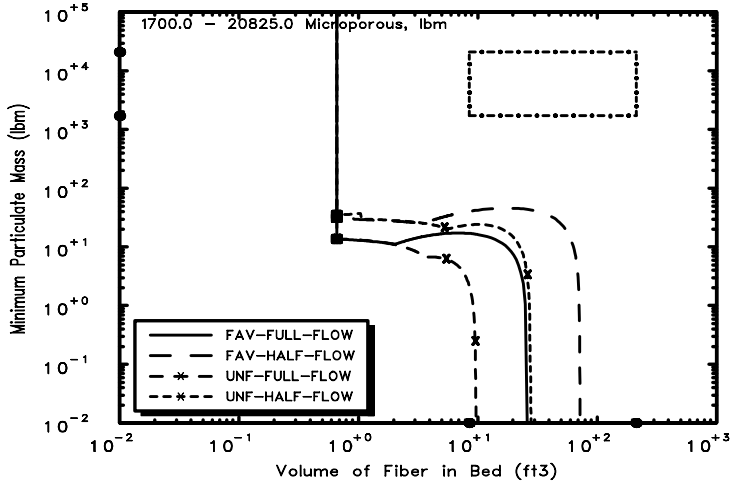

Parametric Case: 35 Large LOCA

Fig. B-35. Parametric Case 35.

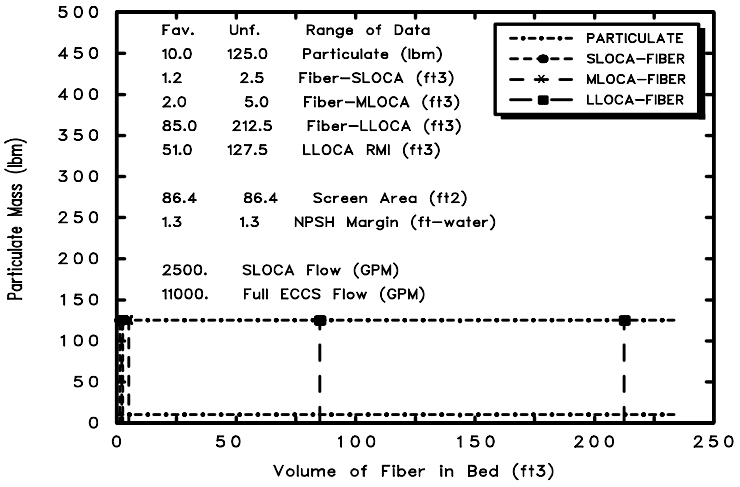

Parametric Case: 36 Debris Potential

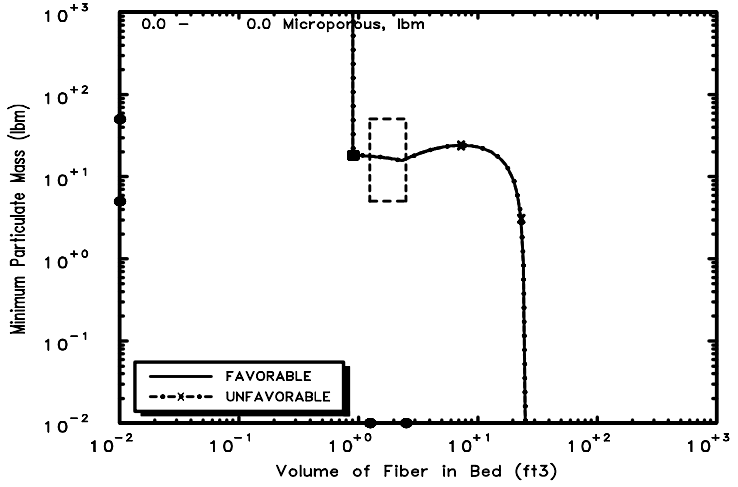

Parametric Case: 36 Small LOCA

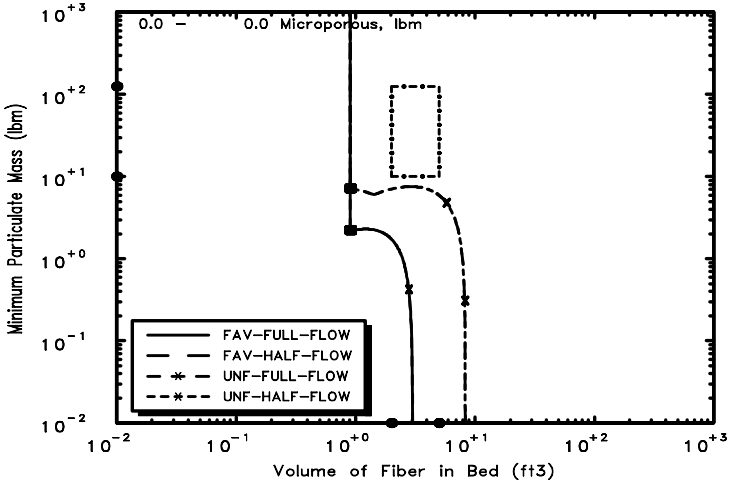

Parametric Case: 36 Medium LOCA

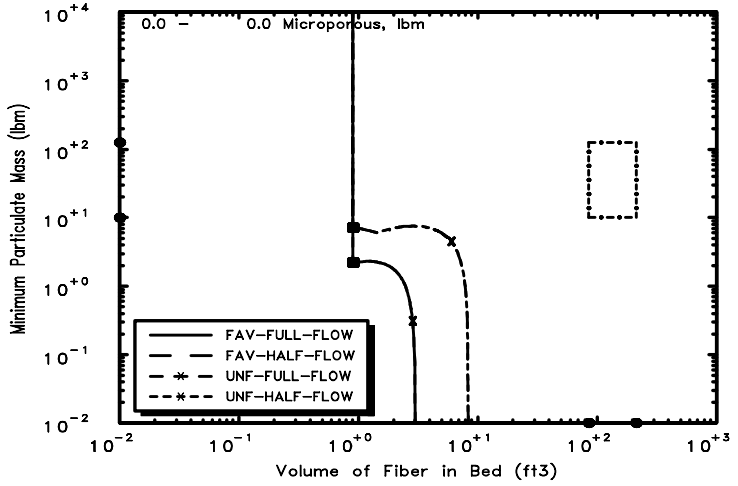

Parametric Case: 36 Large LOCA

Fig. B-36. Parametric Case 36.

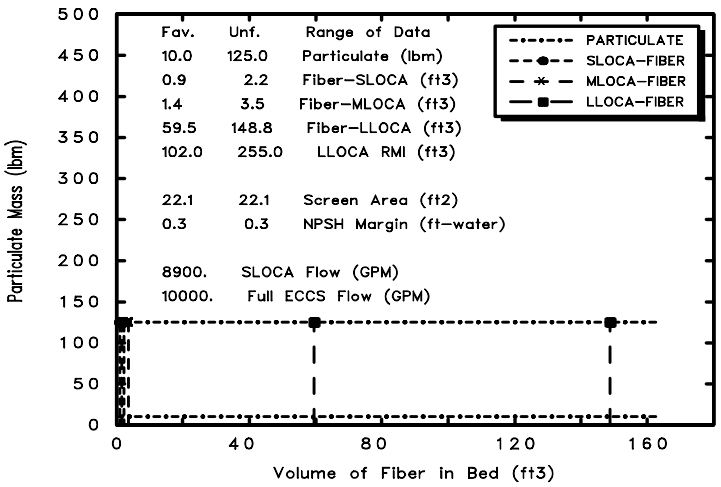

Parametric Case: 37 Debris Potential

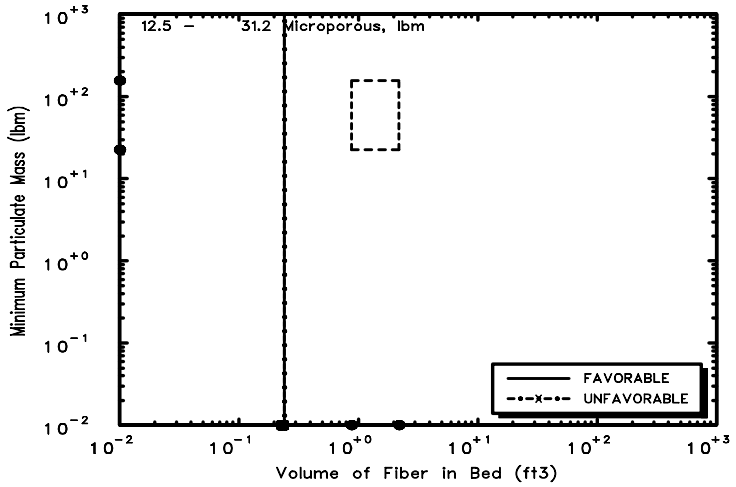

Parametric Case: 37 Small LOCA

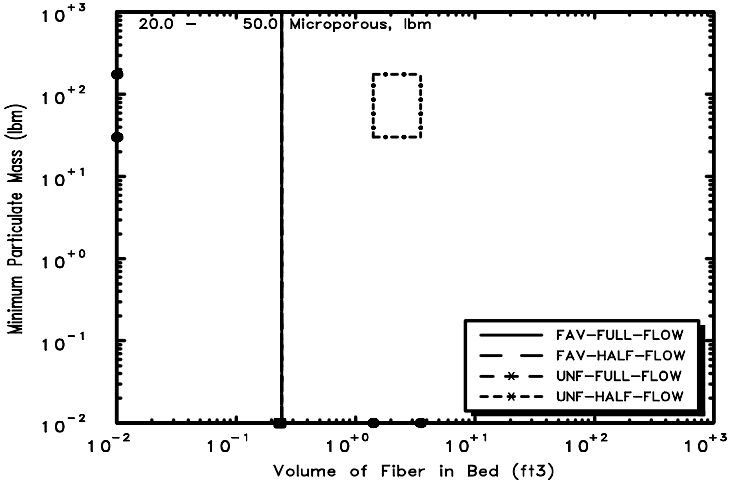

Parametric Case: 37 Medium LOCA

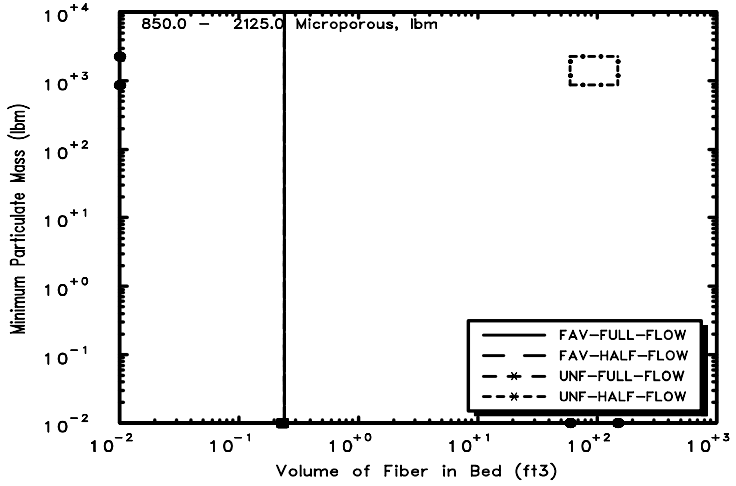

Parametric Case: 37 Large LOCA

Fig. B-37. Parametric Case 37.

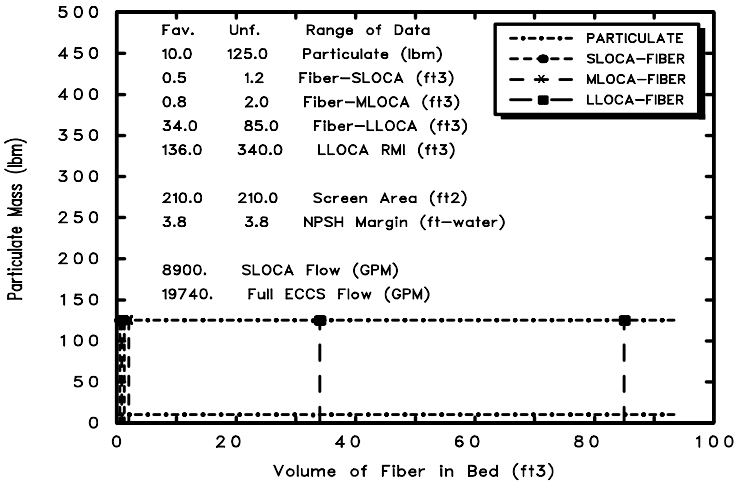

Parametric Case: 38 Debris Potential

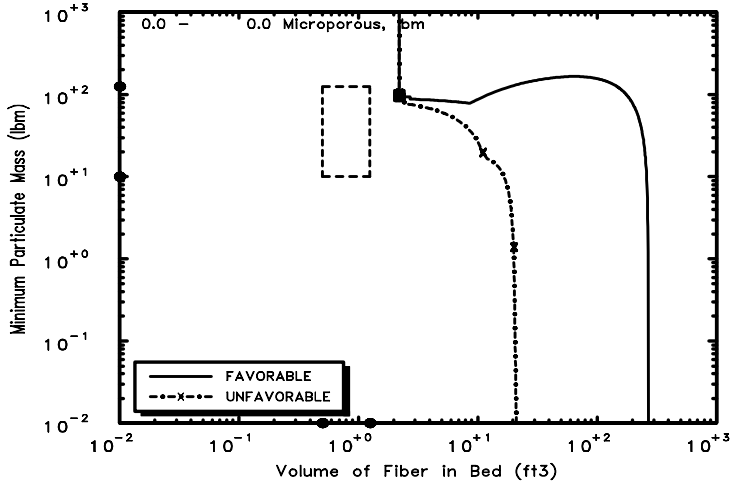

Parametric Case: 38 Small LOCA

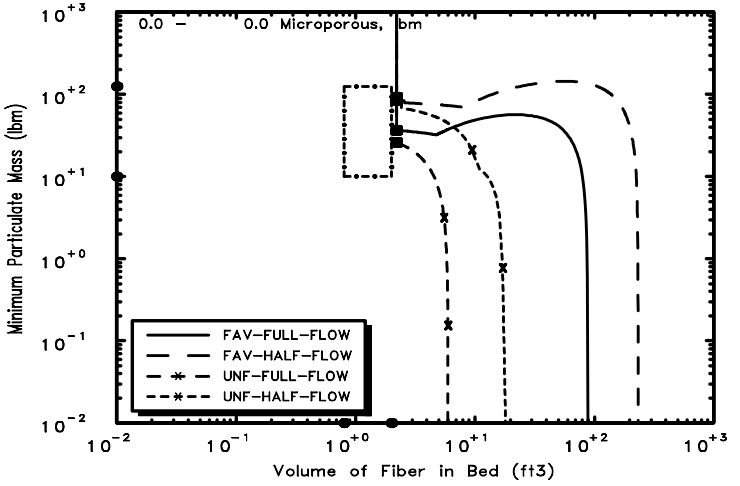

Parametric Case: 38 Medium LOCA

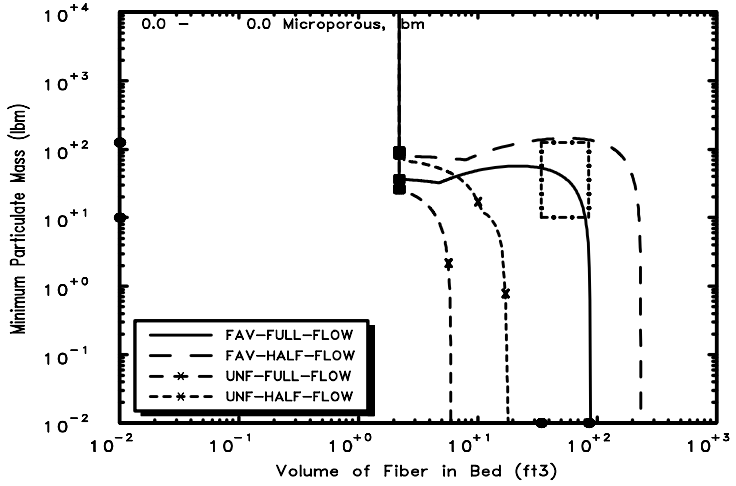

Parametric Case: 38 Large LOCA

Fig. B-38. Parametric Case 38.

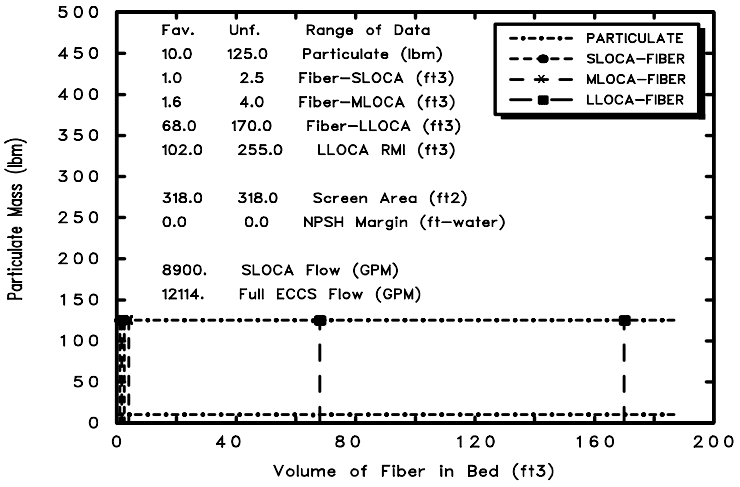

Parametric Case: 39 Debris Potential

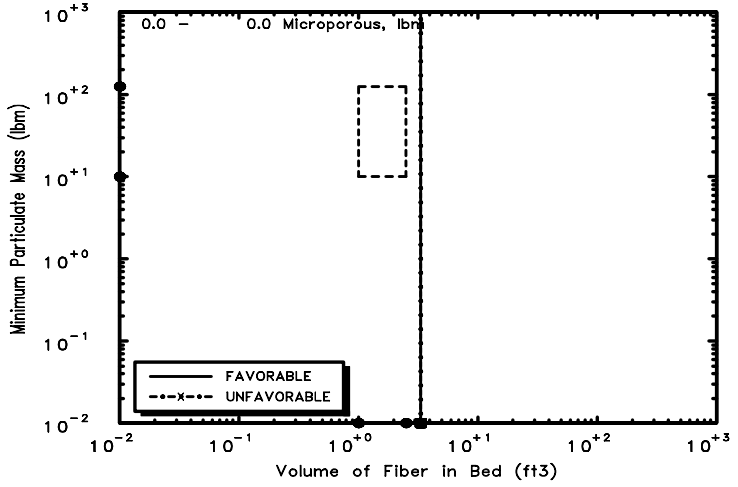

Parametric Case: 39 Small LOCA

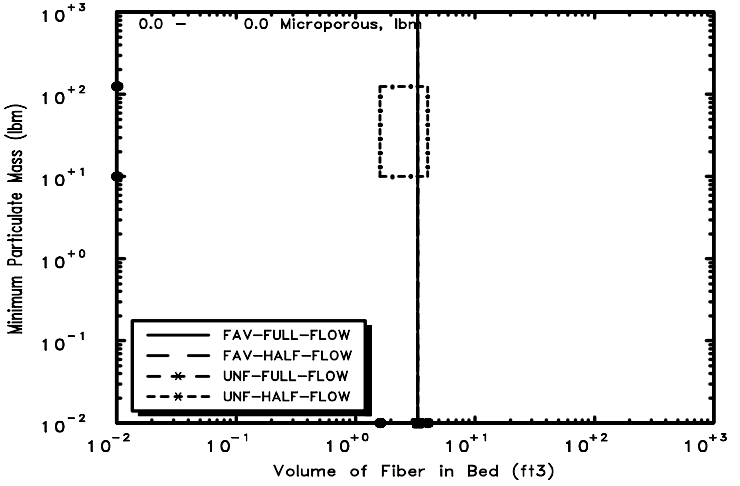

Parametric Case: 39 Medium LOCA

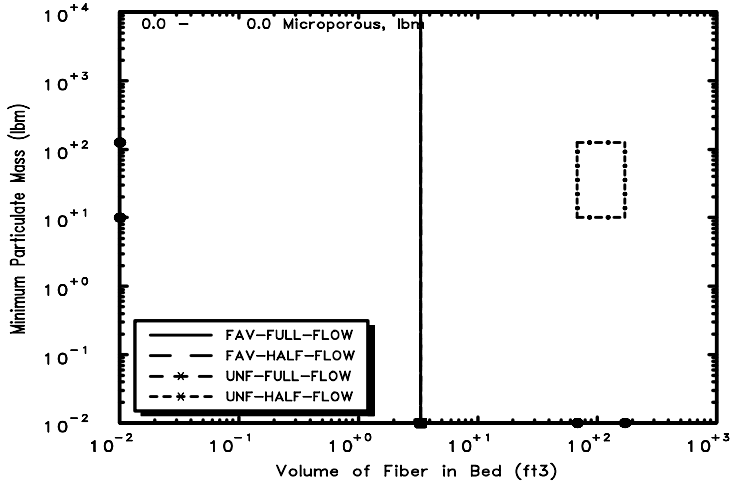

Parametric Case: 39 Large LOCA

Fig. B-39. Parametric Case 39.

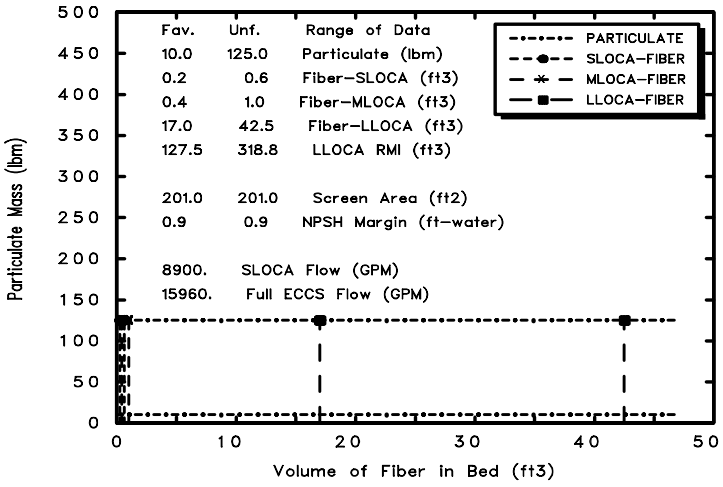

Parametric Case: 40 Debris Potential

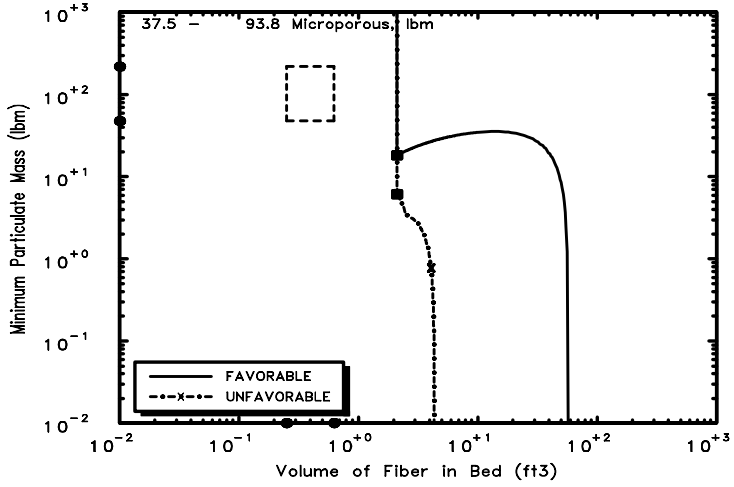

Parametric Case: 40 Small LOCA

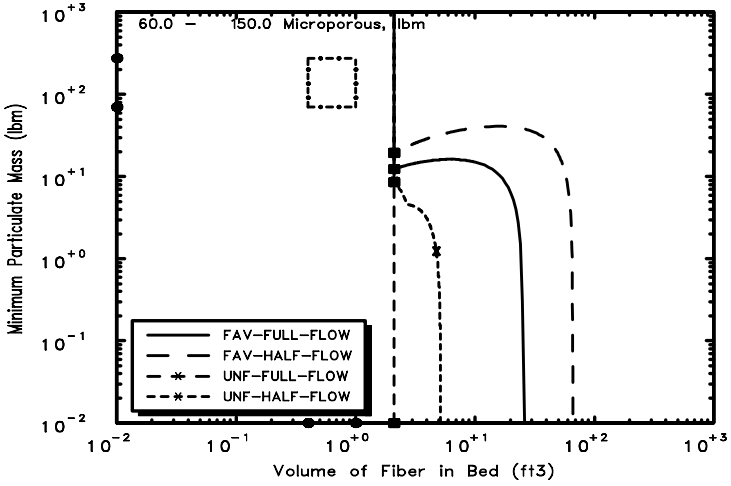

Parametric Case: 40 Medium LOCA

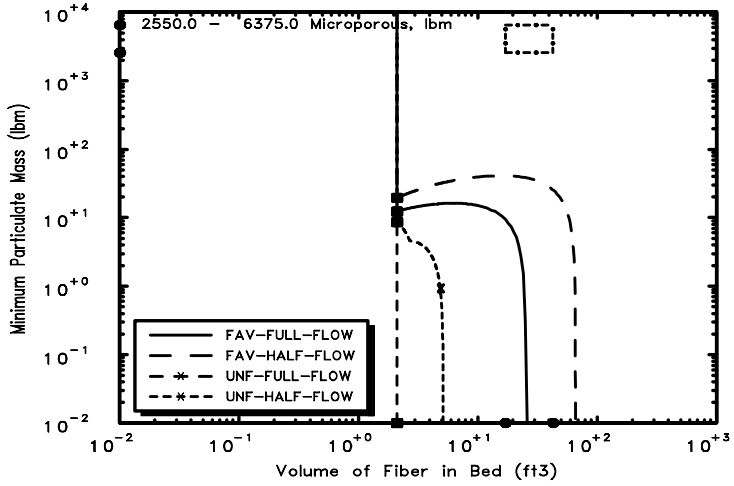

Parametric Case: 40 Large LOCA

Fig. B-40. Parametric Case 40.

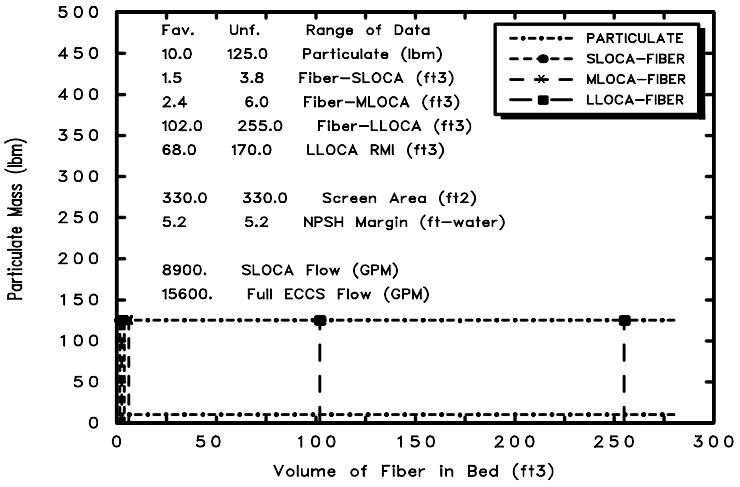

Parametric Case: 41 Debris Potential

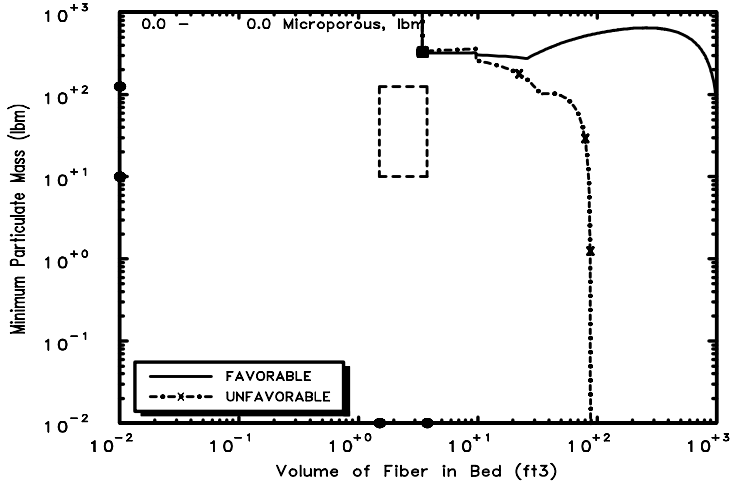

Parametric Case: 41 Small LOCA

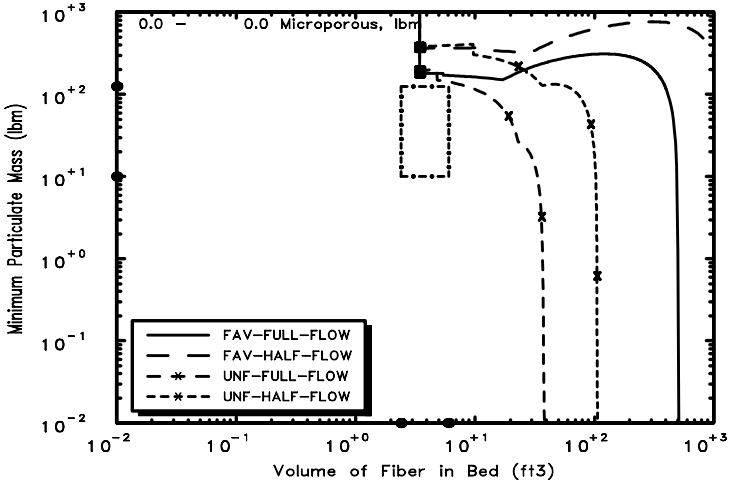

Parametric Case: 41 Medium LOCA

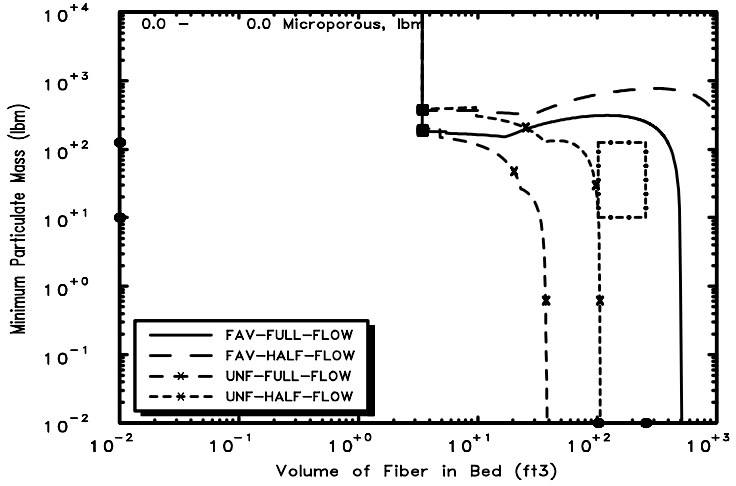

Parametric Case: 41 Large LOCA

Fig. B-41. Parametric Case 41.

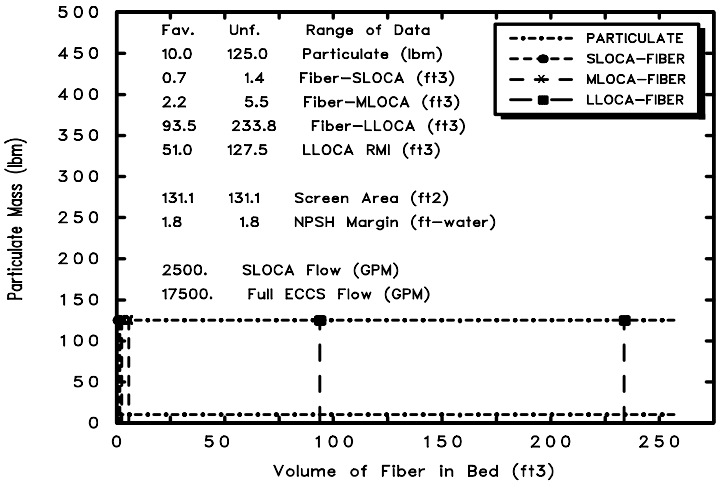

Parametric Case: 42 Debris Potential

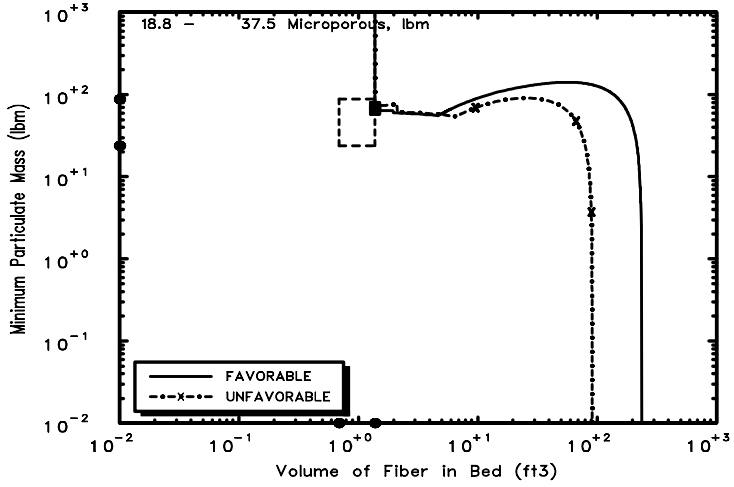

Parametric Case: 42 Small LOCA

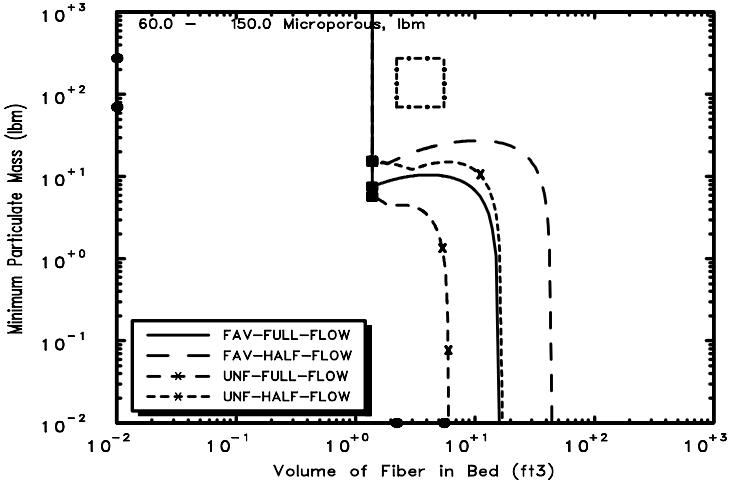

Parametric Case: 42 Medium LOCA

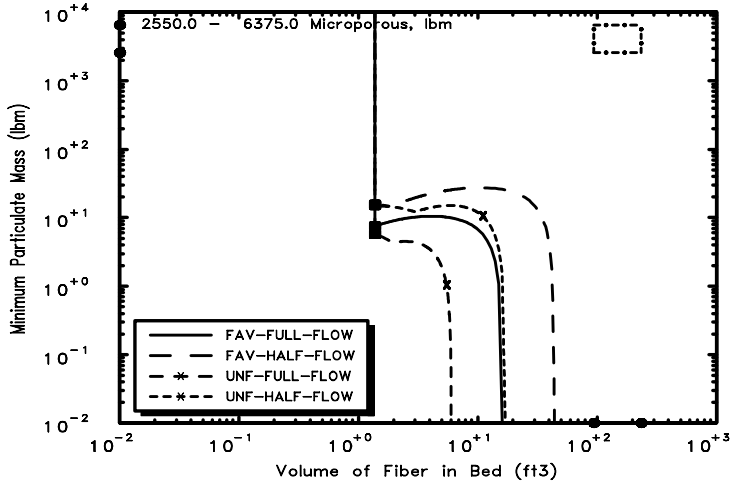

Parametric Case: 42 Large LOCA

Fig. B-42. Parametric Case 42.

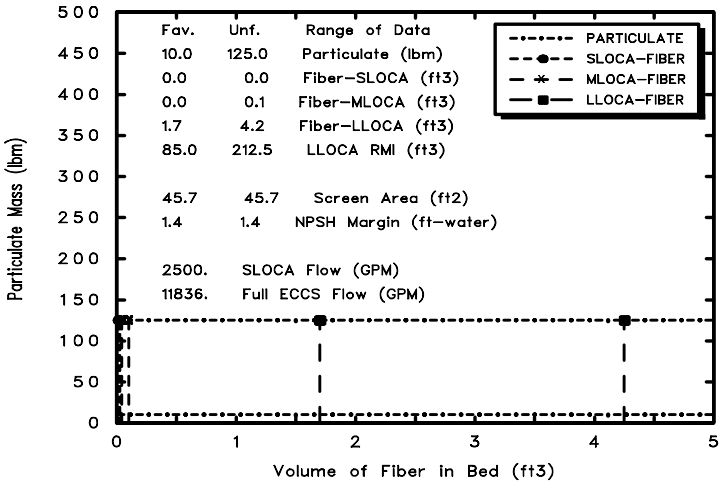

Parametric Case: 43 Debris Potential

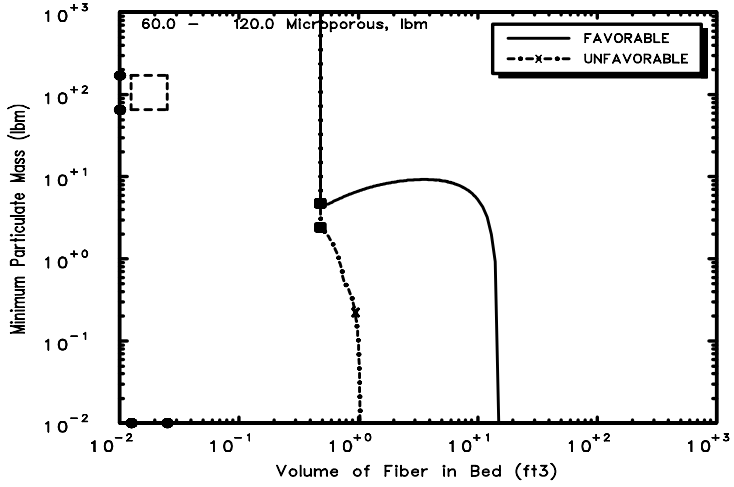

Parametric Case: 43 Small LOCA

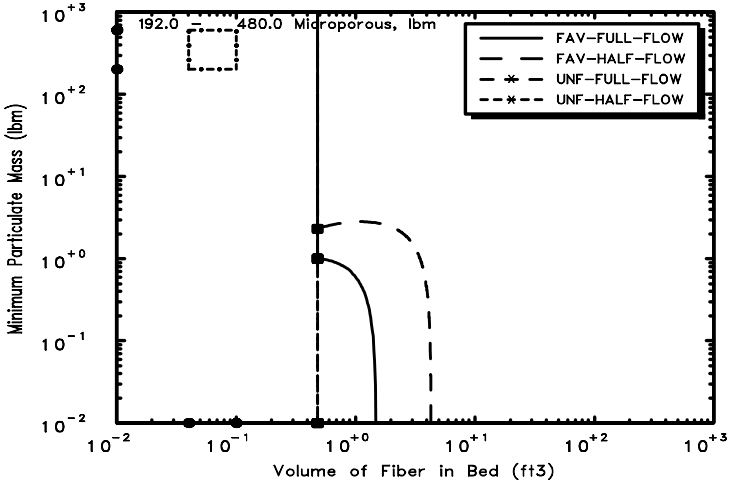

Parametric Case: 43 Medium LOCA

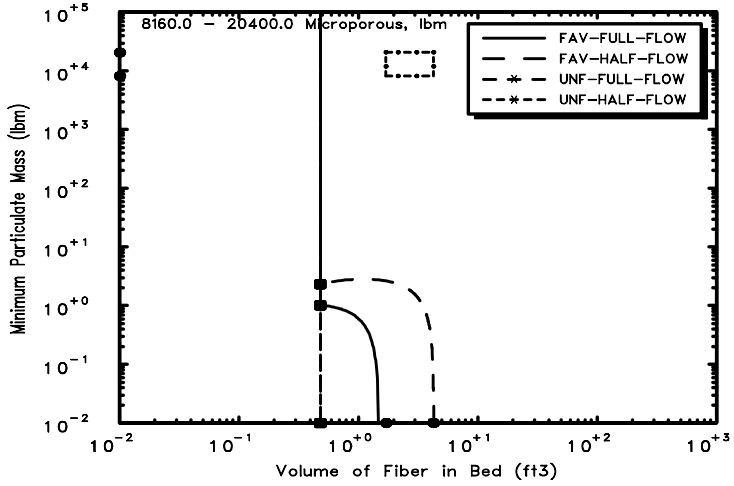

Parametric Case: 43 Large LOCA

Fig. B-43. Parametric Case 43.

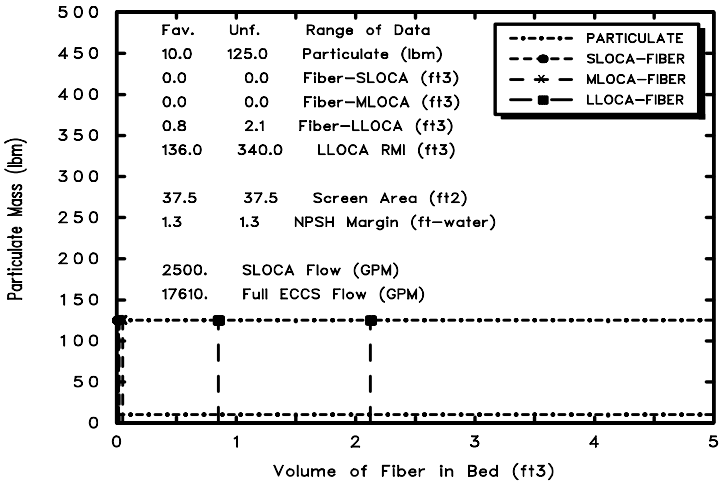

Parametric Case: 44 Debris Potential

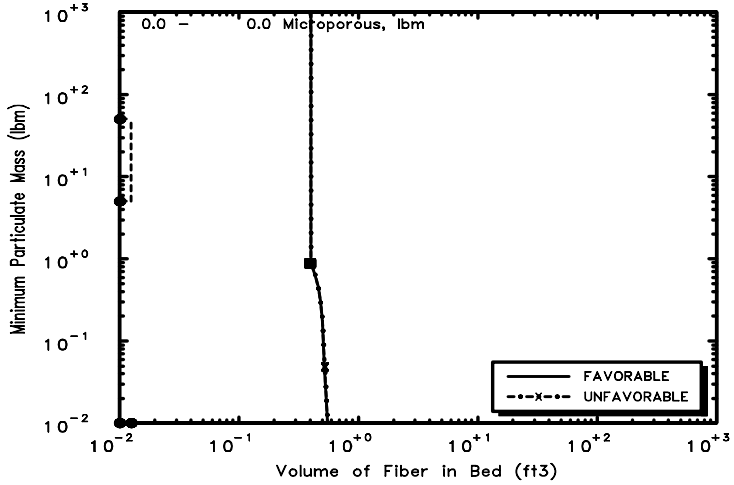

Parametric Case: 44 Small LOCA

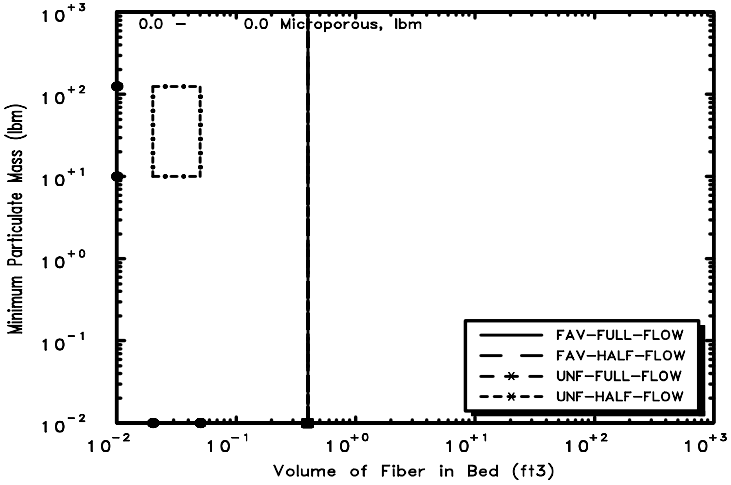

Parametric Case: 44 Medium LOCA

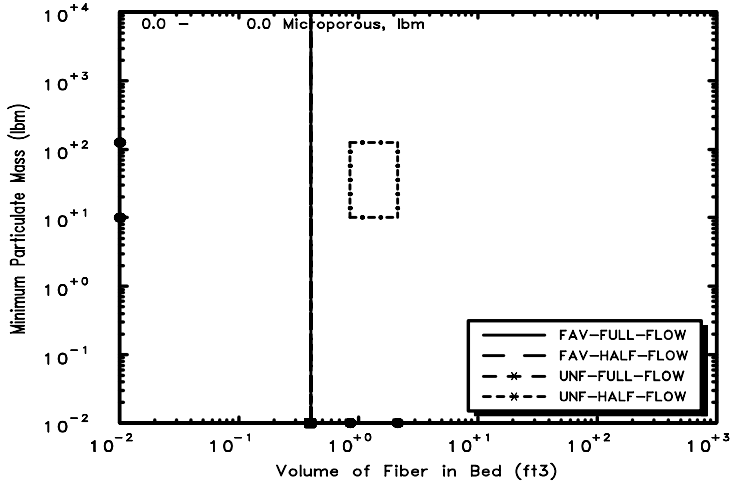

Parametric Case: 44 Large LOCA

Fig. B-44. Parametric Case 44.

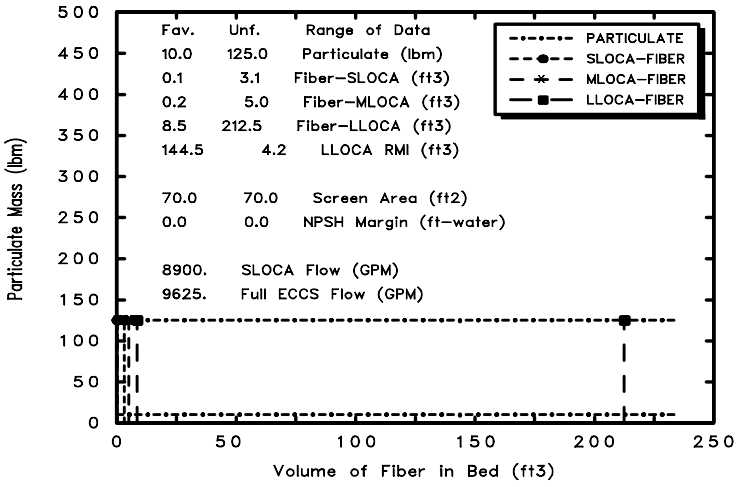

Parametric Case: 45 Debris Potential

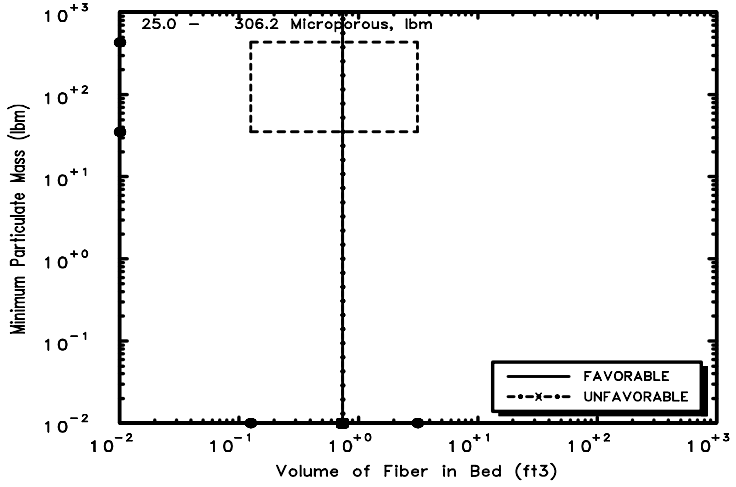

Parametric Case: 45 Small LOCA

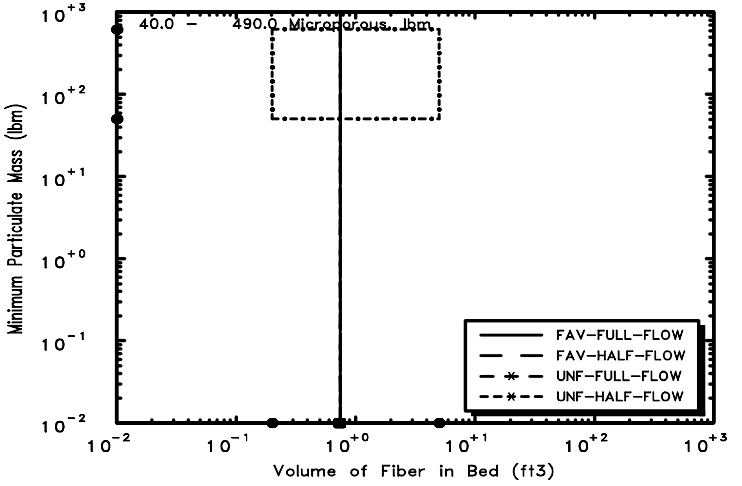

Parametric Case: 45 Medium LOCA

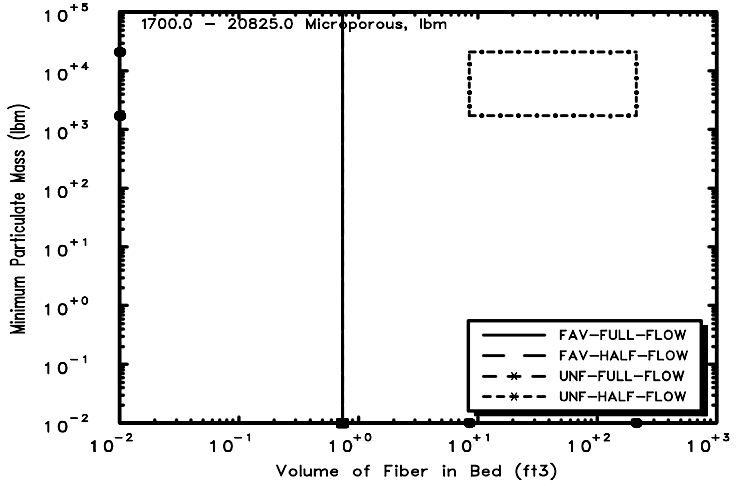

Parametric Case: 45 Large LOCA

Fig. B-45. Parametric Case 45.

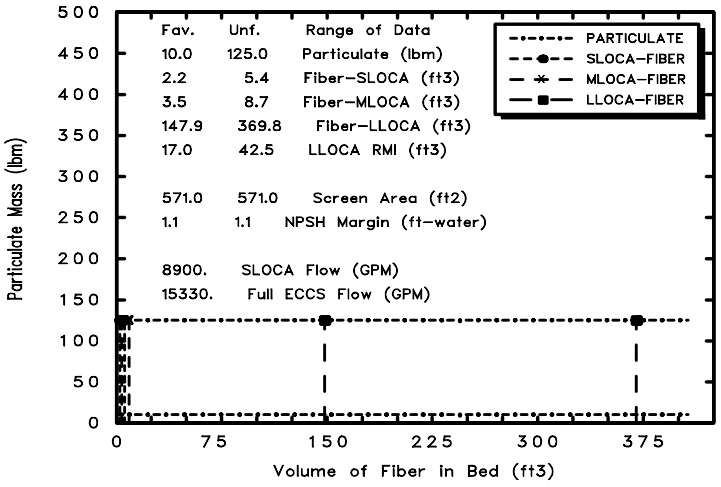

Parametric Case: 46 Debris Potential

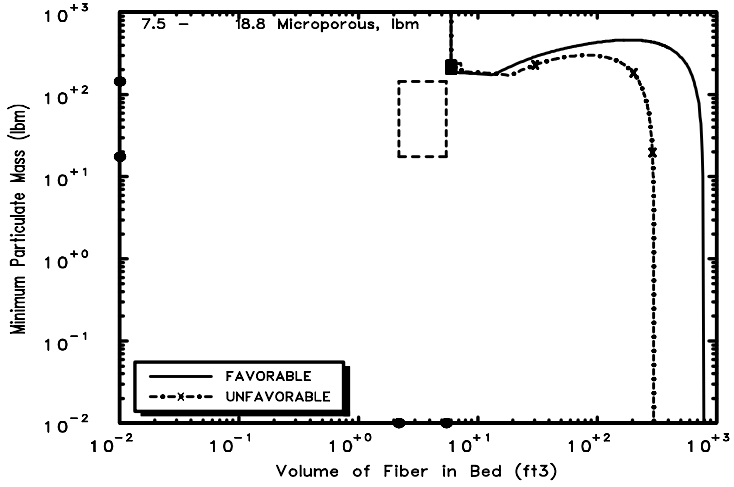

Parametric Case: 46 Small LOCA

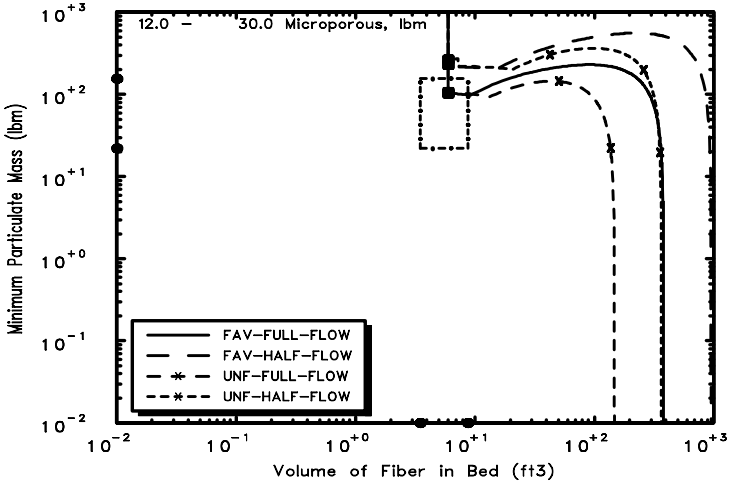

Parametric Case: 46 Medium LOCA

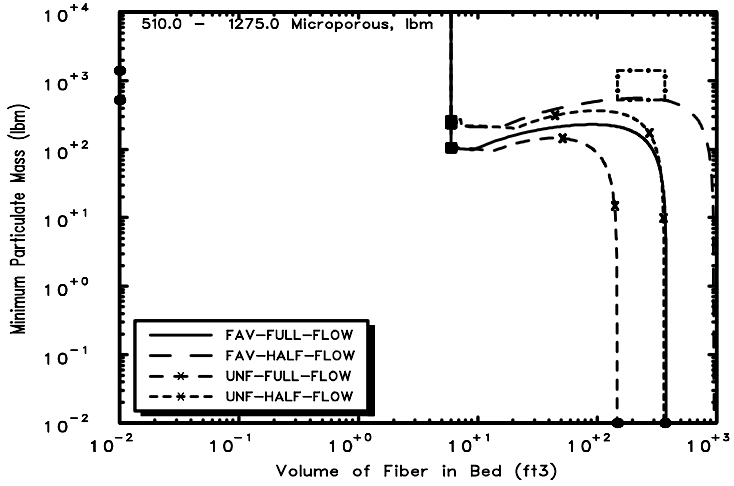

Parametric Case: 46 Large LOCA

Fig. B-46. Parametric Case 46.

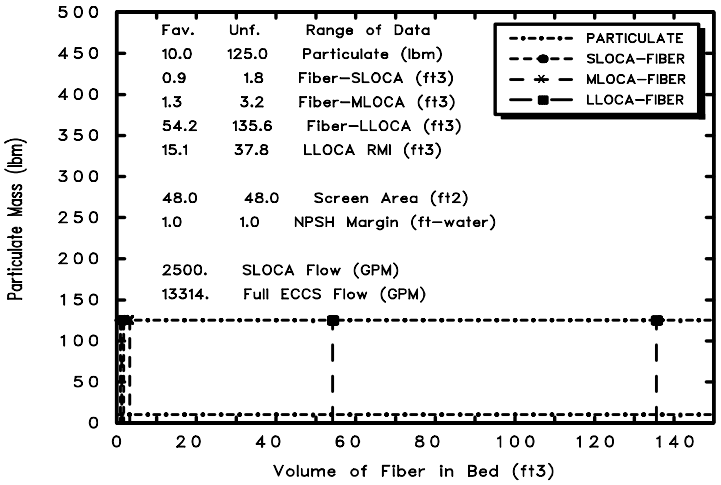

Parametric Case: 47 Debris Potential

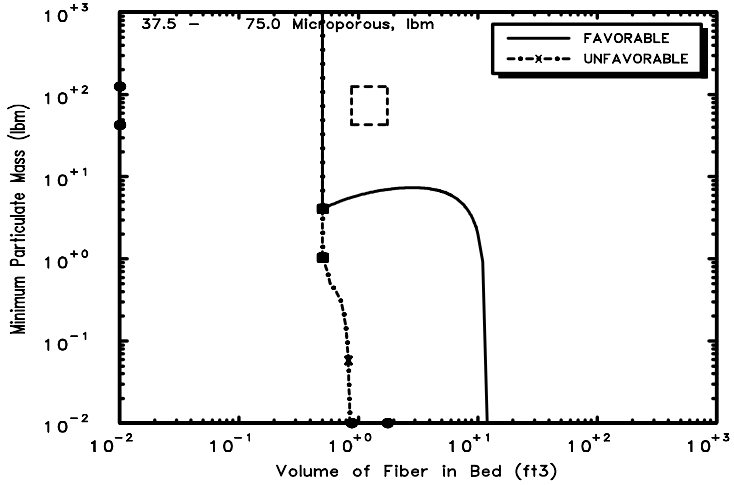

Parametric Case: 47 Small LOCA

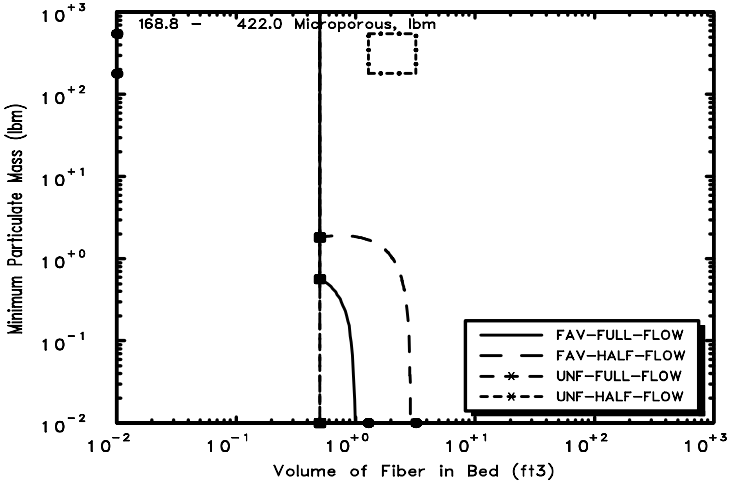

Parametric Case: 47 Medium LOCA

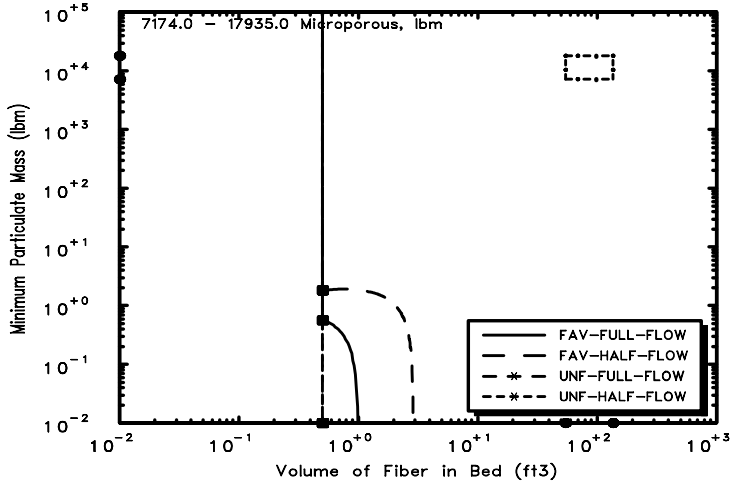

Parametric Case: 47 Large LOCA

Fig. B-47. Parametric Case 47.

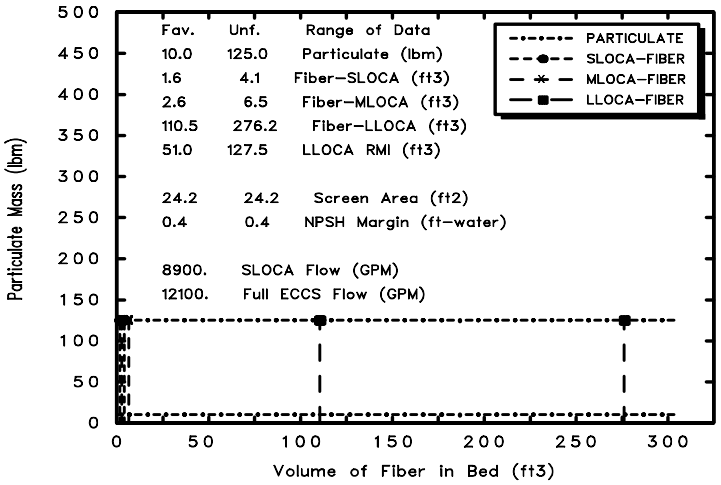

Parametric Case: 48 Debris Potential

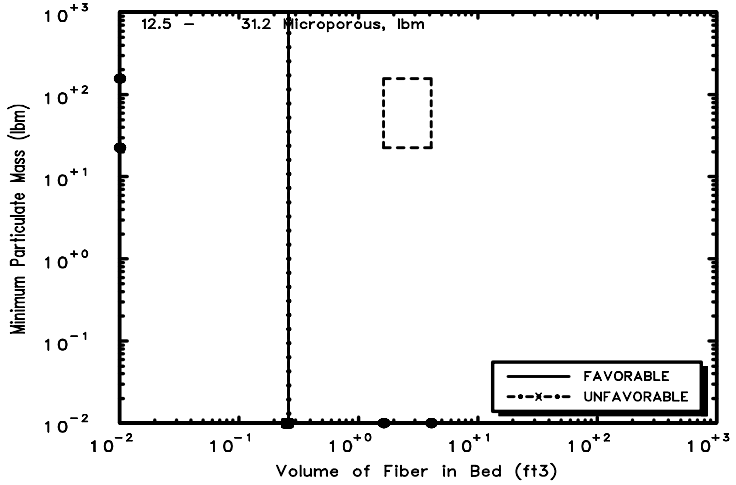

Parametric Case: 48 Small LOCA

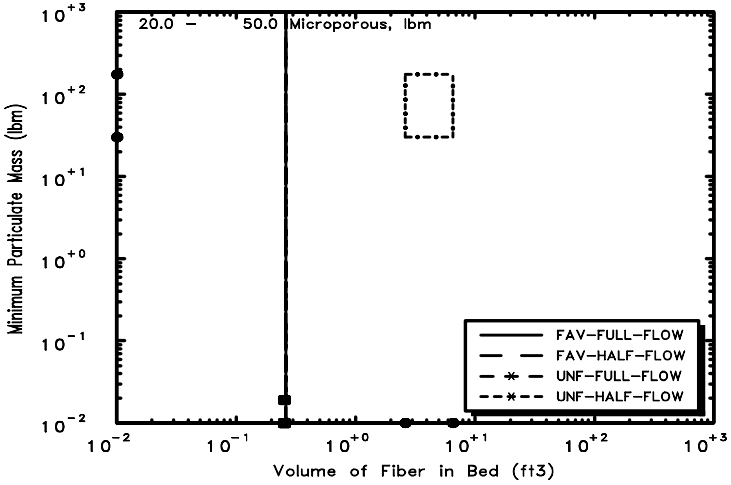

Parametric Case: 48 Medium LOCA

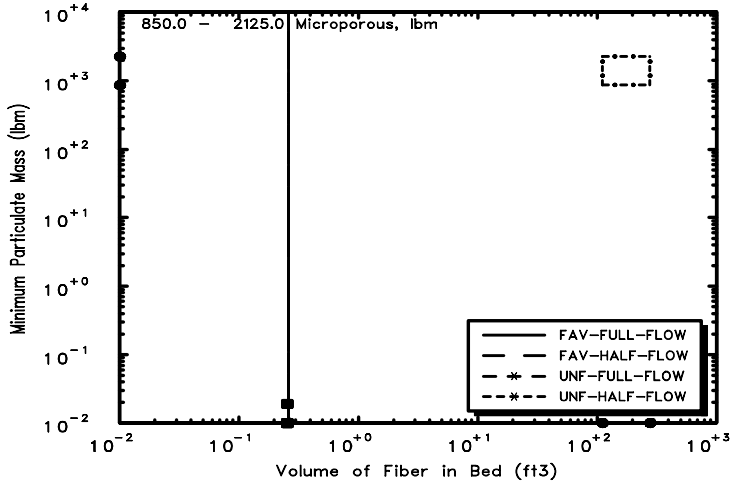

Parametric Case: 48 Large LOCA

Fig. B-48. Parametric Case 48.

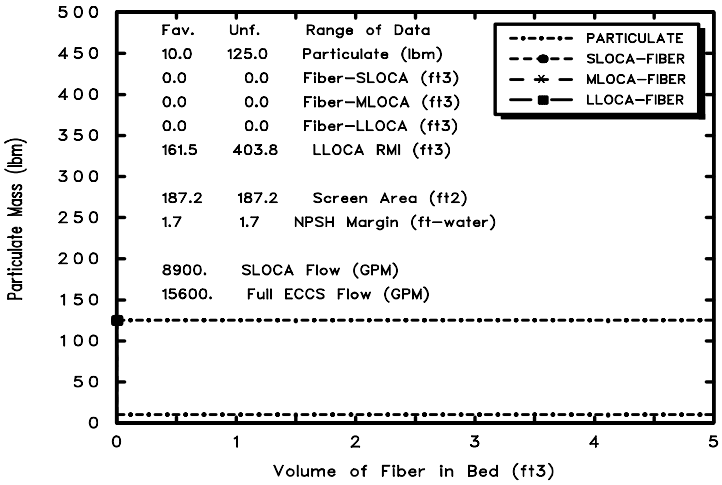

Parametric Case: 49 Debris Potential

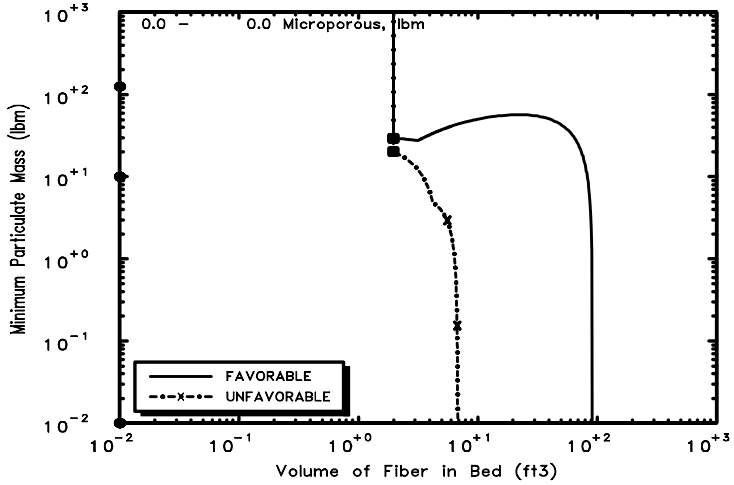

Parametric Case: 49 Small LOCA

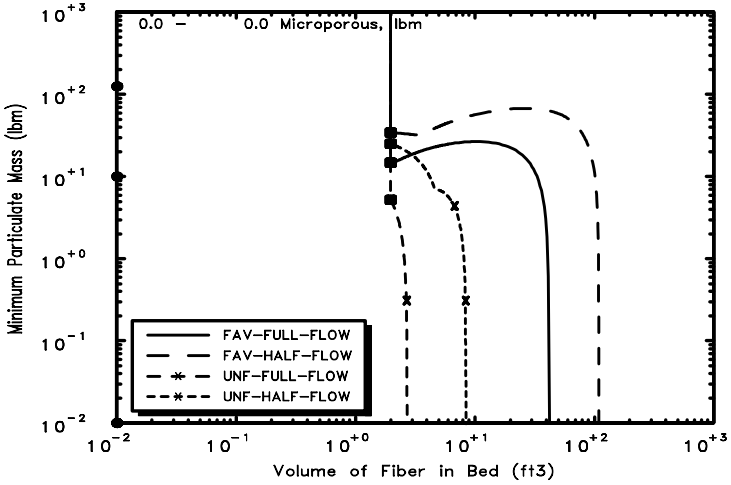

Parametric Case: 49 Medium LOCA

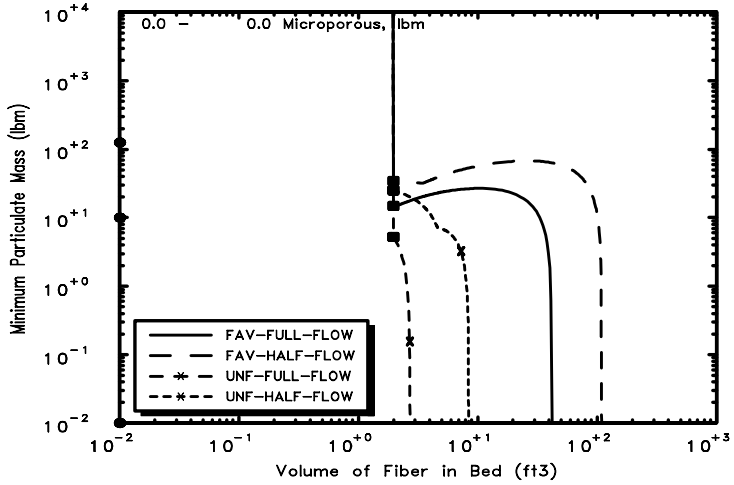

Parametric Case: 49 Large LOCA

Fig. B-49. Parametric Case 49 (Note: No fiber in this case, so no debris boxes presented).

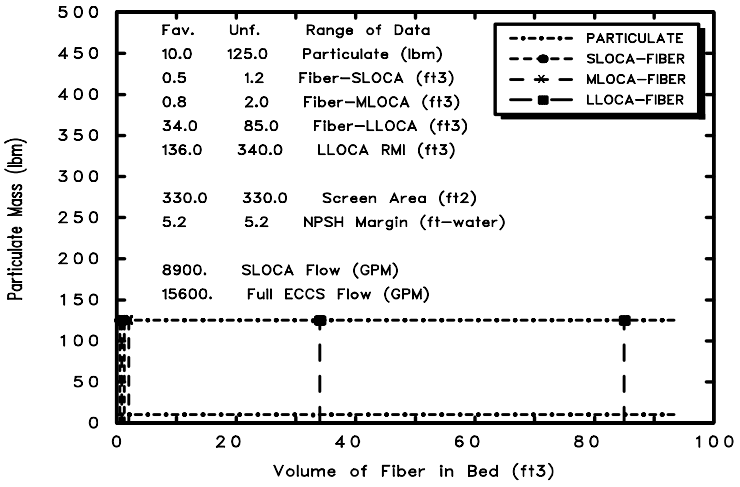

Parametric Case: 50 Debris Potential

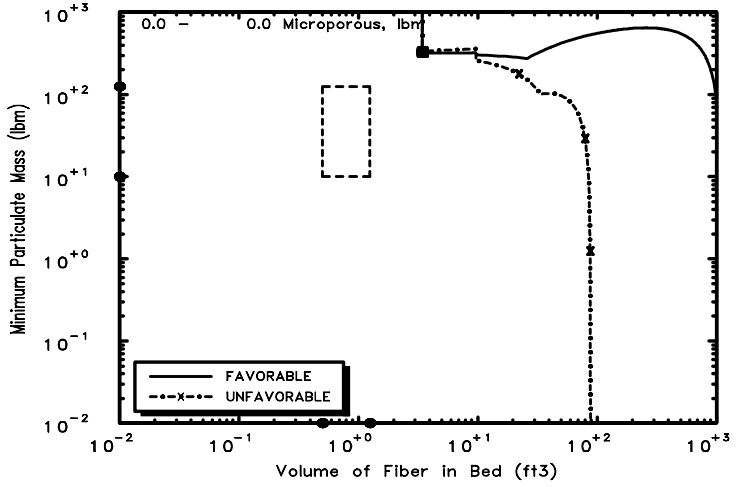

Parametric Case: 50 Small LOCA

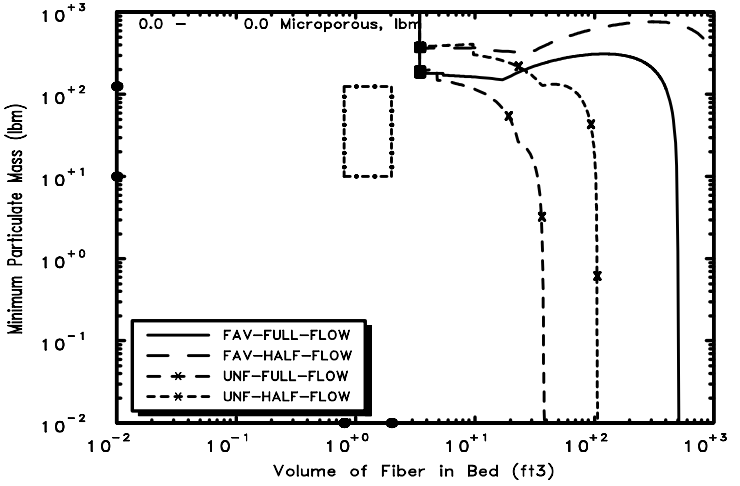

Parametric Case: 50 Medium LOCA

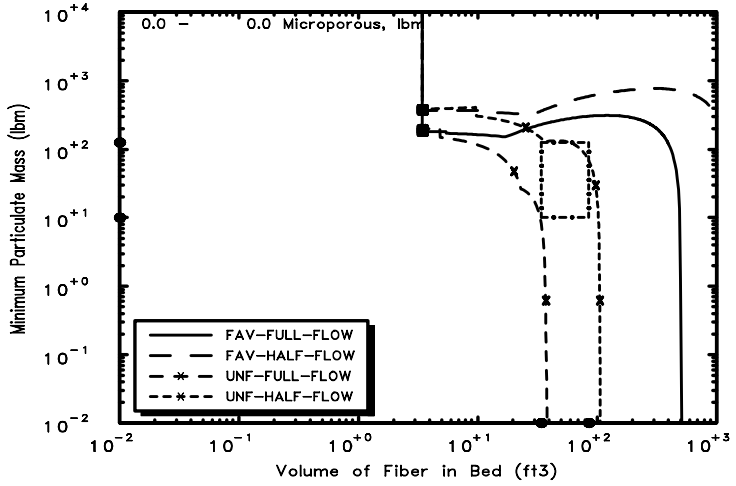

Parametric Case: 50 Large LOCA

Fig. B-50. Parametric Case 50.

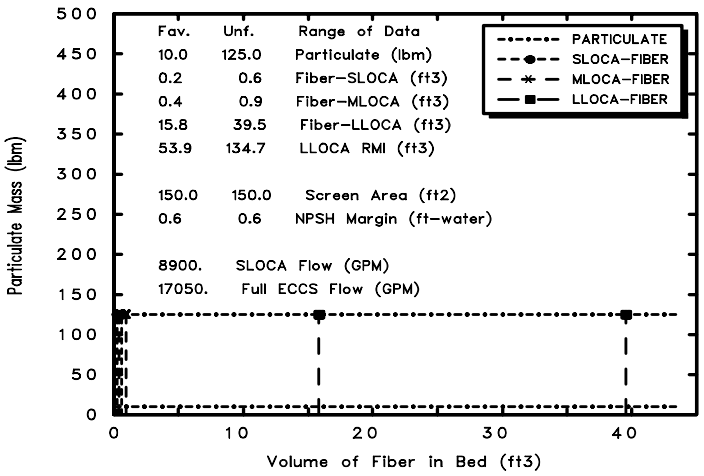

Parametric Case: 51 Debris Potential

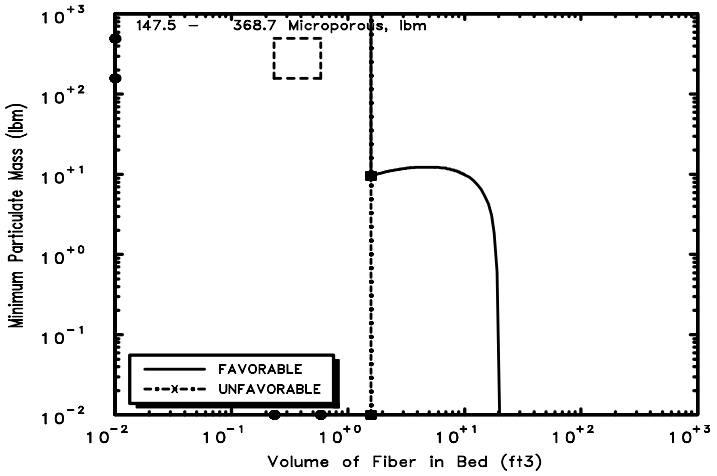

Parametric Case: 51 Small LOCA

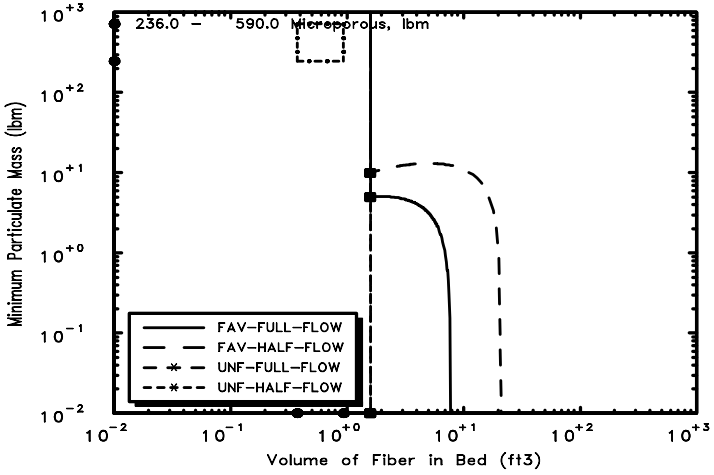

Parametric Case: 51 Medium LOCA

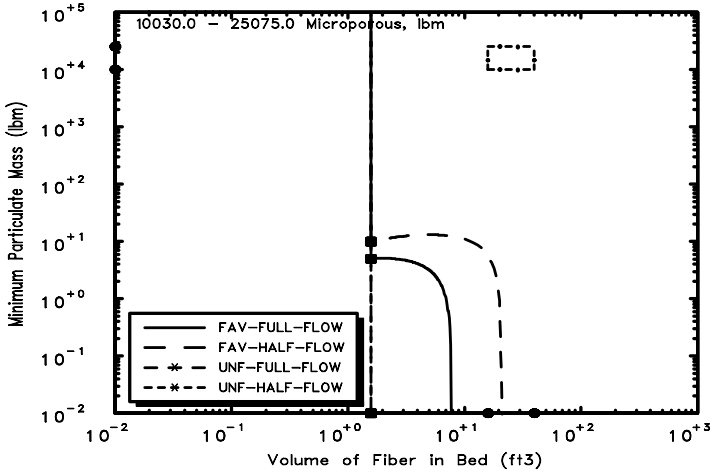

Parametric Case: 51 Large LOCA

Fig. B-51. Parametric Case 51.

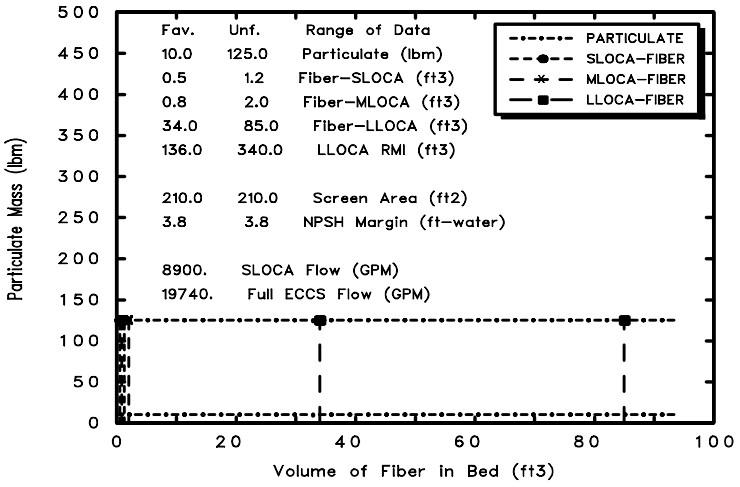

Parametric Case: 52 Debris Potential

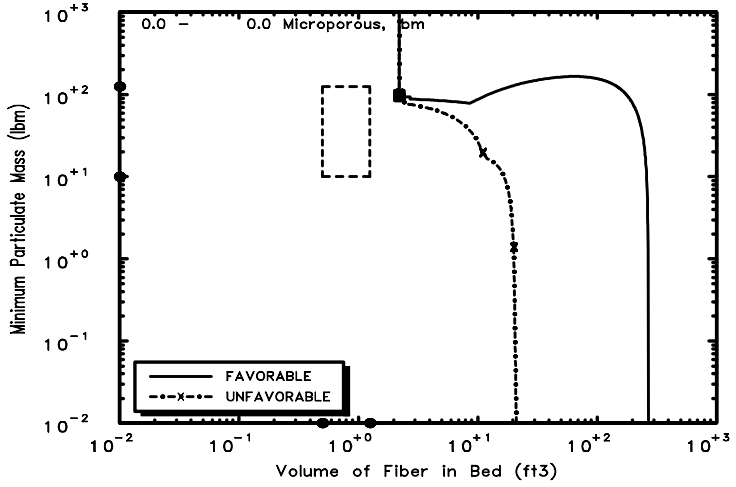

Parametric Case: 52 Small LOCA

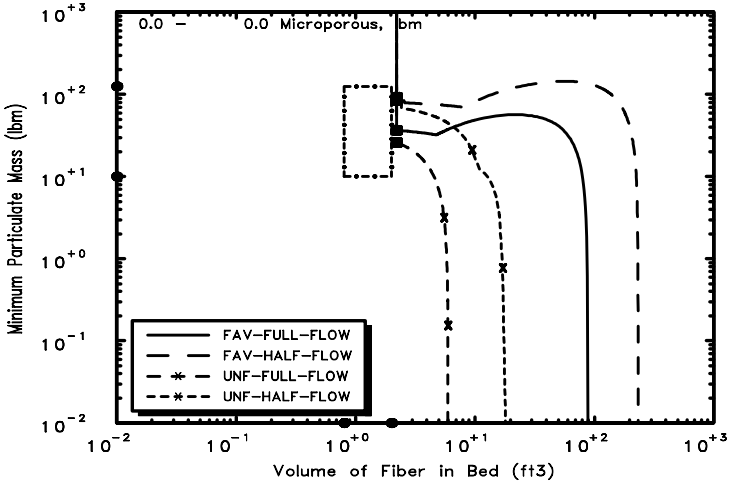

Parametric Case: 52 Medium LOCA

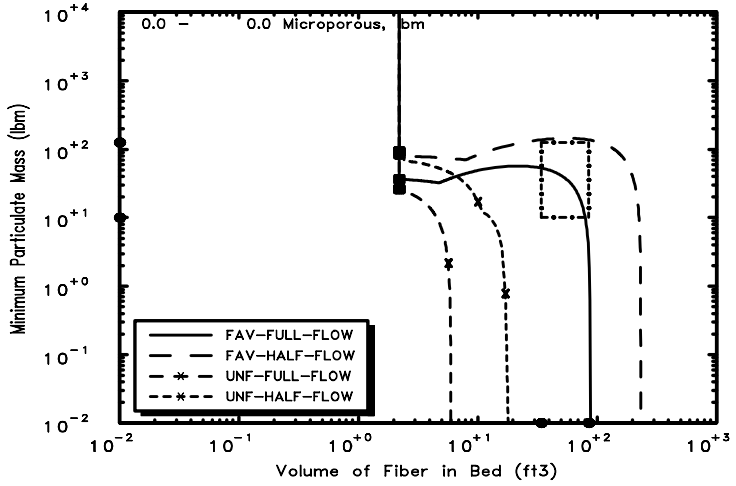

Parametric Case: 52 Large LOCA

Fig. B-52. Parametric Case 52.

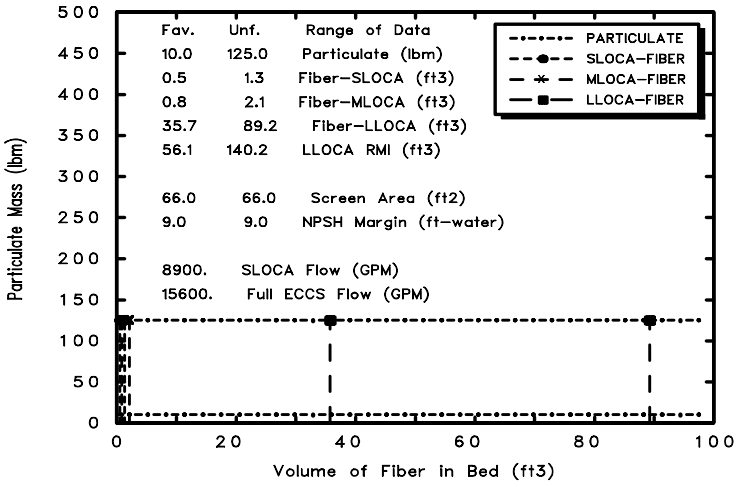

Parametric Case: 53 Debris Potential

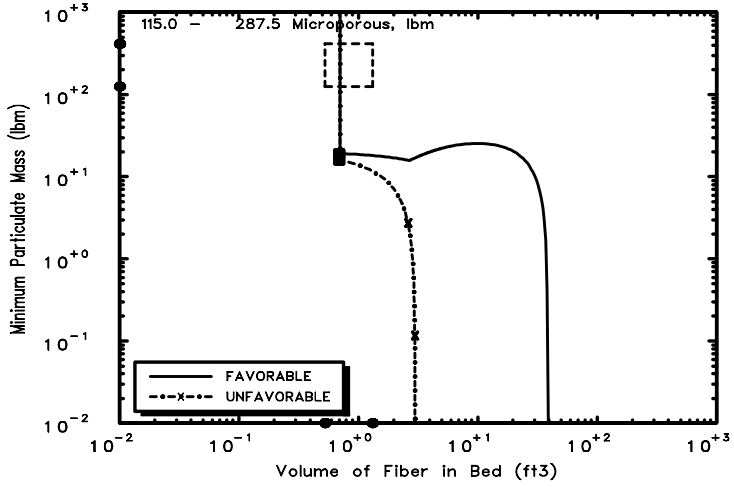

Parametric Case: 53 Small LOCA

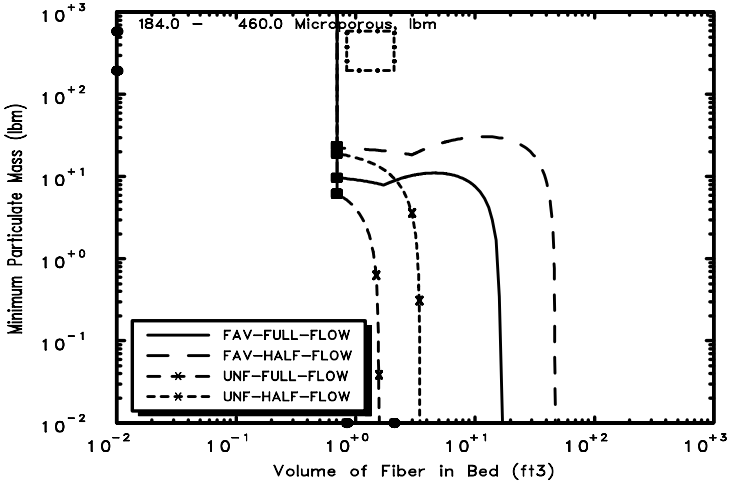

Parametric Case: 53 Medium LOCA

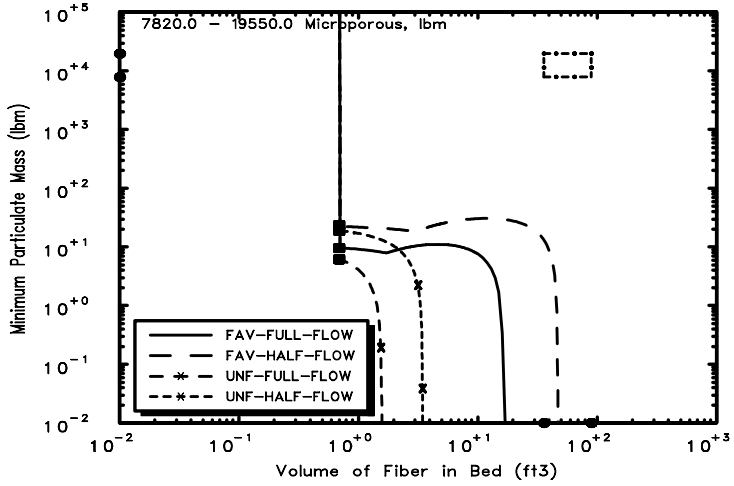

Parametric Case: 53 Large LOCA

Fig. B-53. Parametric Case 53.

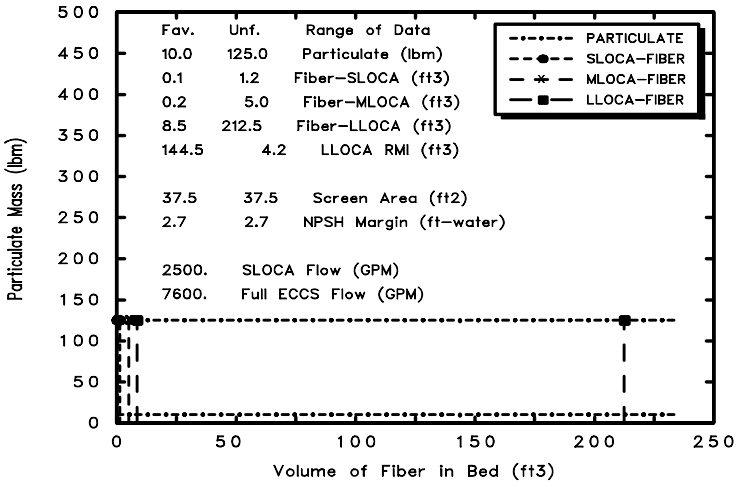

Parametric Case: 54 Debris Potential

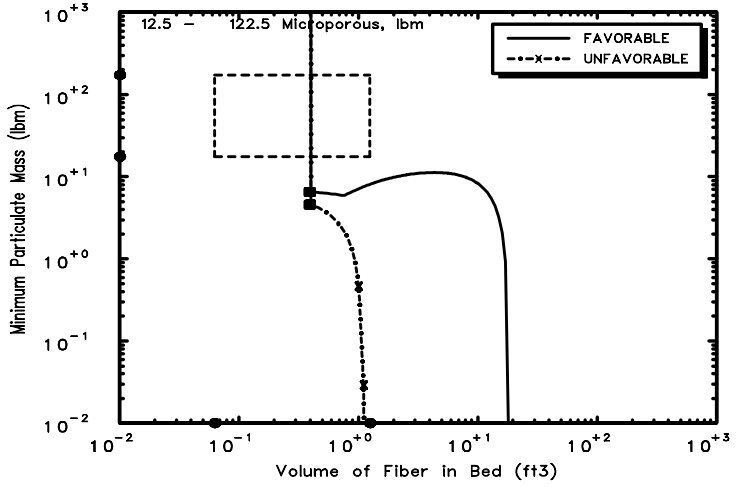

Parametric Case: 54 Small LOCA

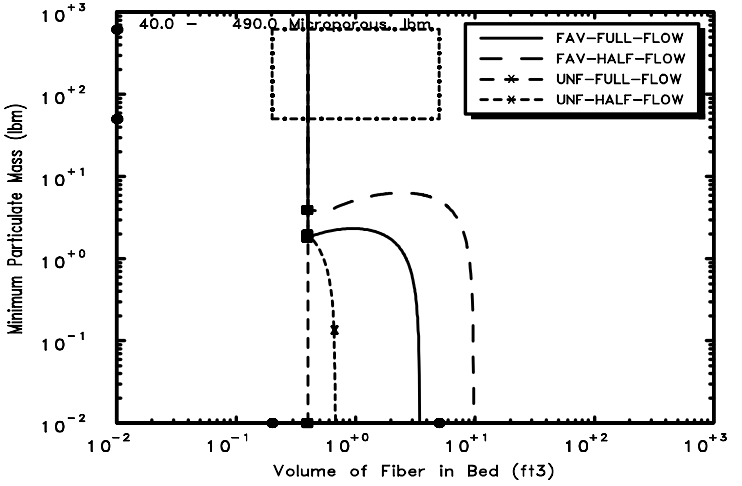

Parametric Case: 54 Medium LOCA

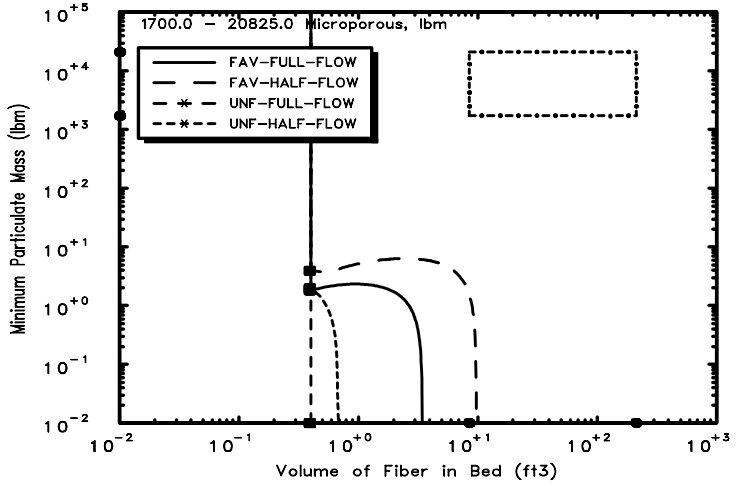

Parametric Case: 54 Large LOCA

Fig. B-54. Parametric Case 54.

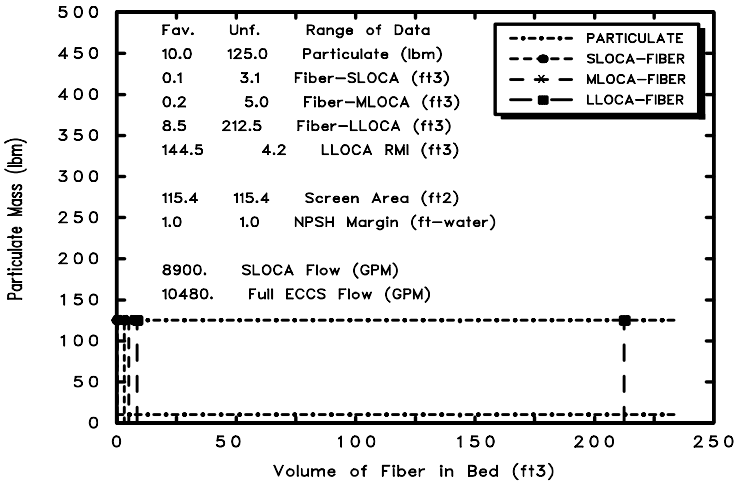

Parametric Case: 55 Debris Potential

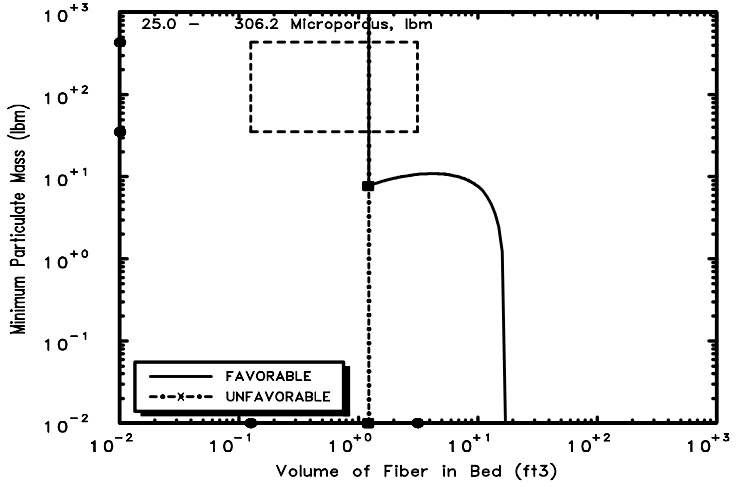

Parametric Case: 55 Small LOCA

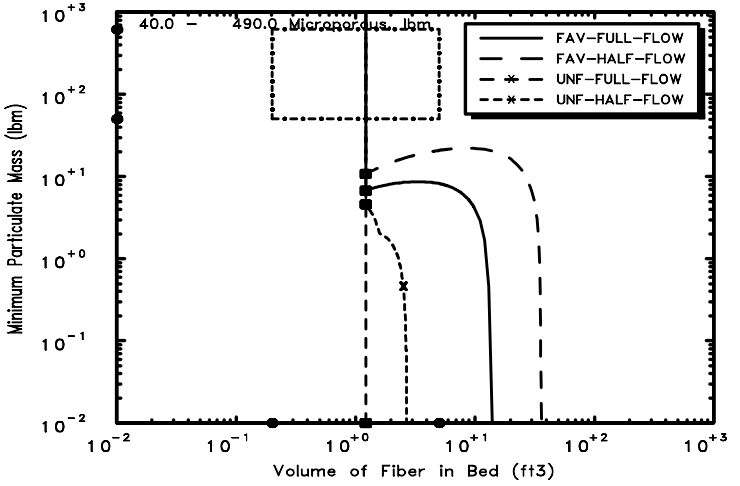

Parametric Case: 55 Medium LOCA

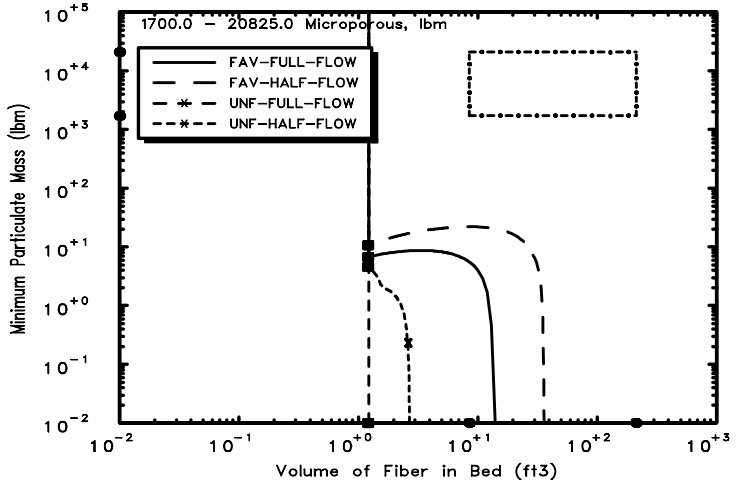

Parametric Case: 55 Large LOCA

Fig. B-55. Parametric Case 55.

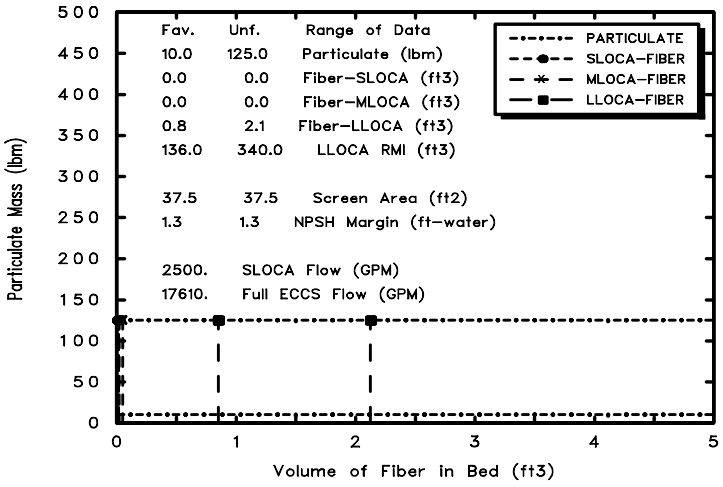

Parametric Case: 56 Debris Potential

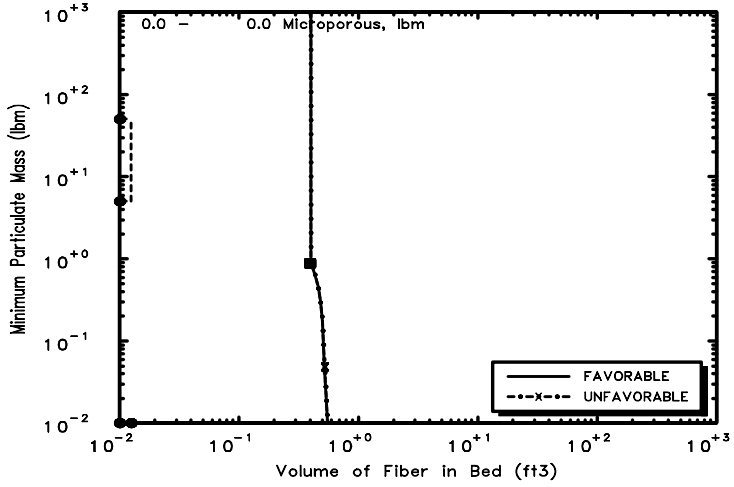

Parametric Case: 56 Small LOCA

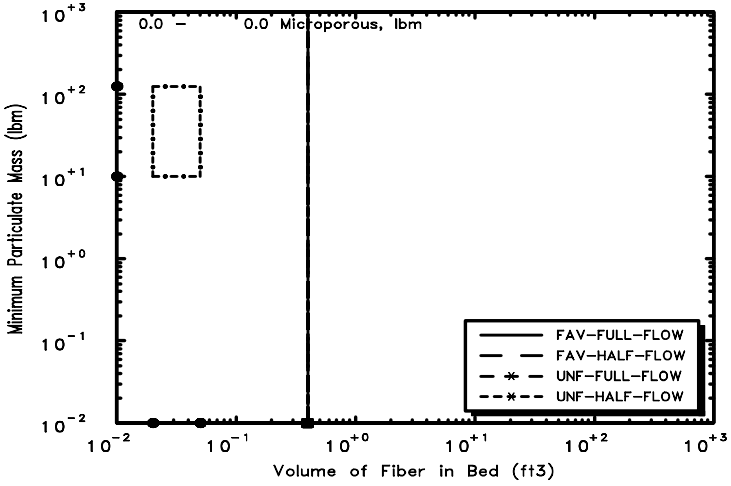

Parametric Case: 56 Medium LOCA

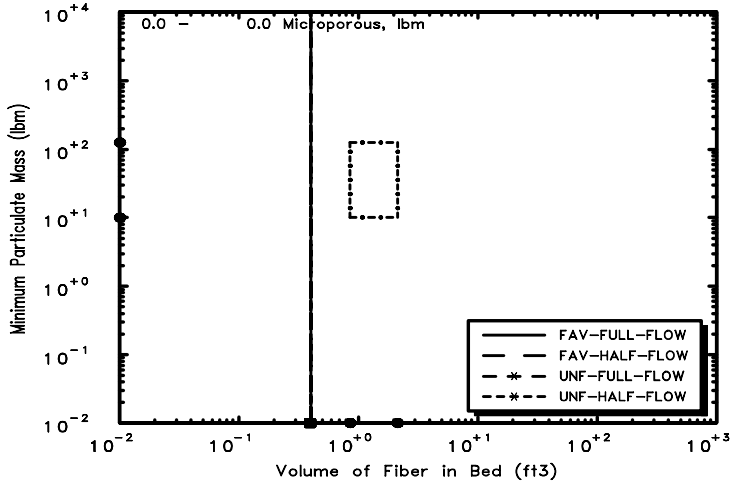

Parametric Case: 56 Large LOCA

Fig. B-56. Parametric Case 56.

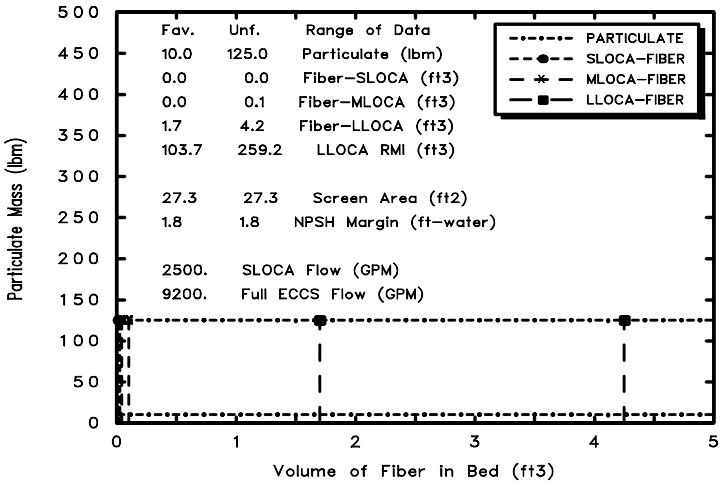

Parametric Case: 57 Debris Potential

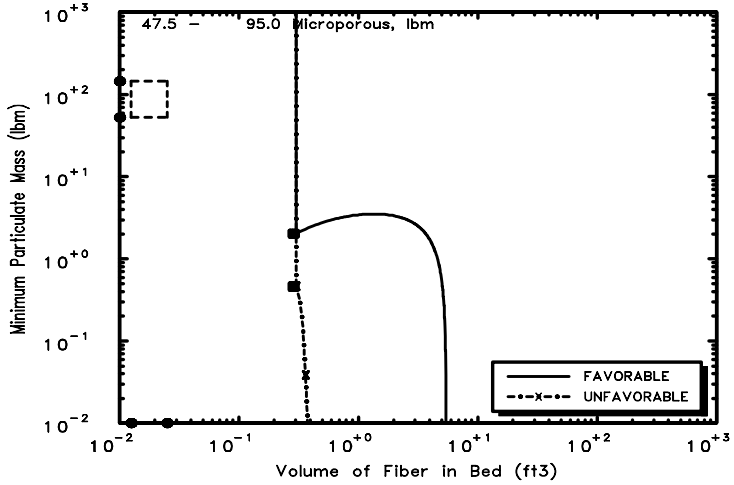

Parametric Case: 57 Small LOCA

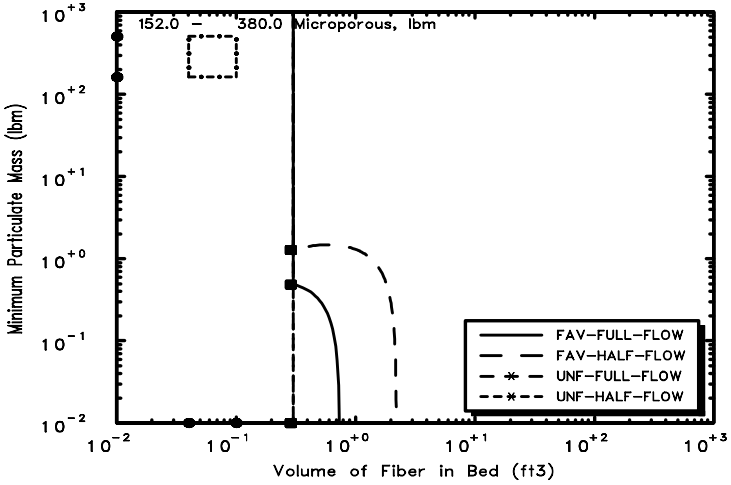

Parametric Case: 57 Medium LOCA

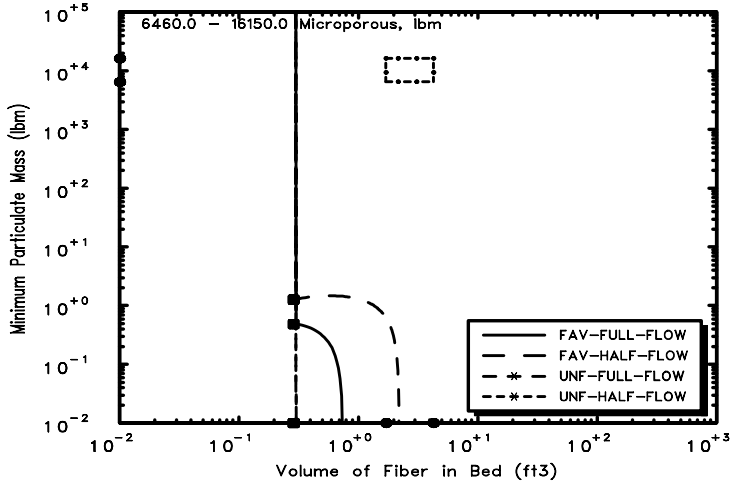

Parametric Case: 57 Large LOCA

Fig. B-57. Parametric Case 57.

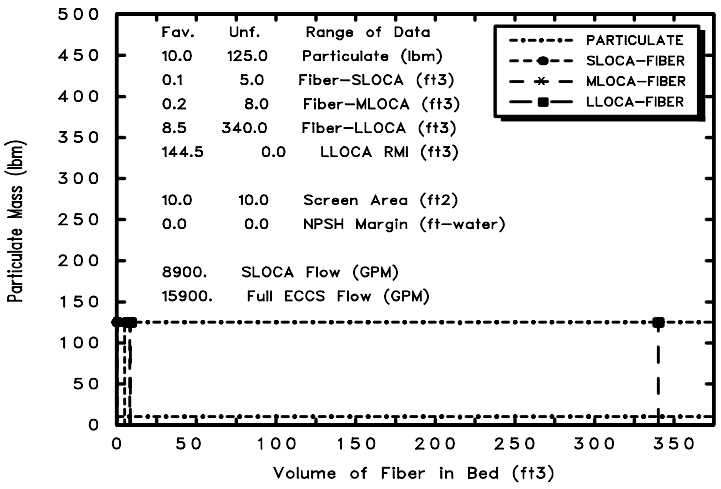

Parametric Case: 58 Debris Potential

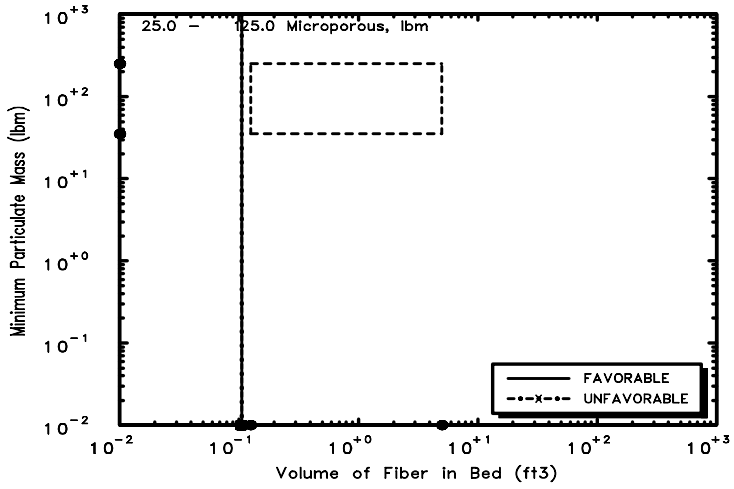

Parametric Case: 58 Small LOCA

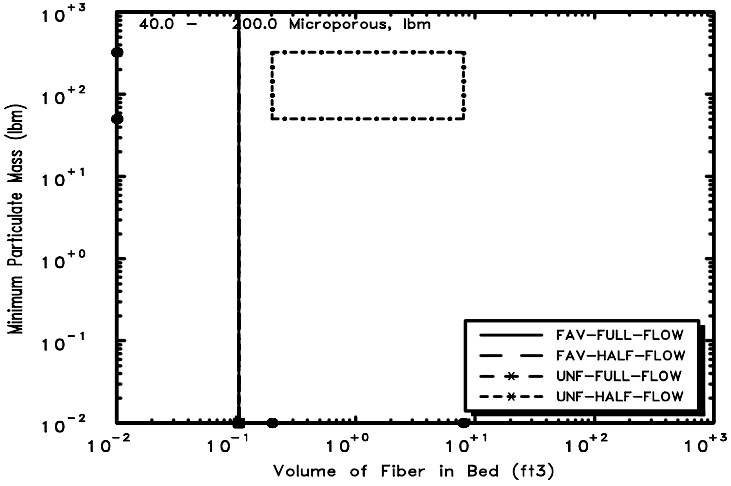

Parametric Case: 58 Medium LOCA

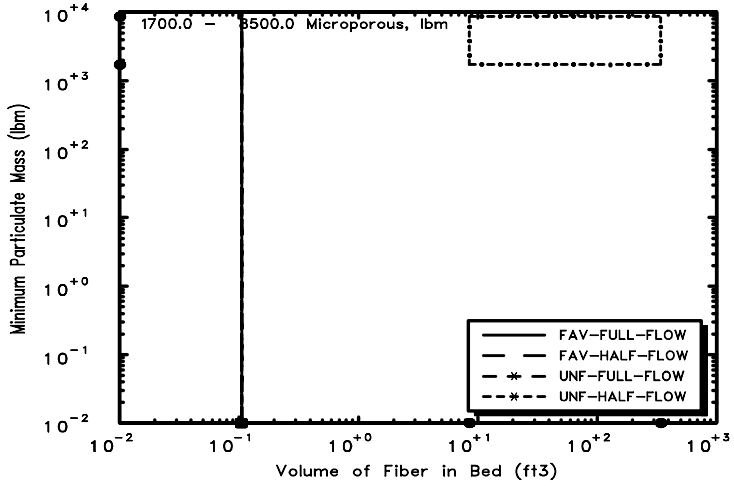

Parametric Case: 58 Large LOCA

Fig. B-58. Parametric Case 58.

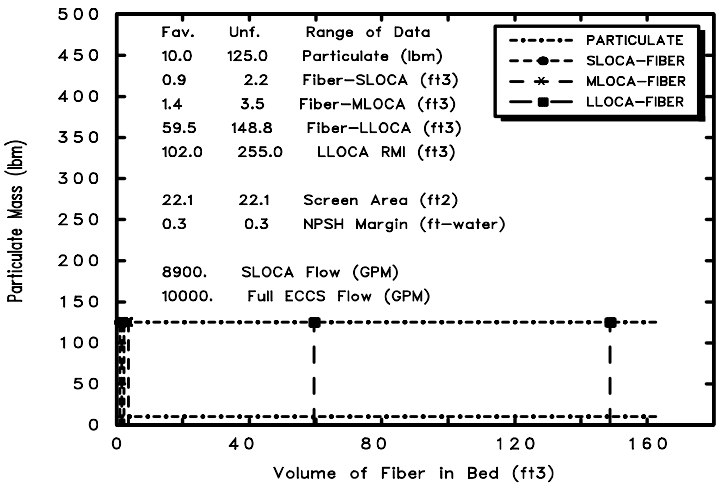

Parametric Case: 59 Debris Potential

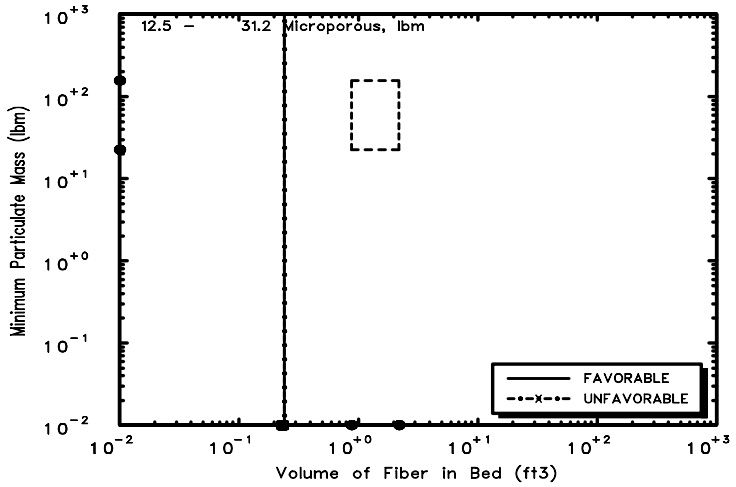

Parametric Case: 59 Small LOCA

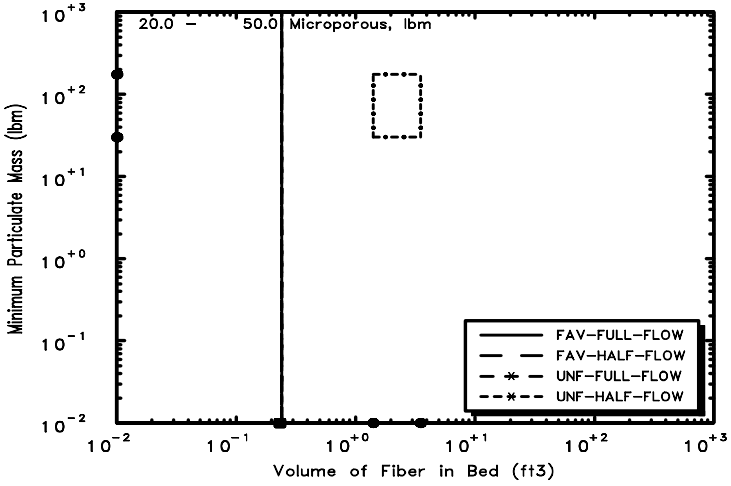

Parametric Case: 59 Medium LOCA

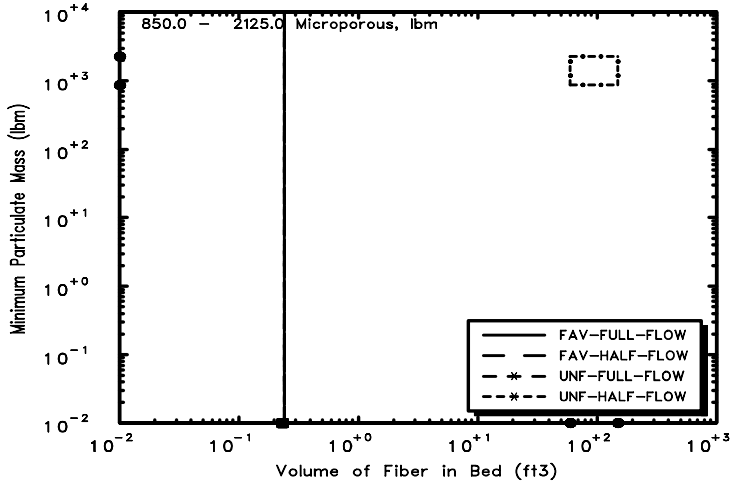

Parametric Case: 59 Large LOCA

Fig. B-59. Parametric Case 59.

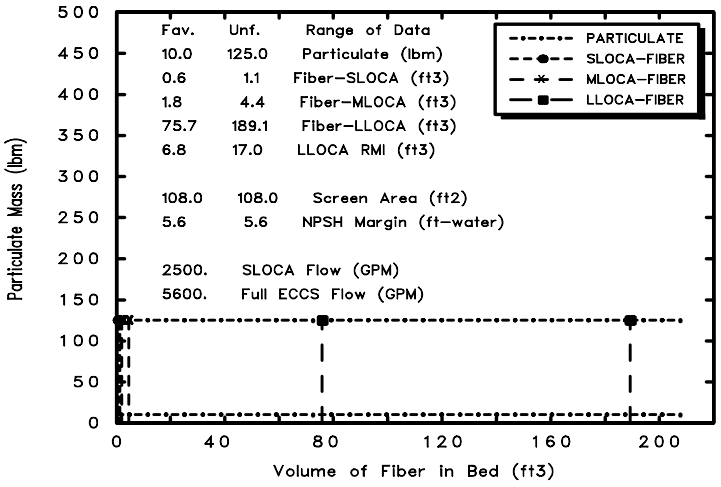

Parametric Case: 60 Debris Potential

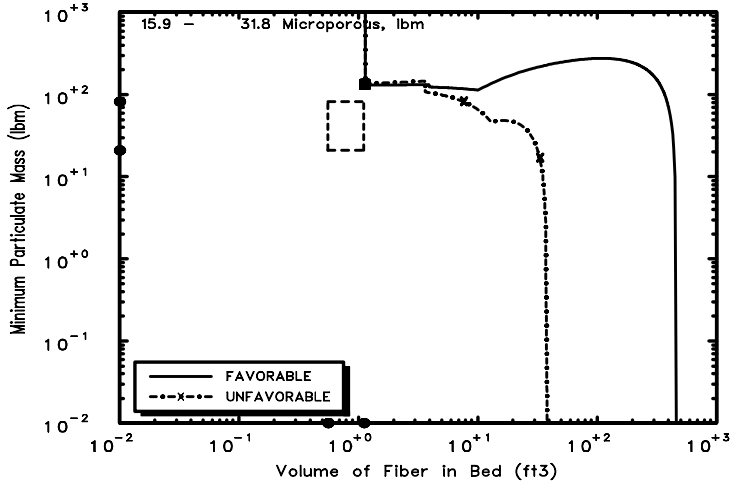

Parametric Case: 60 Small LOCA

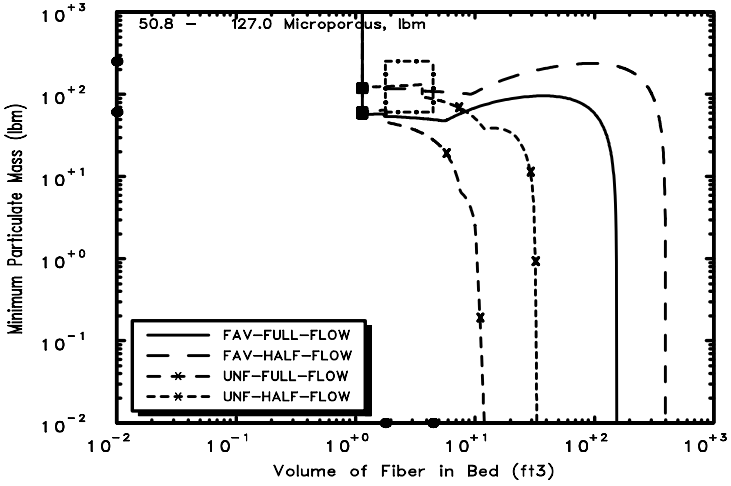

Parametric Case: 60 Medium LOCA

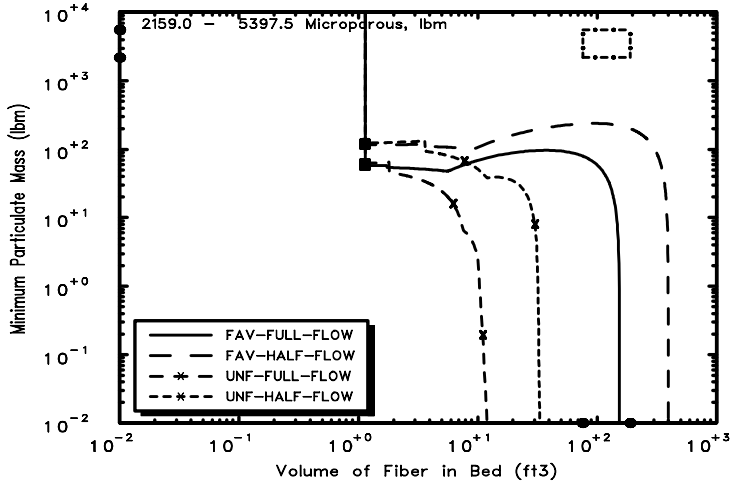

Parametric Case: 60 Large LOCA

Fig. B-60. Parametric Case 60.

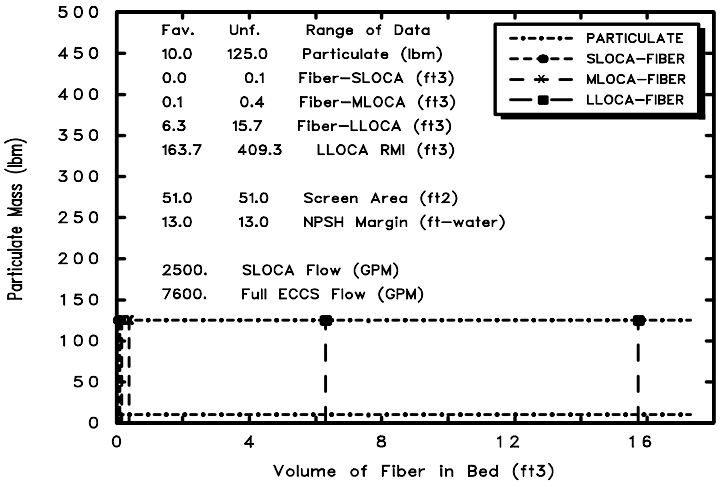

Parametric Case: 61 Debris Potential

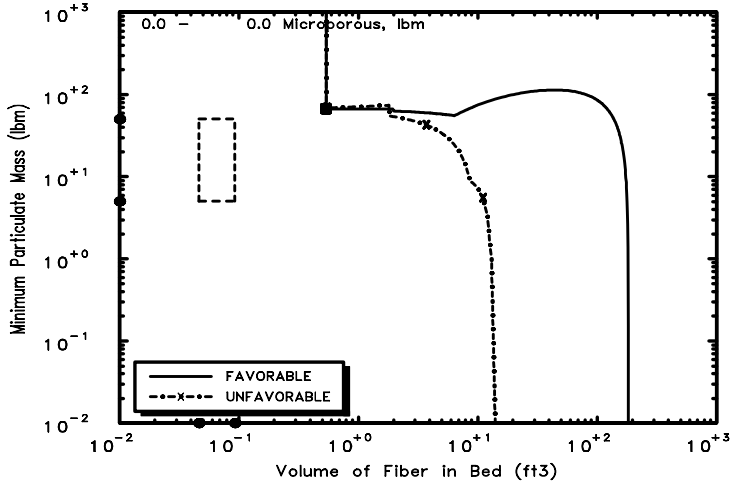

Parametric Case: 61 Small LOCA

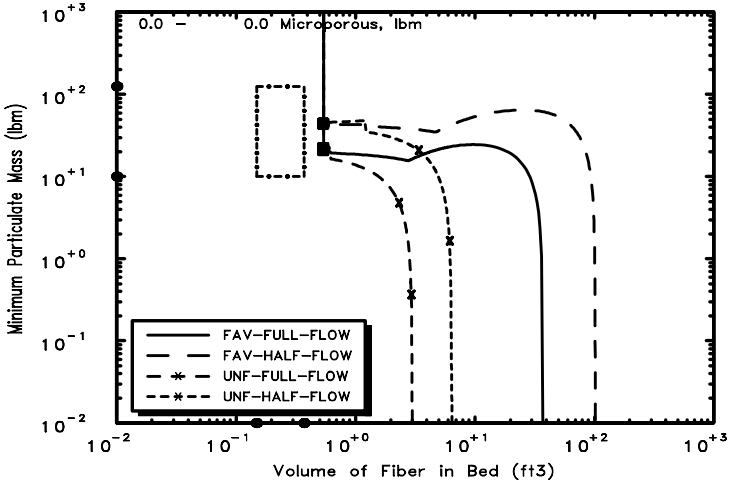

Parametric Case: 61 Medium LOCA

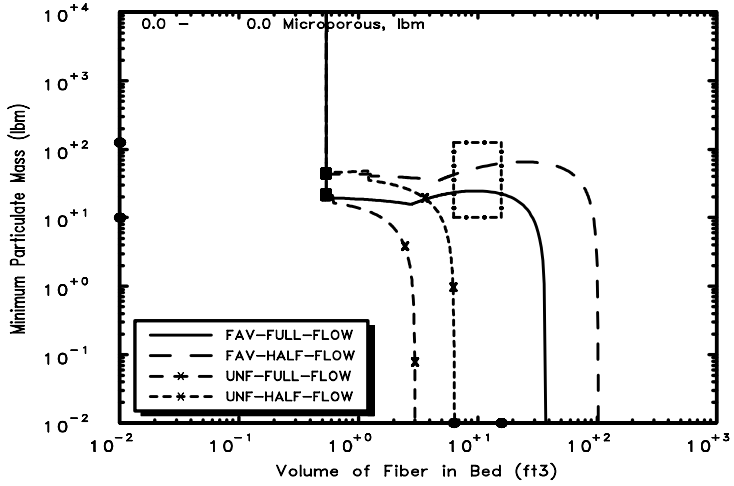

Parametric Case: 61 Large LOCA

Fig. B-61. Parametric Case 61.

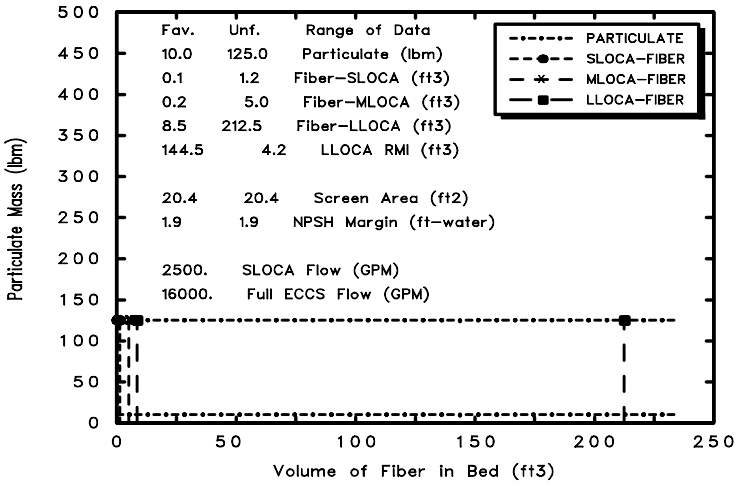

Parametric Case: 62 Debris Potential

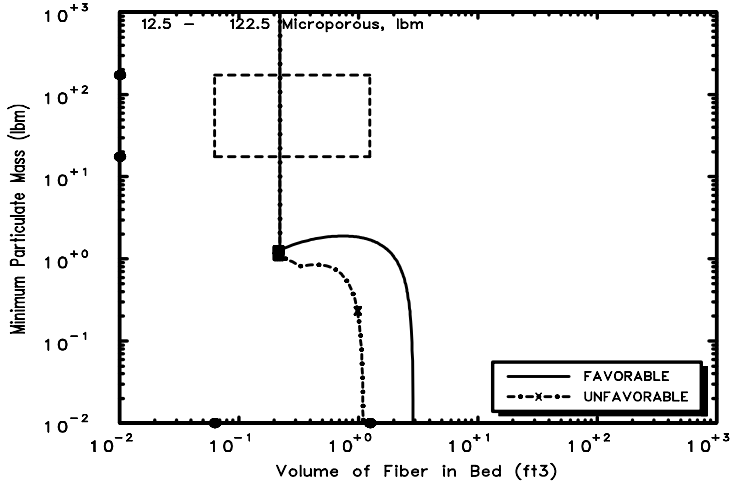

Parametric Case: 62 Small LOCA

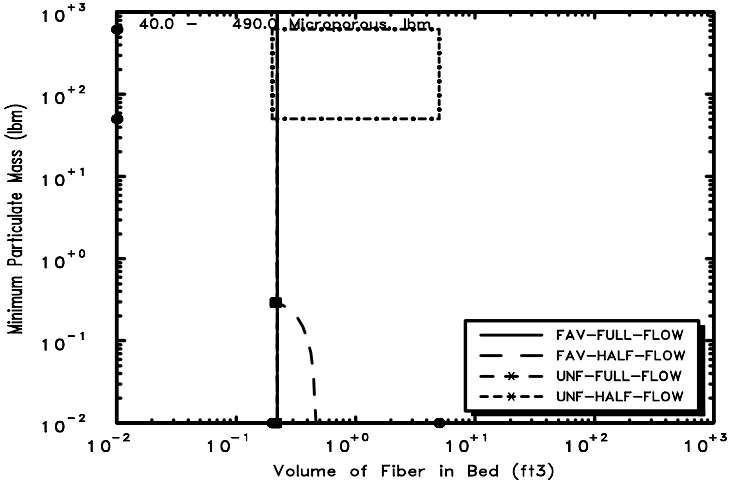

Parametric Case: 62 Medium LOCA

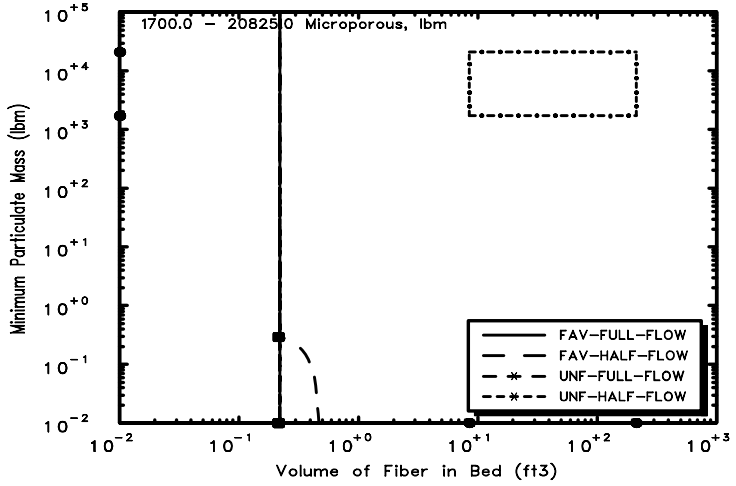

Parametric Case: 62 Large LOCA

Fig. B-62. Parametric Case 62.

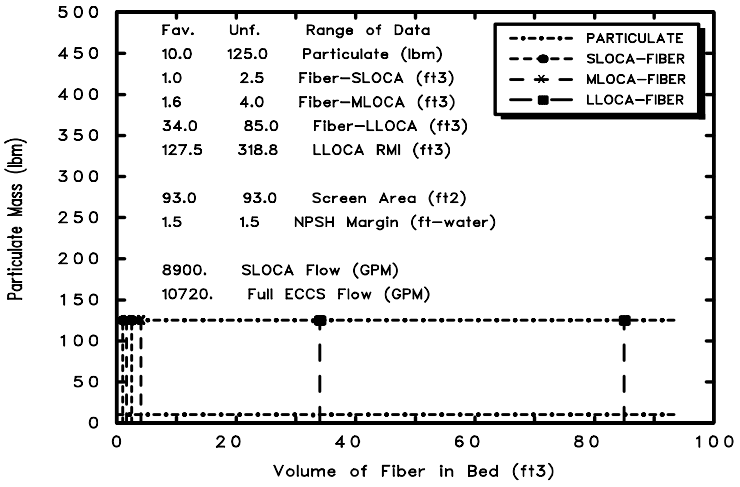

Parametric Case: 63 Debris Potential

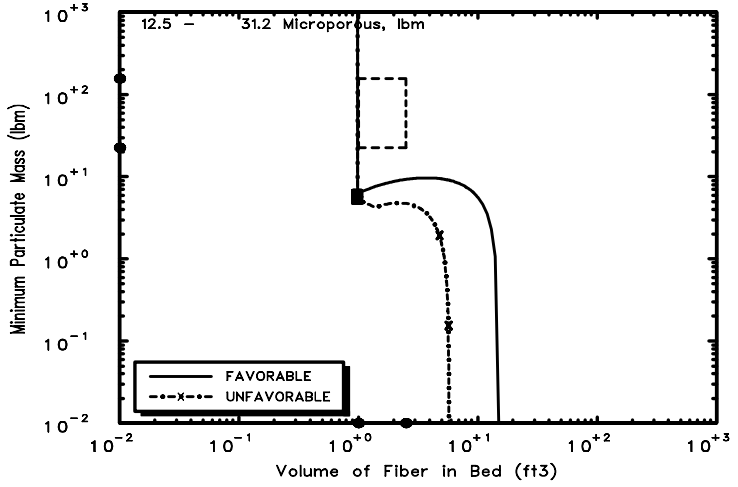

Parametric Case: 63 Small LOCA

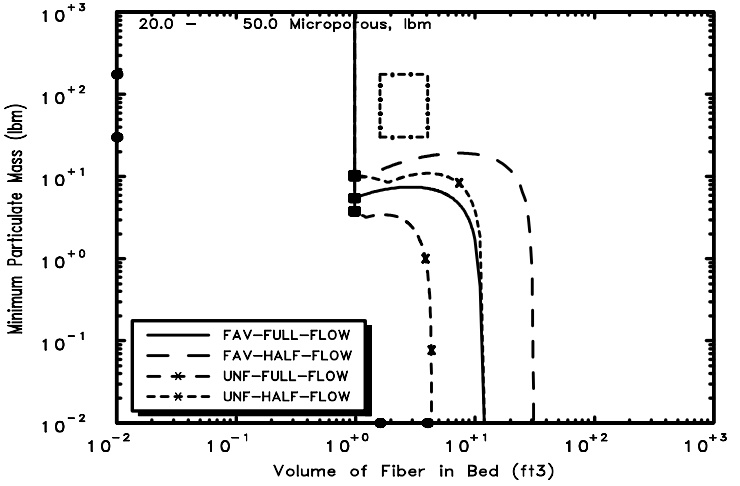

Parametric Case: 63 Medium LOCA

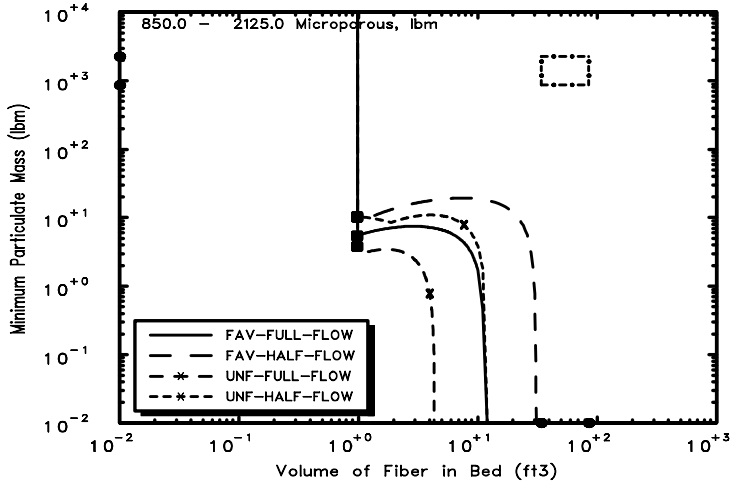

Parametric Case: 63 Large LOCA

Fig. B-63. Parametric Case 63.

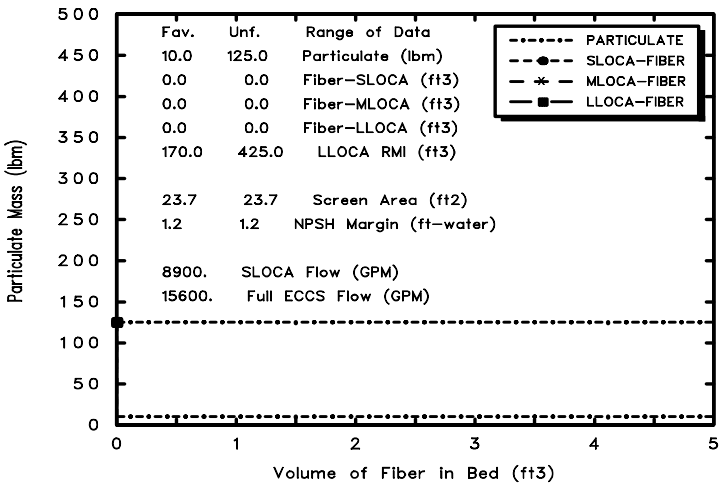

Parametric Case: 64 Debris Potential

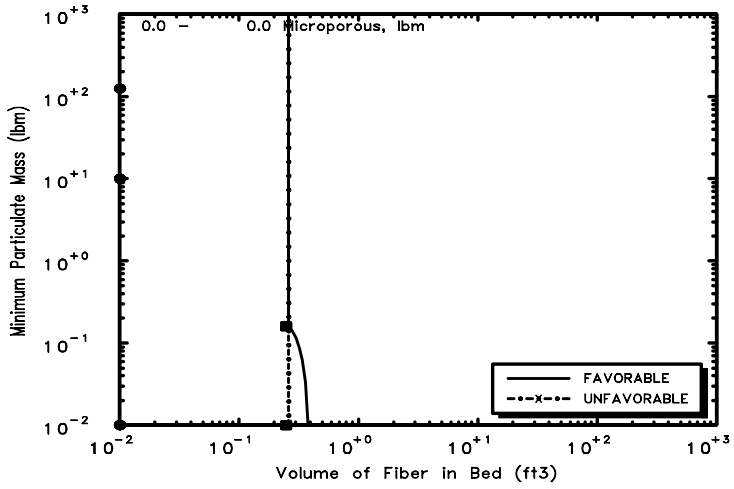

Parametric Case: 64 Small LOCA

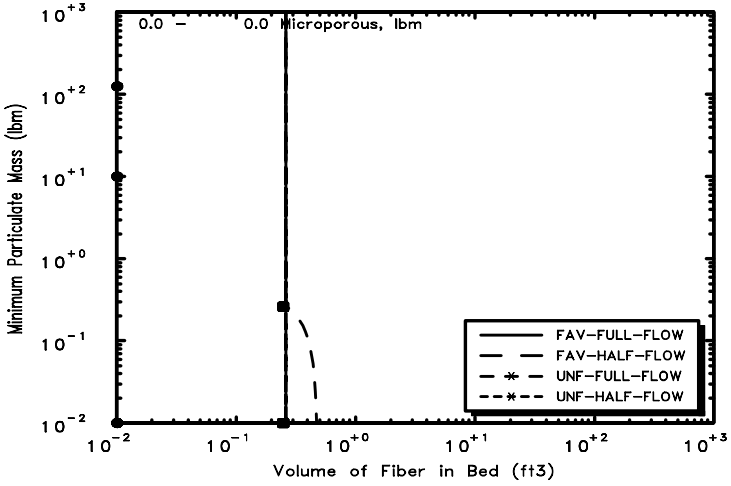

Parametric Case: 64 Medium LOCA

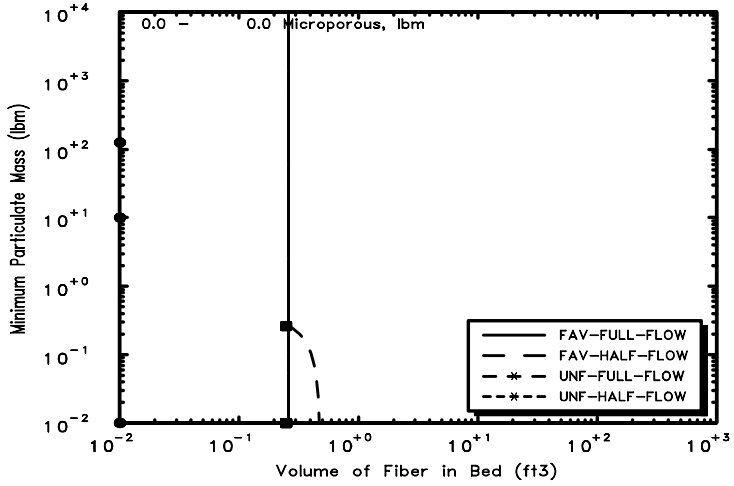

Parametric Case: 64 Large LOCA

Fig. B-64. Parametric Case 64 (Note: No fiber in this case, so no debris boxes presented).

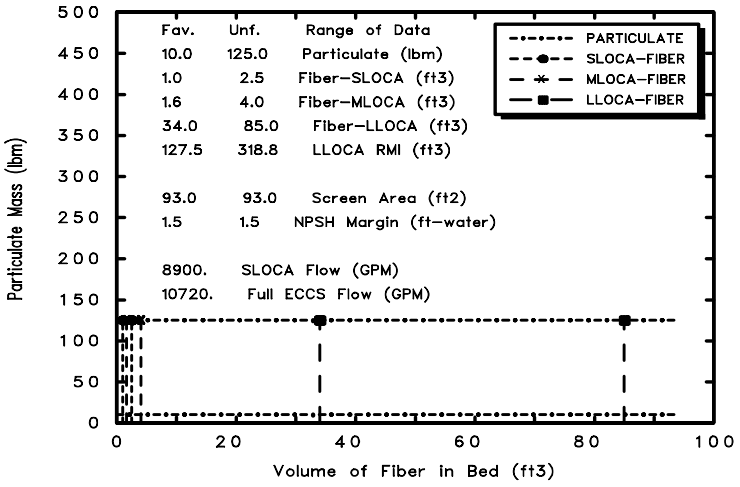

Parametric Case: 65 Debris Potential

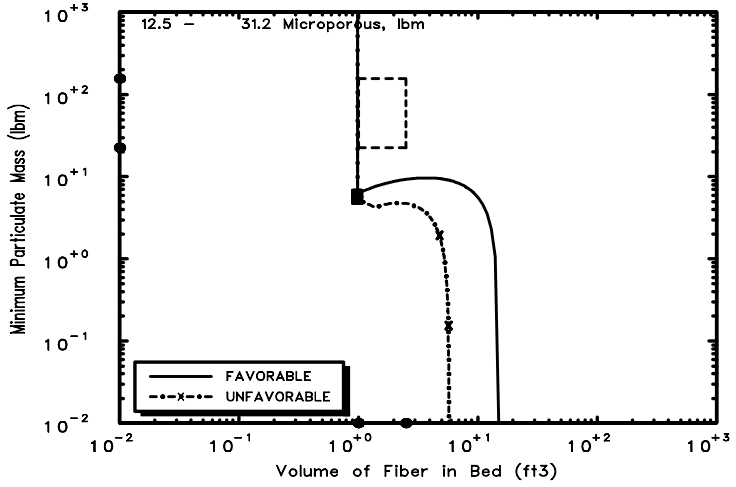

Parametric Case: 65 Small LOCA

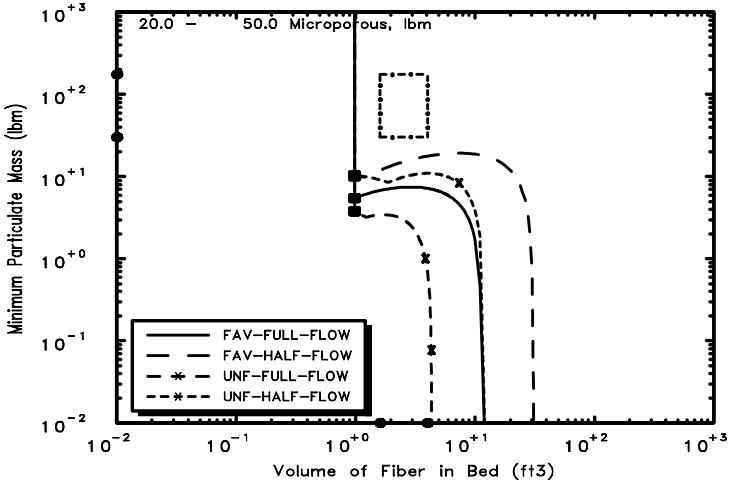

Parametric Case: 65 Medium LOCA

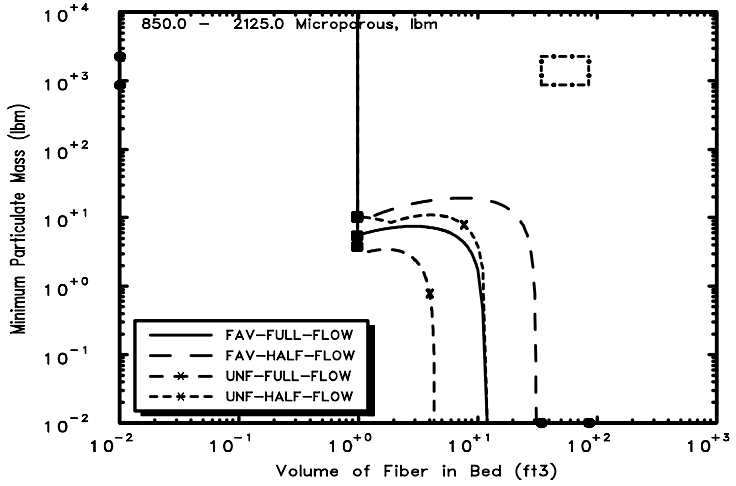

Parametric Case: 65 Large LOCA

Fig. B-65. Parametric Case 65.

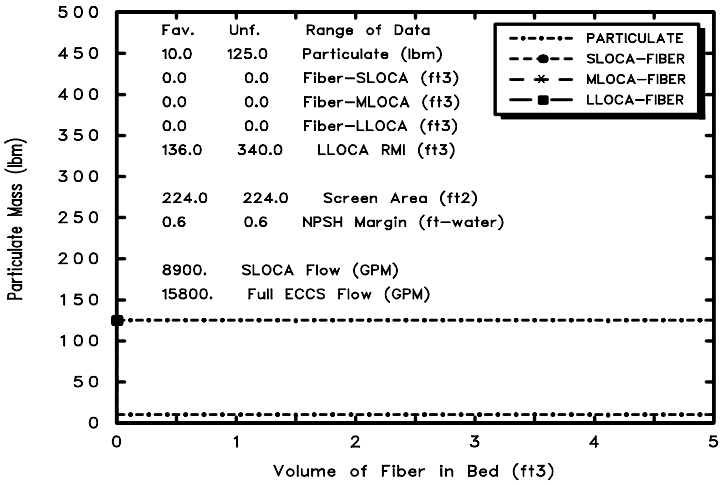

Parametric Case: 66 Debris Potential

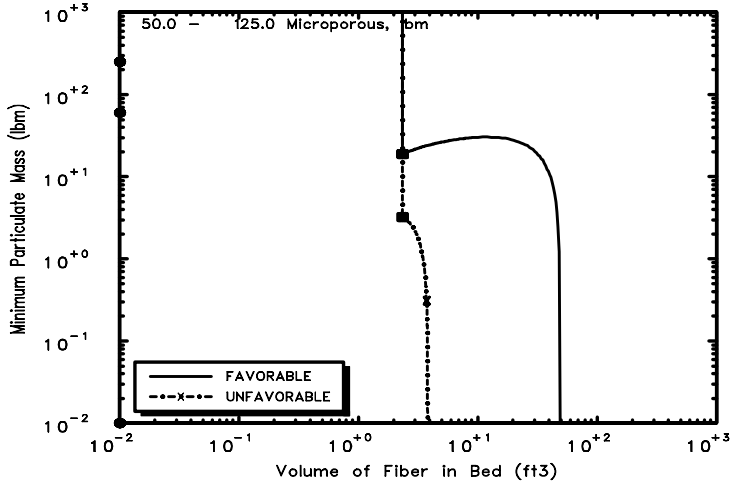

Parametric Case: 66 Small LOCA

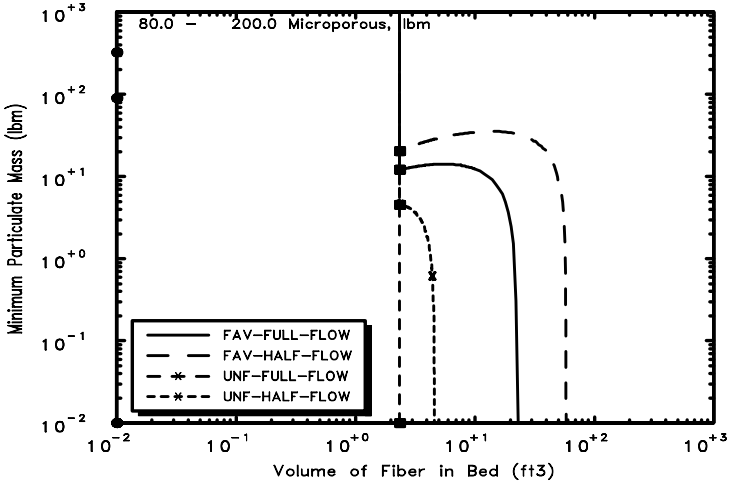

Parametric Case: 66 Medium LOCA

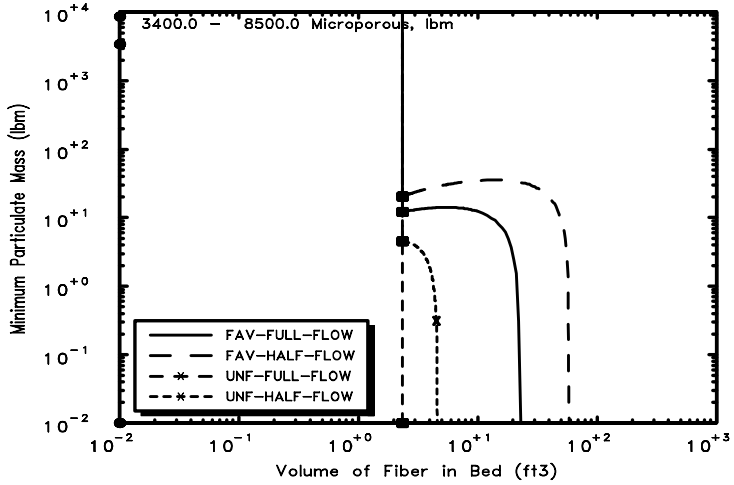

Parametric Case: 66 Large LOCA

Fig. B-66. Parametric Case 66 (Note: No fiber in this case, so no debris boxes presented).

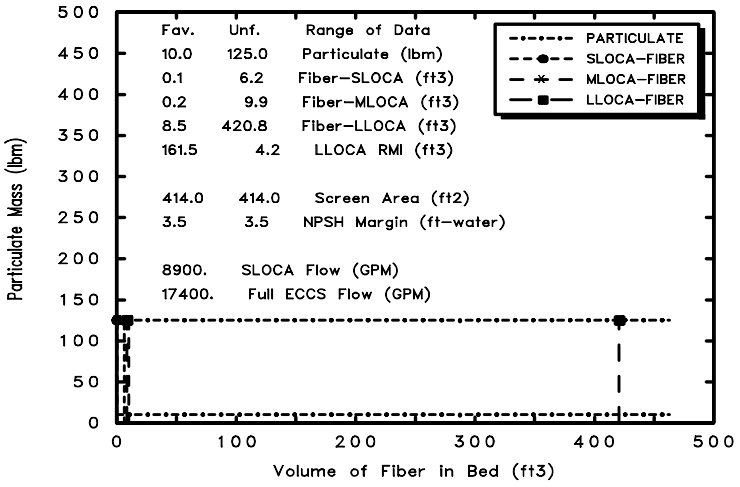

Parametric Case: 67 Debris Potential

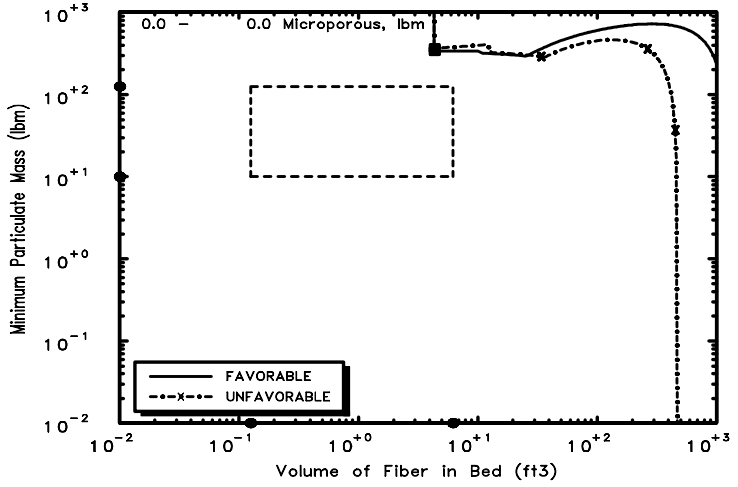

Parametric Case: 67 Small LOCA

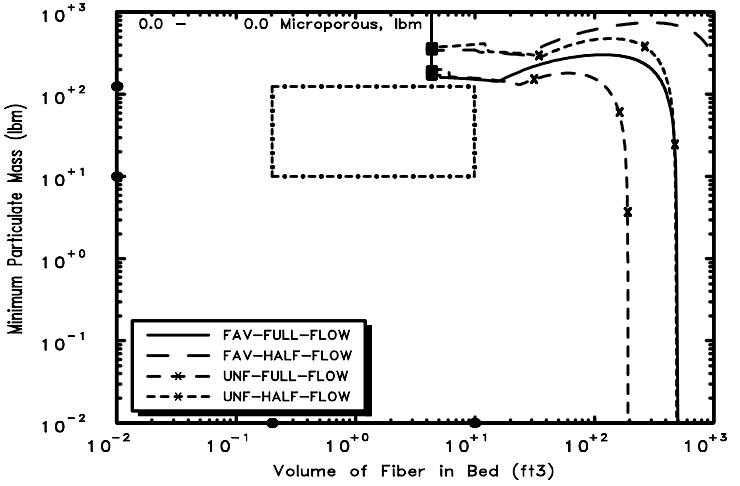

Parametric Case: 67 Medium LOCA

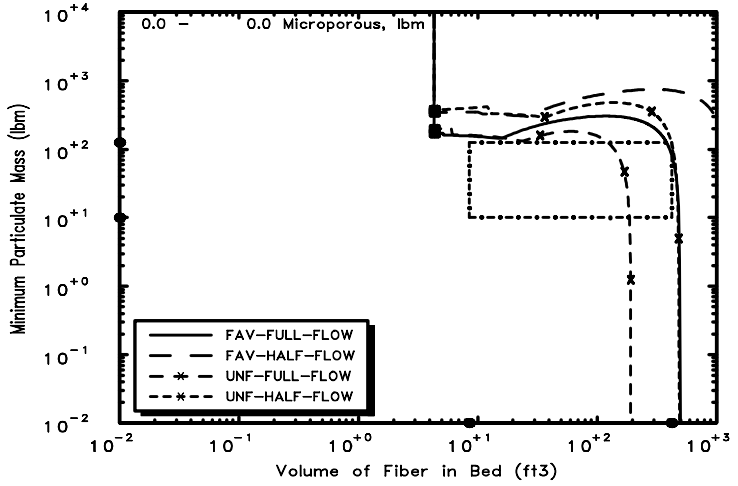

Parametric Case: 67 Large LOCA

Fig. B-67. Parametric Case 67.

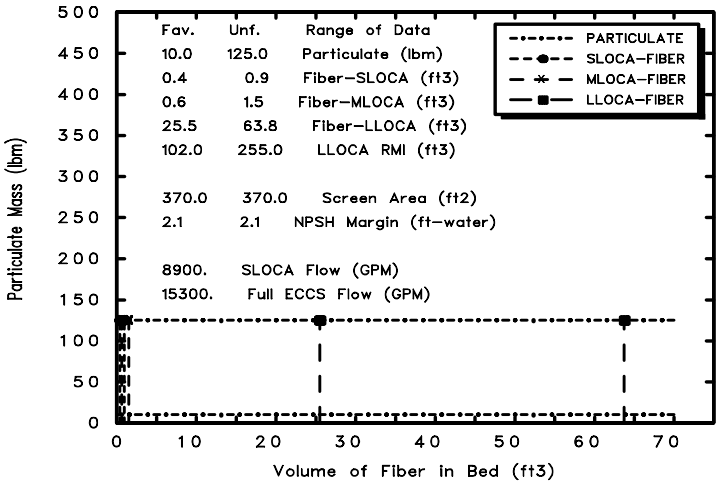

Parametric Case: 68 Debris Potential

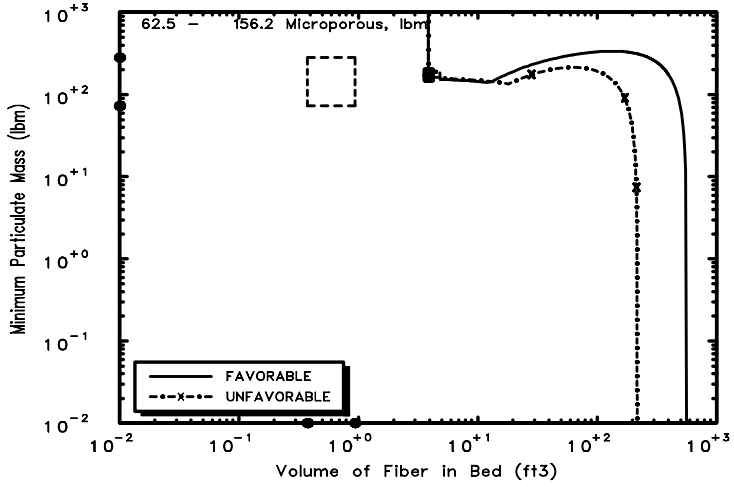

Parametric Case: 68 Small LOCA

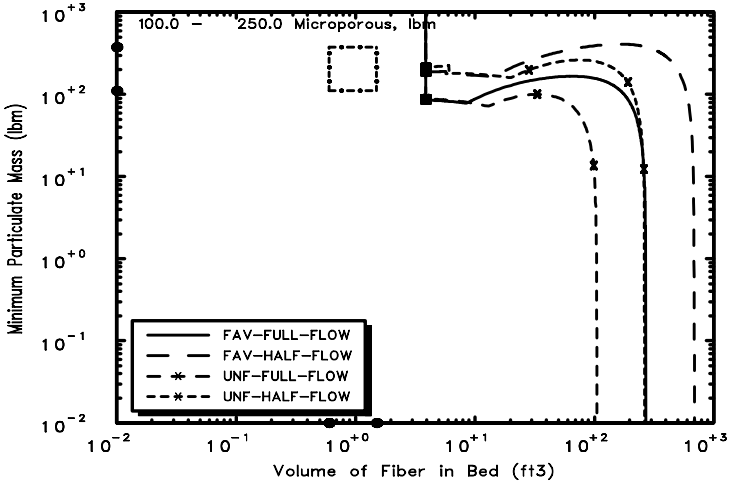

Parametric Case: 68 Medium LOCA

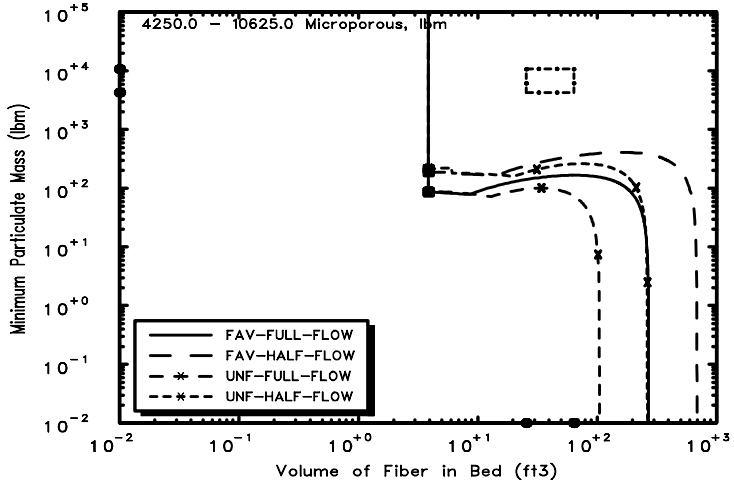

Parametric Case: 68 Large LOCA

Fig. B-68. Parametric Case 68.

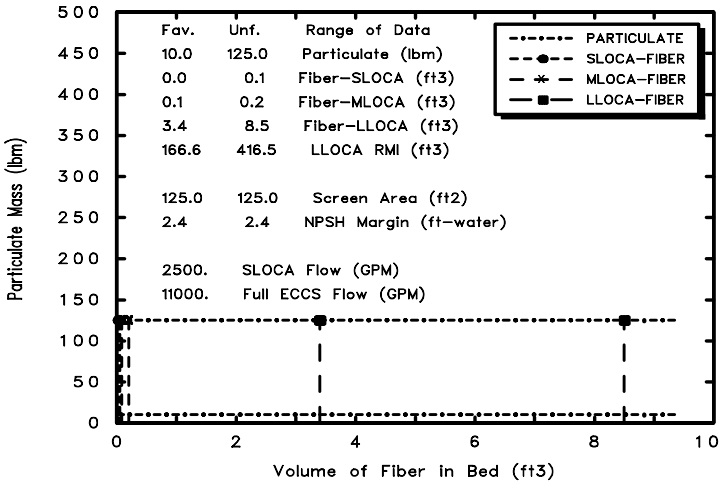

Parametric Case: 69 Debris Potential

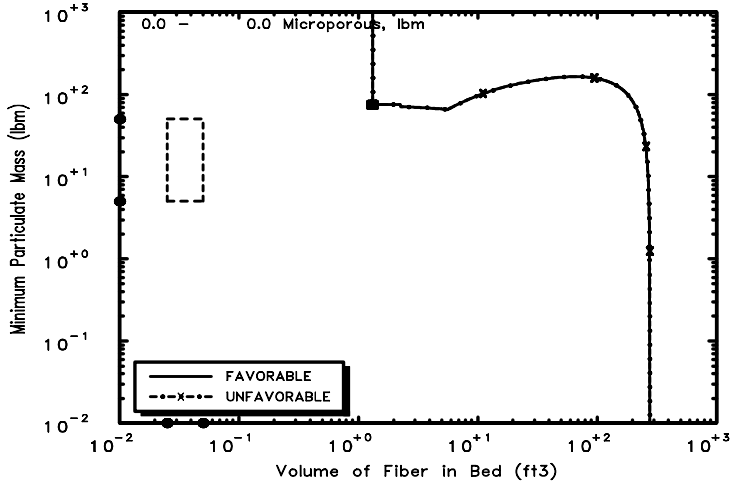

Parametric Case: 69 Small LOCA

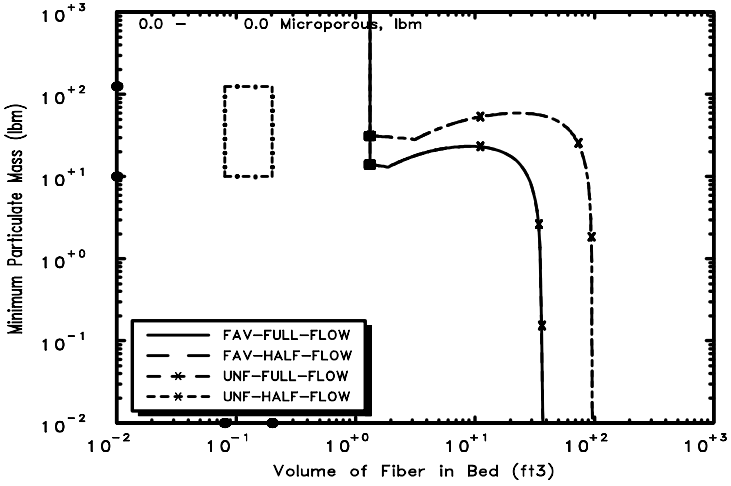

Parametric Case: 69 Medium LOCA

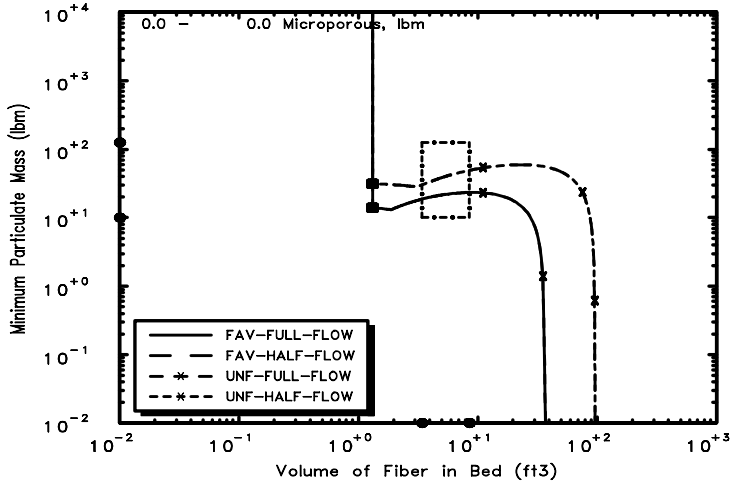

Parametric Case: 69 Large LOCA

Fig. B-69. Parametric Case 69.

Table B-1. Fraction of Debris-Transport Box Above FTDL Curve.

	SLOCA		MLOCA				LLOCA			
	Single Flow		Half Flow		Full Flow		Half Flow		Full Flow	
Case	Fav.	Unfav.	Fav.	Unfav.	Fav.	Unfav.	Fav.	Unfav.	Fav.	Unfav.
1	0.731	0.731	0.96	0.96	0.96	0.96	1	1	1	1
2	0	0	0.459	0.459	0.459	0.459	1	1	1	1
3	0	0	0	0	0	0	0	1	0.821	1
4	1	1	1	1	1	1	1	1	1	1
5	0.867	0.867	0.93	0.93	0.93	0.93	1	1	1	1
6	0.803	0.803	1	1	1	1	1	1	1	1
7	0	0	0	0	0	0	0	0	0	0
8	1	1	1	1	1	1	1	1	1	1
9	1	1	1	1	1	1	1	1	1	1
10	0.88	0.88	0.997	0.997	0.997	0.997	1	1	1	1
11	0.905	0.995	0.781	0.84	1	1	1	1	1	1
12	0.86	0.86	0.921	0.921	0.921	0.921	1	1	1	1
13	0	0	0	0	0	0	1	1	1	1
14	0	0	0	0	0	0	1	1	1	1
15	0	0	0.509	0.509	0.751	0.751	0.997	0.997	1	1
16	0.905	0.995	0.781	0.84	1	1	1	1	1	1
17	1	1	1	1	1	1	1	1	1	1
18	0	0	0	0	0	0	0	0	0	0
19	1	1	1	1	1	1	1	1	1	1
20	1	1	1	1	1	1	1	1	1	1
21	0	0	0	0	0.204	0.438	0	1	0.697	1
22	0.568	0.525	1	1	1	1	1	1	1	1
23	0	0	0.459	0.459	0.459	0.459	1	1	1	1
24	0	0	0	0	0	0	0	0	0	0
25	0	0	0	0	0	0	0	0	0.019	0.644
26	1	1	1	1	1	1	1	1	1	1
27	0.443	0.443	0.918	0.918	0.918	0.918	1	1	1	1
28	0.014	0.013	1	1	1	1	1	1	1	1
29	0	0	0	0	0	0	0	0	0	0
30	0	0	0	0	0	0	1	1	1	1
31	0	0	0	0	0	0	0	0	0	0
32	1	1	1	1	1	1	1	1	1	1
33	0	0	0.634	0.634	0.634	0.634	1	1	1	1

Table B-1. Fraction of Debris-Transport Box Above FTDL Curve (cont).

Case	SLOCA Single Flow		MLOCA Half Flow		MLOCA Full Flow		LLOCA Half Flow		LLOCA Full Flow	
	Fav.	Unfav.	Fav.	Unfav.	Fav.	Unfav.	Fav.	Unfav.	Fav.	Unfav.
34	0	0	0	0	0	0	0.598	1	0.878	1
35	0.828	0.828	0.906	0.906	0.906	0.906	1	1	1	1
36	0.742	0.742	1	1	1	1	1	1	1	1
37	1	1	1	1	1	1	1	1	1	1
38	0	0	0	0	0	0	0	1	0.821	1
39	0	0	0.286	0.286	0.286	0.286	1	1	1	1
40	0	0	0	0	0	0	1	1	1	1
41	0	0	0	0	0	0	0	1	0	1
42	0.005	0.002	1	1	1	1	1	1	1	1
43	0	0	0	0	0	0	1	1	1	1
44	0	0	0	0	0	0	1	1	1	1
45	0.802	0.802	0.89	0.89	0.89	0.89	1	1	1	1
46	0	0	0	0	0.217	0.203	0.973	1	1	1
47	1	1	1	1	1	1	1	1	1	1
48	1	1	1	1	1	1	1	1	1	1
49	0	0	0	0	0	0	0	0	0	0
50	0	0	0	0	0	0	0	0.119	0	1
51	0	0	0	0	0	0	1	1	1	1
52	0	0	0	0	0	0	0	1	0.821	1
53	0.803	0.803	1	1	1	1	1	1	1	1
54	0.731	0.731	0.96	0.96	0.96	0.96	1	1	1	1
55	0.645	0.645	0.791	0.791	0.791	0.791	1	1	1	1
56	0	0	0	0	0	0	1	1	1	1
57	0	0	0	0	0	0	1	1	1	1
58	1	1	1	1	1	1	1	1	1	1
59	1	1	1	1	1	1	1	1	1	1
60	0	0	0.725	0.714	1	1	1	1	1	1
61	0	0	0	0	0	0	0.598	1	0.878	1
62	0.88	0.88	0.997	0.997	0.997	0.997	1	1	1	1
63	1	1	1	1	1	1	1	1	1	1
64	0	0	0	0	0	0	0	0	0	0
65	1	1	1	1	1	1	1	1	1	1
66	0	0	0	0	0	0	0	0	0	0
67	0	0	0	0	0	0	0	0	0.019	0.644
68	0	0	0	0	0	0	1	1	1	1
69	0	0	0	0	0	0	0.729	0.729	0.897	0.897